BIOMECHANICS2020

INTERNATIONAL CONFERENCE
OF THE POLISH SOCIETY OF BIOMECHANICS
9-10 SEPTEMBER 2021,WARSAW

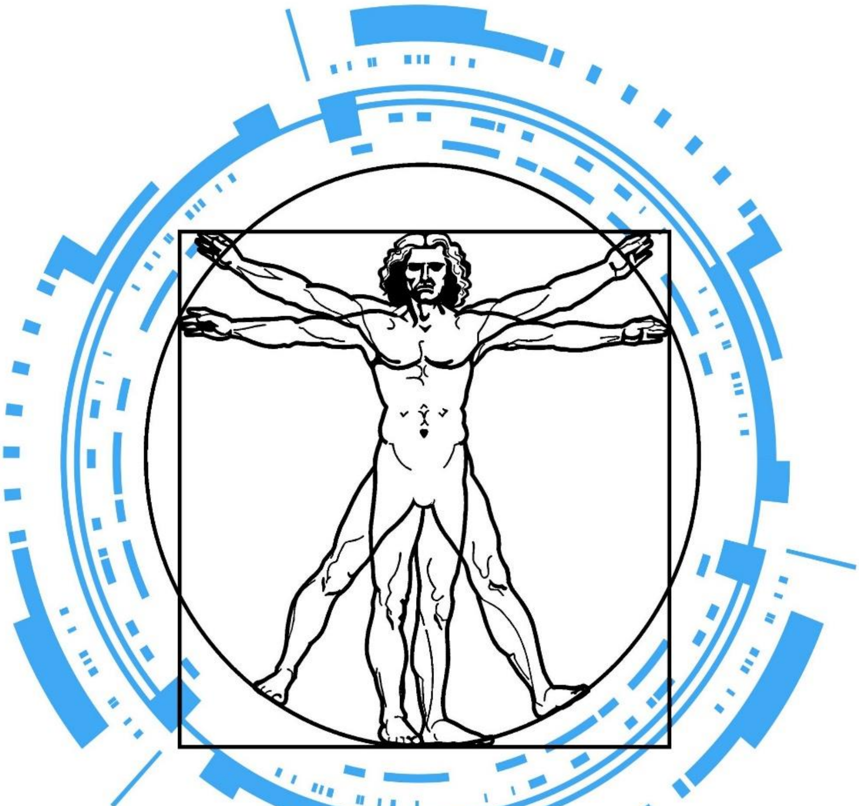

Editors:

A. Hadamus, S. Piszczatowski, M. Syczewska, S. Wójtowicz, D. Białoszewski

INTERNATIONAL CONFERENCE OF THE POLISH SOCIETY OF BIOMECHANICS

BIOMECHANICS 2020

ABSTRACTS BOOK

EDITORS

Anna Hadamus, Szczepan Piszczatowski, Małgorzata Syczewska, Sebastian Wójtowicz, Dariusz Białoszewski

SEPTEMBER 9-10, 2021

ISBN: 978-83-7637-561-8

Editorial office

Medical University of Warsaw,

Department of Rehabilitation, Faculty of Medical Sciences

Księcia Trojdena 2c, 02-109 Warszawa

Technical editor

Sebastian Wójtowicz

Proofreading

Anna Daniluk

Cover design

Dorota Saganowska

ORGANIZERS

The Polish Society of Biomechanics

♦

Department of Rehabilitation, Faculty of Medical Sciences,
Medical University of Warsaw

HONORARY PATRONAGE

Rector of the Medical University of Warsaw,
prof. Zbigniew Gaciong, MD, PhD

♦

Presidium of the Polish Council of Physiotherapists

PATRONAGE

European Society of Biomechanics

♦

European Society for Movement Analysis in Adults and Children

♦

The Committee of Mechanics of the Polish Academy of Sciences

♦

The Committee of Rehabilitation, Physical Education and Social Integration
of the Polish Academy of Sciences

ACKNOWLEDGMENT

Ministry
of Education
and Science

The International Conference of the Polish Society of Biomechanics "Biomechanics 2020" - a task funded under contract 756/P-DUN/2019 by the Ministry of Education and Science allocated for science dissemination activities.

Krajowa Izba
Fizjoterapeutów

The International Conference of the Polish Society of Biomechanics "Biomechanics 2020" was held over the patronage and financial support by The Polish Chamber of Physiotherapists.

ORGANISING COMMITTEE

General Conference Chairperson

Dariusz Białoszewski

Conference Chairperson

Anna Hadamus

Deputy Conference Chairperson

Anna Daniluk

Members

Michalina Błażkiewicz

Aneta Bugalska

Marta Grabowicz

Anna Obszyńska-Litwiniec

Anna Ostaszewska

Marek Pawlikowski

Dorota Saganowska

Małgorzata Syczewska

Piotr Tabor

Karolina Wiaderna

Sebastian Wójtowicz

Zbigniew Wroński

Anna Żelazowska

Students

Kamila Borowska

Anita Gryko

Marta Kijo

Anna Kozicka

Oskar Kuźmicki

Izabela Warzonkiewicz

SCIENTIFIC COMMITTEE

Chairperson of the Scientific Committee

Szczepan Piszczatowski

Co-Chairperson of the Scientific Committee

Małgorzata Syczewska

Honorary Chairpersons of the Scientific Committee

Romuald Będziński

Andrzej Wit

Members

María Ángeles Pérez Ansón, Spain

Michael A. Adams, United Kingdom

Jan Awrejcewicz, Poland

Dariusz Białoszewski, Poland

Michalina Błażkiewicz, Poland

Krzysztof Buśko, Poland

Wiesław Chwała, Poland

Luca Cristofolini, Italy

Adam Czaplicki, Poland

Dariusz Czaprowski, Poland

Thomas Dreher, Switzerland

Lechosław Dworak, Poland

Stephen Ferguson, Switzerland

Jarosław Filipiak, Poland

Jan Gajewski, Poland

Wojciech Glinkowski, Poland

Marek Gzik, Poland

Jaap Harlaar, Netherlands

Danuta Jasińska-Choromańska, Poland

Antoni John, Poland

Ilse Jonkers, Belgium

Marek Jóźwiak, Poland

Grzegorz Juras, Poland

Krzysztof Kędzior, Poland

Natalia Kizilova, Poland

Michał Kuczyński, Poland

Krzysztof Kwiatkowski, Poland

Robert Latosiewicz, Poland

Tomasz Lekszycki, Poland

Tomasz Łodygowski, Poland

Andrzej Maciejczak, Poland

Ewa Majchrzak, Poland

Jerzy Małachowski, Poland

Ryszard Maroński, Poland

Andrzej Mastalerz, Poland

Daniel Matej, Czech Republic

Robert Michnik, Poland

Grzegorz Milewski, Poland

Karol Miller, Australia

David Mitton, France

Bertram Müller, Spain

Zbigniew Nawrat, Poland

Małgorzata Ogurkowska, Poland

Marek Pawlikowski, Poland

Celina Pezowicz, Poland

Stanisław Pomianowski, Poland

Neil Postans, United Kingdom

John Rasmussen, Denmark

Gwendolen Reilly, United Kingdom

Danuta Roman-Liu, Poland

Alicja Rutkowska-Kucharska, Poland

Eugeniusz Sajewicz, Poland

Konstanty Skalski, Poland

Małgorzata Sobera, Poland

Artur Stolarczyk, Poland

Martin Svehlik, Austria

Zdenek Svoboda, Czech Republic

Marek Synder, Poland

Czesław Szymczak, Poland

Wojciech Święszkowski, Poland

Czesław Urbanik, Poland

Wojciech Wolański, Poland

Sebastian Wolf, Germany

Michał Wychowański, Poland

SPONSORS

Qualisys AB

Kvarnbergsgatan 2

411 05 Göteborg

Sweden

Qualisys is a leading provider of motion capture technology and has a long history of supplying research, engineering, entertainment, and sports facilities with high-end camera systems and expertise in capturing and analyzing movements. Qualisys offers a wide range of products and services and has offices in Gothenburg, Chicago, and Shanghai. Qualisys is certified according to ISO 9001:2015, our clinical products are compliant with Medical Device Directive 93/42/EEC and have FDA clearance (K171547).

Tekscan, Inc.

307 West First Street

South Boston, MA

02127-1309 USA

Tekscan, Inc. is the leading manufacturer of ultra-thin, tactile pressure and force sensors and measurement systems in the world. Tekscan's pressure measurement technology is a fundamental tool in key applications in the medical, dental, academia and industrial fields. . Our sensors and systems are used across a wide range of applications; as stand-alone solutions or as embedded technologies, to create better and differentiated products. Our passion for innovation, broad expertise, and commitment to quality help turn your vision into reality.

Over the last several decades, Biomechanical Researchers around the world have incorporated pressure mapping technology as an important research tool in their repertoire. These application-specific systems incorporate an ultra-thin, minimally-invasive pressure sensor to measure relative pressure and force distribution in real time, at high resolutions, and at different scanning speeds. By analyzing movements, forces, and plantar pressure exerted by lower extremities, you are presented with objective data that visual assessments cannot provide.

Preface

The field of biomechanics has been developing rapidly in recent years as advances in medical sciences are contributing to the development of related sciences, a necessary driver of new discoveries. Biomechanics is one of them, providing advanced knowledge about mechanical properties of tissues, fluids, organs and the body at large. Biomechanics also influences sports, both professional and recreational as well as disabled sport, providing information about the effectiveness of human movement. Accordingly, it is crucial for training and sports medicine.

This book contains 72 abstracts submitted for the International Conference of the Polish Society of Biomechanics BIOMECHANICS 2020 and accepted by reviewers from the Conference's Scientific Committee as well as 10 abstracts of the invited lectures.

The first meeting under the name "Biomechanics" was organized in 1959 in Poznan by prof. Aleksander Kabsch as the Ist Symposium of Biomechanics. The formula of the meetings has changed over time, in line with the development of the discipline in Poland, and also according to the needs of researchers, students, and scientists. Since 2001 the International Conference of the Society has been organized biannually. The last conference before this one was BIOMECHANICS 2018 in Zielona Góra. Biomechanics 2020 is taking place in 2021 (and not in 2020 as the number indicates), as the outbreak of the global pandemic of SARS-COV-2 in December 2019 made it impossible to hold the conference as scheduled in September 2020. Therefore, Biomechanics 2020 had to be postponed. At that time, we were hoping that the epidemiological situation would improve and we would be able to meet face-to-face in September 2021. Alas, this is not the case. The pandemic situation is still difficult, and in early spring this year both the Board of Polish Society of Biomechanics and the Organizing Committee decided to go on-line.

This is, of course, not an ideal solution, but it is the best we can offer. Long breaks in meetings and conferences are not good for the scientific community, as the interchange of ideas, discussions, and critical comments pushes research work forward. That was the reason behind the decision to organize the meeting this year rather than postponing it further, and take advantage of this opportunity, even if it is taking place in the virtual world.

Restrictions and lockdowns connected with SARS-COV-2 continue to affect not only everyday life all over the world, but also research. Experimental studies have had to be stopped in numerous institutions, as laboratories had to close and it was not possible to enrol subjects and patients while on-line classes at many universities took more effort on the part of the teachers/researchers than on-site learning, leaving less time for science. In some places, the shortage of financial resources due to the difficult situation connected with the pandemic is a serious problem. Despite all these obstacles, the Organizing Committee of BIOMECHANICS 2020 received many interesting abstracts from various fields of biomechanics, such as sport biomechanics, clinical movement analysis, biomaterials, bioengineering, and many others. After a peer-review process 72 of them were accepted for presentation in oral or poster sessions. This book offers them all, and we hope it can be of interest not only to scientists, but also students, for whom it may be an inspiration for their future research. Readers are encouraged to contact the corresponding authors and continue discussions regarding their research.

We would like to thank all those whose hard work made this abstract book and the BIOMECHANICS 2020 conference possible: organizers, reviewers, sponsors, and, above all, all the authors who have contributed to this book and to our conference.

Editors:
Anna Hadamus, Szczepan Piszczatowski,
Małgorzata Syczewska, Sebastian Wójtowicz,
Dariusz Białoszewski

List of Contents

INVITED LECTURES

In silico experiments on bone adaptation by remodeling

T. ADACHI[1]

Abstract

Bone structure and function dynamically changes by remodeling under changing mechanical environment [1]. From biomechanical viewpoints, in vivo and in vitro studies have been clarifying the underlying molecular and cellular mechanisms. However, due to the complexity of intercellular signaling and the hierarchy in structure-function relationships from cellular to tissue level, the predictions of physiological and pathological bone states are still difficult. We have been developing an in-silico experimental platform [2] to explore bone remodeling by which complex molecular and cellular interactions are linked to macroscopic bone remodeling. The in-silico platform will reproduce bone adaptation to changing mechanical loadings, and metabolic bone diseases such as osteoporosis. Additionally, the platform enables us to conduct in-silico experiments to give perturbation of a specific signaling molecule to observe dynamic changes of bone morphology and mechanical function as well as bone metabolic dynamics. This novel platform provides a quantitative tool to predict the therapeutic effects of drugs against metabolic bone diseases and significantly accelerate basic researches in bone adaptation by remodeling.

References

[1] ADACHI T., TSUBOTA K.-I., TOMITA Y., SCOTT J.H., *Trabecular surface remodeling simulation for cancellous bone using microstructural voxel finite element models*. Journal of Biomechanical Engineering, 2001, 123(5), pp. 403-409.

[2] KAMEO Y., MIYA Y., HAYASHI M., NAKASHIMA T., ADACHI T., I*n silico experiments of bone remodeling explore metabolic diseases and their drug treatment.* Science Advances, 2020, 6(10), #eaax0938..

[1]Taiji Adachi, Biomechanics Laboratory, Institute for Frontier Life and Medical, Sciences Kyoto University, Japan, e-mail: adachi@infront.kyoto-u.ac.jp

Corticospinal adaptation to strength training

J. AVELA[1]

Key words: *Neural adaptation, corticospinal excitability, transcranial magnetic stimulation*

1. Introduction

There is evidence that increase in strength gains due to strength training can be achieved without a significant change in muscle characteristics, which leads to the idea of a contribution from neural factors [1]. To understand the possible mechanisms involved, it is important to look at the features on a more detailed level. The majority of the evidence about neural adaptations in response to strength training is indirect and, therefore can take place at different parts of the corticospinal tract. The corticospinal tract comprises of supraspinal level (corticospinal neurons, subcortical neurons, as well as inhibitory and excitatory intercortical neurons) and the spinal level (motor neurons and inhibitory and excitatory neurons).

It has been shown that transcranial magnetic stimulation -induced (TMS) motor evoked potentials (MEP), which manifests as changes in corticospinal excitability, increases during different types of contractions (submaximal, maximal, repetitive or sustained). Several studies have reported increases in the MEP size following exercise-induced muscle fatigue [E.G. 2], but not all studies have found convergent results. McNeil et al. [3] demonstrated unaffected MEP size after sustained submaximal muscle contractions. On the other hand, a decrease in the MEP size have been shown after fatiguing and sustained submaximal (25-50% of maximal voluntary contractions; MVC) voluntary contractions. However, no changes were observed at higher contractions levels (75–100 % of MVC) [4]. Some studies have also indicated an increment in MEP size at the beginning of a fatiguing task, which then levels off or decreases after a certain point [5]. In addition, cortical silent period, which is an indication of spinal and intracortical inhibition, has been shown to increase in duration during maximal and submaximal fatiguing muscle contractions [6].

In interventional studies of strength training, increases, decreases or no changes in MEP size have been observed following a training period. Reasons for these inconsistent findings might be variations in testing and training protocols, and in the muscles studied. However, there are only few studies in which TMS has been used to study acute neuromuscular fatigue responses during resistance exercise.

Acute neuromuscular fatigue responses after a single hypertrophic type of resistance exercise have been demonstrated previously with methodology that is more conventional. For example, Häkkinen [7] showed decreased electromyographic (EMG) activity and large reductions in maximal force after hypertrophic loading. Furthermore, Walker et al. [8] showed that hypertrophic resistance loading produces neuromuscular fatigue dominated by peripheral factors (interpolated twitch technique), whereas fatigue induced by maximal loading seems to be caused by a reduction in neural drive (EMG) to the muscle. In light of this, previous studies have not provided in more detail the potential sites within the central nervous system that modulate these acute neural responses.

2. Two study examples of acute corticospinal adaptation to strength train

In a study by Ruotsalainen et al. [9] eleven volunteers participated in the upper arm hypertrophic resistance exercise (HRE) including one repetition maximum (1 RM) control contractions and three sets of 13 RM (SET1–3). TMS was applied during MVC contraction at the end of each set and during control contractions. Interpolated twitch technique was utilized in order to evaluate peripheral changes. In this study MVC decreased after each set. MEPs increased first and then decreased slightly (138.7 %, 130.4 % and 113.1 % after SET1, SET2 and SET3, respectively,

[1]Jaane Avela, Neuromuscular Research Center, University Of Jyväskylä, Finland, e-mail: janne.avela@jyu.fi

when compared to pre-exercise value). A significant reduction in MEP area between SET1 and SET3 was observed while silent period duration increased (~151–165 ms) simultaneously between these sets. Twitch force during MVC increased significantly following each set when compared to pre-exercise value. Simultaneously, a significant reduction was observed in resting twitch force over the sets. This study clearly supports the existence of both central and peripheral fatigue during HRE of elbow flexors. However, changes in the MEP area and silent period suggest that during HRE of the elbow flexors, the corticospinal excitability increases first, until at some point, supraspinal fatigue takes over.

In a recent study of Mason et al. [10], corticospinal and motor cortical excitability and inhibition were measured from agonist and antagonist muscles before and after a single session of heavy-resistance wrist flexor training in 18 individuals. Training consisted of four sets of 6–8 repetitions at 80% of 1 RM. Recruitment curves for corticospinal excitability and inhibition of the right wrist flexor and wrist extensor muscles were constructed and assessed by examining the area under the recruitment curve. Intracortical measures were obtained using paired-pulse TMS procedures. After a single training session, corticospinal excitability increased in both the agonist and antagonist muscles. This was parallel to decreases in corticospinal inhibition in both muscles. However, intracortical inhibition was reduced and intracortical facilitation was increased for the agonist muscle only. These results indicate that the corticospinal responses to a single session of strength training are similar between agonist and antagonist muscles; however, the intrinsic cortico-cortical circuitry of the antagonist seems to remain unchanged. These corticospinal excitability changes are very likely due to fatigue of the agonist muscle, which leads to increased co-activation of the antagonist muscle.

3. Conclusions

Acute and long-term responses to resistance exercise can demonstrate which part of the corticospinal system is stressed during the exercise. This information may assist coaches to develop targeted resistance training programs. However, a huge lack of information is still missing about e.g. muscle- training-, age- and even gender specificity on the effect of these responses.

References

[1] AAGAARD P., SIMONSEN E.B., ANDERSEN J. L., MAGNUSSON P., & DYHRE-POULSEN P., *Neural adaptation to resistance training: changes in evoked V-wave and H-reflex responses.* Journal of Applied Physiology, 2002, 92(6), 2309-2318.

[2] HOFFMAN B.W., OVA T, CARROLL T.J, CRESSWELL A.G., *Increases in corticospinal responsiveness during a sustained submaximal plantar flexion.* 2009, J Appl Physiol 107:112–120.

[3] McNEIL C.J., GIESEBRECHT S., GANDEVIA S.C., TAYLOR J.L., *Behaviour of the motoneurone pool in a fatiguing submaximal contraction*. 2011, J Physiol 589(14):3533–3544.

[4] TODD G., TAYLOR J.L., GANDEVIA S.C. *Measurement of voluntary activation of fresh and fatigued human muscles using transcranial magnetic stimulation*. 2003, J Physiol 551(2):661–671.

[5] HUNTER S.K., BUTLER J.E., TODD G., GANDEVIA S.C., TAYLOR J.L. *Supraspinal fatigue does not explain the sex difference in muscle fatigue of maximal contractions*. 2006, J Appl Physiol 101:1036–1044.

[6] SOGAARD K., GANDEVIA S.C., TODD G., PETERSEN N.T., TAYLOR J.L. *The effect of sustained low-intensity contractions on supraspinal fatigue in human elbow flexor muscles*. 2006, J Physiol 573(2):511–523.

[7] HÄKKINEN K. *Neuromuscular fatigue in males and females during strenuous heavy resistance loading*. 1994, Electromyogr Clin Neurophysiol 34(4):205–214.

[8] WALKSER S., DAVIS L., AVELA J., HÄKKINEN K. *Neuromuscular fatigue during dynamic maximal strength and hypertrophic resistance loadings.* 2012, J Electromyogr Kinesiol 22:356–362.

[9] RUOTSALAINEN I., AHTIAINEN J.P., KIDGELL D.J., AVELA J. *Changes in corticospinal excitability during an acute bout of resistance exercise in the elbow flexors.* 2014, European Journal of Applied Phsyiology 114, 7, 1545-1553.

[10] MASON J., HOWATSON G., FRAZER A.K., PEARCE A.J., JABERZADEH S., AVELA J., KIDGELL D.J. *Modulation of intracortical inhibition and excitation in agonist and antagonist muscles following acute strength training*. 2019, European Journal of Applied Physiology, 119: 2185-2199.

Nano-Bio Science: a precursor to Nanomedicine

F. CARUSO[1]

Abstract

A major focus in nanomedicine is the design and engineering of particles for targeted therapy and diagnostics. Self-assembly technologies have been used extensively to engineer a diverse array of particles for such applications [1–4]. This presentation will focus on our research on the development of particles and their interactions with biological barriers. Aspects of the physicochemical properties of the particles as well as post-assembly biological modification through ligand targeting and the formation of a protein corona will be covered. Particle variants based on metal–ligand complexation, assembled through the deposition of metal ions and polyphenols, will also be presented. Our studies are aimed at obtaining detailed knowledge of complex bio–nano interactions, which is expected to aid in the rational design of nanoengineered materials for applications including HIV, hearing loss and cancer targeting.

References

[1] RICHARDSON, J.J., BJÖRNMALM, M., CARUSO, F., *Technology-driven layer-by-layer assembly of nanofilms*, Science 2015, 348, aaa2491.

[2] EJIMA, H., RICHARDSON, J.J., LIANG, K., BEST, J.P., VAN KOEVERDEN, M.P., SUCH, G.K., CUI, J., CARUSO, F., *One-step assembly of coordination complexes for versatile film and particle engineering*, Science 2013, 341, 154.

[3] GUO, J., TARDY, B.L., CHRISTOFFERSON, A.J., DAI, Y., RICHARDSON, J.J., ZHU, W., HU, M., JU, Y., CUI, J., DAGASTINE, R.R., YAROVSKY, I., CARUSO, F., *Modular assembly of superstructures from polyphenol-functionalized building blocks*, Nat. Nanotechnol. 2016, 11, 1105.

[4] BJÖRNMALM, M., THURECHT, K.J., MICHAEL, M., SCOTT, A.M., CARUSO, F., *Bridging bio-nano science and cancer nanomedicine*, ACS Nano 2017, 11, 9594.

[1]Frank Caruso, ARC Centre of Excellence in Convergent Bio-Nano Science and Technology, and the Department of Chemical Engineering, The University of Melbourne, Parkville 3010, Australia,
e-mail: fcaruso@unimelb.edu.au

Do we need motion analysis in orthopaedic surgery?

T. DREHER[1]

Abstract

Motion analysis has been established in clinical use to better understand the biomechanics of walking and to optimize treatment in specific fields. However, it is a relevant question how motion analysis really affects clinical decision making and whether it is effective to improve patient care. The lecture aims to give an answer to this question and to highlight the needs for clinicians to benefit from motion analysis for decision making.

[1] Thomas Dreher, Department of Pediatric Orthopaedics and Traumatology, Children's University Hospital, Balgrist Orthopaedic University Hospital, Zurich, Switzerland, e-mail: thomas.dreher@med.uni-heidelberg.de

Asymmetric running with prosthetic limb

H. HOBARA[1]

Key words: *transfemoral amputation, running-specific prosthesis, asymmetry, amputee locomotion*

1. Introduction

The physical and psychosocial benefits of sports and recreational activities have been widely recognized for individuals with lower limb amputation, but their participation in these activities is still limited. Running has become a common activity for individuals with lower limb amputation participating in sports and recreation. This is partly because that recent technical developments of running-specific prostheses (RSPs) with elastic energy storage/returning functions facilitated the regain of the running activity in individuals with unilateral transfemoral amputation (uTFAs). However, very few studies have characterized the biomechanics of running in uTFAs wearing RSP. Thus, quantifying the biomechanics of running in uTFAs is a critical step that will lead to objective, targeted improvements in rehabilitation and prosthetic designs [1]. In the presentation, biomechanics of uTFAs wearing RSPs during running will be delivered.

2. Asymmetric running mechanics

2.1. Ground reaction forces

Running velocity is constrained by forces that limbs apply to the ground, ie, ground reaction force (GRF), and the time needed for force application, ie, contact time. Thus, GRFs are one of the fundamental biomechanical variables to describe the running mechanics. Previous studies demonstrated that peak vertical GRF in prosthetic limb was significantly smaller than that of intact limb across a range of running speeds [2] and maximal sprinting [3-4]. However, past findings showed that contact time in prosthetic limb was significantly longer than that of intact limb during submaximal running and maximal sprinting [3-4]. Consequently, there are no significant difference in vGRF impulse between the prosthetic and intact limbs in a wide range of running speeds [2-3]. These results suggest that, compared with the intact limb, the prosthetic limb may require longer contact time to exert an equivalent vGRF impulse in order to compensate for a functional limitation in the ipsilateral limb. In other words, uTFAs may be exposed to a greater risk of running-related injuries in their intact limbs compared to the prosthetic limbs, due to the elevated GRF loading [5].

2.2. Joint kinetics

Although joint moment is a commonly-used biomechanical parameter to enhance our understanding of muscular effort and joint control during running, little is known about the joint moment in uTFAs. Using a total of 59 retro-reflective markers, Namiki et al. [6] calculated the joint moments through an inverse dynamics method, where the moments of inertia of the prosthetic shank and foot segments were estimated by assuming that those parts had homogeneous solid cylinder and thin plate forms, respectively. The authors found that all peak flexion and extension moments in the prosthetic limb were lower than those of the intact limb. However, they also found that peak plantarflexion moment of prosthetic limb was significantly greater than that of intact limb. These results suggest that asymmetric joint moment adaptations occur for uTFAs to compensate for replacement of the biological leg with a passive prosthetic knee joint and RSP.

---

[1]Hiroaki Hobara, National Institute of Advanced Industrial Science and Technology (AIST), AI Research Center, Waterfront 3F, 2-3-26, Aomi, Kotoku, Tokyo, Japan, e-mail: hobara-hiroaki@aist.go.jp

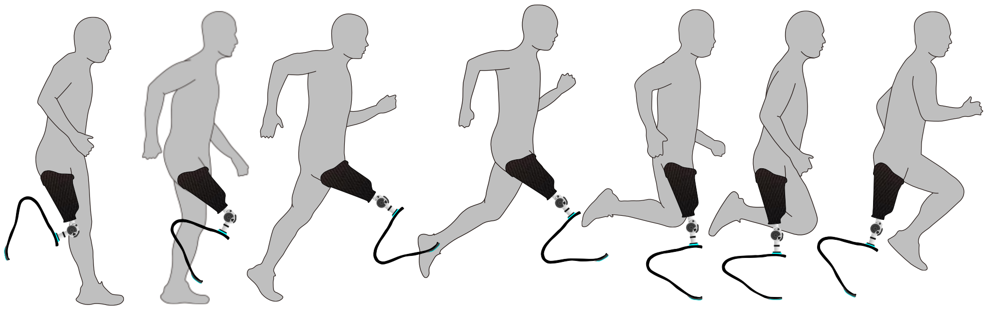

Fig. 1. A schematic representation of running in uTFAs wearing RSP.

2.3. Dynamic balance control

Maintaining dynamic balance is essential to achieve continuous running without a fall. However, little is known about how the whole-body sagittal plane angular momentum ($\vec{H}$) is regulated in uTFAs and the control of the prosthetic and intact limbs. Thus, we compared the positive and negative peaks of whole-body sagittal plane $\vec{H}$ between the prosthetic limb's and intact limb's steps. We found that there was no significant difference in the positive peak of $\vec{H}$ between limbs, while the negative peak of intact limb's step was significantly smaller than that of prosthetic limb's step [7]. These results suggest that uTFAs wearing RSP would adopt a limb-specific strategy to maintain dynamic balance during straight running.

3. Summary

In summary, our results showed that ground reaction forces, joint moments and whole-body sagittal plane angular momentum in uTFAs during sprinting were asymmetric between intact and prosthetic limbs. Therefore, these results suggest that a limb-specific rehabilitation and training strategies should be developed for uTFAs wearing running-specific prostheses.

Acknowledgments: This work was partly supported by JSPS KAKENHI, Grant Number 26702027.

References

[1] HOBARA H. et al., *Leg stiffness in unilateral transfemoral amputees across a range of running speeds.* Journal of Biomechanics, 2019, 84, 67-72.

[2] SAKATA H. et al., *A Limb-specific Strategy across a Range of Running Speeds in Transfemoral Amputees.* Medicine & Science in Sports & Exercise, 2020, 52 (4), 892-899.

[3] MAKIMOTO A. et al., *Ground Reaction Forces During Sprinting in Unilateral amputees.* Journal of Applied Biomechanics, 2017, 33 (6), 406-409.

[4] SANO Y. et al., *Leg stiffness during sprinting in transfemoral amputees with running-specific prosthesis.* Gait and Posture, 2017, 56, 65-67.

[5] HOBARA H. et al., *L Loading rates in unilateral transfemoral amputees with running-specific prostheses across a range of speeds.* Clinical Biomechanics, 2020, 75, 104999.

[6] NAMIKI Y. et al., *Joint moments during sprinting in unilateral transfemoral amputees wearing running-specific prostheses.* Biology Open, 2019, 8, bio039206.

[7] HISANO G. et al., *Whole-body sagittal plane angular momentum during running in unilateral transfemoral amputees.* International Society of Biomechanics (ISB) congress, 2021, PA084.

An integrated, multi-scale approach to understand the role of mechanical loading in cartilage homeostasis and disease: Bridging from joint to chondrocyte

I. JONKERS[1]

Abstract

To design and adapt therapeutic approaches that successfully regenerate native joint cartilage, it is indispensable to understand how articular cartilage is loaded during locomotion. Furthermore, the local cartilage loading needs to be related to the molecular response of the chondrocytes. In my presentation, I will identify biomarkers of early OA during locomotion (using multi-scale modeling), relate the mechanical loading to experimentally measured cartilage deformations (using high-field MRI) and identify the effect of the local mechanical cues to constituent expression (using bioreactor experiments).

Through careful documentation of the mechanobiological response, we will be able to design future rehabilitation approaches and preventive exercise programs that optimize cartilage health.

[1]Ilse Jonkers, The Human Movement Biomechanics Research Group, KU Leuven,
e-mail: ilse.jonkers@kuleuven.be

Challenges of bone tissue engineering: from materials to multiscale modeling

G. NASELLO[1], S. RUSSO[2], J. M. GARCÍA-AZNAR[3], M. A. PÉREZ[4]

Key words: *bone tissue engineering, microfluidics, titanium, biodegradable materials, multiscale modeling*

1. Background and motivation

The worldwide incidence of bone disorders and conditions has trended steeply upward and is expected to double in the next few years, especially in populations where aging is coupled with increased obesity and poor physical activity [1]. Bone Tissue Engineering (BTE) has been viewed as a potential alternative to the conventional use of bone grafts, due to their limitless supply and no disease transmission. However, BTE practices have not been fully integrated to clinical practice due to several limitations and challenges. BTE aims to induce new functional bone regeneration via the synergistic combination of biomaterials, cells and factor therapy. Personalization is an issue with increasing importance in this field that we need to incorporate. Novel technologies based on an organ-on-a-chip based may help to this personalization goal [2].

In BTE, porous materials are used as scaffolding that provide mechanical support and promote onsite tissue growth. Scaffolds require a stiffness similar to bone and a porous geometry that facilitates high cell seeding efficiency, osteoblast adhesion, proliferation and growth [3]. Emerging 3D printing technologies are enabling the design and fabrication of complex geometries using different biomaterials (standard and degradable). In fact, recent advances in scaffold design have demonstrated promising direction for integrating design, modelling, and experiments to develop high-performance scaffolds for clinical applications. Advanced modelling approaches have included computational fluid dynamic simulation for predicting biological tissue growth on complex geometries [4] or multiscale approaches have been used to predict bone regeneration [5]. *In silico* modelling offers an efficient framework to predict and understand the behaviour of biomaterial [6].

Therefore, in this work we aim to present a multidisciplinary *in vivo-in vitro-in silico* platform for bone regeneration therapies customized in patients to allow a faster and better repair of bone tissue.

2. Methods

Different technologies should be combined to achieve previous goal: organ-on-a-chip technology to study patient-specific variability, mechano-driven model of bone ingrowth in a titanium porous scaffold and a physiochemical model of hydrolysis as a predictive tool of degradation for degradable scaffold. A brief overview of each one is here presented.

2.1. Organ-on-a-chip: Bone-on-a-chip

Bone-on-a-chip platforms facilitate the use of cells derived from patients, thus creating models of human physiology with higher clinical impact. Here, we created a 3D cell culture of human osteoblasts for assessment of bone tissue formation *in vitro* in a microfluidic device [2]. This methodology helps to understand how osteoblasts interact with physiological hydrogel (as collagen

---

[1] Gabriele Nasello, University of Zaragoza, Instituto de Investigación en Ingeniería de Aragón-I3A, Spain, e-mail: gnasello@unizar.es
[2] Simone Russo, University of Zaragoza, Instituto de Investigación en Ingeniería de Aragón-I3A, Spain, e-mail: simonerusso@unizar.es
[3] José Manuel García Aznar, University of Zaragoza, Instituto de Investigación en Ingeniería de Aragón-I3A, Aragón Institute of Health Science (IACS), Spain, e-mail: jmgaraz@unizar.es
[4] María Angeles Pérez, University of Zaragoza, Instituto de Investigación en Ingeniería de Aragón-I3A, Aragón Institute of Health Science (IACS), Spain, e-mail: angeles@unizar.es

and fibril) recreating a physiological environment for the cells that promote the formation of novel bone tissue.

2.2. Mechano-driven model of bone ingrowth

A numerical model that elucidates the role of mechanics during bone ingrowth may provide important spatio-temporal information on final shape and speed of pore-filling of scaffolds by cells and the final bone response. A mechano-driven model was here proposed. The model was validated with *in vivo* data on goats, where non-uniform bone ingrowth in 3D printed titanium scaffolds was observed. In fact, bone ingrowth distribution changed depending on insertion point.

2.3. A physiochemical model for scaffold degradation

A key feature of degradable biomaterials used as scaffolds is that they provide temporary mechanical integrity at the defect site until the bone tissue is repaired or regenerated, and normal biomechanical function is restored. Numerical simulation of this degradation process could be certainly important to successful tissue regeneration. A hydrolytic degradation model was proposed. It was experimentally validated using a hybrid PCL/PLGA scaffold. *In vitro* degradation under static, fluid flow and compression load were quantified.

3. Conclusion and Discussion

Summarizing, the field of tissue engineering and in particular, BTE, is rapidly growing. BTE-based products are beginning to be used in clinical practice. Based on the current success, even more BTE technologies are expected to become available to patients in the next few years. Current efforts should be focused in multidisciplinary approaches as the one here presented including patient-specific characteristics and *in silico* modelling. Integrated design approaches that encourage iteration and consideration of diverse processes including design configuration, material selection, and simulation models provide a basis for improving design performance. Current challenges emphasize the direction where new research may lead to significant improvements in personalized medicine and emerging areas in healthcare.

References

[1] BAROLI B., *From natural bone grafts to tissue engineering therapeutics: brainstorming on pharmaceutical formulative requirements and challenges.* Journal of Pharmaceutical Sciences, 2009, 98(4): 137-1375.

[2] DEL AMO C., OLIVARES V., CÓNDOR M., BLANCO A., SANTOLARIA J., ASÍN J., BORAU C., CARCÍA-AZNAR J.M., *Matrix architecture plays a pivotal role in 3D osteoblast migration: The effect of interstitial fluid flow.* Journal of Mechanical Behavior of Biomedical Materials, 2018, 83, 52-62.

[3] EGAN P. F., BAUER I., SHEA K., FERGUSON S. J., *Matrix Mechanics of Threee-Dimensional printed lattices ofr biomedical devices.* Journal of Mechanical Design, 2019, 141, 031703.

[4] GUYOT Y., PAPANTONIOU I., LUYTEN F., GERIS L., *Matrix Coupling curvature-dependent and shear stress-stimulated neotissue growth in dynamic bioreactor cultures: A 3D computational model of a complete scaffold.* Biomechanics and Modeling in Mechanobiology, 2016, 15, 169-180.

[5] SANZ-HERRERA J.A., J. M. GARCÍA-AZNAR, M. DOBLARÉ, *On scaffold designing for bone regeneration: A computational multiscale approach.* Acta Biomaterialia, 2009, 5, 219-229.

[6] GERIS L., LAMBRECHTS T., CARLIER A., PAPANTONIOU I., *Fabric The future is digital: In silico tissue engineering,* Current Opinion in Biomedical Engineering. Tissue Engineering and Regenerative Medicine/Biomaterials, 2018, 6, 92-98.

Surface EMG decomposition: a new tool for evaluating muscle function

J. RICHARDS [1]

Key words: *EMG decomposition, muscle assessment, rehabilitation*

1. Introduction

Surface electromyography (sEMG) has been used over many years to give an indication of the level and timing of muscle activations during static and dynamic tasks, but these methods do not offer sufficient detail to determine individual motor unit (MU) behaviour. The development of decomposition EMG (dEMG) techniques have the potential to provide new insights in how the neuromuscular system controls movement. The recording of MU behaviour has previously been restricted to isometric tasks [1, 2, 3], but it is now possible to decompose cyclic dynamic contractions [4]. Despite this now being possible only a few studies have explored the differences in MU behaviour during concentric and eccentric muscle contractions during different movement tasks.

2. Materials and methods

This talk will consider the methods of data collection using dEMG and inertial measurement unit (IMU) sensors to quantify MU behavior during different functional and rehabilitation tasks. This will consider the effect of speed, load and phase of movement. Data on MU behavior will be presented on Vastus Medialis (VM) and Vastus Lateralis (VL) during squatting and leg raise tasks at different loads and speeds, and Peroneus Longus (PL) during standing balance tasks under different surface conditions in individuals with and without ankle instability.

3. Results

Significant differences in MU behaviour can be seen between different speeds of movement, loads and between the concentric and eccentric phases. Increases in speed are associated with greater MU firing rates, whereas increases in load are associated with greater MU firing rates and the recruitment of larger MUs, with the concentric phase showing higher firing rates than the eccentric. The standing balance stability tests revealed marked differences between those with and without ankle instability, with greater firing rates when these are performed on an unstable surface.

4. Discussion

The ability to conduct surface dEMG signal decomposition during dynamic muscle activations is a recent technological development. The changes in MU behaviour; including firing rates and MU amplitudes, could help our understanding on how load, speed and balance are controlled by the central nervous system, and this is certainly an area worthy of further study.

Acknowledgments: G. Chapman, E. Orantes-Gonzalez, J. Heredia-Jimenez, S.B. Lindley, J. Selfe.

References

[1] DE LUCA, C. J., CHANG, S. S., ROY, S. H., KLINE, J. C., HAMID NAWAB, S., *Decomposition of surface EMG signals from cyclic dynamic contractions. Journal of Neurophysiology.* J Journal of Neurophysiology, 2015 113(6), 1941–1951.

[2] DEL VECCHIO, A., NEGRO, F., HOLOBAR, A., CASOLO, A., FOLLAND, J. P., FELICI, F., & FARINA, D., *You are as fast as your motor neurons: speed of recruitment and maximal discharge of motor neurons determine the maximal rate of force development in humans.* Journal of Physiology, 2019, 597(9), JP277396.

[3] MILLER, J. D., STERCZALA, A. J., TREVINO, M. A., WRAY, M. E., DIMMICK, H. L., HERDA, T. J., *Motor unit action potential amplitudes and firing rates during repetitive muscle actions of the first dorsal interosseous in children and adults.* European Journal of Applied Physiology, 2019, 119(4), 1007–1018.

[1]Jim Richards¸ Allied Health Research unit, University of Central Lancashire, UK, e-mail: jrichards@uclan.ac.uk

The role of biomechanics in engineering functional tissue

W. ŚWIĘSZKOWSKI[1]

Key words: *tissue engineering, biofabrication, biomechanics*

1. Introduction

According to standard definition, biomechanics is the study of mechanical aspects of biological systems, at any level from cells to tissues, organs, and whole organisms. The biological systems sense, react, and adapt to their mechanical environment. Biomechanical factors influence the critical processes in living organisms, such as cell differentiation, tissue growth, maturation, or degeneration. Therefore, biomechanics is one of the key factors in successful tissue engineering and regenerative medicine for musculoskeletal, cardiovascular, skin, and other tissues [1].

This paper aims to review the role of scaffold design and biomechanics in engineering functional musculoskeletal tissues.

2. Methods and results

In the first approach, we designed and fabricated 3D multilayered composite (ML) scaffolds for tendon regeneration. They are formed from electrospun nanofibres coated by thin layers of cell-laden hydrogel (Fig.1) [2]. The composition of the hydrogel was tailored independently to ensure proper support for cellular growth and differentiation. The scaffolds were both biochemically and mechanically stimulated. The concentration of the chemical stimulus (BMP-12) was selected to facilitate the tenogenic differentiation of MSCs. The cultures were mechanically stimulated in a bioreactor showing the positive role of the tested dynamic culture condition on cell alignment and tenogenic differentiation. Our results also demonstrated that adding the selected amount of BMP-12 (10 ng/mL) induces tenogenic differentiation more effectively during dynamic stimulation than static conditions. The synergistic effect of mechanical and biochemical stimulation results in an enhancement of cell proliferation, alignment, and differentiation, illustrating the potential of the scaffold and the bioreactor system for tendon tissue engineering.

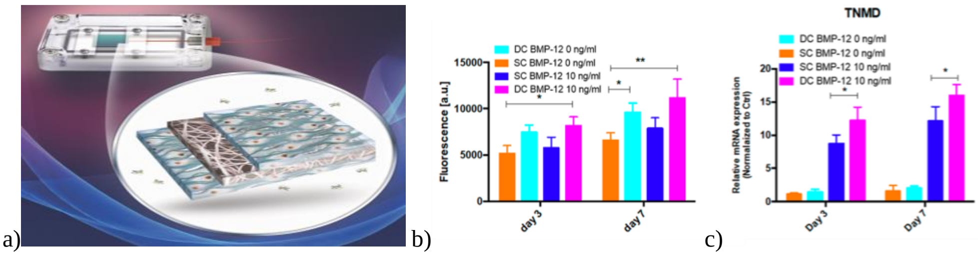

Fig. 1. Mechanical and biochemical stimulation effects on MSCs encapsulated into ML scaffolds (a). Proliferation rate of MSCs was registered to be significantly improved by the combination of the mechanical and biochemical stimuli at each time point (n = 3) (b). Data representing Rt-PCR of mRNA expression of tenomodulin (c). [2]

In the second approach, we designed and fabricated 3D oriented cell-laden hydrogel yarns via a novel system employing a wet spinning technique for tendon tissue engineering (Fig.2a) [3]. Highly aligned yarns recapitulate the structure and morphology of the tendon fascicles, mimicking the native tissue architecture. The scaffolds were statically stretched using a customized system and treated with BMP-12 (Fig.2b). The characteristics of cultured stimulated and non-stimulated scaffolds indicate the positive role of static stretching on cell adhesion, alignment, proliferation, and tenogenic

[1]Wojciech Święszkowski, Faculty of Materials Science and Engineering, Warsaw University of Technology, e-mail: wojciech.swieszkowski@pw.edu.pl

differentiation. Our results also demonstrate that the combination of mechanical and biochemical stimuli effectively improves tenogenic differentiation (Fig.2c).

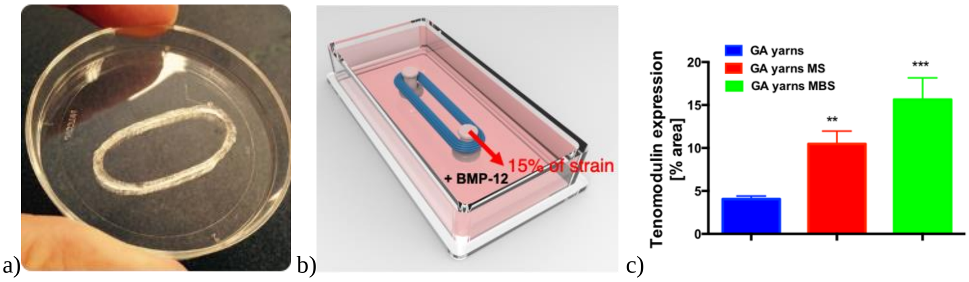

Fig. 2. Highly aligned, densely packed hydrogel fibrous scaffolds are fabricated with wet spinning biofabrication system (a). Cell-laden scaffolds undergo static mechanical and biochemical stimulations in a custom system (b). Combination of mechanical and biochemical stimuli (GA yarns MBS) induces a synergistic effect on key tenogenic gene expression, leading to a more effective tenogenic differentiation of hBM-MSCs compared to non-stimulated condition (GA yarns) and only mechanical stimulation (GA yarns MS). [3]

3. Conclusions

The presented results provide insight into the influence of scaffold designs and culture conditions for engineering biomimetic tendon tissues. The 3D construct compositions were optimized to achieve adequate mechanical and physical properties as well as cell viability and proliferation. Additionally, the combined effects of mechanical and biochemical stimulations result in preferential cell alignment, higher orientation, and an increase of tenogenic differentiation of MSCs compared to non-stimulated conditions. The obtained results suggest that the proposed 3D cell-laden systems can be used for the engineering of tendon tissue.

Further investigations are required to validate how the scaffolds facilitate tissue formation in vivo in animal models, which is essential for the potential clinical translation of the systems.

Acknowledgments: This study was supported by Pol-Nor/202 132/68/2013 (NewJoint), STRATEGMED1/233224/10/NCBR/2014 (START), STRATEGMED3/305813/2/NCBR/2017 (Bionic), STRATEGMED3/306888/3/NCBR/2017 (ITE), and the subvention grant 2021.

References

[1] BUTLER D.L., ET AL. *The impact of biomechanics in tissue engineering and regenerative medicine. Tissue Eng Part B Rev. 2009 Dec; 15(4): 477–484.*

[2] RINOLDI C., ET AL. *Mechanical and Biochemical Stimulation of 3D Multilayered Scaffolds for Tendon Tissue Engineering. ACS Biomater. Sci. Eng. 2019, 5, 2953−2964.*

[3] RINOLDI C., ET AL. *Tendon Tissue Engineering: Effects of Mechanical and Biochemical Stimulation on Stem Cell Alignment on Cell-Laden Hydrogel Yarns. Adv. Healthcare Mater. 2019, 8, 1801218*

How sports biomechanics can foster in-field performance assessment: technical issues and applications in swimming

G. VANNOZZI[1]

Abstract

Sports biomechanics can fruitfully support a successful coaching outcome by a timely feedback to the athlete to objectively target performance aspects and protect from injuries. The systematic monitoring and motor ability assessment, through the analysis of mechanical variables determining the sport-specific performance, can reinforce the link between research and coaching practice, especially in élite sports.

With reference to the ICF framework promoted by the World Health Organization, motor ability is typically assessed using both capacity and performance tests as carried out in laboratory settings and in-field, respectively. Laboratory tests normally use movement analysis equipment such as stereophotogrammetry and dynamometry. Conversely, what typically happens in in-field applications is the adoption of qualitative assessment in sport environments through direct observation, field test batteries, product measurements.

In the last 20 years, the advent of MEMS technology dramatically changed the state of the art and inertial sensor-based applications are rapidly spreading into both research and professional environments. However, robustness and reliability of sensor measurements are still a matter of debate due to a number of methodological issues that still represent an issue for the straightforward application of this technology in real sport settings.

In this talk, the state of the art about the use of magneto-inertial sensors into in-field sport settings for motor ability assessment will be provided. A specific emphasis will be placed on the need to take into account sensors limitations (static bias, drift, sensors-to-body movements), and on the opportunity to follow good practice rules for a better exploitation of their potential.

From a methodological standpoint, main activities are addressed to the estimation of spatio-temporal parameters, the definition of body segment orientation, and the estimation of kinetic and energy-like quantities. This quantitative approach will integrate with, or eventually substitute for, the evaluation tests currently adopted in in-field settings, joining objectivity with field applicability.

References to the most recent approaches in terms of sensor systems (e.g smart textiles) or advanced processing (e.g machine learning) will be also provided. A specific reference to swimming biomechanics applications will be presented as a paradigmatic case presenting several technical challenges and potential applications.

[1]Giuseppe Vannozzi¸Department of Motor, Human and Health Sciences, University of Rome “Foro Italico”, Rome, Italy, e-mail: giuseppe.vannozzi@uniroma4.it

ABSTRACTS

Kinematics of topspin backhand in female table tennis players – a comparative analysis

Z. BAŃKOSZ[1], S. WINIARSKI[2]

Keywords: *kinematics; table tennis, sports technique, statistical parametric mapping;*

1. The aim of the research

The research aimed to compare the kinematics between female table tennis players from two countries - Poland (POL) and China (CHIN) during the performance of a topspin backhand stroke (so-called quick topspin).

2. Material and Methods

The study involved eight female table tennis players at a high, comparable sports skill level, playing in Poland's highest league. Four of them were national team members of Poland (age: 20.5±1.8). Four others were players from China (age: 20.0±0.0). Kinematics was measured using Inertial Measurement Unit (IMU) system - MR3 myoMuscle Master Edition. The participants performed topspin backhand as a response to a topspin ball (played by table tennis robot), repeated 15 times (Fig. 1). As a calculating tool a Statistical Parametric Mapping (calculated using SPM1D in a Python package) method was used.

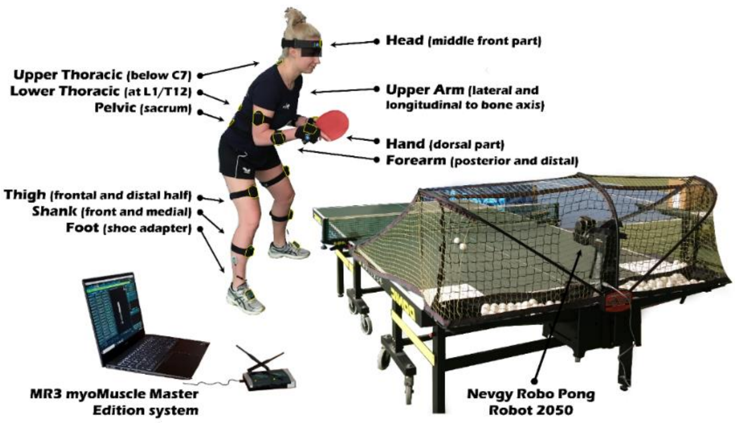

Fig. 1. Measurement site and scheme.

3. Results, Discussion and Conclusions

The differences found in the research (Fig. 2) are probably mainly due to differences in the training methodologies caused by different coaching systems. The observed differences include greater use of the so-called small steps in order to adapt and be ready during the back to ready position and backswing phases, which gives the CHIN players slightly better conditions for preparation for the next plays. The CHIN players' position is also more universal than the POL players and favours a quicker transition from the backhand to the forehand play. This difference is

[1]Department of Biomechanics, Faculty of Physical Education and Sports, University School of Physical Education in Wroclaw, Poland, e- mail: ziemowit.bankosz@awf.wroc.pl

[2]Department of Biomechanics, Faculty of Physical Education and Sports, University School of Physical Education in Wroclaw, Poland, e-mail: slawomir.winiarski@awf.wroc.pl

probably related to the difference in the dominant playing styles of the groups studied. Despite the differences in movement patterns in both groups, the exact value of the acceleration of playing hand was achieved. This may be a manifestation of the phenomenon of equifinality and compensation.

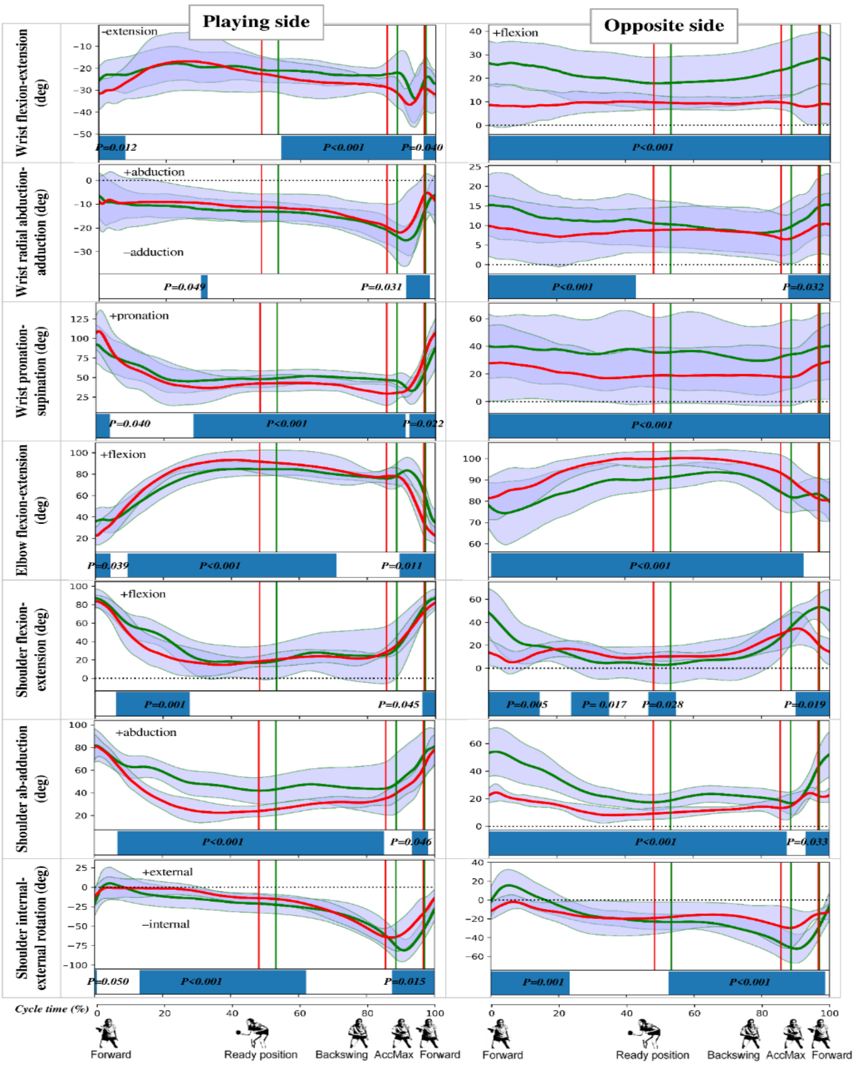

Fig. 2. Upper extremity kinematics

References

[1] BARTLETT R., WHEAT J., ROBINS M., *Is movement variability important for sports biomechanists?* Sports Biomechanics, 2007, 6, 224-243.

[2] STERGIOU N., DECKER L.M., *Human movement variability, nonlinear dynamics, and pathology: Is there a connection?* Hum Mov Sci, 2011, 30, 869-888.

[3] BAŃKOSZ Z., WINIARSKI S., *Statistical Parametric Mapping Reveals Subtle Gender Differences in Angular Movements in Table Tennis Topspin Backhand.* International Journal of Environmental Research and Public Health, 2020, 17, 6996.

[4] PATAKY T.C., ROBINSON M.A, VANRENTERGHEM J., *Vector field statistical analysis of kinematic and force trajectories.* J Biomech, 2013, 46, 2394–2401.

[5] SHEPPARD A., LI F.X. *Expertise and the control of interception in table tennis*. Eur J Sport Sci, 2007, 7, 213-222.

[6] BAŃKOSZ Z., WINIARSKI S., MALAGOLI LANZONI I., *Gender Differences in Kinematic Parameters of Topspin Forehand and Backhand in Table Tennis.* International Journal of Environmental Research and Public Health, 2020; 17(16): 5742.

[7] IINO Y., MORI T., KOJIMA T., *Contributions of upper limb rotations to racket velocity in table tennis backhands against topspin and backspin*. Journal of Sports Sciences, 26, 287-293.

[8] IINO Y., *Hip joint kinetics in the table tennis topspin forehand: relationship to racket velocity.* Journal of Sports Sciences, 2017, 36, 1-9.

[9] XIA R., DAI B., FU W., GU N., WU Y., *Kinematic comparisons of the shakehand and penhold grips in table tennis forehand and backhand strokes when returning topspin and backspin balls.* Journal of Sports Science and Medicine, 2020, 19, 637-644.

Comparison of optoelectronic and IMU-based systems used in the assessment of Nordic Walking gait

A. BARTOSZEK[1], A. STRUZIK[2], S. JAROSZCZUK[3], B. PIETRASZEWSKI[4], M. WOŹNIEWSKI[5]

Key words: *inertial measurement unit; motion analysis; validity; wearable sensors*

1. Introduction

Although the validity of joint kinematic variables recorded with inertial measurement unit-based (IMU) systems has been confirmed for optoelectronic systems, the measurement accuracy of each system must be evaluated and cannot be easily compared. Therefore, this study compared the lower limb joint angle values during the Nordic Walking gait recorded using IMU-based and optoelectronic motion analysis systems.

2. Material and methods

The study subject was a long-time Nordic Walking instructor characterized by the following basic features: 1.73 m of body height and 68.8 kg of body mass. The task in the experiment was to cover a distance of 12 metres (14 attempts with 5 gait cycles) at a velocity preferred for the Nordic Walking gait. The trials were simultaneously recorded by MyoMotion (IMU-based) and BTS (optoelectronic) motion analysis systems. The study was carried out in the Biomechanical Analysis Laboratory at the University School of Physical Education in Wrocław, Poland.

3. Results

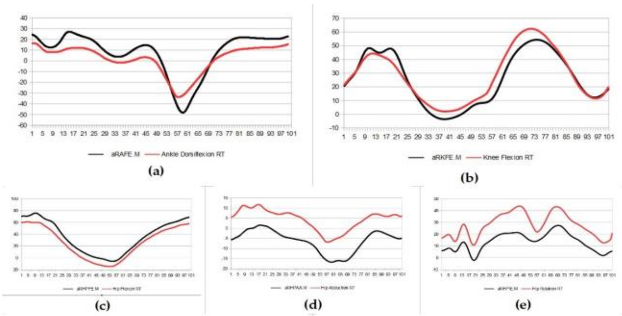

Fig. 1. Comparison of right lower limb joint angles throughout the movement cycles of Nordic Walking gait obtained from BTS Smart DX (black) and MyoMotion (red) systems for: ankle flexion-extension (a), knee flexion-extension (b), and hip flexion-extension (c), abduction-adduction (d) and rotation (e)

Table 1. Within-rater (between systems) comparison of kinematic parameters for right lower limb (mean values)

Segments	Systems	Variables

[1]Department of Biomechanics, University School of Physical Education, Wrocław, Poland,
e-mail: amadeusz.bartoszek@awf.wroc.pl
[2]Department of Biomechanics, University School of Physical Education, Wrocław, Poland,
e-mail: artur.struzik@awf.wroc.pl
[3]Department of Biomechanics, University School of Physical Education, Wrocław, Poland,
e-mail: sebastian.jaroszczuk@awf.wroc.pl
[4]Department of Biomechanics, University School of Physical Education, Wrocław, Poland,
e-mail: bogdan.pietraszewski@awf.wroc.pl
[5]Department of Rehabilitation in Internal Diseases, University School of Physical Education, Wrocław, Poland,
e-mail: marek.wozniewski@awf.wroc.pl

			MIN [°]	MAX [°]	ROM [°]	BIAS [°]	SSE	r	95% LoA	RCI
Ankle	FE	BTS	-48.3	26.7	75.1	-5.9	0.22	0.98	14.1	28.1
		MyoM	-33.8	16.2	50.0					
Knee	FE	BTS	-3.6	54.4	58.0	2.5	0.29	0.96	10.5	20.9
		MyoM	2.0	62.3	60.3					
Hip	FE	BTS	-6.2	75.5	81.6	-9.4	0.09	1.00	5.2	10.4
		MyoM	-14.8	60.5	75.3					
	AA	BTS	-16.9	1.4	18.3	10.6	0.31	0.96	3.2	6.3
		MyoM	-11.6	7.0	18.5					
	IE	BTS	-2.4	27.4	29.8	0.8	1.60	0.53	12.6	25.3
		MyoM	7.5	23.2	15.7					

BIAS – the mean of the difference between the systems angle values; a minus (-) with the bias result means that BTS shows a higher value than MyoMotion; SEE – standardized error of estimate; *r* – Pearson correlation coefficient; 95% LoA – the 95% limits of agreement; RCI – range of compliance interval

4. Discussion

This study aimed to compare two technologically different ways of collecting data by motion analysis systems based on inertial measurement unit (IMU) and optoelectronic measurements for comparison of joint angles provided by them in complex motion task like Nordic Walking gait. The BTS and MyoMotion systems showed very strong mutual correlation for the measurement of examined lower limb joints, except for the hip rotation (r = 0,53). Moreover despite of good similarity in joint angle waveforms (Figure 1), results given by BIAS or even calculated values of MIN and MAX (Table 1) are definitely too much discrepancy.

5. Conclusions

As a Nordic Walking is quite a complex movement characterized by high velocity reaching up to 2.1 m/s and based on literature [1,2,3], it was recognized that if the discrepancy between the measurements were within ±10° the validity of measuring still should be good. However, results related to range of compliance interval (RCI) and BIAS between systems put this thesis on for consideration. The observed discrepancies between the IMU-based and optoelectronic motion analysis systems were likely due to differences between the biomechanical models used by these two systems which makes it impossible to say unequivocally whether the kinematic data on the angles obtained from the tested systems cannot be directly compared with each other without further research.

References

[1] RICHARDS J.G., *The measurement of human motion: a comparison of commercially available systems.* Human Movement Science, 1999, 18(5), 589-602.

[2] GRIBBLE P, HERTEL J, DENEGAR C, BUCKLEY W., *Reliability and validity of a 2-D video digitizing system during a static and a dynamic task.* Journal of Sport Rehabilitation, 2005, 14(2), 137-149.

[3] HUBER M.E, SEITZ A.L, LEESER M, STERNAD D., *Validity and reliability of Kinect skeleton for measuring shoulder joint angles: a feasibility study.* Physiotherapy, 2015, 101(4), 389-393.

Assessing fall risk in older women

P. Bobowik[1], I. Wiszomirska[2]

Key words: *fall risk, elderly, seniors*

1. Introduction

One-third of older people experience a fall each year [1]. Falls are a consequence of many factors: reduced muscle strength, degenerative changes in the vestibular and visual systems, deterioration of motor control, and environmental factors [2,3].

Although fall risk assessment should take place in a dynamic environment [4], it is important to identify which static balance-related indices may be predictors of falls in the elderly.

2. Material and methods

The study involved fifty-six women aged 71.77 ± 7.43 (SD). Balance was assessed with the use of a Biodex Balance System SD (BBS) platform. A Postural Stability Test (PST) was performed using the stability platform with eyes open (EO) and eyes closed (EC). On this basis, the following static stability coefficients were determined: an overall stability index (OSI), an anterior-posterior stability index (APSI) and a medial-lateral stability index (MLSI). A Fall Risk Test (FRT) was also performed with eyes closed at various levels of platform instability from 12-6, on the basis of which a dynamic stability factor, i.e. a fall risk index (FRI) 12-6, was determined.

A regression analysis was performed in order to determine which static stability-related independent variables make it possible to predict FR (FRI 12-6) in older women. A transformation of indices with a distribution different from the normal was performed, finding the logarithm of the measurement data. A significance level of $p < 0.05$ was adopted.

3. Results and discussion

A model was built based on the following static stability parameters with eyes open and closed: OSI OO, APSI OO, MLSI OO, OSI EC, APSI EC and MLSI EC. The obtained results allow FR to be predicted with an accuracy of just 39% on the basis of the medial-lateral stability index (MLSI) with eyes open. The regression results are shown in Table 1.

Table 1. The results of the regression analysis for static stability factors in fall risk.

R2= 0.3894; F(6,48)= 5.1010						
parameter	**OSI EO [-]**	**APSI EO [-]**	**MLSI EO [-]**	**OSI EC [-]**	**APSI EC [-]**	**MLSI EC [-]**
b	0.0916	-0.1121	0.5282	-0.7587	0.5804	0.1500
p	0.794	0.664	0.002*	0.163	0.117	0.458

Legend 1.
b – regression coefficient; p –probability value; OSI- overall stability index; APSI- anterior-posterior stability index; MLSI- medial-lateral stability index; EO-eyes open; EC- eyes closed;

By means of backward stepwise regression analysis using the above model, a variable that significantly influences FR in seniors was distinguished, namely MLSI EO. The above analysis shows that this indicator may predict the risk of falls in older women in 35% of cases. The results of the above analysis can be found in Table 2.

[1]Józef Piłsudski University of Physical Education in Warsaw, Faculty of Rehabilitation,
e-mail: patrycja.bobowik@awf.edu.pl
[2] Józef Piłsudski University of Physical Education in Warsaw, Faculty of Rehabilitation,
e-mail: ida.wiszomirska@awf.edu.pl

Table 2. Results of backward stepwise regression analysis as regards fall risk

parameter	b	R2	p
MLSI EO [-]	0.484011	0.3458	0.000002*

Legend 2.
b- regression coefficient; p- probability value; MLSI- medial-lateral stability index; EO-eyes open;

4. Conclusions

Fall risk assessment should be conducted in dynamic conditions. The results of the above analysis suggest that medial-lateral swaying with eyes open is also a strong fall risk predictor in older women.

Acknowledgments: This work was made possible due to support from the Ministry of Science and Higher Education in the years 2020-2022. It was carried out by Research Group no. 3 at the Józef Piłsudski University of Physical Education in Warsaw "Motor system diagnostics in selected dysfunctions as a basis for planning the rehabilitation process".

References

[1] GRANT A., MACKENZIE L., CLEMSON L., *How do general practitioners engage with allied health practitioners to prevent falls in older people? An exploratory qualitative study.* Australasian Journal on Ageing, 34, 149–154.

[2] GOUVEIA É.R., GOUVEIA B.R., IHLE A., KLIEGEL M., MARQUES A., FREITAS D.L., *Balance and mobility relationships in older adults: a representative population-based cross-sectional study in Madeira, Portugal*. Archives of Gerontology and Geriatrics, 2019, 80,65–69.

[3] BOBOWIK P., WISZOMIRSKA I., LEŚ A., KACZMARCZYK K., *Selected tools for assessing the risk of falls in older women*. Biomed Research International, 2020, 2020:2065201.

[4] BOBOWIK P., WISZOMIRSKA., *Diagnostic dependence of muscle strength measurements and the risk of falls in the elderly*. International Journal of Rehabilitation Research, 2020, 43(4), 330-336.

Influence of direction of bone conduction stimulation applied to the otic capsule on the human cochlea

P. BORKOWSKI[1], P. MAREK[2], K. NIEMCZYK[3], M. LACHOWSKA[4]

Key words: *FE analysis, temporal bone, cochlea, inner ear, bone conduction*

1. Introduction

The effectiveness of stimulation for bone conduction (BC) implants located on the skull surface (BAHA) depends on the site of implantation [1]. Similarly, in the case of an implant placed on the otic capsule, the intensity of vibration of individual parts of the inner ear can differ, depending on the stimulation direction. For some directions, despite the intense vibration of the promontory bone, vibration amplitudes of the basilar membrane inside the cochlea can be relatively small [2]. The use of numerical analysis is of great importance, because in the case of experimental studies, only vibrations observed on the outer side of the cochlea are measured [3, 4]. Obtaining good results of BC stimulation on the outer part of the cochlea is not equivalent to the effective stimulation of the basilar membrane. Before choosing the direction of stimulation, especially for the stimulator placed on the otic capsule, the anatomy of the bone tissue in the vicinity of semicircular canals should be considered to ensure secure location of the implant [5].

2. Material and methods

2.1. Numerical model of the temporal bone

A finite element model of the temporal bone with the inner ear was used to conduct a harmonic analysis of BC stimulation on the otic capsule [2]. A force was applied to the titanium stimulator located next to the labyrinth (Fig. 1). The constant force magnitude of 0.1 N was assumed for the entire frequency range 0.2 to 10 kHz [3]. Material properties of cortical bone and the round window membrane were viscoelastic, other properties were isotropic and linear elastic. The perilymph fluid inside the cochlea was assumed as viscous and compressible. Stiffness and damping of the basilar membrane and spiral lamina were changing from the base to the apex of the cochlea. The boundary of the temporal bone was fixed. The stapes footplate was immobilized (otosclerotic condition).

2.2. Effectiveness of bone conduction stimulation

The two directions of stimulation were considered: a) the first giving the highest amplitude of the volume displacement on the round window membrane, which was calculated relatively to vibration of the surrounding bone, b) the second giving the highest amplitude of the promontory bone vibration (Fig. 1). The effectiveness of BC stimulation inside the cochlea was calculated based on vibration amplitudes along the basilar membrane and the spiral lamina. The effectiveness for the outer part of the cochlea was represented by amplitudes of the volume displacement on the round window membrane and the relative vibration at its centre. The volume displacement value obtained for the first direction of stimulation at a given frequency was taken as a reference level for scaling other amplitudes to obtain similar results as those obtained for the cochlea stimulated by stapes vibrations (air conduction).

[1]Warsaw University of Technology, The Faculty of Power and Aeronautical Engineering, Warsaw, Poland,
e-mail: pbork@meil.pw.edu.pl
[2]Warsaw University of Technology, The Faculty of Power and Aeronautical Engineering,
e-mail: pmarek@meil.pw.edu.pl
[3]Medical University of Warsaw, Department of Otolaryngology, Warsaw, Poland,
e-mail: kniemczyk@wum.edu.pl
[4]Medical University of Warsaw, Department of Otolaryngology, Warsaw, Poland,
e-mail: mlachowska@wum.edu.pl

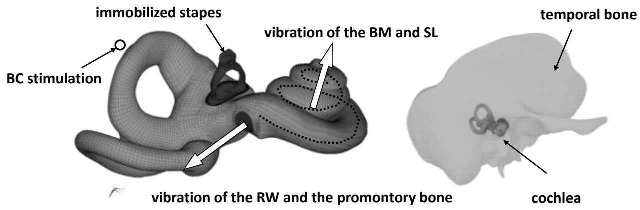

Fig. 1. Location of bone conduction (BC) stimulation and vibration directions (left), the temporal bone (right)

2.4. Results

For the first direction of stimulation, the effectiveness of BC stimulation inside the cochlea was several times higher and more evenly distributed compared to the direction causing intense bone vibrations (Fig. 2). The results on the round window membrane were also significantly lower for the second direction, however the decrease in effectiveness was frequency dependent.

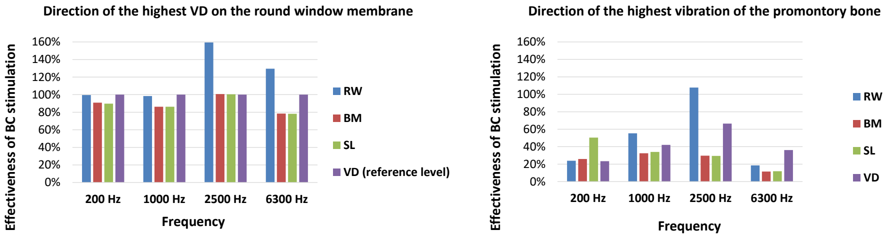

Fig. 2. Effectiveness of bone conduction (BC) stimulation applied on the otic capsule: at the round window centre (RW), along the basilar membrane (BM) and spiral lamina (SL)

2.5. Conclusions

Results on the outer side and inside of the cochlea may vary depending on the direction of bone conduction stimulation. Numerical simulation showed that the effectiveness of the basilar membrane stimulation is not directly related to the promontory bone vibration observed in the experiment.

Acknowledgments: This research was supported by the National Centre for Research and Development: PBS3/B7/25/2015

References

[1] Dobrev I., Stenfelt S., Röösli C., Bolt L., Pfiffner F., Gerig R., Huber A, Sim JH., *Influence of stimulation position on the sensitivity for bone conduction hearing aids without skin penetration*. Int J Audiol, 2016, 55(8), 439-46.

[2] Borkowski P, Marek P, Niemczyk K, Lachowska M, Kwacz M, Wysocki J., *Bone conduction stimulation of the otic capsule: a finite element model of the temporal bone*. Acta Bioeng Biomech, 2019, 21(3), 75-86.

[3] Kwacz M., Niemczyk K., Wysocki J., Lachowska M., Borkowski P., Małkowska M., Sokołowski J., *Round Window Membrane Motion Induced by Bone Conduction Stimulation at Different Excitation Sites: Methodology of Measurement and Data Analysis in Cadaver Study*. Ear Hear, 2019, 40(6), 1437-1444.

[4] Niemczyk K., Lachowska M., Kwacz M., Wysocki J., Borkowski P., Małkowska M., Sokołowski J., *Effectiveness of Bone Conduction Stimulation Applied Directly to the Otic Capsule Measured at Promontory: Assessment in Cadavers.* Audiol Neurootol, 2020, 25(3): 143-150.

[5] Wojciechowski T., Lachowska M., Niemczyk K., *Detailed Analysis of the Space between the Semicircular Canals for the Purpose of Direct Bone Conduction Stimulation of the Inner Ear*. Audiol Neurootol, 2021, 26(1), 35-44.

The design of ankle rotary exercise device

P. BORKOWSKI[1], J. ZUZDA[2], R. LATOSIEWICZ[3]

Key words: *rehabilitation, rotation exercises, device, ankle joint*

1. Introduction

Musculoskeletal disorders are in the top of five diagnostic groups in the European Union and lead to significant costs of healthcare and social support. One of the problems of musculoskeletal disorders is associated with dysfunctions in the musculoskeletal system in the area of the lower extremities - the ankle joint. The ankle joint allows the foot to be positioned correctly on the ground and adapts it to uneven ground during walking. Walking, jumping, running or even standing without proper ankle function is difficult. The ankle joint is one of the body's most burdened and vulnerable joints. It`s structure causes that even a small, inappropriate movement can affect the function [1,2].

2. Rehabilitation

Injuries of the ankle joint require appropriate treatment and rehabilitation. Early medical intervention and a well-programmed exercise program can help restore and maintain muscle balance, decrease pain by reducing muscle tone and use physiological reflexes from receptors located in muscle attachments, increase the range of motion, and prevent secondary injuries [3,4]. The literature review suggests that currently there are no devices that allow for the exercise and active and passive rehabilitation of ankle joints implemented through rotational multidirectional movements instead of commonly used isolated single-plane exercises.

3. Rehabilitation device

The ankle joint rehabilitation device allows the exercise and rehabilitation in both active and passive forms, implemented through rotational multiplane movements. At the same time, after blocking the rotational movements, exercises in isolated planes (flexion–extension, eversion–inversion and rotation movement around the vertical axis of the tibia) of the ankle joint are possible. The subject of the invention, shown in Fig. 1, consists of three main units:

- exercise module (1);
- a supportive arm for rehabilitated person (2);
- optional supportive arm for physiotherapist (3).

Exercise module (1) allows for multiplane active and/or passive ankle joint movements. Supportive arm (2) is used to support and control exercises by a rehabilitated person. Optional supportive arm (3) is used for training or supervision exercises by an assisting person/health professional.

[1]Bialystok University of Technology, Institute of Biomedical Engineering; e-mail: p.borkowski@pb.edu.pl,
[2]Bialystok University of Technology, Institute of Management and Quality Science; e-mail: j.zuzda@pb.edu.pl,
[3]Medical University of Lublin, Poland, Department of Physiotherapy and Rehabilitation;
e-mail: r.latosiewicz@umlub.pl

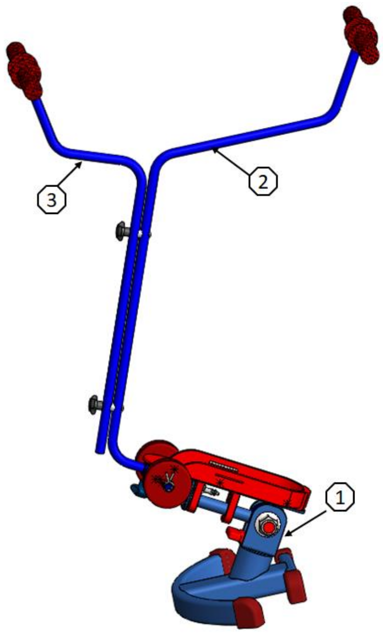

Fig. 1. The device for ankle joint exercises with rotatory movements

4. Conclusions

The presented device allows for multiplane ankle joint movements. Together with the developed exercise program, it is a comprehensive solution for rehabilitation of even severe injuries. The device is a continuation of scientific works related to the rehabilitation by means of rotational improvement of human joints [5]. The construction of the device has been reported to the Patent Office of the Republic of Poland.

References

[1] Musculoskeletal Health in Europe. Report v 5.0. Eumusc.net, 9-10, 34-37, 130.

[2] SCHÜNKE M., SCHULTE E., SCHUMACHER U., VOLL M., WESKER K., (2007). LernAtlas der Anatomie. Allgemeine Anatomie und Bewegungssystem. Thieme, New Yor.k

[3] FLETCHER GF., BALDY GJ., AMSTERDAM EA., (2001). Exercise standards for testing and training a statement for healthcare professionals from the American Heart Association. Circulation, 104:1694-1740.

[4] https://orthoinfo.aaos.org/en/diseases--conditions/?bodyPart=Ankle.

[5] Urządzenie do rotacyjnych ćwiczeń stawu biodrowego. Zgłoszenie patentowe P.42669.

Identification of the heterogeneous shear modulus distribution through isogeometric inverse analysis

B. BORZESZKOWSKI[1], I. LUBOWIECKA[1], R. A. SAUER[1,2,3]

Keywords: *biomembrane, incompressible Neo-Hooke, inverse analysis, material identification, nonlinear Kirchhoff-Love shells*

1. Introduction

Many soft biological materials consist of membrane- or shell-like structures [1]. Examples are lung, ocular, and skin tissues. These structures usually are heterogeneous and nearly-incompressible. Computer models of these structures, based on the Finite Element Method (FEM), require knowledge of constitutive parameters to establish their mechanical response. In this work, the Finite Element Model Updating (FEMU) [2] method is used to identify heterogeneous shear modulus distributions using a Kirchhoff-Love shell formulation [3].

2. Materials and methods

The considered tissue sample consists of a flat square sheet, in which boundary conditions induce uni-axial tension (Fig. 1). The material is modeled with the incompressible Neo-Hookean model [4] with *a priori* defined analytical distribution

$$\mu = 1 + 0.9 \cdot \cos(\pi X) \cos(\pi Y) \,. \qquad [1]$$

The obtained deformation with the addition of 4% random noise is used to mimic experimental data. The material distribution is discretized by 64 elements with 81 nodal (shear modulus) values being design variables to be identified. Minimization of the objective function, which expresses the discrepancy between finite model prediction and experiment is solved iteratively with the use of an algorithm based on trust-region approach [5].

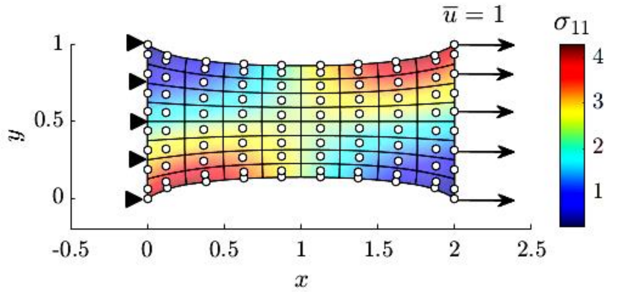

Fig 1. Uniaxial tension: deformed configuration colored by the membrane stress.

3. Results

81 nodal unknown shear modulus values are identified with a mean relative percentage error of 1.9 % and a standard deviation of 0.07%.

[1] Gdańsk University of Technology, Faculty of Civil and Environmental Engineering, Gdańsk, Poland, e-mail: bartosz.borzeszkowski@pg.edu.pl
[2]Aachen Institute for Advanced Study in Computational Engineering Science (AICES), RWTH Aachen University, Aachen, Germany,
[3] Department of Mechanical Engineering, Indian Institute of Technology, Kanpur, India

4. Conclusions

Despite large geometrical nonlinearities, the presence of 4% noise, and high variance of the material distribution, the algorithm showed very good performance and robustness in the heterogeneous shear modulus identification.

Acknowledgments: This work has been partially supported by the National Science Centre (Poland) under [Grant No. 2017/27/B/ST8/02518]. Calculations have been carried out at the Academic Computer Centre in Gdańsk.

References

[1] HUMPHREY J. D., *Computer methods in membrane biomechanics*. Computer Methods in Biomechanics and Biomedical Engineering, 1998, 1(3), 171-210.

[2] STÉPHANE A., et al, *Overview of identification methods of mechanical parameters based on full-field measurements*. Experimental Mechanics, 2008, 48.4, 381.

[3] SAUER R.A., DUONG T.X., *On the theoretical foundations of thin solid and liquid shells*. Math. Mech. Solids, 2017, 22(3), 343-371.

[4] SAUER R.A., DUONG T.X., CORBET,C.J., *A computational formulation for constrained solid and liquid membranes considering isogeometric finite elements*. Computer Methods in Applied Mechanics and Engineering, 2014, 271, 48–68.

[5] CONN A.R., *Trust region methods*. Siam, 2000, Vol. 1.

Influence of strength and time parameters of hip adductor and adductor muscles on maintaining balance in the frontal plane in young healthy women

A. BUGALSKA[1], S. WÓJTOWICZ[2], A. DANILUK[3], K. WIADERNA[4], M. GRABOWICZ[5], A. HADAMUS[6]

Key words: *isokinetics, balance, isometrics, adductors*

1. Introduction

Balance enables the human body to function properly on a motor basis and requires proper interaction between the musculoskeletal system and the nervous system. Damage at any stage of stimulus transmission - damage to receptors, spinal pathways, brain centers, or effectors - can result in balance-related dysfunctions in both the sagittal and frontal planes. The gluteus medius muscle, along with the gluteus minor muscle and the broad fascia stressor, is one of the strongest frontal stabilizers of the pelvis, and thus their synergistic action should influancethe quality of body balance [1,2].

The aim of the present study was to determine the effect of hip adductor muscle strength assessed under isometric and isokinetic conditions in healthy subjects on the quality of balance maintenance under static conditions.

2. Materials and methods

The study group consisted of 51 healthy women, aged between 18 and 25 years. Balance measurement according to the M-CTSIB protocol and single-leg standing tests (eyes open and eyes closed) were performed using the BIODEX Balance System platform. Isokinetic testing performed at 30°/s and isometric testing of the hip extensors, performed after a prior 10-minute uniform warm-up using the Humac Norm system. Several parameters of strength, power and time were evaluated.

3. Results

Regression analysis for swing ratio (SW) and stability ratio (ST) during standing with both feet showed significant results for the presence of visual feedback (SW R=-0.922; p<0.0001; ST R=-0.613; p=0.0493), unstable ground (SW R=1.253; p<0.0001; R=2.547; p<0.0001). More significant results in the isokinetic test of hip adductors were observed for the ST parameters: time required to reach maximum force moment (R=4.865; p=0.0019), lag time (R=9.608; p=0.0319), force moment decrease time (R=-2.80728; p=0.0105), work per repetition (R=0.156; p= 0.001) and mean muscle power (R=-0.171485; p=0.0083). There was no correlation of SW and ST coefficient with anthropometric parameters or? the variety of physical activity, sit and reach test score, strength parameters in the isokinetic test or any parameters obtained in the isometric test.

[1]Department of Rehabilitation, Faculty of Medical Sciences, Medical University of Warsaw, Poland, e-mail: aneta.bugalska @wum.edu.pl
[2]Department of Rehabilitation, Faculty of Medical Sciences, Medical University of Warsaw, Poland, e-mail: sebastian.wojtowicz@wum.edu.pl
[3]Department of Rehabilitation, Faculty of Medical Sciences, Medical University of Warsaw, Poland, e-mail: anna.daniluk@wum.edu.pl
[4]Department of Rehabilitation, Faculty of Medical Sciences, Medical University of Warsaw, Poland, e-mail: karolina.wiaderna@wum.edu.pl
[5]Department of Rehabilitation, Faculty of Medical Sciences, Medical University of Warsaw, Poland, e-mail: marta.grabowicz@wum.edu.pl
[6]Department of Rehabilitation, Faculty of Medical Sciences, Medical University of Warsaw, Poland, e-mail: anna.hadamus@wum.edu.pl

Regression analysis for single-leg standing showed the dependence of the overall swing ratio (overall) in single-leg standing, the anterior-posterior (AP) swing ratio and the side-to-side (ML) swing ratio on the time required to reach the maximum moment of force in isometric contraction in the direction of abduction (overall: R = 0.769; p = 0.0005; AP: R= 0.565; p=0.008; ML: R= -1.74; p<0.05) and on the test conditions.

4. Discussion

Correct activation of the hip abductor muscles may be important for bipedal and single leg stance balance maintenance in young people both during standing with both feet and standing on one leg. The obtained results prove there is a need for prospective, randomized studies on larger groups with different age and gender of subjects.

References

[1] CZERWIŃSKI E., BOROWY P., JASIAK B., *Współczesne zasady zapobiegania upadkom z wykorzystaniem rehabilitacji.* Ortopedia Traumatologia Rehabilitacja. 2006;4(6):380-7.

[2] RIMLAND J.M., et al. *Effectiveness of non-pharmacological interventions to prevent falls in older people: a systematic overview.* The SENATOR Project ONTOP Series. PloS one. 2016;11(8):e0161579.

[3] ZAK M., SWINE C., GRODZICKI T., *Combined effects of functionally-oriented exercise regimens and nutritional supplementation on both the institutionalised and free-living frail elderly (double-blind, randomised clinical trial).* BMC Public Health. 2009;9:39.

Investigation on mechanics for use of PLA in total hip arthroplasty using FEM analysis

E. CELIK[1], F. ALEMDAR[2], M. BATI [3], M. F. DASDEMIR [4], O. A. BUYUKBAYRAKTAR [5], M. KARA [6], K.N. CHETHAN [7], Ş. MIHÇIN[8]

Key words: *PLA, FEA, Total Hip Arthroplasty, Plastic Liner, Biomaterial*

Abstract

Polylactic acid (PLA) is a biodegradable non-toxic, biocompatible polymer used as a popular filament material in biomedical applications with the advance of 3D printing technologies. PLA is considered a suitable implant material due to its contribution to bone regeneration. In this study, the use of PLA in Total Hip Arthroplasty (THA) as a liner material was assessed. In this regard, the PLA liner with different material combinations in THA was examined to provide evidence for its potential. The hip implant model was drawn using a computer-aided design tool then transferred into a commercial finite element analysis (FEA) software. The models consisted of assemblies of PLA with titanium, chrome cobalt, stainless steels, dense NiTi shape-alloys, and Alumina-Zirconia. Simulations were run under static loading conditions. To evaluate and compare the results for the optimum design; factor of safety, total deformation and von Mises stress analysis were used. When Al-Zi combined with PLA, it produced the least deformation and reasonable Von Mises stress values. PLA might perform best when used with Al-Zi. As a next step, experimental pre-clinical tests are planned to assess its clinical potential.

Acknowledgments

This research was funded by TUBITAK 2232 International Outstanding Researchers Funding Scheme with Grant No of 118C188 'New Generation Implants for All' project.

The authors thank the Mechanical Engineering, Department of Izmir Institute of Technology for providing the high computational facility to carry out this research.

References

[1] TOMČÍKOVÁ, ZITA, et al. *Influence of plasticizer and bioplasticizer on the structure and mechanical properties of the pla fibres.*

[1]Department of Mechanical Engineering, Izmir Institute of Technology, Urla, Izmir, TURKEY,
[2]Department of Mechanical Engineering, Izmir Institute of Technology, Urla, Izmir, TURKEY
[3]Department of Mechanical Engineering, Izmir Institute of Technology, Urla, Izmir, TURKEY
[4]Department of Mechanical Engineering, Izmir Institute of Technology, Urla, Izmir, TURKEY
[5]Department of Mechanical Engineering, Izmir Institute of Technology, Urla, Izmir, TURKEY
[6]Department of Mechanical Engineering, Izmir Institute of Technology, Urla, Izmir, TURKEY,
e-mail: mustafakara0512@gmail.com
[7]Department of Aeronautical and Automobile Engineering, Manipal Institute of Technology, Manipal Academy of Higher Education, Manipal-576104, Karnataka, INDIA
[8]Department of Mechanical Engineering, Izmir Institute of Technology, Urla, Izmir, TURKEY

[2] OKOLIE, OBINNA, et al. *3D Printing for Hip Implant Applications: A Review.* Polymers, 2020, 12.11: 2682.

[3] DEDUKH, N. V.; MAKAROV, V. B.; PAVLOV, A. D. *Polylactide-based biomaterial and its use as bone implants (analytical literature review).* Pain, Joints, Spine, 2019, 9.1: 28-35.

[4] MEROLA M., AFFATATO S., *Materials for hip prostheses: A review of wear and loading considerations.* Materials, 2019, 12.3: 495.

[5] HU C.Y., YOON T.R., *Recent updates for biomaterials used in total hip arthroplasty*. Biomaterials research, 2018, 22.1: 1-12.

[6] CHETHAN, K. N., et al. *Static structural analysis of different stem designs used in total hip arthroplasty using finite element method.* Heliyon, 2019, 5.6: e01767.

[7] CHOWDHURY M.A., et al. *Experimental investigation on friction and wear of stainless steel 304 sliding against different pin materials.* World Applied Sciences Journal, 2013, 22.12: 1702-1710.

[8] GUEZMIL M., BENSALAH W., MEZLINI S. *Tribological behavior of UHMWPE against TiAl6V4 and CoCr28Mo alloys under dry and lubricated conditions.* Journal of the mechanical behavior of biomedical materials, 2016, 63: 375-385.

[9] PEREPELKINA S., et al. *Investigation of Friction Coefficient of Various Polymers Used in Rapid Prototyping Technologies with Different Settings of 3D Printing.* Tribology in Industry, 2017, 39.4.

[10] TRIYONO J. et al. *Investigation of Meshing Strategy on Mechanical Behaviour of Hip Stem Implant Design Using FEA.* Open Engineering, 2020, 10.1: 769-775.

[11] BAHRAMINASAB M., SAHARI B. B., *NiTi shape memory alloys, promising materials in orthopedic applications.* Shape Memory Alloys-Processing, Characterization and Applications, 2013, 261-278.

Numerical determination of the degree of mechanical anisotropy of the trabecular bone

A. CICHAŃSKI[1], K. NOWICKI[2]

Key words: *trabecular bone structure, cancellous bone anisotropy, MIL analysis*

1. Introduction

The stiffness of the trabecular bone is influenced not only by the content of the mineral fraction but also by its distribution. Principal Component Analysis of the relationship between bone structure indices and mechanical properties indicates that one of the more independent indices is degree of anisotropy DA [2]. The accuracy of DA determination does not depend on either the scanning resolution or the resolution of the structure reconstruction [3]. In order to ensure the representativeness of the apparent module determined FE, models to be simulated are made from images of the structure processed along it principal mean intercept length MIL axis [4].

The aim of the study was to compare the effectiveness of MIL and FEM analysis to determine the degree of anisotropy for the trabecular bone structure. Direction of occurrence of the maximum apparent modulus for the MIL was directly determined. An important issue resolved in work was to indicate direction and value of the maximum apparent modulus during the FE analysis.

2. Material and methods

Tests were performed on samples of the trabecular bone structure. Specimens were obtained from patients by dissecting them from the neck of the femur obtained after hip arthroplasty surgery. Cylindrical samples with a diameter of ø10 mm and a height of 7.7 mm were cut from the slices. Sample were scanned at a resolution of 36μm on a μCT80 microtomograph. The verification of the proposed method was performed on the basis of 11 samples selected from set n = 33. As a result of the scanning, 214 scans were recorded. Based on the scans, geometric models for cylindrical samples were prepared and meshed with element size 36μm. From this mesh, cube-shaped samples with a side of 5.4 mm were cut at the angle α in the 0XY plane and the angle γ in the 0XZ plane **Fig. 1**. Samples were compressed by 1%. Analyzes were performed in the APDL environment of the ANSYS program. The isotropic material properties E = 10GPa and $\nu = 0.3$ were adopted for the analyzes [1].

In the course FE analyzes, the values of the apparent modulus were determined for samples cut at angles $0^o < \gamma < 180^o$ with a step of 5^o. For each position described by the γ angle, a set of analyzes was performed for samples cut at the angles $0^o < \alpha < 360^o$ with a step of 5^o. On the basis of the so determined courses of variability of the apparent modulus, it was established modulus maximum value and direction of it occurrence. Next, the apparent modules for two perpendicular axes to the predetermined direction of the maximum E was determined. The minimum value of the apparent modulus determined in this way related to the maximum value was used to calculate the DM values using formula $DM=1-E_{min}/E_{max}$.

3. Results

The differences between the indicators values of the degree of structural anisotropy DA of the trabecular structure determined by the MIL analysis and the degree of mechanical anisotropy of the trabecular structure DM determined by the numerical FE analyses are summarized in **Fig. 3**.

[1]UTP University of Sciences and Technology in Bydgoszcz, Faculty of Mechanical Engineering, Bydgoszcz, Poland, e-mail: artur.cichanski@utp.edu.pl
[2]UTP University of Sciences and Technology in Bydgoszcz, Faculty of Mechanical Engineering, Bydgoszcz, Poland, e-mail: krzysztof.nowicki@utp.edu.pl

The Shapiro-Wilk tests for the normality of the distribution for the values of DM and DA showed that in the case of DM the distribution can be considered normal (p-value = 0.6239). However, for DA, this hypothesis is invalid (p-value = 0.0026). Therefore, the non-parametric Wilcox test for the occurrence of differences between the distributions of DM and DA was performed, obtaining the p-value=8×10^{-5}. Thus, the hypothesis about the compatibility of the distributions was rejected.

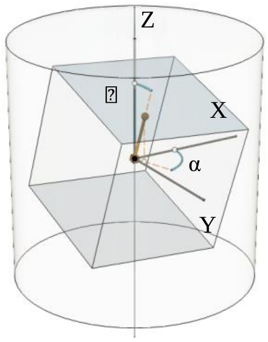

Fig. 1. Scheme for defining sample cutting angles.

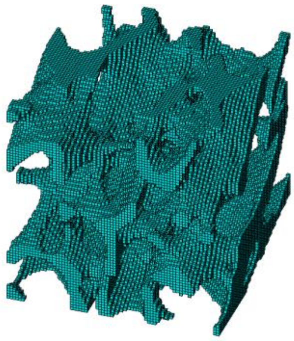

Fig. 2. Trabecular structure sample slice, BV/TV=0.248, α=0º, γ=0º.

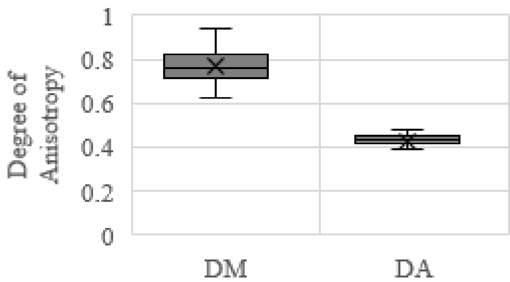

Fig. 3. Comparison of structure indicators DM and DA.

4. Conclusions

The values of the DM coefficient are different from the values of the DA coefficient as shown in **Fig. 3**. Due to the differences in the method of determining the directions of the trabecular structure between the methods, it can be indicated that the DM method, which is not based on an ellipsoid approximation as in the case of DA, tends to capture an increase in local stiffness in the structure. The use of approximation in the DA method leads to the omission of such structure features. The sensitivity of the DM method to local structural disturbances may be proved by a much higher value of the range of variability of the DA method.

References

[1] BEVILL G., KEAVENY T.M., *Trabecular bone strength predictions using finite element analysis of micro-scale images at limited spatial resolution*. Bone, 2009, 44, 579-84.

[2] CICHAŃSKI A., NOWICKI K., MAZURKIEWICZ A., TOPOLINSKI T., *Investigation of statistical relationships between quantities describing bone architecture, its fractal dimensions and mechanical properties*. Acta of Bioengineering and Biomechanics, 2010, 12, 69-77.

[3] KIM D.G., CHRISTOPHERSON G.T., DONG X.N., FYHRIE D.P., YENI Y. N., *The effect of microcomputed tomography scanning and reconstruction voxel size on the accuracy of stereological measurements in human cancellous bone*. Bone, 2004, 35, 1375-82.

[4] NIEBUR G.L., YUEN J.C., HSIA A.C., KEAVENY T.M., *Convergence behavior of high-resolution finite element models of trabecular bone*. Journal of Biomechanical Engineering-Transactions of the Asme, 1999, 121, 629-635.

Minimal shoes improve stability in persons with a history of falls

T. CUDEJKO [1], J. GARDINER [2], A. AKPAN [3], K. D'AOÛT [4]

Key words: *ageing, falls, gait, stability, footwear*

1. Introduction

Postural and gait instabilities contribute to falls in older adults [1]. Given that shoes affect human stability and that visual and cognitive systems deteriorate during aging [2], we aimed to: (i) compare the effects of footwear type on stability in persons with a history of falls, and (ii) determine whether these effects are altered by an experimentally induced absence of visual input or by a cognitive load.

2. Methods

Thirty persons with a history of falls (mean age 68.6 ± 4.4 years; 57% female) attended a university movement laboratory and performed standing and walking trials in three footwear conditions, i.e. (i) conventional shoes (cushioned-supportive), (ii) minimal shoes (flat-flexible), and (iii) barefoot. The outcomes were: (i) postural stability (movement of the center of pressure (CoP) assessed via posturography during eyes open/closed), and (ii) walking stability (Margin of Stability (MoS) in the sagittal and frontal plane assessed via 3-D motion analysis system during normal/dual-task walking). MOS was calculated by subtracting the position of the extrapolated center of mass from the position of the base of support.

3. Results

Minimal shoes and barefoot condition were more beneficial for postural stability than conventional shoes (Table 1).

Table 1. Mean values (SD) for the CoP metrics of postural stability

	Conventional	Minimal	Barefoot
Eyes open			
AP velocity (mm/s)	13.4 (4.7)$^{1\ 2}$	9.7 (2.7)	9.0 (2.4)
AP max range (mm)	3.5 (1.2)$^{1\ 2}$	2.7 (1.1)	2.7 (1.0)
ML velocity (mm/s)	9.1 (4.3)$^{1\ 2}$	5.6 (1.9)	6.1 (2.4)
ML max range (mm)	2.4 (1.0)$^{1\ 2}$	1.6 (0.6)	1.7 (0.7)
Eyes closed			
AP velocity (mm/s)	18.8 (8.4)$^{1\ 2}$	13.2 (3.9)	11.9 (3.5)
AP max range (mm)	4.0 (1.6)$^{1\ 2}$	3.1 (0.9)	2.9 (1.0)
ML velocity (mm/s)	11.7 (7.1)$^{1\ 2}$	6.4 (2.5)	6.3 (3.2)
ML max range (mm)	2.6 (1.4)$^{1\ 2}$	1.7 (0.8)	1.6 (1.0)

Lower values are indicative of better postural stability; AP – anterior-posterior, ML – medial-lateral; ^{1} - significantly ($p<0.05$) diffrent than ML; ^{2} significanlty diffrent than BF

Minimal shoes were more beneficial for walking stability in the sagittal plane (MoS AP) than conventional shoes and barefoot ($p<0.05$), but not in the frontal plane ($p>0.05$). This can be seen visually in the Figure 1. The distribution of the extrapolated center of mass position for minimal shoes

[1]Department of Musculoskeletal and Ageing Science, University of Liverpool, Liverpool, United Kingdom, e-mail: cudejkot@cardiff.ac.uk
[2]Department of Musculoskeletal and Ageing Science, University of Liverpool, Liverpool, United Kingdom, e-mail: J.D.Gardiner@liverpool.ac.uk
[3]Department of Musculoskeletal and Ageing Science, University of Liverpool, Liverpool, United Kingdom, e-mail: Asangaedem.Akpan@liverpool.ac.uk
[4]Department of Musculoskeletal and Ageing Science, University of Liverpool, Liverpool, United Kingdom, e-mail: Kristiaan.Daout@liverpool.ac.uk

is typically more condensed and further away from the anterior-posterior border (horizontal line) of the base of support resulting in larger values of the MoS and improved stability during walking in minimal shoes compared to barefoot and conventional shoes

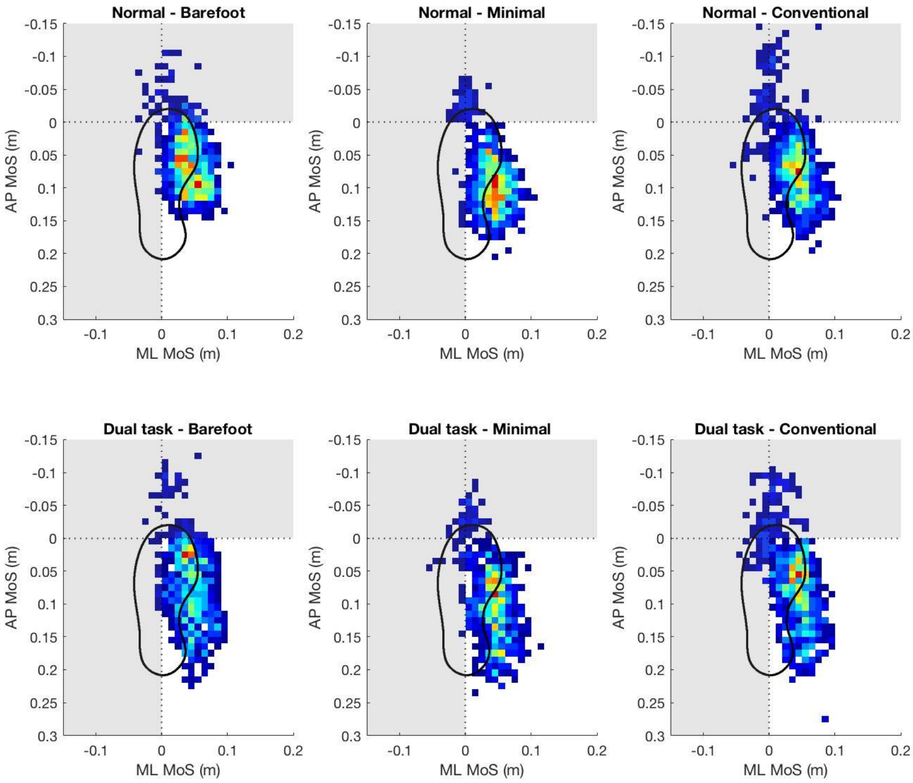

Fig. 1. Two-dimensional histogram of extrapolated centre of mass position at heel strike for walking trials. Hotter colours indicate extrapolated centre of mass at heel strike was positioned in that area more frequently. Greyed out areas represent regions considered 'unstable'. Lower values of the Margin of Stability are indicative of worse walking stability. The boundary of support (dotted lines) is defined by the calcaneus marker for medio-lateral direction and hallux for the anterior-posterior direction. Data are plotted for all steps (left and right foot) from all participants for each condition.

There was no interaction between footwear type and visual/walking condition for postural stability, nor for walking stability.

4. Conclusions

This study supports the need for longitudinal studies investigating whether minimal footwear is more beneficial for real-life fall prevention in older people than conventional footwear.

Acknowledgments: The funding was provided through the Innovate UK, part of UK Research and Innovation, under grant number 1570.

References

[1] RUBENSTEIN L. (2006) Age and ageing, 35, ii37-ii41.
[2] DAVIS A. et al. (2019). Footwear Science, 11, 13-23.

Barbell squat power measurement methods – experimental comparison

S. CYGAN[1], J. KRÓL[2], M. GROSZYK[3]

Key words: *sports biomechanics, power measurement, weight lifting, barbell squat*

1. Introduction

Power measurements are an established method for monitoring performance improvement and fine-tuning training settings for professionals, becoming also popular in amateur sports. Studies have shown that adjusting training for maximum power output provides benefits in many sports disciplines [1]. Interest in power measurements was enabled by fast developments of various devices for different sports including weight training [2].

2. Materials and Methods

2.1. Developed vertical displacement measurement methods

First of the developed power measurement methods uses a rotary encoder 400P/R (DFRobot, China) driven by a retractable line via a roller with 125 mm diameter. The encoder is connected to an Arduino board which passes the rotation data further to a PC computer, where it is received in real time by a Python based program for further processing. The rotation data is sampled at 100 Hz with approx. 1 mm resolution. During the measurement the device is placed directly under the bar and the retractable line is attached to the bar. The user has to provide the program with the mass of the lifted weight, body mass and height of the subject.

Second of the developed methods uses a video motion tracking method (by template matching) for obtaining vertical displacements of a marker placed on the bar. Motion tracking is carried out in post-processing using a purposefully developed program in Matlab environment. The recording can be done with any standard camera – here a cell phone camera was used (Xiaomi Redmi Note 8 Pro). As a result displacement data is obtained at sampling rate equal to the frame rate of the video recording (here 30 Hz) with resolution depending on the recording resolution and distance from the camera (here 1.73 mm). The program requires the user to manually point the marker to be tracked along with another marker for distance scaling. The user also provides the measured distance between the two markers used for scaling as well as the mass of the lifted weight, body mass and hight of the subject.

2.2. Power calculation

Both methods provide continuous displacements data enabling calculation of velocities and accelerations and further the power based on the mass of the lifted weight and the mass of the subject using the following equation:

$$P = P_w + P_{ub} + P_t = (m_w + m_{ub}) \cdot \left(g + \frac{dv}{dt}\right) \cdot v + m_t \cdot \left(g + \frac{d(kv)}{dt}\right) \cdot kv$$

where P is the sought power, P_w, P_{ub} and P_t are the power values associated with lifting the barbell weight (mass m_w), the upper body (m_{ub}) and the thighs (m_t) respectively. v is the velocity of the bar calculated directly as a derivative of displacement. It is assumed that the upper body moves at the same vertical velocity. Velocity kv is the vertical velocity of the centre of mass of the thighs, calculated using the coefficient k being the relative location of the centre of mass of the thigh provided by the regression equations developed by Zatsiorsky et al. [3]. The masses of the upper body and the thighs are calculated also using regression method provided in [3]. Power calculations were

[1]Warsaw University of Technology, Institute of Metrology and Biomedical Engineering, Warsaw, Poland, e-mail: szymon.cygan@pw.edu.pl

[2]W.U.T., Institute of Metrology and Biomedical Engineering, e-mail: julia.krol.stud@pw.edu.pl

[3]W.U.T., Inst. of Metrology and Biomedical Eng., e-mail: maciej.groszyk.stud@pw.edu.pl

carried out for each method separately in respective programs and thus they differed in details such as velocity and acceleration filtering methods.

2.3. Experimental verification

The two proposed methods were tested against a reference method – a commercially available linear MuscleLab encoder (Ergotest Innovation AS, Norway) measuring displacements at 200 Hz with 0.019 mm resolution. Measurements with all methods were taken simultaneously for one subject (male, 78 kg, 188 cm) at six different loads (Table 1.) with 8 repetitions at each load.

3. Results

Obtained results of displacements and velocities measurements for different loads showed good agreement with reference. For the encoder based method average displacement for all repetitions was 70.6±1.7 cm with -2.1% error vs reference (72.1±3.1 cm), average velocity 94.5±0.8 cm/s with 0.48% error vs reference. For the video based method average displacement was 72.5±2.5 cm with 0.5% error and velocity 96±3.9 cm/s with 0.7% error. The peak velocities (v_{max}) showed higher error (-2.4% and -1.3% for the two methods respectively) when compared to reference data as seen in Table 1.

Values of peak power (P_{max}) generated for each load, averaged for all the repetitions are given in Table 1.

Table 1. Results of peak velocity and peak power measurements.

	Mechanical				Video			
load [kg]	v_{max} [cm/s]	vs v_{ref}	P_{max} [W]	vs P_{ref}	v_{max} [cm/s]	vs v_{ref}	P_{max} [W]	vs P_{ref}
20	154,6±5,8	-2,4%	1362±71	32,5%	155,0±9,1	-2,1%	1017±130	-1,1%
25	-	-	-	-	165,6±13,3	-0,1%	1158±200	-1,3%
30	161,7±4,3	-1,7%	1430±71	18,4%	163,0±10,1	-0,9%	1105±70	-8,5%
35	151,7±3,0	-3,0%	1344±61	11,8%	155,4±11,9	-0,6%	1088±185	-9,5%
40	146,2±2,5	-2,7%	1276±58	7,3%	148,6±9,4	-1,1%	979±133	-17,7%
45	139,4±3,5	-2,5%	1212±62	2,3%	138,5±10,9	-3,1%	878±111	-25,9%

4. Discussion and conclusions

Results of displacements and averaged velocities for each repetition measurements show good agreement with the reference method. Peak velocities differ more from the reference which most probably results from different data smoothing approaches used in both developed methods. Reported peak power values show large discrepancies with the reference. Unknown data processing methods implemented in the MuscleLab encoder software makes it impossible to interpret the discrepancies, but they can be probably partially attributed to the sensitivity of acceleration calculation to any noise and the way it may be filtered/smoothed. This does not entirely explain the tendencies of the encoder based method to overestimate and the video based method to underestimate the peak power and the fact that both methods show the same tendency for different loads.

Developed methods have been shown to measure displacements correctly and provide access to all the raw data enabling much more detailed analysis than the commercial encoder. The video analysis based method requires no dedicated hardware making it the most available and versatile method. Adapting those methods to different exercise like bench-press requires only the implementation of appropriate body segments mass calculation.

References

[1] N. Kawamori and G. G. Haff, “The optimal training load for the development of muscular power,” *Journal of Strength and Conditioning Research*, vol. 18, no. 3. pp. 675–684, 2004.

[2] S. Lorenzetti, T. Lamparter, and F. Lüthy, “Validity and reliability of simple measurement device to assess the velocity of the barbell during squats,” *BMC Res. Notes*, vol. 10, no. 1, p. 707, Dec. 2017.

[3] V. Zatsiorsky, V. Seluyanov, and L. Chugunova, “In Vivo Body Segment Inertial Parameters Determination Using A Gamma Scanner Method,” in *Biomechanics of Human Movement: Applications in Rehabilitation, Sports and Ergonomics*, 1990, pp. 186–202.

Modelling record scores in the clean lift and its derivatives in the training of young weightlifters: a longitudinal study

A. CZAPLICKI[1], **P. SZYSZKA**[2]

Key words: *clean lift, record scores, annual macrocycle, time trends*

1. Introduction

The clean lift (C) and its derivatives, the power clean (PC), hang clean (HC) and hang power clean HPC), belong to basic weightlifting exercises. They are also used in strength training in many sports disciplines [1]. Despite the unquestionable importance of these exercises, no research has been conducted to analyze time trends of record scores of the C and its derivatives during several years of training. The estimation of such trends may facilitate the forecasting of future results and support the selection of appropriate training loads during the annual macrocycle, which is particularly important for young or beginning athletes. Considering the above, the aim of the current paper is to determine the time trajectories of the record scores in the C and its derivatives during a two-year training cycle in young weightlifters.

2. Material and methods

The study involved a group of 17 young weightlifters (age: 17.1 ± 2.8 years; weight: 75.6 ± 16.8 kg) who were tested seven times at three-month intervals in two annual macrocycles in 2018 and 2019.

Each measurement session started on Monday and the tests were conducted in a random order for four consecutive days. The lifters performed 3 maximal lifts with progressive increases in load, starting from a load equal to or greater than 90% of 1 RM. The repetition with the highest load (1 RM) was recorded as the final result of the test. Because of the differences in body mass between subjects and its within-subject variations during the research, the lifters' body mass changes were recorded regularly and the results achieved in particular lifts were converted into Sinclair points.

The weightlifters were provided with information on the research process and profits related to participating in the study. The research was completed in accordance with the ethical standards of the Helsinki Declaration and was approved by the University Research Ethics Committee.

The empirical data were primarily verified for normality of distribution and homogeneity of variances by means of the Shapiro-Wilk test and Bartlett's test. Subsequently, a multilevel model was built containing repeated measurements nested within a particular subject [2]. The statistical analysis and modelling were performed in the R environment (R Foundation for Statistical Computing, Austria) using the basic *lmer* function from the *lmerTest* package [2,3].

3. Results

Figure 1 shows the time trajectories of the C record scores computed with the *lmer* function. The differences between the individual trajectories and the differences between these trajectories and the mean trajectory (red thick line) can be easily recognized. A comparison of the mean trajectories for the C and its derivatives is presented in Figure 2. A similar pattern of the C and HC, and PC and HPC curves is clearly visible. The largest increases for record scores were recorded for the HC.

[1]Józef Piłsudski University of Physical Education in Warsaw, Faculty of Physical Education and Health in Biała Podlaska, Department of Natural Sciences, Biała Podlaska, Poland, e-mail: adam.czaplicki@awf.edu.pl
[2]Józef Piłsudski University of Physical Education in Warsaw, Faculty of Physical Education and Health in Biała Podlaska, Department of Sport Sciences, Biała Podlaska, Poland, e-mail: paulina.szyszka@awf.edu.pl

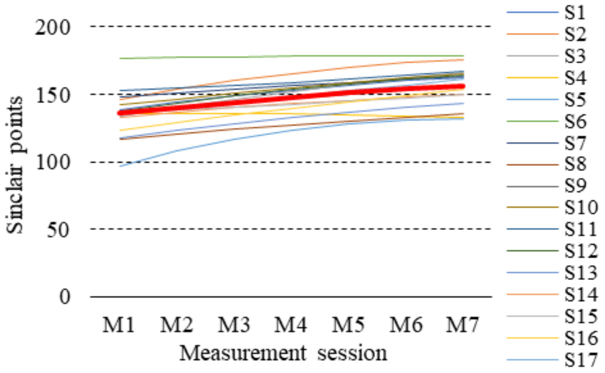

Fig. 1. Computed individual trajectories for the C and the mean trajectory.

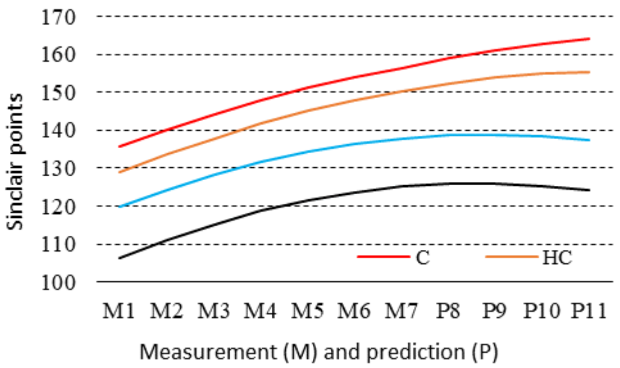

Fig. 2. Computed mean trajectories for the C and its derivatives.

4. Discussion

The aim of the study was to identify the time trajectories of the record scores achieved in C and its derivations during a two-year training cycle in young weightlifters. The results of the computations showed that tracking record scores at regular intervals in the C and its derivatives makes it possible to identify time trends in these scores and second-degree polynomial approximation was sufficient.

The study showed that the time trajectories of the record scores in the HC were similar to those in the C and the trajectories of the PC were in line with the trajectories of the HPC.

We believe that the knowledge of the time trends in the C and its derivatives may be important both for the coaches of young weightlifters and young weightlifters themselves. It makes it easier to choose an adequate selection of special exercises for training as well as their volume and intensity.

References

[1] POLETAEV P., CERVERA V., *The Russian approach to planning a weightlifting program*. Strength Cond. 1995, 17(1), 20-26.

[2] CZAPLICKI A., SZYSZKA P., SACHARUK J. JASZCZUK J., *Modeling record scores in the snatch and its variations in the long-term training of young weightlifters.* Plos One, 2019, 14(12), e0225891.

[3] KUZNETSOVA A., BROCKHOFF P.B., CHRISTENSEN R.H.B. *lmerTest package: Tests in linear mixed models.* J. Stat. Softw., 2017, 82(13), doi:10.18637/jss.v082.i13.

A method to evaluate the muscle synergy of spine stabilization muscles in the deadlift exercise. Single case analysis.

A. DANECKA[1], A. RUTKOWSKA-KUCHARSKA [2], R. MICHNIK[1]

Key words: *relative synchronization, electromyography, load*

1. Introduction

Muscle synergy is defined as coordinated recruitment of muscle groups [1]. Muscle synergy analysis (MSA) is a mathematical technique to define a set of muscle group activation patterns, which are used by the CNS to generate proper coordination for a given biomechanical task [2,3]. The literature presents a number of algorithms enabling the identification of synergy from the most popular ones, i.e. NMF (non-negative matrix factorization) or PCA (principal component analysis) to less known FA (factor analysis), ICA (independent component analysis) or pICA (non-negative independent component analysis algorithm) [4]. Another method of muscle synergy assessment may be the analysis of time and amplitude parameters of the EMG signal related to motion time (the so-called relative synchronization). Proper coordination of muscles responsible for spinal stabilization is particularly important in heavy-duty exercises. This kind of exercise is 'deadlift'. [5]. In the conditions of maximum and submaximum loads, the share of the so-called tertiary stabilizers is important.

The aim of the study is to develop a method to evaluate the synergism of selected spinal stabilizing muscles and to describe their interaction in deadweight exercise with maximum load.

2. Materials and methods

The measurements were taken by 1 man who is a strength training instructor, knows the technique of performing a deadlift, and applies this exercise in his daily workout.

2.1 Measurement procedure

Before the measurements were taken, surface electrodes were placed on the body of the test person. Surface electrodes with solid gel Ag/AgCl (NORAXON Inc., USA) were placed in a bipolar configuration on a m. back rectifier (ES), a m. upper and lower abdomen straight (RAu and RAl) and an external oblique (OE) right and left side. The reference electrode was placed on the front upper hip spike [5]. The EMG signal was measured with TeleMyo2400TG2 (Noraxon Inc., USA). The electrogoniometer (Twin Axis Goniometers SG150 model) was placed in the axis of the knee joint on the right and left lower limb.

2.2 Description of the motor task

The examined person performed a classic deadlift [6] with a 2.2 m long and 20 kg weight Olympic barbell). The exercise was performed with the maximum load (DL 100%) and with the load amounting to 70% of the weight lifted during DL 100%. The maximum load was the weight of the barbell with which the test person could perform technically correct dead thrust once (1RM). The test person performed 3 series of 4 DL70% cycles each. For the purpose of motion analysis, the exercise was divided into the preparatory phase (1), barbell lifting phase (2), barbell lowering phase (3), final phase, return to posture without a barbell (4).

[1]Department of Biomechatronics, Faculty of Biomedical Engineering, Silesian University of Technology, Zabrze, Poland, e-mail: aneta.danecka@polsl.pl
[2]Biomechanics Department, University School of Physical Education, Wroclaw, Poland

2.3 EMG signal analysis

The raw EMG signal was digitally processed in Matlab software, where high pass filtration was used to remove ECG artifacts, a cleaning operation and a smoothing algorithm (sliding window algorithm). In the next stage, the processed signals were used to detect the beginning of motion recording by the electrogoniometer - at the beginning and end of muscle activity for each muscle examined. Automatic detection of the beginning of muscle activity was implemented using the method of calculating the range of standard deviations for the EMG baseline, each time before the beginning of a given activity. For the study, a multiplier was established that if the SD range is exceeded by 5%, the moment of muscle group activation is determined. In addition, to eliminate the treatment of single discharges as the moment of activation (which exceed the designated SD range), a time of minimum time of the subperiod (MTS), during which the EMG signal should constantly remain above the threshold value, was determined. Verification of the reliability of the established threshold values for the conducted tests was performed using graphic methods. The division into individual phases (initial phase (PP), concentric phase (CP), eccentric phase (EP) and final phase (FP)) was made in relation to the division criterion for dorsal rectifier muscle activity. To determine CP and EP the maximum and minimum values achieved for the goniometer were determined.

From the signal obtained from the electrogoniometer the duration of motion (s) and the duration of concentric phase (s) and eccentric phase (s) of the exercise were determined. Then for each muscle was determined:

- maximum value of EMG signal in phases 1, 2, 3, 4 [μV] - in the summary the results are shown only for phases 2 and 3,
- time of achieving maximum muscle EMG activity in phases 2 and 3 [s],
- relative EMG activity time in phases 2 and 3 [%],
- relative time to reach maximum EMG activity in phases 2 and 3 [%].

3. Results

Table 1. *Time to achieve maximum muscle EMG activity in the CP and EP phases compared to the beginning of a given phase*

muscle		OE_r	OE_l	RAu_r	RAu_l	RAl_r	RAl_l	ES_r	ES_l
EMG (μV)	CP	82,3	110,9	24,9	25,08	21,9	24,7	619,3	640,8
	EP	43,5	27,0	8,0	6,1	16,1	15,3	403,4	368,1

CP – concentric phase, EP – eccentric phase, OE - external oblique muscle, RAl - rectus abdominalis lower muscle, RAu - rectus abdominalis upper muscle, ES - erector spinae muscle, r – right, l – left

Table 2. *Relative time to reach maximum EMG activity*

muscle		OE_r	OE_l	RAu_r	RAu_l	RAl_r	RAl_l	ES_r	ES_l
Time (%)	CP	86,1	87,0	86,5	85,3	43,2	87,3	64,6	64,4
	EP	65,0	72,7	62,5	37,4	65,0	76,3	49,0	70,9

CP – concentric phase, EP – eccentric phase, OE - external oblique muscle, RAl - rectus abdominalis lower muscle, RAu - rectus abdominalis upper muscle, ES - erector spinae muscle, r – right, l – left

Table 3. *Relative EMG activity time*

muscle		OE_r	OE_l	RAu_r	RAu_l	RAl_r	RAl_l	ES_r	ES_l
Time (%)	CP	22,5	22,3	29,4	27,7	25,2	24,8	20,1	19,4
	EP	18,4	18,2	24,1	22,6	20,6	20,3	16,4	15,8

CP – concentric phase, EP – eccentric phase, OE - external oblique muscle, RAl - rectus abdominalis lower muscle, RAu - rectus abdominalis upper muscle, ES - erector spinae muscle, r – right, l – left

The EMG activity of the examined muscles was higher during the barbell lifting phase, both for the dorsal and abdominal muscles. It should be remembered that for the dorsal muscles it is a concentric phase and for the abdominal muscles it is eccentric. Also, the duration of activity of the examined muscles is longer in the barbell lifting phase than in the lowering phase. The relative duration of activity of the tested muscles is similar in both phases of barbell movement. We cannot relate our results to other authors studies, as the interest of EMG activity researchers in the deadlift exercise concerns the shoulder and shoulder muscles as well as the lower limbs and hip rim [7].

References

[1] D'AVELLA A. *Muscle Synergies*. In: Binder M.D., Hirokawa N., Windhorst U. (eds) Encyclopedia of Neuroscience. 2009, Springer, Berlin, Heidelberg.

[2] SOOMRO MH, CONFORTO S, GIUNTA G, RANALDI S, DE MARCHIS C. *Comparison of initialization techniques for the accurate extraction of muscle synergies from myoelectric signals via nonnegative matrix factorization*. 2018, Appl Bionics Biomech, Rome, Italy

[3] BANKS CL, PAI MM, MCGUIRK TE, FREGLY BJ, PATTEN C. *Methodological choices in muscle synergy analysis impact differentiation of physiological characteristics following stroke*. 2017, Front Comput Neurosci; 11,1–12.

[4] TRESCH MC, CHEUNG VCK, D'AVELLA A. *Matrix factorization algorithms for the identification of muscle synergies: Evaluation on simulated and experimental data sets.* 2006, J Neurophysiol; 95,2199–212.

[5] NG J.K., KIPPERS V., RICHARDSON C.A. *Muscle fibre orientation abdominal muscles and suggested surface EMG electrode positions.* Electromyogr Clin Neurophysiol, 1998, 38 (1), 51-58.

[6] BIRD S., B. BARRINGTON HIGGS. *Exploring the deadlift.* Strength and Conditioning Journal, 2010, 32(2), 46-51.

[7] MARTIN-FUENTES I., OLIVA-LOZANO J.M., MUYOR J.M. *Electromyographic activity in deadlift exercise and its variants. A systematic review*. PLoS ONE; 2020 15(2):e0229507.

Muscle performance of hip abductor and adductor in healthy and osteitis pubis professional soccer players: A comparative study.

W.M. ELSAIS [1], **W.S. MOHAMMAD** [2]

Key words: *Muscle performance, Neuromuscular control, Soccer players, Osteitis pubis*

Abstract

Background: Although, the strength of hip adductor and abductor has been investigated in healthy and osteitis pubis soccer players, the imperfection in muscle performance for hip muscles still ambiguous. **Objective:** The present study aimed at comparing the muscle performance parameters of hip abductor and adductor muscles in both concentric and eccentric mode of contraction in soccer players suffering from osteitis pubis and healthy players at high angular velocity. **Materials and Methods:** Using A cross-sectional study, an isokinetic dynamometer at a speed of 180°/s was used to test 34 male soccer players with osteitis pubis and 18 healthy soccer players. **Results:** When compared to healthy group, players with osteitis pubis had significantly longer time to peak torque, acceleration and deceleration times (p 0.05), but no significant difference in muscle strength. **Conclusions:** The current study found that soccer players with osteitis pubis had a decrease neuromuscular response. As a result, these muscles' reaction time is important, and the diminution could lead to enlarged stresses and/or improper load distribution across the musculotendinous structure of the anterior pelvis, possibly leading to the development of osteitis pubis. Incorporating the current study's findings into clinical practice could provide critical information when evaluating the hip muscles in soccer players with osteitis pubis for pre-screening, improve the quality of the rehabilitation programs, and guide the decision to return to sports after injury.

[1] Buraydah Private Colleges, College of Applied Medical Sciences, Physiotherapy Department,
e-mail: w.m.e.elsais@edu.salford.ac.uk
[2] Cairo university, Faculty of Physical therapy, biomechanics Department, e-mail: walaa.sayed@pt.cu.edu.eg

Problem of body configuration of physiotherapy students while lifting a load

W. S. Erdmann[1], E. Prętkiewicz-Abacjew[2], M. Opanowska[3]

Key words: *lifting load, body configuration, physiotherapy students*

1. Introduction

Lifting of the objects is often an action in everyday life. This is practiced at home, during professional work, at the sports. Unfortunately, the technique of movement of lifting is often improper. People hold their trunk in horizontal position and have straighten lower extremities (Fig. 1). Within the medical profession lifting of heavy persons takes place by the members of the rescue team during lifting of victims of accidents, lifting of patients by nurses, lifting of patients by physiotherapy personnel during kinesitherapy exercises. Low back pain is one of the most common symptoms motivating people to seek medical help [1]. One of the reasons for that kind of pain is wrong approach to lifting of heavy load. The aim of the presentation is a description of physiotherapy students' knowledge aiming at lifting of heavy object. This is a continuation of [2].

A **B**

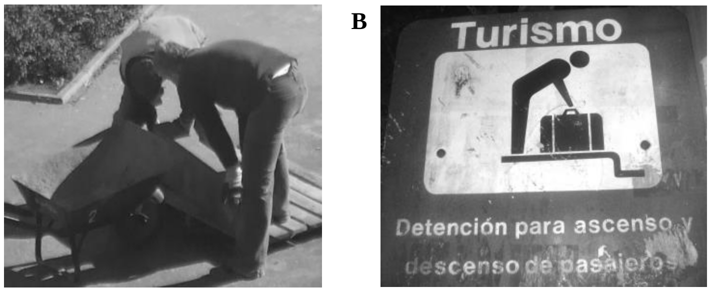

Fig. 1. Wrong lifting of heavy objects: **A** – by construction workers; **B** – shown on a road sign.

2. Material and Methods

2.1. Investigated subjects

The subjects were 65 students (39 females and 26 males) of physiotherapy major. They were 20 years old, 170.3 cm (females) and 182.1 cm (males) of height, and 60.7 kg (females) and 82.6 kg (males) of body mass. All students were at the beginning of biomechanics classes before teaching on optimal load carrying behaviour.

2.2. Method

Students were asked to mark (pretend) of lifting of a heavy object. i.e. a light plastic box with 5 reams of paper inside. The total mass of a paper was m = 12 kg. Students stayed in front of a box with self-acquired distance and with self-acquired configuration of the body. Students then were photographed from the side (in sagittal plane). On the photographs distances and angles of body configuration were measured.

[1]Gdansk University of Physical Education and Sport, Chair of Health and Natural Sciences, Gdansk, Poland,
e-mail: wlodzimierz.erdmann@awf.gda.pl
[2]Gdansk College of Health, Faculty of Physiotherapy and Health Sciences, Gdansk, Poland,
e-mail: elabacjew@op.pl
[3]Gdansk University of Physical Education and Sport, Dept. of Methodology of Phys. Ed., Gdansk, Poland,
e-mail: monkao84@wp.pl

3. Results

The distance of students' toes from the box was in mean data 9.1 and standard deviation 6.4 cm for women and 7.3 (6.2) cm for men. Only 4 women and 3 men had their toes 0 cm from the box. The furthest distance was 21 cm. The angle of leaning the trunk was for women in mean data 74.9 (16.7) degrees from the vertical line and for men it was 78.3 (22.8) deg. 17 women and 16 men had their trunk leaned over 80 deg. Arm angle between vertical line and arm line for women was 12.9 (7.4) and for men was 10.7 (10.0) deg. Knee angle was for women 54.4 (39.0) and for men 38.4 (43.1) deg. Nine women and nine men had their knee angle below 10 deg, i.e. close to straighten legs.

4. Discussion and Conclusion

Several physiotherapy students, both women and men had their position during lifting a load in wrong configuration (Fig. 2). The most improper position was for the trunk. Leaning the trunk over 80 degrees, and this was for half of the subjects, was very dangerous for lumbar part of the vertebral column. The proper body position during lifting a load is shown in Fig 3. It is necessary to teach all people proper configuration of the body during lifting a load, especially for people who in their professional work need to carry heavy loads.

A B

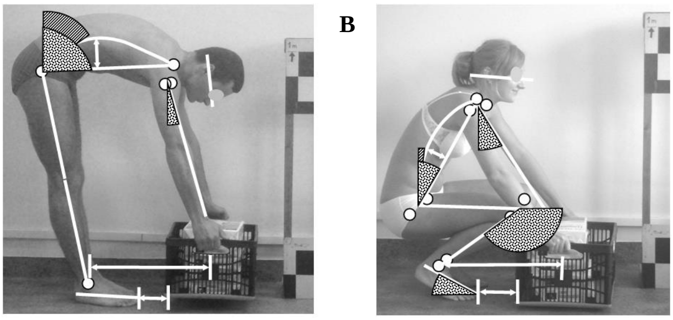

Fig. 2. Wrong positions acquired during lifting a load: trunk curved, feet too far from the load, hence upper extremities moved forward. In addition: **A** – straighten lower extremities, trunk and head in horizontal position; **B** – knees flexed, but here they are flexed too much, heels raised over the ground.

A B

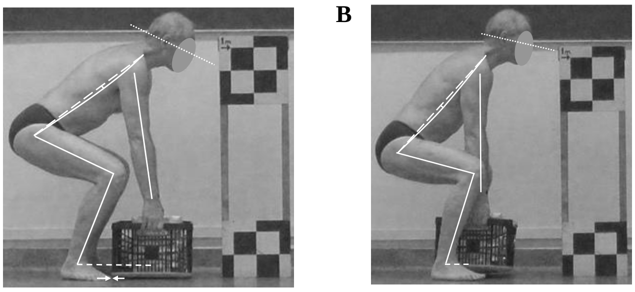

Fig. 3. Proper position of the body during lifting a load, i.e. head moved backward, straighten trunk with leaning at about 45 deg., hip and knee joints flexed at 80- 90 deg. Heels touch the ground. Load near feet (**A**) or even between feet (**B**).

References

[1] Allegri M., Montella S., Salici F. Valente A., Marchesisni M., Compagnone C., Baciarello M., Manferdini M.E., Fanelli G. *Mechanism of back pain: a guide for diagnosis and therapy,* F1000Res. 2016. Doi: 10.12688/f1000research.8105.2.

[2] Erdmann W.S., Prętkiewicz-Abacjew E., Orzechowska [now Opanowska] M. *Body configuration of physiotherapy students during lifting a load as counter-injury prophylaxis (in Polish).* Abstracts of Symposium "Movement analysis – theory and praxis in clinical applications". Warsaw: Institute "Monument – Centre of Child Health", 2010.

A correlational analysis of shuttlecock velocity and flighting angle kinematic determinants in the badminton forehand smash

A. FERREIRA[1], M. GÓRSKI[2], P. TABOR[3] J. GAJEWSKI[4],

Keywords: *technique, biomechanical, determinants, racket, speed*

1. Introduction

Badminton forehand smash is one of the most important strokes in professional badminton, resulting in shuttlecock's high velocity and steep downward angle [1]. Correct technique of this offensive shot leads to decreased opponent's reaction time and causes difficulty with shuttlecock defence [2]. The aim of this study was to examine the biomechanical parameters of elite badminton players while performing forehand smash and conduct correlation analysis of the shuttlecock's speed and flight angle kinematic determinants.

2. Materials and methods

2.1. Examined subject

Twenty-one elite professional badminton players (12 males and 9 females) – members of the Polish National Badminton Team participated in the study (see basic information in table 1). None of them reported any injuries for six months prior the study. The study received Ethical approval from the Senate Research Ethics Committee of Józef Piłsudski University of Physical Education in Warsaw, Poland.

	Age (years)	Training practice (years)	Body mass (kg)	Body height (cm)	BMI	% FAT (%)
Members of Polish National Badminton Team (n=21)	22.4 (± 4.4)	13.4 (± 4.1)	70.0 (± 10.6)	175.1 (± 11.6)	22.7 (± 1.9)	17 (± 7)

2.2. Methods

In order to measure kinematic variables during the forehand smash, the Vicon 3D motion capture system with 10 cameras (MX T40S, 200 Hz) was used. Three cameras were placed on the floor and 7 on the walls. Thirty-nine reflective markers were placed on the participant's body, following Plug-in-Gait markers' placement and reflective tape was placed on the shuttlecock's cork base.

Every player's task was to perform multiple forehand smashes, giving to the shuttlecock the highest possible velocity. Five smashes were recorded, in which the shuttlecock had to pass above the badminton net (155 cm) and under a colourful string visible for the athlete, placed 30 cm over the net (Fig.1.). In order to ensure the repeatability of the measurement conditions, the shuttlecock was released by the Leopard Smart shuttlecock's feeding machine during the performance of every smash. Rests between the attempts were administered at the request of the athlete. Kinematics variables (angles, angular velocities, centre of player's body mass) of the fastest smash of each participant were

[1]Józef Piłsudski University of Physical Education in Warsaw, Poland, Faculty of Physical Education,
e-mail: anna.glebocka@interia.pl
[2]Institute of Sport – National Research Institute, Department of Kinesiology, Warsaw, Poland,
email: michal.gorski@insp.waw.pl
[3]Józef Piłsudski University of Physical Education in Warsaw, Poland, Faculty of Physical Education,
e-mail: piotr.tabor@awf.edu.pl
[4]Józef Piłsudski University of Physical Education in Warsaw, Poland, Faculty of Physical Education,
e-mail: jan.gajewski@awf.edu.pl

calculated. Relationships between the variables were assessed by calculating the Spearman's rank correlation coefficient. Computations were performed with STATISTICA software (v. 13.3, StatSoft, USA) and MS Excel.

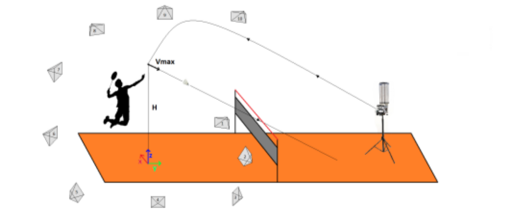

Fig. 1. Scheme of measuring station

3. Results

Mean shuttlecock velocity (V_{sh}) was 75 m/s (± 8.1) and mean shuttlecock flight angle (shuttlecock velocity vector inclination to the horizontal plane) (α_{sh}) was 11.8° (± 3.8). Statistical significant ($p<0.05$) positive correlation was found between both V_{sh} and α_{sh} and: height of the shuttlecock in the moment of contact with the racket (r=0.67; r=0.85 respectively); the height of the jump before the hit (r=0.74; r=0.85 respectively) and length of flight faze (r=0.59; r=0.44 respectively). Positive significant ($p<0.05$) relationship between both V_{sh} and α_{sh} was found also with: elbow flexion angle during shuttle and racket contact (r=0.47; r=0.58 respectively); angular velocity of shoulder internal rotation at the moment of shuttle and racket contact (r=0.63; r=0.46 respectively) and in its maximum moment r=0.66; r=0.51 respectively). Statistical significant ($p<0.05$) negative correlation was found for V_{sh} and: wrist abduction angle in the moment of the hit (r=-0.52) which means that a bigger wrist adduction angle results in a greater V_{sh}; wrist extension angle at the moment of the hit (r= -0.45), which means that a bigger wrist flexion angle results in a greater V_{sh}. Positive statistical significant relationship ($p<0.05$) was found between α_{sh} and: spine flexion angle in the moment of contact of shuttlecock with racket (r=0.77), at its maximal angular velocity (r=0.65); and maximal spine rotation angular velocity (counter clockwise direction for right-handed players) (r=0.55).

4. Conclusion

Positive significant correlation between V_{sh}, α_{sh} and height of jump before the hit, the height of shuttle in the moment of hit and flight faze time emphasise the importance of the jumping ability in badminton, for which a lot of general development training time should be dedicated. The relationship between V_{sh}, wrist flexion and adduction angle demonstrates the importance of a proper wrist movement for a successful smash. The relation between α_{sh} and spine flexion proves the importance of abdominal muscles activation during the smash performance. The impact of shoulder internal rotation and trunk rotation on the badminton forehand smash is consistent with the research of other scientists [1, 2].

Acknowledgments: Financial support: Project DM-61 implemented at the Józef Piłsudski University of Physical Education in Warsaw, Poland. DSN Scientific project implemented under contract No. 18/07/104.06/2019/WIN at the Institute of Sport – National Research Institute, Warsaw, Poland.

References

[1] ZHANG Z, LI S, WAN B, VISENTIN P, JIANG Q, DYCK M, LI H, SHAN G. *The influence of X-factor (trunk rotation) and experience on the quality of the badminton forehand smash.* Journal of human kinetics, 2016, 53(1), 9-22.

[2] KING M, TOWLER H, DILLON R, MCERLAIN-NAYLOR S. *A correlation analysis of shuttlecock speed kinematic determinants in the badminton jump smash.* Applied Sciences, 2020, 10(4), 1248.

Optimization on mechanical behaviour of hip implant designs

H. Göktaş[1], E. Subaşı[2], M. Uzkut[3], M. Kara[4], H. Biçici[5], E. Celik[6], H. Shirazi[7], K.N. Chethan[8], Ş. Mihçin[9]

Key words: *hip implant, Finite Element Method, static analysis, von Mises stress, total deformation*

Abstract

Total Hip Arthroplasty (THA) is one of the best advancements in healthcare. THA is required when the hip joint causes immobility and pain. The designed hip implants vary in geometry with different geometrical parameters. The geometry plays an important role in the mechanical behavior of the hip implant. In this study, the optimum selection of hip implant under static loading was evaluated using finite element modeling (FEM). Hip implants with three different stem cross-sections incl. (a) elliptic, (b) oval, and (c) trapezoidal were designed using a commercial Computer-Aided Design (CAD) software package. The FEM analysis was carried out via ANSYS R2019 to assess the key mechanical parameters of the implants such as stress distribution and deformation. The results were evaluated for the best stress and strain values. The optimum design had equivalent stress (von Misses) of 258,1 MPa, equivalent strain of 0.004, with total deformation of 0.24 mm and frictional stress of 0.362 MPa producing best values for trapezoidal cross-sectioned design. The findings of this study provided an insight into the selection of appropriate hip implant design with certain geometric design parameters to produce optimum results in clinical applications.

Acknowledgments

This research was funded by TUBITAK 2232 International Outstanding Researchers Fellowship Funding Scheme; Grant No of 118C188 'New Generation Implants for All' project.

The authors thank the Mechanical Engineering, Department of Izmir Institute of Technology for providing the high computational facility to carry out this research.

References

[1] Merola M., Affatato S., *Materials for hip prostheses: A review of wear and loading considerations.* Materials, 2019, 12(3), 495. doi:10.3390/ma12030495

[2] Ridzwan M., Shuib S., Hassan A., Shokri A., Mohamad Ib M., *Problem of stress shielding and improvement to the hip implant designs: A review.* Journal of Medical Sciences, 2007, 7(3), 460-467. doi:10.3923/jms.2007.460.467

[3] Mattingly D. A., *Cemented long-stem femoral components in revision total hip arthroplasty.* Revision Total Hip Arthroplasty, 1999, 239-243. doi:10.1007/978-1-4612-1406-9_32

[4] Ulrich S.D. et. al., *Total hip arthroplasties: what are the reasons for revision?* 2008 Oct;32(5):597-604.doi: 10.1007/s00264-007-0364-3. Epub 2007 Apr 19. PubMed PMID:17443324; PubMed PMCID : PMC2551710.

[1]Department of Mechanical Engineering, Izmir Institute of Technology, Urla, Izmir, TURKEY, e-mail: mustafakara0512@gmail.com

[2]Department of Mechanical Engineering, Izmir Institute of Technology, Urla, Izmir, TURKEY

[3]Department of Mechanical Engineering, Izmir Institute of Technology, Urla, Izmir, TURKEY

[4]Department of Mechanical Engineering, Izmir Institute of Technology, Urla, Izmir, TURKEY, e-mail: mustafakara0512@gmail.com

[5]Department of Mechanical Engineering, Izmir Institute of Technology, Urla, Izmir, TURKEY

[6]Department of Mechanical Engineering, Izmir Institute of Technology, Urla, Izmir, TURKEY

[7]Department of Mechanical Engineering, Izmir Institute of Technology, Urla, Izmir, TURKEY

[8]Department of Aeronautical and Automobile Engineering, Manipal Institute of Technology, Manipal Academy of Higher Education, Karnataka, INDIA

[9]Department of Mechanical Engineering, Izmir Institute of Technology, Urla, Izmir, TURKEY

[5] COLIC K., SEDMAK, A., GRBOVIC A., SEDMAK S., DORDEVIC B., *Finite Element Modeling of Hip Implant Static Loading*. Procedia Engineering, 2016, 149:257-262,DOI:10.1016/j.proeng.2016.06.664

[6] WANG L., THOMPSON J., *Finite element analysis of polyethylene wear in total hip replacement: A literature review,* Proc IMechE Part H: J Engineering in Medicine, 2019, DOI: 10.1177/0954411919872630

[7] BAURA G. D. *Total hip prostheses.* Medical Device Technologies, 2012, 381-404. doi:10.1016/b978-0-12-374976-5.00018-9

[8] KAYA F., İNCE G., AVCAR M., YÜNLÜ L. *Kalça protezi tasariminin sonlu elemanlar yöntemi ile statik analizi.* Mühendislik Bilimleri Ve Tasarım Dergisi, 2021, 9(1), 199-208. doi:10.21923/jesd.839995

[9] DAMM P., DYMKE J., ACKERMANN R., BENDER A., GRAICHEN F., HALDER A., BERGMANN G. *Friction in total hip joint prosthesis measured in vivo during walking.* PLoS ONE, 2013, 8(11). doi:10.1371/journal.pone.0078373

[10] RAMOUTAR D.N., CROSNIER E.A., SHIVJI F., MILES A.W., GILL H.S., *Assessment of Head Displacement and Disassembly Force With Increasing Assembly Load at the Head/Trunnion Junction of a Total Hip Arthroplasty Prosthesis.* J Arthroplasty. 2017 May;32(5):1675-1678. doi: 10.1016/j.arth.2016.11.054. Epub 2016 Dec 14. PMID: 28063775.

[11] RAWAL B., YADAV A., PARE V. *Life estimation of knee joint prosthesis by combined effect of fatigue and wear.* Procedia Technology, 2016, 23, 60-67. doi:10.1016/j.protcy.2016.03.072

[12] DARWICH A., NAZHA H., DAOUD M., *Effect of Coating Materials on the Fatigue Behavior of Hip Implants: A Three-dimensional Finite Element Analysis,* J. Appl. Comput. Mech., 2020¸6(2) 284-295, DOI:10.22055/JACM.2019.30017.1659

[13] CHANGQI L., et. al., *Femoral Stress Changes after Total Hip Arthroplasty with the Ribbed Prosthesis: A Finite Element Analysis*, BioMedResearchInternational, vol. 2020, Article,ID 6783936, 8 pages, 2020. https://doi.org/10.1155/2020/6783936

[14] ABDULLAH A.H., ASRI M., ALIAS M.S. TARDAN GIHA, *Finite Element Analysis of Cemented Hip Arthroplasty: Influence of Stem Tapers,* Proceedings of the International MultiConference of Engineers and Computer Scientists 2010 Vol III, IMECS 2010,March 17-19,2010, Hong Kong

[15] TANNER K.E., YETTRAM A.L., LOEFFLER M., GOODIER W.D., FREEMAN M.A., BONFIELD W., *Is stem length important in uncemented endoprostheses?* 1995 Jun;17(4):291-6, doi: 10.1016/1350-4533(95)90854-5.PubMed PMID:7633757.

[16] GRIZA S., REIS M., REBOH Y., REGULY A., STROHAECKER T.R. *Failure analysis of uncemented total hip stem due to microstructure and neck stress riser.* Engineering Failure Analysis, 2008, 15(7), 981–988. doi:10.1016/j.engfailanal.2007.10.012

[17] GRIZA S., ZANON G., SILVA E. P., BERTONI F., REGULY A., STROHAECKER T. R. *Design aspects involved in a cemented THA stem failure case.* Engineering Failure Analysis, 2009, 16(1), 512–520. doi:10.1016/j.engfailanal.2008.06.016

The effectiveness of original balance training programme on postural balance in middle-aged women – a pilot study

M. Grabowicz[1], A. Daniluk[2], A. Bugalska[3], S. Wójtowicz[4], K. wiaderna[5], A. Hadamus[6]

Key words: *postural balance, exercise*

1. Introduction

Postural balance enables the human body to maintain an upright posture and is essential to perform activities of daily living normally.

It has been proven that balance training implemented in healthy subjects is a good tool for the prevention and treatment of mechanical injuries [1], is a prerequisite for becoming a professional athlete [2] and is also important in the view of prevention of balance disorders in an older age [3]. Moreover, balance training may improve motor coordination [4], cognitive functions [5], proprioceptive input, reaction time and specified muscular strength [6].

The above reasons indicate that implementing balance training is crucial regardless of the age. Therefore new original training programmes as well as different training durations should be examined.

The aim of the present study was to investigate the effectiveness of an original training programme on postural balance in middle-aged healthy women. The secondary objective was to examine the training duration with positive effects on postural balance.

2. Material and methods

11 healthy middle-aged women were involved in this study (mean age = 55.07 ± 7.92, BMI = 27.29 ± 4.8). Participants performed a 4 week long progressive balance training with the frequency of exercises 3 times a week for 30 minutes per session. The training involved a warm up, a cool down and a main part with exercises subdivided into 4 sections: lower limbs muscles strengthening exercises; trunk muscles strengthening exercises; static balance exercises and dynamic balance exercises. The progression was reached by decreasing a base of support, adding an unstable surface and an exclusion of vision.

Each participant underwent postural balance assessments on the Biodex Balance System posturographic platform, including the Modified Clinical Test of Sensory Interaction for Balance (mCTSIB) 3 times: pre-training (Examination 1), in the middle of the training duration – after two weeks of exercises (Examination 2) and post-training – after four weeks of training (Examination 3). The level of statistical significance was set at $p<0.05$.

3. Results

[1]Department of Rehabilitation, Faculty of Medical Sciences, Medical University of Warsaw, Warsaw, Poland, e-mail: marta.grabowicz@wum.edu.pl
[2] Department of Rehabilitation, Faculty of Medical Sciences, Medical University of Warsaw, Warsaw, Poland, e-mail: anna.daniluk@wum.edu.pl
[3]Department of Rehabilitation, Faculty of Medical Sciences, Medical University of Warsaw, Warsaw, Poland, e-mail: aneta.bugalska@wum.edu.pl
[4]Department of Rehabilitation, Faculty of Medical Sciences, Medical University of Warsaw, Warsaw, Poland, e-mail: sebastian.wojtowicz@wum.edu.pl
[5]Department of Rehabilitation, Faculty of Medical Sciences, Medical University of Warsaw, Warsaw, Poland, e-mail: karolina.wiaderna@wum.edu.pl
[6]Department of Rehabilitation, Faculty of Medical Sciences, Medical University of Warsaw, Warsaw, Poland, e-mail: anna.hadamus@wum.edu.pl

The results demonstrated a significant difference in sway index in condition two of mCTSIB (eyes closed, firm surface) between Examination 1 and 3 (p=0.047), and between Examination 1 and 2 (p=0.045), but not between Examination 2 and 3 (p>0.05). However demonstrated difference was an increase of sway index. The other three conditions of mCTSIB (eyes open, firm surface; eyes open, foam surface; eyes closed, foam surface) did not indicate any significant differences between performed assessments.

4. Discussion and conclusion

A review of literature, in opposite to the present study showed that a balance training can be an effective tool for improving postural balance parameters in middle-aged women [7, 8]. Although, in the study of Anderson et al. similarly to the present study a 4 weeks-long progressive postural balance training with the frequency of 3 times per week was implemented, one training session lasted for 50 minutes, instead of 30 minutes like in the present study [7]. This might indicate that the 30 minutes is not enough to gain postural balance improvement after 12 exercise sessions. Another reason for this divergence between exisiting literature and the present study might be the selection of specific exercises and progression. The study of Nepocatych et al., demonstrated a significant improvement of sway index scores in conditions with altered vision and surface for the group which performed exercise programme on BOSU compared to the group which used STEP for exercise routine [8]. This might show that more exercises with altered surface should be conducted in order to improve postural balance.

Regardless of the age of the participants in the available studies, different durations of balance training have been included, varying from 2 to 32 weeks [1]. Interestingly, according to the systematic review of Lesinski et al. the most effective balance training period is 11-12 weeks. This is consistent with the present study which showed no significant improvement after 4 weeks of training.

Limitations of the present study include: short duration of the training programme, small sample size and no follow-up examination after finishing the exercise programme.

The present study has indicated that neither 2-week long, nor 4-week long postural balance training, performed 3 times a week is sufficient to improve postural balance in static conditions. Further research investigating different balance training programmes, possibly individually tailored, instead of group exercises and different training durations among various age groups should be conducted.

References

[1] LESINSKI M, HORTOBAGYI T, MUEHLBAUR T et al. *Dose-response relationships of balance training in healthy young adults: a systematic review and meta-analysis.* Sports medicine, 2015, 45(4), 557-576.

[2] GEBEL A, LESINSKI M, BEHM D.G et al. *Effects and Dose-Response Relationship of Balance Training on Balance Performance in Youth: A Systematic Review and Meta-Analysis.* Sports Medicine, 2018, 48(9), 2067-2089.

[3] SUNDSTRUP E, JAKOBSEN M.D, ANDERSEN J.L et al. *Muscle function and postural balance in lifelong trained male footballers compared with sedentary elderly men and youngsters*. Scandinavian Journal of Medicine and Science in Sport, 2010, 20(1), 90-97.

[4] OLIVEIRA A.S, SILVA P.B, LUND M.E et al. *Motor Coordination During a Perturbed Sidestep Cutting Task.* Journal of Orthopaedic and Sports Physical Therapy, 2017, 47(11), 853-862.

[5] ROGGE A.K, RODER B, ZECH A et al.. *Balance training improves memory and spatial cognition in healthy adults.* Scientific Reports, 2017, 5661(7):1-10.

[6] YAGGIE J.A, CAMPBELL B.M. *Effects of balance training on selected skills*. Journal of Strength and Conditioning Research, 2006, 20(2), 422-428.

[7] ANDERSON G.S, DELUIGI F, BELLI G. *Training for improved neuro-muscular control of balance in middle aged females*. Journal of Bodywork and Movement Therapies, 2016, 20(1), 10-18.

[8] NEPOCATYCH S, KETCHAM C.J, VALLABHAJOSULA S et al. *The effects of unstable surface balance training on postural sway, stability, functional ability and flexibility in women.* Journal of Sports Medicine and Physical Fitness, 2018, 58(1-2), 27-34.

Trends in balance maintaining rehabilitation based on review of currently used virtual reality using systems

G. GRUSZKA[1], P. WODARSKI[2], M. PLES[3], M. CHMURA[4], A. BIENIEK[5], J. JURKOJĆ[6]

Key words: *Virtual Reality, Balance maintaining, Physical rehabilitation*

1. Introduction

Physical rehabilitation of human ability to maintain balance is a process taking long time and requiring a close and strict cooperation between the patient and her/his physiotherapist. This process is known to be discouraging to patients due to its monotonousness, lack of noticeable changes in short amounts of time and problems with access to facilities responsible for conducting the rehabilitation process. Throughout classic physical rehabilitation process physiotherapists do not have access to any form of quantitive data which would allow them to evaluate whether exercises performed by their patients give any positive results, thus prolonging the entire process. Qualitative data, being the only accessible to therapists, is unobjective and therefore can lead to various results, depending on interpretation of therapists themselves. One of possible solutions to those difficulties and inconveniencies is introduction of virtual reality (VR) to physical rehabilitation process.

Restoring patient's ability to maintain balance very often requires use of various supporting devices, which cause the process to be more efficient or make it possible at all to restore one's balance maintaining ability. Patients have to be constantly supervised by one if not more physiotherapists in order to assure patient's safety and correctness of performed exercises. This leads to increase in costs of rehabilitation and problems with terms of rehabilitation start. All of aforementioned issues cause patients to lose their will to complete rehabilitation process and decide to drop out before regaining their health [1].

In past two decades physical rehabilitation was getting increasingly improved by introduction of new systems, exercising devices and changes in approach. VR and Augmented Reality (AR) have been becoming progressively more recognizable means of enhancing the rehabilitation process, giving patients the aspect of fun and gamification to boring and monotonous process of regaining balance maintaining ability, while at the same time providing therapists with valuable quantitative data. More and more publications state that not introducing VR or AR to physical rehabilitation is unreasonable, since reported results conclude, that use of these technologies is either beneficial or neutral to patients [2].

2. Methodology

Publication bases we reviewed include: Mendeley (prior to version 1.19.8), Pubmed, Researchgate and Google Scholar. In order to include a paper to our article it had to research use of VR, AR or "exergaming" in relation to physiological rehabilitation. Papers describing use of standalone VR/AR systems as rehabilitation equipment or conventional rehabilitation equipment converted or adapted to make use of VR/AR equipment, or researching the topic of "exergaming" with descriptions of used systems were included, unless the principles of working or the components of custom made systems were not described. No particular illness, impairment, dysfunction or disease was focused on, neither the duration of research and amount of participating patients/research subjects were taken into account. Papers no older than from 2010 were taken into account. To find

[1]Department of Biomedical Engineering, SUT, Zabrze, Poland, e-mail: grzegorz.gruszka@polsl.pl
[2]Department of Biomedical Engineering, SUT, Zabrze, Poland, e-mail: piotr.wodarski@polsl.pl
[3]Department of Biomedical Engineering, SUT, Zabrze, Poland, e-mail: marek.ples@polsl.pl
[4]Department of Biomedical Engineering, SUT, Zabrze, Poland, e-mail: marta.chmura@polsl.pl
[5]Department of Biomedical Engineering, SUT, Zabrze, Poland, e-mail: adnrzej.bieniek@polsl.pl
[6]Department of Biomedical Engineering, SUT, Zabrze, Poland, e-mail: jacek.jurkojc@polsl.pl

publications to review following strings were typed in each of publication bases: “VR rehabilitation”, “VR ‘AND’ rehabilitation”, “Virtual reality rehabilitation”, “virtual reality ‘AND’ rehabilitation”, “Exergaming”, “VR Balance”, “Virtual Reality balance rehabilitation”, “Virtual Reality Balance”. Duplicates were discarded and over 100 publications were reviewed.

2. Findings and discussion

24 publications were taken into consideration after applying the inclusion criteria. A table giving a short description of systems used in each of the publications and methods of evaluating the rehabilitation results was created. Review of selected publications allowed us to divide systems used in considered publications into two groups: not-widely available, made purely for research/rehabilitation purposes, allowing replication of scenarios at high similarity to real life situations “big” systems, and widely and easily accessible to everyone, not taking much space “small” systems made mainly for entertainment purposes or altered conventional equipment.

Analysis of our findings allowed us to get into conclusions: the big and less accessible systems are used less frequently for commencing research that is later described in publications. Reasons for such outcome are multiple – their availability is smaller, making regular measurements over greater duration of time more troublesome, commencing alterations to those systems is not simple and their rehabilitative value is small due to inaccessibility. Small systems allow patients to train comfortably in their homes or at local rehabilitation facilities, the gamification factor is usually already included (for example with Nintendo Wii Balance Board or the Microsoft Kinect), and none to little changes in the hardware or software have to be made in order to perform research. It can be checked whether just using the systems in their stock state increases the ability to maintain balance [3], or custom hardware, scenarios and programs to gather data from devices can be created and allow different kinds of research [4].

From the performed review we can conclude that small, easy to access and to customise “small” systems are becoming progressively more popular, and are starting to be just as valuable research and rehabilitation equipment as the “big” systems. What is more, patients can use them whenever they want or are advised to due to accessibility of those systems and their small size. On the other hand, the “big” systems use highly more advanced components and provide data inaccessible through use of small systems, for example because of their smaller maximum sampling frequency or lack of effectors used for simulation of conditions which would provide data corresponding more to real life stimulis, and therefore cannot be discarded as research tools.

References

[1] G. C. Burdea, “Virtual Rehabilitation - Benefits and Challenges,” *Methods Inf. Med.*, vol. 42, no. 5, pp. 519–523, 2003, doi: 10.1055/s-0038-1634378.

[2] D. Cano Porras, P. Siemonsma, R. Inzelberg, G. Zeilig, and M. Plotnik, “Advantages of virtual reality in the rehabilitation of balance and gait: Systematic review,” *Neurology*, vol. 90, no. 22, pp. 1017–1025, 2018, doi: 10.1212/WNL.0000000000005603.

[3] H. Bateni, “Changes in balance in older adults based on use of physical therapy vs the Wii Fit gaming system: A preliminary study,” *Physiother. (United Kingdom)*, vol. 98, no. 3, pp. 211–216, 2012, doi: 10.1016/j.physio.2011.02.004.

[4] M. M. Lee, K. J. Lee, and C. H. Song, “Game-based virtual reality canoe paddling training to improve postural balance and upper extremity function: A preliminary randomized controlled study of 30 patients with subacute stroke,” *Med. Sci. Monit.*, vol. 24, pp. 2590–2598, 2018, doi: 10.12659/MSM.906451.

Numerical analysis of scoliosis brace

S. GRYCUK[1], P. MROZEK[2]

Key words: orthotics, FEM, principal stress vector, principal stress trajectories

This article presents the results of numerical finite element method (FEM) simulations in the Ansys environment of a Boston orthopaedic brace. A reverse engineering methodology based on digitization by means of a three-dimensional (3D) optical scanner was employed to develop the geometric model. Special attention was paid to applying the same loads and boundary conditions as in numerical simulations during experimental testing. The force flow lines characterizing the brace and indicating the general working method of the orthosis's structure were determined using the FEM model. Identification of the main areas of the orthosis, carrying loads correcting the spine and of the positions of sites exerting little effort, from the perspective of their participation in the orthosis's essential therapeutic application, was carried out. Methods for mechanical optimization of the brace's design can be proposed based on the results obtained. As the conducted analysis is universal in character, it can be adapted to other types of orthopaedic braces.

References

[1] CHAN W.Y., YIP J., YICK K.L., NG S.P., LU L., CHEUNG K.M.C., ... TSE C.Y,. *Mechanical and clinical evaluation of a shape memory alloy and conventional struts in a flexible scoliotic brace*, Annals of Biomedical Engineering, 2018, 46(8), 1194-1205.

[2] CHUNG C.L., KELLY D.M., STEELE J.R., DIANGELO D.J., *A mechanical analog thoracolumbar spine model for the evaluation of scoliosis bracing technology*, Journal of Rehabilitation and Assistive Technologies Engineering, 2018, 5, 2055668318809661.

[3] GUAN T., ZHANG Y.F., *Determination of three-dimensional corrective force in adolescent idiopathic scoliosis and biomechanical finite element analysis,* Frontiers in Bioengineering and Biotechnology, 2020, 8.

[4] KELLY D.W., TOSH M.W., *Interpreting load paths and stress trajectories in elasticity*, Engineering Computations, 2000, 17(2), 117-135.

[5] KHLIF M., MASMOUDI N., BRADAI C., *Polypropylene tensile test under dynamic loading*, Journal of KONES, 2014, 21.

[6] NG K.J., DUKE K., LOU E., *Investigation of future 3D printed brace design parameters: evaluation of mechanical properties and prototype outcomes*, Journal of 3D Printing in Medicine, 2019, 3(4), 171-184.

[7] NIJSSEN J.P., RADAELLI G., HERDER J.L., KIM C.J., RING J.B., *Design and analysis of a shell mechanism based two-fold force controlled scoliosis brace*, International Design Engineering Technical Conferences and Computers and Information in Engineering Conference. American Society of Mechanical Engineers, 2017, V05AT08A014.

[8] RAUX S., KOHLER R., GARIN C., CUNIN V., ABELIN-GENEVOIS K., *Tridimensional trunk surface acquisition for brace manufacturing in idiopathic scoliosis*, European Spine Journal, 2014, 23(4), 419-423.

[9] RIGO M., JELAČIĆ M., *Brace technology thematic series: the 3D Rigo Chêneau-type brace*, Scoliosis and Spinal Disorders, 2017, 12(1), 1-46.

[1] Institute of Biomedical Engineering, Faculty of Mechanical Engineering, Bialystok University of Technology, Bialystok, Poland, e-mail: s.grycuk@doktoranci.pb.edu.pl

[2] Institute of Biomedical Engineering, Faculty of Mechanical Engineering, Bialystok University of Technology, Bialystok, Poland

Assessment of the effectiveness of rehabilitation after total hip replacement surgery using sample entropy

A. HADAMUS[1], M. BŁAŻKIEWICZ[2], D. BIAŁOSZEWSKI[3], K. WYDRA[4], A.J. KOWALSKA[5], E. URBANIAK[6], R. BORATYŃSKI[7], A. KOBZA[8], W. MARCZYŃSKI[9]

Key words: *body balance, osteoarthritis, postural control, sample entropy, total hip arthroplasty*

1. Introduction

Patients after total hip replacement (THR) load the feet asymmetrically during both standing and walking as well as during other activities of daily living. This may affect body balance [1,2]. Methods of re-education of postural stability include Virtual Reality (VR) training, which is also used to teach the patient how to correct limb loading [3]. Nonlinear measures, such as sample entropy, can capture the temporal component of the center of pressure (CoP) displacement. These measures make it possible to quantify the regularity, complexity, and efficiency or 'automaticity' of postural control [4,5]. The aim of this study was to assess the impact of additional virtual reality training on postural control changes.

2. Materials and methods

2.1. Participants and intervention

Fiftysix patients were randomly assigned to the experimental group (E-group; N=30) and control group (C-group; N=26). All patients had undergone THR within 2 to 12 weeks before the beginning of the study.

The C-group underwent standard post-operative rehabilitation (4 weeks, 5 times per week), while a VR training program (12 sessions – 3 times a week, 30 minutes each) was used in the E-group as an additional rehabilitation tool.

2.2. Measurements and calculations

The postural stability data were recorded using AMTI AccuSway platform during both legs standing tests with eyes open (EO) and with eyes closed (EC) (each 3 trials). The second attempt was analysed. Sample entropy (SampEn) was calculated for both CoP components: medio-lateral (ML) and anterior-posterior (AP) with the following equation:

---

[1]Department of Rehabilitation, Faculty of Medical Sciences, Medical University of Warsaw, Poland, e-mail: anna.hadamus@wum.edu.pl
[2]Faculty of Rehabilitation, The Józef Piłsudski University of Physical Education in Warsaw, Poland, e-mail: michalinablazkiewicz@awf.edu.pl
[3]Department of Rehabilitation, Faculty of Medical Sciences, Medical University of Warsaw, Poland, e-mail: dariusz.bialoszewski@wum.edu.pl
[4]Professor Adam Gruca Independent Public Teaching Hospital in Otwock, Rehabilitation Clinic, Otwock, Poland, e-mail: kamil.wydra@interia.eu
[5]Professor Adam Gruca Independent Public Teaching Hospital in Otwock, Rehabilitation Clinic, Otwock, Poland, e-mail: aleksandra.macheta@wp.pl
[6]Professor Adam Gruca Independent Public Teaching Hospital in Otwock, Rehabilitation Clinic, Otwock, Poland, e-mail: edyta.urbaniak@wp.pl
[7]Professor Adam Gruca Independent Public Teaching Hospital in Otwock, Rehabilitation Clinic, Otwock, Poland, e-mail: borek14@interia.eu
[8]Professor Adam Gruca Independent Public Teaching Hospital in Otwock, Rehabilitation Clinic, Otwock, Poland, e-mail: akobza@poczta.fm
[9]Medical Centre for Postgraduate Education, Professor Adam Gruca Independent Public Teaching Hospital in Otwock, Orthopaedics Clinic, Otwock, Poland, e-mail: wmarczynski@interia.pl

$$SampEn(m,r,N) = -ln\left(\frac{A^m(r)}{B^m(r)}\right)$$

SampEn was calculated using MATLAB (MathWorks, Natick, MA, U.S.A.) codes obtained from the Physionet tool [6] with "default" parameter values of m = 2 and r = 0.2*(standard deviation of the data). Statistical analysis was performed using Statistica 13.1 software with the p-value set at 0.05. Non-parametric tests were used.

3. Results

No differences were found between groups, neither before, nor at the end of the rehabilitation program. SampEn values increased after rehabilitation in E-group for test with EO and decreased for the test with EC. In the C-group SampEn values increased only for ML direction in the test with EO, while other values of SampEn (AP direction with EO, both directions with EC) decreased. All these changes were not statistically significant.

4. Discussion

The results obtained above are similar to those obtained before using classical body balance measures [7,8]. The results of the E-group are slightly better than in C-group. Higher values of SampEn in the test with eyes open indicate, that postural control in this condition is better after 4-weeks of rehabilitation. The fact that these changes were not statistically significant may be caused by a relatively small sample size or, more likely, slow recovery of joint function after 3rd week post-THR [9]. Hesseling et al. [9] confirmed with their study, that the physical outcome of over 95% of the patients after THR stays at the same level or slightly decreases after the 3rd week following surgery [9], which can partially explain why SampEn values for EC-tests decreased.

Acknowledgments: The study was financed from the NCBiR fund as part of the VB-Clinic project Strategmed III program.

References

[1] MIURA N., TAGOMORI K., IKUTOMO H., NAKAGAWA N., MASUHARA K., *Asymmetrical loading during sit-to-stand movement in patients 1 year after total hip arthroplasty.* Clin Biomech (Bristol, Avon), 2018, 57, 89-92.

[2] ZENI J.JR., ABUJABER S., FLOWERS P., POZZI F., SNYDER-MACKLER L., *Biofeedback to promote movement symmetry after total knee arthroplasty: a feasibility study.* J Orthop Sports Phys Ther, 2013, 43(10), 715-26.

[3] JURAS G., BRACHMAN A., MICHALSKA J. ET AL., *Standards of virtual reality application in balance training programs in clinical practice: a systematic review.* Games Health J, 2019, 8(2), 101-11.

[4] DONKER S.F., ROERDINK M., GREVEN A.J., BEEK P.J. *Regularity of center-of-pressure trajectories depends on the amount of attention invested in postural control.* Exp Brain Res, 2007, 181(1), 1-11.

[5] KĘDZIOREK J., BŁAŻKIEWICZ M., *Nonlinear measures to evaluate upright postural stability: a systematic review.* Entropy, 2020, 22, 1357.

[6] GOLDBERGER A.L., AMARAL L.A., GLASS L. ET AL., *Physiobank, Physiotoolkit, and Physionet: components of a new research resource for complex physiologic signals.* Circulation 2000, 101(23), E215-20.

[7] HADAMUS A., BIAŁOSZEWSKI D., URBANIAK E., ET AL., *The impact of training in virtual reality on balance in patients after total knee replacement is relatively slight*. Gait Posture 2020, 81(Suppl.1), 134-5.

[8] HADAMUS A., BIAŁOSZEWSKI D., KOWALSKA A.J., ET AL., *There is little impact of balance training in virtual reality on selected balance parameters in patients after hip arthroplasty*. Gait Posture 2020, 81(Suppl.1), 588.

[9] HESSELING B., MATHIJSSEN N.M.C., VAN STEENBERGEN L.N., MELLES M., VEHMEIJER S.B.W., PORSIUS, J.T., *Fast starters, slow starters, and late dippers: trajectories of patient-reported outcomes after total hip arthroplasty.* J Bone Joint Surg, 2019, 101(24), 2175-86.

Small unsecured objects transported in a vehicle and their impact on human head injury – blunt injury criterion approach

J. HRUBY[1], B. PARKER WHAM[2], Z. KROBOT[3], M. SEMELA[4]

Keywords: *Experiment, HIC, Impactor, Human Head, Interaction*

1. Introduction

The presented study deals with a familiar situation when unsecured objects are transported in a vehicle. Unsecured objects have a character of objects dedicated to daily usage – work purposes or personal purposes. That generally means laptops, cell phones, tablets, drinks in a glass bottle, objects for sports, and others. Objects of interest are considered stiff/rigid with an insignificant portion of deformability.

The study focuses on the interaction between unsecured objects placed inside a vehicle and vehicle occupants – if a traffic accident happens. If an unsecured object is randomly placed inside the vehicle's inner structure and the vehicle crashes into the barrier, the unsecured objects act like projectiles. These projectiles may, in some cases, interact with occupants' bodies. The interaction may cause, in specific cases, a severe occupant injury. Regarding the human body, the critical part taken for the study purposes is a human head – respectively rear part of a human head with a theoretically insignificant skin thickness. The blunt injury potential (when an unsecured object interacts with a human head) is calculated through Head Injury Criterion (HIC) and Blunt Criterion (BC). Blunt Criterion plays in the presented study a significant role because it serves as a HIC comparison and verification, and the inputs to Blunt Criterion must be carefully selected. If not, the correlation between Head Injury Criterion and Blunt Criterion is not adequately justified. The presented case study shows the selection of the proper and improper values for the Blunt Criterion computations and the influence of the selected values on obtained Blunt Criterion results.

2. Methods

The used equipment for the experimental investigation are as follows: Self-developed airgun with implemented pressure vessel, valves, and optical barriers for impactor velocity measurement; Vehicle seat with restraint system not including the seat head restraint; Hybrid III dummy for the frontal crash including measurement instrumentation and data acquisition system; Self-developed "stiff" impactors with different mass; Data Acquisition System DEWE A4 for object/impactor speed measurement.

[1]Institute of Forensic Engineering, BUT, Brno, e-mail: jaroslav.hruby@colorado.edu
[2]University of Colorado Boulder, 1111 Engineering Drive UCB 428, ECOT 441, e-mail: brad.wham@colorado.edu
[3]University of Defence, Brno, e-mail: zdenek.krobot@unob.cz
[4]Institute of Forensic Engineering, BUT, Brno, e-mail: marek.semela@usi.vutbr.cz

Fig. 1. Experimental Setup for Head Injury Investigation

NI DIADEM software with Crash Analysis Toolkit was used for the computation of HIC (equation (1) and (2)) [2]. Blunt Criterion was calculated through equation (3) [1] from projectile velocity and specific anthropometric values related to human anatomy. All necessary aspects of HIC and Blunt Criterion computations can be found in [1] and [2].

$$\mathrm{HIC}=\max_{t_1,t_2}\left\{\left(\frac{1}{t_2-t_1}\int_{t_2}^{t_1} a\,dt\right)^{2.5}(t_2-t_1)\right\} \quad (1)$$

$$a=\sqrt{a_x^2+a_y^2+a_z^2} \quad (2)$$

$$\text{Blunt Criterion} = \ln\left(\frac{{}^{1}/{}_{2}\cdot M\cdot V^2}{W^{1/3}\cdot T\cdot D}\right) \quad (3)$$

3. Results

Test results obtained from the experimental analysis (Blunt Criterion and HIC results) show that the critical impactor (unsecured object in the vehicle) speed, which can harm a vehicle occupant, is around 50 [km/h] – see Figure 2.

The experimental results also show that the increasing mass (from 0.5 [kg] to 1.5 [kg]) of the impactor (unsecured object in the vehicle) has a significant effect on the critical impactor (loose object in the vehicle) speed (mass increases = critical speed decreases; see Table 1).

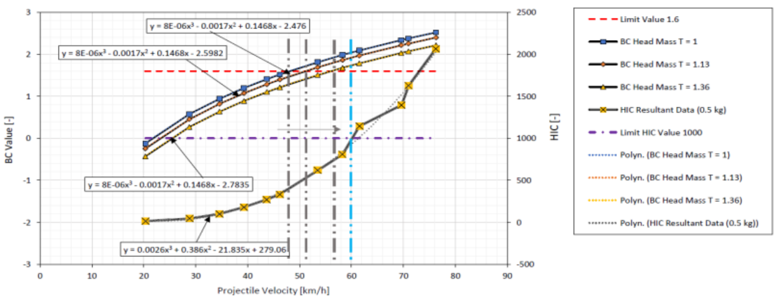

Fig. 2. Example: Obtained Results Based on Head Injury Criterion (HIC) and Blunt Criterion Calculations for Projectile with Mass 0.5 [kg] – Comparison with Critical HIC Value 1000 and Blunt Criterion Value 1.6 (for Blunt Criterion Calculations is used Variable skull and Soft Tissue Thickness)

3. Discussion

The experimental approach described above does not consider head movement during the vehicular crash and head interaction with airbags and other vehicle parts. It is because the experimental setup will be difficult to build. Also, HIC and Blunt Criterion analysis will be complicated to solve – problematic to find and analyze the proper impulse response. The length of the impact impulse is short (around 1.5 [ms]), and other tools are used to verify the injury potential calculated through HIC (Blunt Criterion usage).

References

[1] MACKAY M., *The Increasing Importance of the Biomechanics of Impact Trauma*, Sadhana, 2007, 397-408

[2] M. Frank, B. Bockholdt, D. Peters, J. Lange, R. Grossjohann, A. Ekkernkamp, P. Hinz, "Blunt Criterion trauma model for head and chest injury risk assessment of cal. 380 R and cal. 22 long blank cartridge actuated gundog retrieval devices ", Forensic Science International, Volume 208, Issues 1–3, Pages 37-41, 2011, ISSN 0379-0738

Using spherical contact pairs to model the contact areas in the joints of the wrist

P. IKONIAK[1], A. CISZKIEWICZ[2]

Key words: *Bone Contact, Sphere Fitting, Optimization*

1. Introduction

The wrist contains eight bones, which can be subdivided into two sets: proximal and distal. It is a bridge between the digits and the elbow joint. In total, the wrist connects fifteen bones in twenty-two joints, which makes it one of the most complex structures in the human body.

Many different approaches to wrist modelling are available in literature. The most common approach is to substitute the wrist with only a single or dual constraint, usually in the form of hinge joints [1,2]. However, this approach can be somewhat limiting when considering the contact mechanics in the joint. In these cases, the finite element method (FEM) is often employed [3,4]. The FEM offers better results but at a cost of numerical complexity. On the other hand, deformable contact pairs have been successfully employed for other body joints [5]. The approach provides more accurate results than simple constraints and is less computationally expensive than FEM. To the best of our knowledge, it has never been applied to the joints of the wrist.

Therefore, this study aimed to analyse whether the contact areas in all twenty-two subjoints in the wrist could be simplified using deformable spherical contact pairs. This study was limited to a geometrical analysis of the bone profiles.

2. Method

2.1. Acquiring the contact pairs

In this study, the geometrical models of wrist's joints were based on computer tomography (CT) scans downloaded from embodi3d.com. The details regarding the scans were as follows:

- filename: *ct wrist 1.0.0* by *Mahipal* at *https://www.embodi3d.com/files/file/38758-ct-wrist/*, under *CC – Attribution* license and accessed: 13.10.2020,
- filename: *my wrist 1.0.0* by *rajwardhan19* at *https://www.embodi3d.com/files/file/41972-wrist/*, under *CC – Attribution* license and accessed: 29.04.2021.

These CT scans were imported into *3D Slicer*, in which they were segmented using thresholding. The obtained meshes of the bones in the wrist were then cleaned out and smoothed in *Meshmixer*. *Meshmixer* was also used to select and cut the areas of the meshes corresponding to the contact regions in the subjoints of the wrist. The contact patches were selected taking into account the anatomical placement of the joint's cartilage. This was done for all twenty-two subjoints of the wrist in the first model and two selected subjoints in the second model. After that, a script was written in Python to fit spheres to the contact surfaces. The sphere fitting was performed with an optimizational approach and the script also allowed for visualization of the contact pair in *mayavi* and *matplotlib*.

2.2. Checking the quality of the contact pairs

The quality check of the obtained contact pairs was performed in two ways. We employed the standard deviation to assess the quality of the sphere fitting procedure for each sphere in all contact pairs. Then, visual representations of the contact pairs were used to check whether the pairs were valid in an anatomical sense. Based on the initial assessment of the results, we distinguished three different cases: a valid contact pair rated at 1.0 points – the anatomically smaller sphere was

[1]Faculty of Mechanical Engineering, Cracow University of Technology, Cracow, Poland,
e-mail: pawel.ikoniak@gmail.com
[2]Faculty of Mechanical Engineering, Cracow University of Technology, Cracow, Poland,
e-mail: adam.ciszkiewicz@pk.edu.pl

contained within the anatomically larger sphere (see Fig. 1), a partially invalid contact pair rated at 0.5 point, in which the two spheres intersected and an invalid contact pair rated at 0.0 points, in which the spheres did not form a ball-and-socket joint.

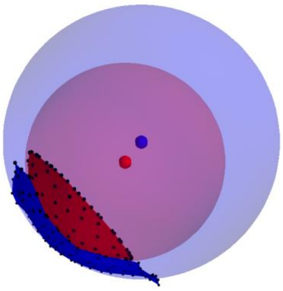

Fig. 1. A contact pair forming a proper ball-and-socket joint with the original meshes of the contact regions.

3. Results and discussion

Valid contact pairs were obtained in almost 60% of the studied subjoints, while the invalid contact pairs constituted only 23% of the cases. Notably, the proper pairs were observed mostly for the joints occurring in the proximal part of the wrist, involving the scaphoid and lunate bones. The worst results were obtained for the joints, which connect the wrist to the digits.

The results also contained several instances, in which the fitting procedure failed to deliver plausible results. This was reflected by unusually large values of radius for some pairs. Although we were unable to fully ascertain the cause of these results, our suspicion is that it was a failure of the fitting procedure. Nonetheless, a large value of radius might also suggest that plane-sphere contact should be employed. This issue requires further study.

4. Conclusions

The study presented an analysis of the contact areas of the joints of the wrist. In total, twenty-two unique subjoints were analysed in terms of whether the geometry of their articular surfaces could be simplified to simple sphere-sphere contact pairs. The contact pairs were obtained through a sphere fitting procedure with input based on two segmented CT datasets.

Our results were promising. In total, almost 60% of the studied joints, the articular surfaces could be simplified with a sphere-sphere contact pair. These cases corresponded mostly to the proximal part of the wrist. At the same time, for 23% of the joints in the distal part of the wrist, we were unable to obtain valid spherical contact pairs. This might suggest that contact pairs of different geometry should be employed in these joints.

References

[1] HOLZBAUR K.R.S., MURRAY W.M., DELP S.L., *A model of the upper extremity for simulating musculoskeletal surgery and analyzing neuromuscular control.* Ann. Biomed. Eng., 2005, 33, 829–840.

[2] QIN J., LEE, D., LI Z., CHEN H., DENNERLEIN J.T., *Estimating in vivo passive forces of the index finger muscles: Exploring model parameters*, J. Biomech., 2010, 43, 1358–1363.

[3] VARGA P., SCHEFZIG P., UNGER E., MAYR W., ZYSSET P.K., ERHART J., *Finite element based estimation of contact areas and pressures of the human scaphoid in various functional positions of the hand*, J. Biomech., 2013, 46, 984–990.

[4] MACHADO M., FLORES P., CLARO J.C.P., AMBRÓSIO J., SILVA M., COMPLETO A., LANKARANI H.M., *Development of a planar multibody model of the human knee joint*, Nonlinear Dyn., 2009, 60, 459–478.

The test of application a new structure in 3D printing elements of rehabilitation exoskeleton

M. JOHN-BANACH[1], A. JOHN[2]

Key words: *3D printing, rehabilitation exoskeleton, inverse honeycomb structure, FEM simulation, three-point bending test*

1. Introduction

Successful attempts to create and test samples of the modified (inverse) honeycomb structure gave rise to the design and testing of selected elements of rehabilitation exoskeletons for children. Proposing children as final recipients of designed and manufactured elements is connected with a few conditions. The first, affecting further research, is related to the available equipment and production capabilities of 3D printers. Available printers are Prusa i3 MK2 and Prusa i3 MK2S. The main restriction concerns the size of the manufactured elements. The second conditioning concerns the possibility of quickly introducing changes to the manufactured elements. It is associated with the rapid growth of children, especially limbs, as well as sometimes with the need to correct the shape of elements during rehabilitation.

You should also pay attention to aesthetic values - incremental technique can produce elements in different coulors, the surface of the elements can have a different texture (they can even be geometric patterns or taken from nature). These should be child-friendly structures. The costs of preparing and manufacturing a given product also play an important role. In this case, the costs are minimized due to the price of the raw material (ABS) as well as the production technology and necessary equipment (incremental technology, 3D printer). It was important to look for a light and durable structure. In the next step, technology was sought that would give the opportunity to create a given internal structure and external form personalized to a particular patient. In the case of children and the specifics of their bodies - continuous and rapid growth - it was important that the technology allowed for relatively quick and cheap creation of new elements.

2. Proposed structure

Based on previous studies of the honeycomb structure, it has been noticed that by introducing proportionally small changes, it is possible to produce acceptable in terms of quality samples of the modeled structure [1]. On this basis, it was decided to modify the honeycomb structure. As a result, a structure has been proposed, which can be described as inverse honeycomb structure. The proposed structure simultaneously eliminated problems with edge modeling and setting boundary conditions. At the same time, attempts were made to model a structure that would have variable geometry along both length and height. These types of issues are related to topological optimization, however, this paper did not address the issue of optimization but only used the results quoted in the literature.

The quantities that were determined during the simulation of the three-point bending test are the maximum linear displacement (deflection) and the maximum reduced and normal stress. The changes introduced in the sample structure reduce the maximum displacement and stress value in the tested samples. Strength tests were carried out on the MTS Insight 10 machine specially prepared for this test. The stand had to be adapted to the tested samples with small dimensions and applied forces. Six series of tests were carried out, five samples each. They differed in sizes of smaller and larger cells. As a result, they had different volume and mass. The sample volume with voids was equalized to the same but complete sample.

[1]Department of Fundamentals of Machinery Design Faculty of Mechanical Engineering Silesian University of Technology, Gliwice, Poland, e-mail: malgorzata.john@polsl.pl

[2]Department of Computational Mechanics and Engineering Faculty of Mechanical Engineering, Silesian University of Technology Gliwice, Poland, e-mail: antoni.john@polsl.pl

3. Application of the structure

Considering the above results, it was decided to develop, produce and numerically test a child's upper limb orthosis or exoskeleton rehabilitation element from the wrist to the elbow depending on the scope of application and cooperation with other elements of the device. Taking into account the results of previous studies [2, 3], a reverse honeycomb structure was proposed in a single-layer and double-layer version (Fig.1). The material used was generally available ABS (two colors: gray and black) and sample elements were made on the Prusa i3 MK3S printer. Dimensions were based on anatomical data - they were selected for a 12-year-old 50 Centile child (data for the North American population).

It was also assumed that the element must be relatively easy to make, have adequate strength and stiffness, and have a simple geometric shape. Modifications were introduced during the tests: thickness was changed, rounding was introduced, internal structure was changed.

a) b)

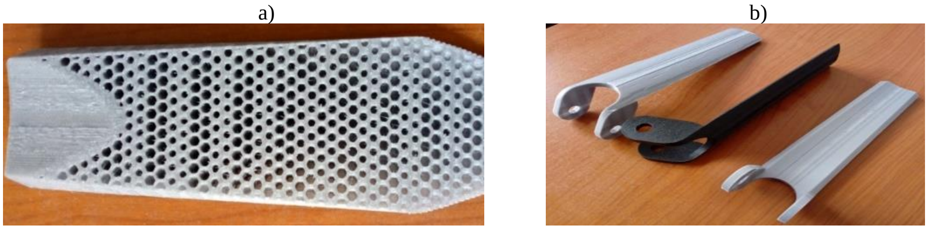

Fig.1. Manufactured elements: a) two-layers structure, b) orthosis components

The study attempts to show that the proposed structure allows, based on the analysis of stress and displacement, to select such geometrical parameters of the structure as to best match strength and stiffness to the requirements of given elements of an exoskeleton or orthosis, taking into account the minimization of production costs. Analysis of the results of numerical simulations made allowed to introduce further changes to improve the functionality of the structure.

4. Summary

Given the high potential of rapid prototyping techniques and the wide field of application in this paper the goal was formulated as: To develop a light structure that can be produced by rapid prototyping techniques. In addition, several restrictions have been imposed. This structure should: carry the load given; enable it to be adapted to a specific external shape; be relatively light; enable changes depending on the requirements; allow execution by means of the equipment owned; allow for relatively quick production (its structure and shape).

It was also assumed that the purpose of the work is not to search for new material, but to develop a new structure based on known and available materials. The obtained results indicate great possibilities of using new structures based on traditional materials. They are also the basis for more extensive research and simulation of applications in various fields, not only in biomechanics.

References

[1] JOHN M., JOHN A., *The influence of the model parameters of «honeycomb» structure on mechanical properties*, Mechanika, 2015, p. 116

[2] JOHN M., JOHN A., SKARKA W., *Numerical examination of like-honeycomb structures*, in AIP Conference Proceedings, 2018, t. 1922, nr 1, p. 80005

[3] JOHN M., JOHN A., SKARKA W., *The Inverse Honeycomb Structures in Numerical Modeling and Experiment*, Mechanika, 2018, t. 24, nr 3, pp. 299–304.

Model of the extraocular muscles control by information from vestibular system

R.R. KASPRANSKY[1], **A.P. KRUCHININA**[2], **Y.Y. MINYAYLO**[3]

Key words: *Vestibular system, vestibulo-ocular reflex, semicircular channels, extraocular muscles*

1. Eye movement

The vestibulo-ocular reflexes (VORs) are essential for maintaining clear vision during locomotion [2]. Mechanism of VOR is based on the relationship between the vestibular system and the extraocular muscles. The aim of the paper is to describe movement of eyeball as function of information from vestibular system.

The vestibular system exists to sense motion of the head and the orientation of the head with respect to gravity. Six oculomotor muscles provide movement of the eyeball. There are four rectus muscles: medial, lateral, superior and inferior, and there are two obliques: superior and inferior. Each muscle rotates the eye relative to some axis, which passing through the geometric center of the eye sphere. The position of this axis is determined by the geometric characteristics of each individual muscle and the position of the eye at the time of activation of the muscle. The combined contraction of these muscles allows you to move your gaze to any point lying in the field of view.

2. Eye rotation model

We consider eyeball as sphere rigid body with fixed geometric center. The origin of an orthogonal eye-fixed frame of reference with the X-, Y-, and Z-axes is placed in the eyeball center.

Rotation of rigid body describing by two parameters: axis of rotation and angle. we can find coordinates of rotation axis by calculating vector of force moment, as it's directed along the axis of rotation. Each of six muscles deliver its own force moment from initial position of eyeball. In this sense we can describe any movement of eyeball as forces moments composition of the activated muscles.

During the experiments the vertical semicircular channels were stimulated. According to Sentagotai's work [1] these channels are connected to the vertical rectus and oblique muscles. So our linear math model has form:

$$\vec{M}_{\text{eye up}} = a \cdot \vec{M}_{IO} + b \cdot \vec{M}_{SR}$$
$$\vec{M}_{\text{eye down}} = a_{\text{down}} \cdot \vec{M}_{SO} + b_{\text{down}} \cdot \vec{M}_{IR}$$

where $\vec{M}_{\text{eye up}}$ – the axis of rotation when the eye moves up, $\vec{M}_{\text{eye down}}$ – the axis of rotation when the eye moves down. Axis were fund from experiment.

The coefficients a and b reflect the quantitative contribution of the muscle to the observed movement: the greater the coefficient, the greater the contribution of the muscle.

We present the coefficients a and b as the sum of the information coming from the otoliths (the first term) and the information from the semicircular channels (the second term). The projection of gravitational acceleration on the otolith organs was proportional to cabin rotation angle. As a result the control coming from the otolith organs is proportional to the sine (in the case of coefficient a) or cosine (in the case of coefficient b) of the cabin rotation angle α.

The control coming from the semicircular channels proportional to the angular acceleration of the head ε.

[1]Gagarin Cosmonaut Training Center, Zvezdniy Gorodik, Moscow Russia, e-mail: r.kaspranskiy@gctc.ru
[2]Lomonosov Moscow State University, Moscow, Russia, e-mail: anna.kruchinina@math.msu.ru
[3] Lomonosov Moscow State University, Moscow, Russia,

$$a = a_o \cdot \sin\ \alpha + a_c \cdot \varepsilon$$
$$b = b_o \cdot \cos\ \alpha + b_c \cdot \varepsilon$$

3. Results

Testing the model on three experiments with the registration of the vestibulo-ocular reflex in response to rotations in the planes of functional pairs of vertical semicircular channels showed that the decomposition of the moment found experimentally in the form of a linear combination of the moments of forces of the activated muscles exists. In addition, the control can be decomposed into otolith and channel components. Each of them proportional to the corresponding information about the movement of the head - the control from the semicircular channels is proportional to the angular acceleration, and the otolith component is proportional to the projection of the gravitational acceleration on the plane of the macula of the otoliths.

References

[1] SZHENTAGOTHAI J., *Das Rolle Der Einzelnen Labyrinthrezeptoren Bei Der Orientation Von Augen Un Copf Im Raume.* // Academiai Kiado, Budapest, –1952

[2] GOLDBERG J. M., WILSON V. J., CULLEN K. E. *The vestibular system. A sixth sense.*– Oxford University Press – 2012.

Effects of various stance widths on postural control during squat

J. KĘDZIOREK[1], M. BŁAŻKIEWICZ[2]

***Key words**: squat, sample entropy, center of pressure, postural control*

1. Summary

Squatting is known as a core exercise which requires coordinated actions of all major body joints. This enables individuals to select different movement strategies to perform squats. The aim of the study was to evaluate effect of various stance widths during squat on postural control. Twenty healthy individuals participated in this study. Each participant performed ones each type of squat cycle with narrow stance (NS), hip stance (HS) and wide stance (WS). In WS squat, the strategy (high LyE), amount of irregularity (high SampEn), and complexity in terms of the roughness of time-series (high FD) were significantly affected. It can therefore be concluded that in terms of complexity of postural control, this squat is the best.

2. Introduction

Postural control is a fundamental motor skill that provides the basis for most movement tasks [1, 2]. The postural control system regulates the body's motion through the complex interaction of somatosensory, visual and vestibular sensory feedback networks, numerous brain regions, and the musculoskeletal system. Squatting is known as a core exercise for many purposes. This is as a complex movement which requires coordinated actions of the torso and all major joints of the lower extremities. Furthermore, this complexity enables individuals to select different movement strategies to perform the squat. One of such strategies is back foot loading, which should minimize anterior displacement of the knee. Unfortunately, such a strategy with different foot settings can lead to a fall. The aim of the study was to evaluate the effect of various stance widths on postural control during squat.

3. Methods

Twenty healthy individuals (24.36 ± 1.86 yrs; 62.14 ± 8.34 kg; 168.5 ± 4.05 cm) participated in this study. The study included 3 different types of squats, depending on stance widths (Fig. 1). The following foot settings were taken into account: narrow stance (NS), hip stance (HS) and wide stance (WS), with foot angle placements set at 0 degree.

Fig. 1. Foot placement during squats: A. Narrow (NS), B. Hip (HS), C. Wide (WS).

Each participant performed each type of squat cycle (duration 15 sec). A single squat cycle was defined with participants starting in an upright position (duration 5 sec), moving downwards to the lowest point possible, and returning to the upright position (remaining time). During the squat, the feet could not leave the floor. Center of pressure (CoP) trajectories in the anterio-posterior (AP) and medio-lateral (ML) directions were measured using the Zebris FDM at a sampling rate of 100Hz. The study used three nonlinear measures to assess CoP dynamics: sample entropy (SampEn), largest

[1]Józef Piłsudski University of Physical Education in Warsaw, Poland, e-mail: justyna.kedziorek@awf.edu.pl
[2]Józef Piłsudski University of Physical Education in Warsaw, Poland, e-mail: michalinablazkiewicz@gmail.com

Lyapunov exponent (LyE) and fractal dimension (FD). The nonlinear coefficients were counted using MatLab software. The SampEn, LyE and FD were calculated according to [1, 2]. All statistical analysis was performed using Statistica software. One-way Anova and post-hoc Tukey HSD test was used in order to assess differences between the squats.

4. Results and Discussion

It was demonstrated that the CoP path length was significantly longer for WS squat compared to the others (Fig. 2). For nonlinear parameters, significant differences were found for all nonlinear parameters in the AP direction between NS, HS and WS squats (Fig. 2).

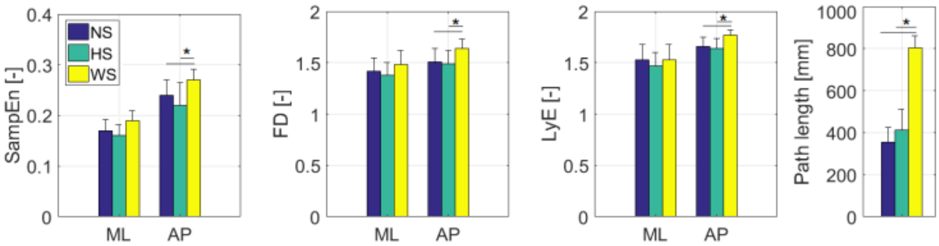

Fig. 2: Mean and standard deviation of nonlinear and linear parameters during all type of squats, * - significant differences.

It is worth adding that the values of all nonlinear parameters were significantly higher in the AP direction in relation to the ML direction for each type of squat.

5. Conclusions

Higher value of CoP path length for the WS squat allows to reach the conclusion that this squat was the least stable. However, looking at the high values of nonlinear parameters, it can be concluded that WS squat, due to the wide spacing of the feet, allowed for a much greater range of motion in the sagittal plane. Presence of high LyE values in AP direction indicates elasticity in adapting to the environment. Thus, in wide squat, the strategy (high LyE), amount of randomness, or irregularity (high SampEn), and complexity in terms of the roughness of time-series (high FD) were significantly affected. It can therefore be concluded that, in terms of complexity, this squat is the best.

Acknowledgments: This work was supported by the Ministry of Science and Higher Education in the year 2020-2022 under Research Group no 3 at Józef Piłsudski University of Physical Education in Warsaw “Motor system diagnostics in selected dysfunctions as a basis for planning the rehabilitation process”.

References

[1] BŁAŻKIEWICZ M., *Nonlinear measures in posturography compared to linear measures based on yoga poses performance.* Acta of Bioengineering and Biomechanics, 2020, 22(4), 15-21.

[2] KĘDZIOREK J., BŁAŻKIEWICZ M., *Nonlinear Measures to Evaluate Upright Postural Stability: A Systematic Review*. Entropy, 2020, 22(12), 1357

Using nonlinear measures to evaluate postural control in healthy adults during bipedal standing on an unstable surface

J. KĘDZIOREK[1], M. BŁAŻKIEWICZ[2], K. KACZMARCZYK[3]

Key words: *center of mass, visual control, sample entropy, fractal dimension, Lyapunov exponent*

1. Introduction

Postural control while maintaining an upright standing posture is a fundamental motor skill that provides the basis for most movement tasks. The aim of this study, therefore, was to assess the complexity of postural control in healthy adults during bipedal standing on an unstable surface in eyes-open and eyes-closed trials, in particular using three nonlinear indicators: sample entropy (SampEn), fractal dimension (FD), and the Lyapunov exponent (LyE).

2. Material and Methods

2.1. Participants and protocol

Fourteen young adults (8 men and 6 women) participated in this study, with mean age 24.07±7.32 years, mean body mass 68.57±10.68 kg and mean height 174.36±8.48 cm. No participants had any musculoskeletal or neurological deficiencies. The postural stability data for each subject, located 54 cm above ground, were recorded using the Biodex Balance System SD (BBS, Biodex, Shirley, NY) tilting platform. The BBS system was synchronized with a motion capture system (Vicon Motion Systems Ltd, Oxford, UK) consisting of 9 infra-red cameras (sampling rate 100 Hz). Vicon was employed to collect kinematics data on center of mass (CoM) displacement. 34 spherical markers were placed at anatomical landmarks of each person according to the biomechanical model full body PlugInGait standards available within the Vicon system.

Each participant underwent 3 trials in the following order: bipedal standing on BBS plate with eyes open (EO), and with eyes closed (EC), and also a Fall Risk (FR) test – all three with arms held downward alongside the trunk of the body. Each measurement took 20 seconds, with a 5 minute break between trials. During the EO and EC tests, the stability of the BBS plate was set at level one (the least stable platform); during the FR test the platform changed stability from very unstable to slightly unstable (from 6 to 2). Each test was recorded once for each participant, in order to reduce the potential effects of learning and fatigue.

2.2. Data calculations and nonlinear analysis

From the Vicon system, displacements of CoM data in each direction (x, y, z) were exported. All subsequent calculations were made using MatLab software (MathWorks, USA). The 3D CoM path length (CoM_pl) was calculated. Moreover, CoM path length was calculated in each plane: sagittal (yz), transverse (xy) and coronal (xz). For each of the CoM components: x – medio-lateral (ML), y – anterior-posterior (AP), z – proximal-distal (PD), three nonlinear indexes were calculated: sample entropy (SampEn) [1], the Lapunov exponent (LyE) [2] and fractal dimension (FD) [3].

Statistical analysis was performed using the Statistica software (StatSoft, USA), with the p-value set at 0.05. Normality of data distribution was assessed using the Shapiro-Wilk test. A factorial Anova was used to check whether the disabling of visual feedback and the direction of movement as well as the interaction of these two factors significantly affect changes in nonlinear parameters. Post-hoc analyses was performed using Tukey's HSD test.

[1]Józef Piłsudski University of Physical Education in Warsaw, Poland, e-mail: justyna.kedziorek@awf.edu.pl
[2]Józef Piłsudski University of Physical Education in Warsaw, Poland, e-mail: michalina.blazkiewicz@awf.edu.pl
[3]Józef Piłsudski University of Physical Education in Warsaw, Poland, e-mail: katarzyna.kaczmarczyk@awf.edu.pl

3. Results

Application of the factorial Anova and post-hoc Tukey HSD test showed a significant effect of visual feedback, direction and the interaction effect (visual feedback x direction) on postural stability assessed with nonlinear parameters. The main effect of visual feedback was significant ($F(3, 76) = 28.747$, $p = 0.0001$) for all nonlinear parameters. SampEn, FD and LyE values were significantly higher during trials with eyes closed compared to those with eyes open (Fig. 1A-C).

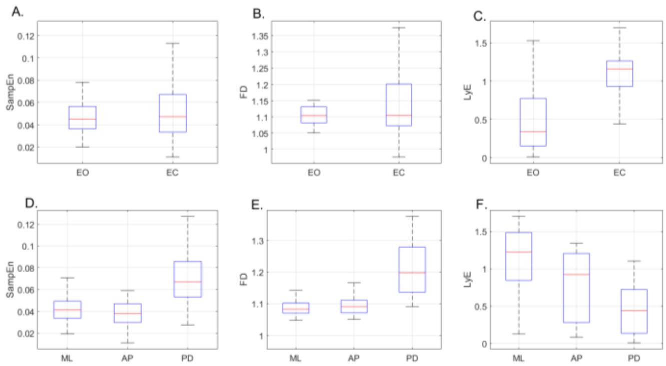

Fig. 1. The main effect of visual feedback and direction for nonlinear parameters: A., D. Sample Entropy; B., E. fractal dimension; C., F. Lyapunov exponent. The central mark indicates the mean, and the bottom and top edges of the box indicate the 25^{th}, 75^{th} percentiles, respectively. The whiskers extend to the most extreme data points.

The main effect of sway direction was also significant ($F(6, 152) = 31.096$, $p = 0.0001$). SampEn and FD values were significantly higher in the PD direction compared in the ML direction. Opposite results were obtained for LyE; here the values were the highest for the ML direction and the lowest for the PD direction (Fig. 1D-F).

4. Discussion

Excluding visual feedback was found to cause a significant increase in linear and nonlinear parameters. Moreover, SampEn and FD values were found to be significantly higher in the PD direction as compared to AP or ML, whereas LyE values in this direction were minimal. Results show that the three nonlinear measures provide a useful way of evaluating postural control in healthy adults. Moreover, it seems that introducing an unstable surface meant that the projection of the CoM was not perpendicular to the surface, but rather set at a certain continually changing angle, forcing the whole system to adapt to chaotic and unpredictable conditions. Such refined changes in conditions can be evaluated in a precise way only by using nonlinear measures.

Acknowledgments: This work was supported by the Ministry of Science and Higher Education in the year 2020-2022 under Research Group no 3 at Józef Piłsudski University of Physical Education in Warsaw "Motor system diagnostics in selected dysfunctions as a basis for planning the rehabilitation process".

References

[1] GOLDBERGER A.L., ET AL., *PhysioBank, PhysioToolkit, and PhysioNet: components of a new research resource for complex physiologic signals*, Circulation, 2000, 101(23), E215-20.

[2] RAZJOUYAN J., ET AL. *A neuro-fuzzy based model for accurate estimation of the lyapunov exponents of an unknown dynamical system*, International Journal of Bifurcation and Chaos, 2012, 22(03), 1250043.

[3] HIGUCHI T., *Approach to an irregular time series on the basis of the fractal theory*, Physica D: Nonlinear Phenomena, 1988, 31(2), 277-283.

Biomechanical aspects of in vitro fertilization

N. KIZILOVA[1], L. BATYUK[2], A. KHALIN[3]

Key words: *computational fluid dynamics, embryo transfer, viscoelasticity, in vitro fertilization,*

1. Introduction

In vitro fertilization (IVF) is one of the widely known types of assisted reproductive technologies that includes artificial fertilization of the preliminary collected eggs, their culture during 4-6 days, further embryo transfer (ET) and its implantation into the uterus [1]. Mechanical factors play an essential role in cell divisions and embryo development, locomotion and invasion, differentiation and mechanotransduction that determines the success of the IVF [2]. In this study the biomechanical factors crucial for successful IVF are summarized. The patient specific ET technique based on CFD computations on individual geometry is proposed.

2. Aims

The study of the embryo injection, movement with the basic fluid and the cumulative stress experienced by the embryo during its movement in order to estimate the influence of the injection speed, size and viscoelastic properties of the embryo, and individual geometry of the uterus on success of the IVF. The adequate simplified models of the embryo as a viscoelastic sphere and the uterus with its patient-specific geometry are essential for correct quantitative estimations of possible damaging factors that may cause unsuccessful ET. CFD analysis is the most proper tool for the through analysis of this complex biomechanical process.

3. Methods

The following methods were used:

- Development of a rheological model of the embryo as modified viscoelastic Zener body,
- Development of simplified geometry of the uterus with individual shape, size and inclination angle,
- Performance of the CFD computations of embryo velocity and stress-strain state at different injection speeds,
- Analysis of the flow parameters and cumulative stress at the embryo surface obtained as a result of CFD simulations.

4. Results and discussion

A scheme of the displacements of the injected embryo in the uterus is presented in Figure1a. The mathematical problem formulation for the multiphase flow [3] (fluid, air bubbles and viscoelastic particles) is described by the steady Navier-Stokes equations at low Reynolds numbers $Re=10^{-3}$-10^{-1}. The pressure, velocity, normal and shear stress in the flow region and over the particles have been computed with AnSys2020R3. The particles of d=0.1 mm (smaller embryos) and d=0.1 mm (larger embryos) were located at different distances r/R=0; 0.25; 0.5; 0.75 (0,1,2,3 in Figure 1b) from the

[1]Warsaw University of Technology, Institute of Aeronautics and Applied Mechanics, Department of Power and Aeronautical Engineering, e-mail: n.kizilova@gmail.com
[2] Kharkiv National Medical University, Department of Department of Medical and Biological Physics, e-mail: liliyabatyuk24@gmail.com
[3] V.N. Karazin Kharkov National University, Faculty of Mathematics and Informatics, Department of Applied Mathematics, e-mail: anat.khalin@gmail.com

walls near the centre of the uterus (location **a** in Figure 1a), and their trajectories from the outlet of the injection tube to the fundus (locations **h, g, f, e** in Figure 1a) have been computed.

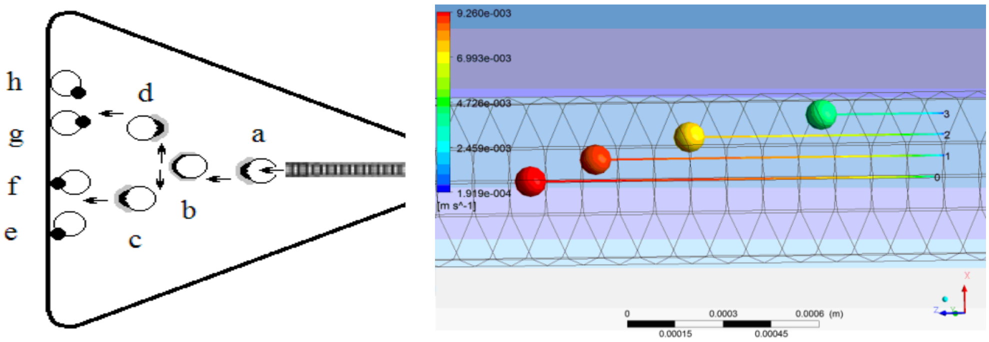

a b

Fig.1. Possible trajectories of the bubbles (white) with embryos (black) and transported liquid (grey); e,f and g,h are successful and unsuccessful locations of the bubbles at the wall (a), and the computed trajectories of the particles located at different distances from the wall.

As it was shown in [4], the shear stress experienced by the embryo during its movement and fluid-structure interaction may be a damaging signal and induce the embryo death due to the stress-activated apoptosis. The stress level could be well below the critical stress τ^* produced mechanical damage of the outer surface of the embryo. The cumulative stress experienced by the particle during its complex movements with fluid flows in the uterus (Figure 1a) is proposed here as a damage accumulation factor (DAF) computed as

$$\mathrm{DAF} = \frac{1}{\mathrm{IT} \cdot \Sigma \tau^*} \int_0^{\mathrm{IT}} \int_\Sigma \sqrt{\tau_{12}^2 + \tau_{13}^2 + \tau_{23}^2}\, \mathrm{d}\Sigma \mathrm{d}t\,, \qquad (1)$$

where Σ is the surface of the particle, τ_{ik} is the shear stress tensor computed at the surface of the particle. Fast injection may produce high DAF due to high shear stresses especially when the embryo is closer to the wall, while the slow injection may also give higher DAF values due to longer IT procedure.

The proposed approach will allow standard ultrasound-based measurements of individual geometry, in vitro estimation of individual viscoelastic parameters, and fast CFD computations of the proposed model with optimal location of the injection point and speed.

References

[1] ELAD, D., JAFFA, A. J., AND GRISARU, D., *Biomechanics of Early Life in the Female Reproductive Tract.* Physiology. 2020. 35(2): 134-143.

[2] YANIV, S., ELAD, D., JAFFA, A. J., EYTAN, O. *Biofluid aspects of embryo transfer*. Annals of Biomedical Engineering. 2003. 31:1255–1262.

[3] FENG, J.Q. *A long gas bubble moving in a tube with flowing liquid*. International Journal of Multiphase Flow. 2009. 35:738–746.

[4] XIE, Y., WANG, F., ZHONG, W., ET AL. *Shear stress induces preimplantation embryo death that is delayed by the zona pellucida and associated with stress-activated protein kinase mediated apoptosis.* Biology of Reproduction. 2006. 75:45–55.

3D Bioreactors for cell culture: fluid dynamics aspects

N. KIZILOVA[1] **J. ROKICKI**[2]

Key words: *tissue engineering, cell culture, fluid mechanics, mechanoelectric stimulation, computational fluid dynamics*

Abstract

Reconstructive therapy is essential in functionality restoration of the tissues impaired by congenital disorders, degenerative diseases and trauma that needs authentic cells for transplantation and tissue engineering. Petri dish and Cell Culture Flasks produce the cells which properties were changed by the contacts between the cells and the walls of the vessel. A bioreactor for tissue engineering applications should: (i) facilitate uniform cell distribution; (ii) provide and maintain the physiological requirements of the cell (e.g., nutrients, oxygen, growth factors); (iii) increase mass transport by diffusion and convection using mixing systems of culture medium; (iv) expose the cells to vital physical stimuli; and (v) enable reproducibility, control, monitoring and automation. Besides, bioreactors should present a simple reliable design preventing possible stagnation and allowing an easy access to the engineered tissue if any problem arises in the reactor during the operational period. In this paper the state-of-the-art review on different types of the reactors existed in the market, and their benefits is presented. The review is mostly concentrated on the fluid dynamics aspects of 3D dynamic cell culture technologies.

[1] Warsaw University of Technology, Institute of Aeronautics and Applied Mechanics, Poland,
V.N. Karazin Kharkov National University, Kharkiv, Ukraine, e-mail: e-mail: n.kizilova@gmail.com
[2] Warsaw University of Technology, Institute of Aeronautics and Applied Mechanics, Poland

Assessing the feasibility of using spherical contact pairs to model the contact regions in the joints of the index finger

K. KLUZA[1], A. CISZKIEWICZ[2]

Key words: *Multibody System Method, Bone Contact, Digit, Shape Fitting*

1. Introduction

The index finger is a complex structure in the human body, which contains three major joints:

- distal interphalangeal (DIP),
- proximal interphalangeal (PIP),
- metacarpophalangeal (MCP).

Each one of these joints connects two bones through the cartilage and a system of ligaments. In the available studies, the joints of the finger are usually replaced with simple constraints, such as revolute or spherical joints under the multibody system framework [1, 2], or modelled with complex geometry using the finite element method [3, 4]. The main aim of this research was to assess whether the contact areas in the three joints of the finger could be replaced with simple spherical contact pairs. This was motivated by the fact that such contact pairs would allow for more accurate contact analysis than the simplified constraints, while still being less computationally than the finite element method.

2. Method

2.1. Obtaining the contact pairs

Two computer tomography datasets of the index finger were acquired from *embodi3d.com* under the Creative-Commons By Attribution license. The details regarding the datasets were listed below:

- filename: *Hand surface scan 1.0.0* by *Krishna Josyula* at *https://www.embodi3d.com/files/file/40118-hand-surface-scan/* under *CC – Attribution license* and accessed: 25.11.2020,
- filename: *Kosci_dloni_3 1.0.0* by *MABC* at *https://www.embodi3d.com/files/file/22155-kosci_dloni_3/* under *CC – Attribution license* and accessed: 25.11.2020.

The scans were then imported into *3D Slicer* and the software was used to segment the datasets by thresholding with manual adjustments. The obtained meshes of the bones were then imported into *Meshmixer*, in which the actual contact regions were selected and cut. Based on the initial analysis of the geometry of the studied joints, we decided on two approaches to contact region selection: one sphere per bone in MCP and two variants for DIP/PIP: one sphere per bone or two spheres per bone (lateral and medial). This resulted in 28 mesh cuts composed into 14 contact regions. The mesh cuts were then imported into custom Python software, which was used to fit the spheres to them using an optimizational approach. The script also allowed for the visualization of the obtained contact pairs.

2.2. Evaluating the contact pairs

Our main goal was to assess whether spherical contact pairs were a viable option for modelling the joint of the index finger. Therefore, after obtaining the spheres, we evaluated their quality as follows using two different criteria. Firstly, the visualized pairs were analysed in terms of whether they formed valid contact pairs – their spheres did not intersect. An example of a valid contact pair was given in Fig. 1. In addition, we also computed parameters to judge the geometry and the quality

[1]Faculty of Mechanical Engineering, Cracow University of Technology, Al. Jana Pawła II 37,31-864 Cracow, Poland, e-mail: karolkluzaa@gmail.com
[2]Faculty of Mechanical Engineering, Cracow University of Technology, Al. Jana Pawła II 37, 31-864 Cracow, Poland, e-mail: adam.ciszkiewicz@pk.edu.pl

of the sphere fit – such as the radius, the maximal deviation from the sphere and the standard deviation.

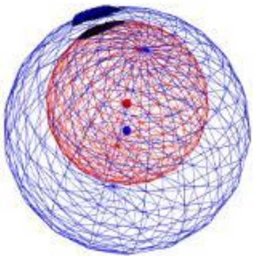

Fig. 1. A sample valid contact pair.

3. Results and discussion

The approach employing a single sphere per bone worked well for the MCP, in which the bone shapes corresponded to spheres. Nevertheless, this simplification proved to be incorrect for the DIP and PIP. In these cases, the procedure returned mathematically correct pairs, but with very large dimensions (for instance: radii of the spheres in DIP: 48.65 mm and 30.45 mm). This was especially evident with the spheres compared to the assumed mesh cuts or the size of the joint itself. This meant that the subtle curvature of the bone profiles was completely lost – the procedure essentially flattened the whole surface with a large sphere, which was reflected by the relatively high value of the maximal difference between the points of the mesh cuts and the fitted spheres (up to 1.22 mm).

The dual-sphere approach returned significantly better results for DIP and PIP. In this case, the fitted spheres were smaller for DIP/PIP and represented the curvature of the bone profiles more closely, with a maximal difference of only 0.56 mm.

In terms of visual assessment, over 85% of the studied pairs formed a proper ball-and-socket joint, corresponding to the anatomical features of the finger joints.

4. Conclusions

The results showed that it might be possible to replace the contact areas in the joints of the index finger with simple spherical contact pairs. Moreover, in two of the joints, better results were obtained when using two contact pairs – medial and lateral – instead of one for the whole contact region.

References

[1] HU D., HOWARD D., REN L., *Biomechanical analysis of the human finger extensor mechanism during isometric pressing*, PLoS One, 2014, 9.

[2] BROOK N., MIZRAHI, J., SHOHAM M., DAYAN J., *A biomechanical model of index finger dynamics*, Med. Eng. Phys, 1995, 17, 54–63.

[3] FAUDOT B., MILAN J., MONSABERT, B.G. DE, CORROLLER T. LE, VIGOUROUX L., *Estimation of joint contact pressure in the index finger using a hybrid finite element musculoskeletal approach,* Comput. Methods Biomech. Biomed. Engin., 2020, 1–11.

[4] WU J.Z., WELCOME D.E., KRAJNAK K., DONG R.G., *Finite element analysis of the penetrations of shear and normal vibrations into the soft tissues in a fingertip,* Med. Eng. Phys., 2007, 29, 718–727.

Effect of dissection on the mechanical properties of human ascending aorta aneurysm

M. KOZUŃ[1], M. KOBIELARZ[2], T. PŁONEK[3], M. JASIŃSKI[4]

Key words: *delamination, dissection, aneurysm, human ascending aorta*

1. Introduction

Dissection is an important problem from a medical, social and scientific point of view, and the number of people suffering from it is constantly increasing. The etiology and development process of dissection is still unknown.

Most of the work related to the analysis of the dissection process concerns biological factors that can have a significant impact on the formation and development of this disease. These factors include qualitative and quantitative changes of elastin fibers, collagen, smooth muscle cells as well as the importance of increasing proteoglycans content in the middle aortic wall layer. These structural elements determine passive and active mechanical properties of the vessel wall, and degenerative processes may lead to changes in the mechanical properties of the aortic wall, its individual layers and the connection between them, and thus loss of integrity of the entire wall.

There is still no answer to how the development of aneurysm affects the resistance to the dissection of human artery. Therefore, the presented work aims to determine the mechanical properties of the interface between layers of the ascending aortic aneurysm wall, in which spontaneous dissection occurred.

2. Material and Method

2.1. Material

The research material was the human ascending aorta aneurysm (n=17). The vessels were collected during cardiac surgery from patients (men, average age: 50±13) who underwent replacement of the ascending aorta segment due to the occurrence of a dissected aneurysm (Bioethical Commission approval number: KB-14/2019). The dissection was spontaneous (type A according to Stanford classification) and occurred between the interface between the inner layer and the complex of the middle and outer layers (I-MAC).

2.2. Method

Rectangular specimens with length (25mm) and width (5mm) in circumferential and longitudinal direction were cut out from each vessel. The mechanical properties were determined on the basis of a peeling test with a 2mm/min load speed, using the MTS Synergie 100 testing machine. The load was applied perpendicularly to a plane of the specimen dissection (T-peeling test configuration).

During the mechanical test, propagation of the previously initiated dissection was forced and the changes in the value of force and displacement were recorded. Next, the force/specimen width vs. displacement curves were prepared and the mechanical properties: stiffness coefficient (k), energy dissipated during delamination (W), the average value of force during delamination (F_{AVER}) were calculated.

3. Results

[1]Department of Mechanics, Material and Biomedical Engineering, Wroclaw University of Science and Technology, Wrocław, Poland, e-mail: marta.kozun@pwr.edu.pl,
[2]Department of Mechanics, Material and Biomedical Engineering, Wroclaw University of Science and Technology, Wroclaw, Poland, e-mail: magdalena.kobielarz@pwr.edu.pl
[3]The Clinic of Cardiac Surgery, Wroclaw Medical University, Wrocław, Poland, tomasz.plonek@umed.wroc.pl
[4]The Clinic of Cardiac Surgery, Wroclaw Medical University, Wrocław, Poland, marek.jasinski@umed.wroc.pl

For each force/width vs displacement curve the jagged plateau region corresponding to the propagation of dissection characterizes oscillations in obtained values of the force. The oscillation is often referred to in the rubber mechanics as "unstable" or stick-slip "tearing".

The results indicate that the values of the analysed mechanical parameters (energy dissipated during delamination, mean force, and stiffness) change with the direction. Values (median) of mechanical parameters are higher for circumferential specimens (Table 1).

Table 1. Values (median) of mechanical parameters obtained for I-MAC interface

direction	k [mN/mm]	W [mJ/cm2]	F_{AVER}[mN/mm]
circumferential	0,118	0,10	0,056
longitudinal	0,110	0,08	0,040

4. Discussion

The presented work concerns the problem of dissection of the blood vessel wall, which is now more and more often treated in clinical practice as a separate disease entity. The dissecting aneurysms of ascending aorta were examined. The mechanical parameters of the interface between the intima the media-adventitia complex (peeling test) were determined. It should be emphasized that dissection occurred spontaneously between the above-mentioned layers, and was not forced for the needs of research, which has not been presented in the literature so far. Based on the determined mechanical parameters, the dissection properties have been characterized by the underlying aortic dissection.

The delamination curves revealed an oscillation. This indicates that dissection does not propagate at a steady rate. It arrests and reinitiates at somewhat irregular intervals [2]. According to the Pasta et. al [2], such a course of the curve results from damage to a large number of elastin fibers during propagation of dissection and their high extensibility during dissection testing. Consequently, this leads to an increase in the peel test magnitude [2]. The obtained results showed that the wall of the ascending aortic aneurysm was characterized by a lower value of the maximum force and energy dispersed during the dissection process of the examined interface in comparison with dissected ascending aorta [1], therefore patients with ascending aortic aneurysm are more prone to dissection.

References

[1] KOZUŃ M., PŁONEK T., JASIŃSKI M., FILIPIAK T., *Effect of dissection on the mechanical properties of human ascending aorta and human ascending aorta aneurysm,* Acta of Bioengineering and Biomechanics, 2019, 2:127-134.

[2] PASTA S., PHILLIPPI J.A., GLEASON T.G., VORP D.A., *Effect of aneurysm on the mechanical dissection properties of the human ascending thoracic aorta,* The Journal of Thoracic and Cardiovascular Surgery, 2012, 460-467.

Patient-specific modeling for evaluation of blalock–taussig shunt performance

A.G. KUCHUMOV[1], A. KHAIRULIN[2]

Key words: *modified Blalock–Taussig shunt, blood, aorta*

1. Introduction

Obstructive lesions of the right ventricular output tract, isolated or combined with other congenital heart defects, account for 25–30% of congenital heart anomalies [1]. Surgical treatment, as the main method of treatment of congenital heart defects with obstruction of the right ventricle output can be represented as radical correction or stage treatment [2]. A breakthrough solution in the surgical treatment of cyanotic congenital heart defects was the creation of an intersystem shunt (in particular, a modified Blalock–Taussig shunt) [3]. It is important to note that the modified Blalock–Taussig shunt continues to be a high-risk procedure with a total mortality of 2.3% to 16% [4]. The main complications of the modified Blalock–Taussig shunt are associated with the development of shunt thrombosis. Therefore, the choice of the optimal shunt diameter is a very important task, which is not solved to date. Mathematical modelling and biomechanics methods allow estimating prognostic data, reconstruct realistic and accurate three-dimensional models that take into account the level of blood pressure, detailed anatomy, feedback mechanisms in the circulatory system and deformation of the vessel wall. The clinician can noninvasively determine temporal and spatial variable hemodynamic parameters that cannot be studied by imaging or clinical measurements.

2. Materials and methods

2.1. Patients

Contrast-enhanced multislice computed tomography of the heart and arteries for four patients was performed in S.G. Sukhanov Federal Center of Cardiovascular Surgery.

2.2. Images adopting and 3D processing

Three-dimensional aortic models with installed shunts were constructed by using ITK-Snap. Then, for each model, additional shunting options were created using the SPACECLAIM graphical package processing (three configurations were considered: central shunt, left shunt, right shunt).

2.3. Problem statement

Incompressibility equation and Navier–Stokes equation describing blood flow can be written as follows

$$\nabla \cdot u = 0, \tag{1}$$

$$\rho\left(\frac{\partial u}{\partial t} + u \cdot \nabla u\right) = \nabla \cdot \sigma + f, \tag{2}$$

where ρ is the constant density, u is the velocity vector, σ is the stress tensor, f is a body force.

3. Results

[1]Perm National Research Polytechnic University; Perm, Russia, e-mail: kychymov@inbox.ru
[2]Perm National Research Polytechnic University; Perm, Russia, e-mail: s.xayrulin@mail.ru

As a result of the problem solution, the hemodynamic parameters distributions (velocity, pressure, wall shear stress, time-averaged wall shear stress, oscillatory shear index, relative residence time) were found. The most interesting results correspond to the maximum value of the blood flow rate.

Fig. 1 shows the distribution of velocity characteristics of the blood flow. In the aortic region, blood flow has a uniform distribution. As blood move away from the descending part of the aorta, there is an equalization of blood flow velocity. The reverse situation can be observed in the pulmonary artery, where mainly a vortex blood flow with the exception of model 3 due to its geometric features can be seen. At the peak of systole, the maximum values of blood flow are shifted to the shunt region. Local blood velocity increase occurs due to the lumen narrowing and heterogeneity of the shunt shape (right shunt configuration).

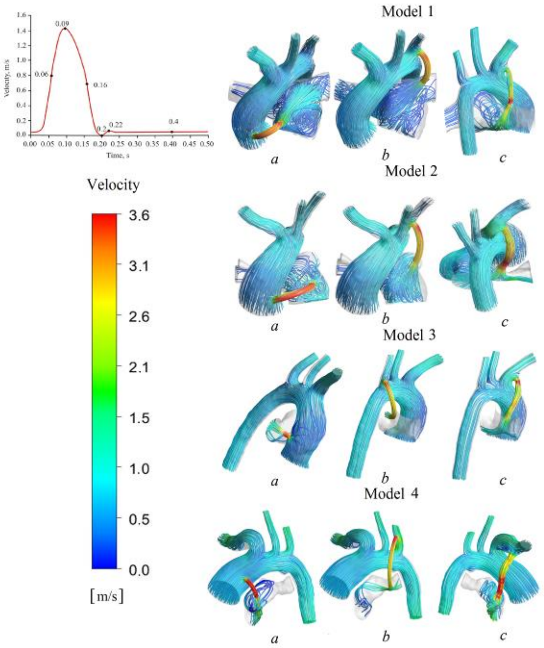

Fig. 1. *Veocity distribution:* a *– central shunt,* b *– right shunt,* c *– left shunt*

Acknowledgments: Part of the work was supported by the Perm Region government grant for the development of the scientific school "Computer biomechanics and digital technologies in biomedicine". The reported study was funded by RFBR and Perm Territory, project number 20-41-596005.

References

[1] DRISCOLL D.J, MICHELS V., GERSONY W. *Occurrence risk for congenital heart defects in relatives of patients with aortic stenosis, pulmonary stenosis, or ventricular septal defect.* Circulation, 1993, 87, 114-120.

[2] MCKENZIE E.D., KHAN M.S., SAMAYOA A.X. *The Blalock-Taussig shunt revisited a contemporary experience.* J. Am. Coll. Surg., 1988, 216, 699-704.

[3] DE LEVAL M.R., MCKAY R., JONES M., STARK J., MACARTNEY F.J. *Modified Blalock-Taussig shunt. Use of subclavian artery orifice as flow regulator in prosthetic systemic-pulmonary artery shunts*. Thorac. Cardiovasc. Surg., 1981, 112-119.

[4] CURZON C.L., MILFORD-BELAND S., LI J.S. *Cardiac surgery in infants with low birth weight is associated with increased mortality: analysis of the Society Of Thoracic Surgeons Congenital Heart Database*. J. Thorac. Cardiovasc. Surg., 2008, 135, 546-555.

Kinematic criteria for the evaluation of technique of dance sport athletes

S. KULIŚ[1], J. GAJEWSKI[2]

Key words: *dancesport, kinematic, technique, sport*

1. Study aim

The use of accelerometery to measure pelvic and upper body accelerations in sports couples may prove useful in assessing its repeatability and the degree of coordination of the dancers. The aim of the research is to formulate kinematic criteria for the assessment of motion technique, taking into account the analysis of the acceleration of the pelvic girdle and thoracic spine of the dance athletes.

2. Methods

24 dancesport athletes (12 athletes of the intermediate level and 12 athletes of elite level) took part in the research. Each of them performed 3 times basic Viennese waltz figure "natural turn". Each attempts consisted of 3 figures danced continuously to the same music (60 bars per minute) in the dancehall. A device for recording triaxial accelerations and triaxial rotational angular velocities was mounted on the dorsal part of the pelvic girdle and on the thoracic spine of athlete.

3. Results

Statistical analysis of the obtained results of the athletes revealed statistically significant differences between the elite athletes and the intermediate level athletes in rotational angular velocities of the thoracic spine around the tranverse axis (elite females r=0,5535 p>0,05; males r=0,5705 p>0,05 versus intermediate females r=0,2280 p>0,05 males r=0,2587 p>0,05) and around the sagittal axis (elite females r=0,5322 p>0,05; males r=0,6069 p>0,05 versus intermediate females 0,1334 p>0,05 males 0,3204 p>0,05).

Statistically significant correlations were found in between dancesport partners of intermediate level couples (r varied between -0,7737 and 0,8714 p>0,05 for various parameters) as well as elite couples (r varied between -0,9105 and 0,9480 p>0,05 for various parameters). Higher correlations were achieved by elite athletes, especially in rotational angular velocities of the upper body.

However the general pattern of the movement for intermediate and elite dancers is similar in some parameters, elite dancers achieve higher maximum and minimum values of the rotational angular velocities and show higher consistency and coordination.

4. Conclusions

The proposed measurement method, presentation and analysis of the pattern of the pelvic girdle and thoracic spine motion of dancesport athletes in "natural turn" in Viennese Waltz represents a good tool for fast and effective qualitative and quantitative kinematic evaluation of movement technique components.

References

[1]Department of Physical Education, Józef Piłsudski University of Physical Education in Warsaw, e-mail: szymon.kulis@gmail.com

[2] Department Of Physical Education, Józef Piłsudski University of Physical Education in Warsaw, e mail: jan.gajewski@awf.edu.pl

[1] HARTMANN, M., MAVROLAMPADOS, A., ALLINGHAM, E., CARLSON, E., BURGER, B., TOIVIAINEN, P., *Kinematics of perceived dyadic coordination in dance.* Scientific Reports, 2019, 9(1). https://doi.org/10.1038/s41598-019-52097-6

[2] SHIOYA T., *Analysis of Pivot Turn and Related Movements in Ballroom Dancing.* The Proceedings of the Symposium on Sports and Human Dynamics, 2019(0), C–2. https://doi.org/10.1299/jsmeshd.2019.c-2

[3] YOSHIDA Y., BIZOKAS A., DEMIDOVA K., NAKAI S., NAKAI R., NISHIMURA T., *Partnering Effects on Joint Motion Range and Step Length in the Competitive Waltz Dancers.* Journal of Dance Medicine & Science : Official Publication of the International Association for Dance Medicine & Science, 2020, 24(4), 168–174. https://doi.org/10.12678/1089-313X.24.4.168

[4] YOSHIDA Y., BIZOKAS A., DEMIDOVA K., NAKAI S., NAKAI R., NISHIMURA T., *Determining Partnering Effects in the "Rise and Fall" Motion of Competitive Waltz by the Use of Statistical Parametric Mapping.* Baltic Journal of Sport and Health Sciences, 2021, 1(120), 4–12. https://doi.org/10.33607/bjshs.v1i120.1047

Evaluation of structure of a hydrogel material based on sodium alginate under deformation

J. KUROWIAK[1], T. KLEKIEL[1], A. MACKIEWICZ[1], R. BĘDZIŃSKI[1]

Key words: *hydrogel, regenerative medicine, sodium alginate, elasticity, micro DIC*

1. Introduction

The obstruction of the urethral canal, affecting mainly men, is caused by the narrowing. Urethra stricture is most often caused by scarring, which is the result of replacing the spongy tissue with scar tissue. The sooner urethral stricture is diagnosed, the more effective it is to treat it. The most promising treatment method is stenting, which is systematically improved. Ideal stents are those that do not migrate from the site of implantation, are biocompatible with the surrounding tissue and retain urine flow trajectories [1, 2]. The challenge remains to come up with the best solution that is medically perfect. Urethra stents should be characterized by high deformability, the value of which will be similar to that characteristic of the tissue forming the urogenital system.

The presented research concerned the determination of mechanical properties, local surface deformation - micro strain and degradation of hydrogel material based on sodium alginate (SA). The main task was to determine changes in the structure of the material depending on the concentration of SA, the type of cross-linking agent and, above all, the different cross-linking time of the sample. It was observed that the higher the concentration of SA the better mechanical properties of the material. Innovative studies of digital image correlation-μDIC (micro Digital Image Correlation) have allowed for the assessment of micro deformations determining precisely the changes occurring in the structure of the material produced.

2. Materials and methods

The study was carried out using: alginate acid salts with the parameters: viscosity 15-25 cP, 1% H2O, pH 6.5-8.5, molecular weight 120-190g/mol and density 1.601g/cm3 as well as $CaCl_2$ and $BaCl_2$. The artificial urine solution was prepared according to the recipe of Mayrovitz and Sims [3]. Degradation tests, a static tensile test and a micro-deformation analysis (μDIC) were carried out on the tubular samples. The preparation of SA has been described in previous studies [4-5]. The samples were produced by the sol-gel immersion method. The material was divided into four groups depending on the cross-linking time: I-2h, II-24h, III-48h and IV-72h. The variable cross-linking time was to determine physical and mechanical properties of the material changed for the SA/$CaCl_2$ and SA/$BaCl_2$ combinations.

3. Results and discussion

The results of strength analysis (Fig. 1A-B) show that 24-hour crosslinking of the hydrogel material with 1.5 M $BaCl_2$ solution of 7g/100ml SA is sufficient for the material to reach the value of Young's modulus oscillating within 3 MPa. The most unstable material was the one with 5g/100ml SA crosslinked with 1.5M $CaCl_2$ solution. From the analysis of the obtained μDIC results (Fig. 1C), it can be concluded that the material crosslinked with Ba^{2+} cations had a higher repeatability of results, the material exhibited higher elasticity and stiffness compared to the samples crosslinked with Ca^{2+} cations. Weaker crosslinking of the structure was observed for the samples with Ca^{2+} cations, which caused discrepancies in the results obtained for these samples. he CaCl2 cross-linked samples were more susceptible to damage already at the stage of mounting them on the cardiological balloon. Based on the degradation studies (Figure 1D), it was observed that the SAMBa5 sample degraded the fastest. The SAMBa5 sample crosslinked for 24 and 48 hours on day 5 showed complete degradation.

[1]Department of Biomedical Engineering, Faculty of Mechanical Engineering University of Zielona Gora, Zielona Góra, Poland, e-mail: j.kurowiak@iimb.uz.zgora.pl

It was observed that the degradation rate for samples crosslinked with Ca^{2+} cations for all crosslinking times (2, 24, 48, and 72 hours) was relatively constant and ranged between 40 and 55% on test day 7.

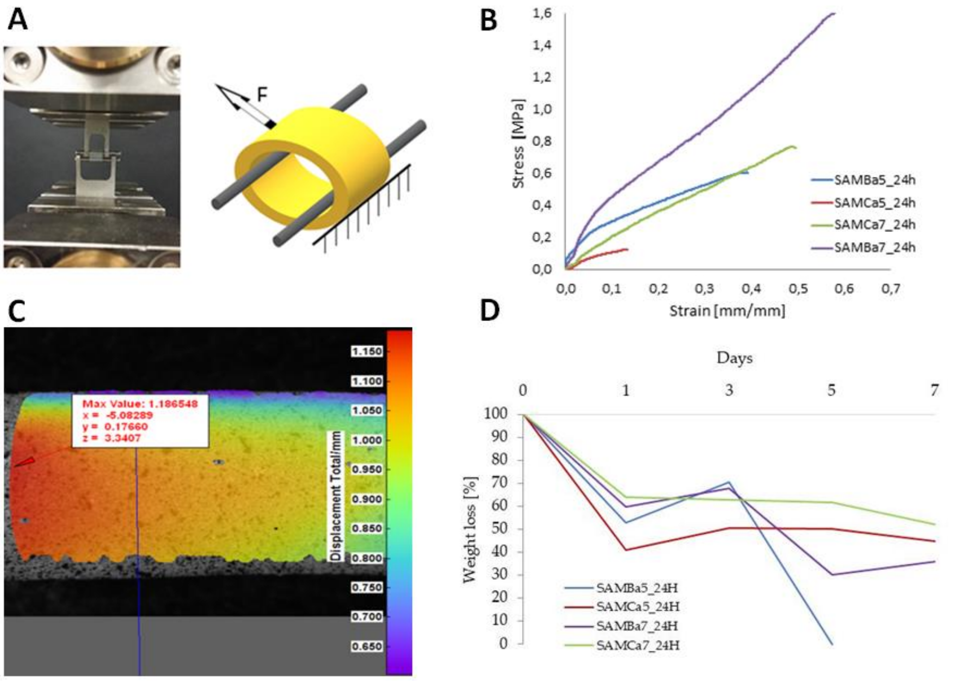

Figure 1. ***Example test results: strain-strain analysis for 24 h crosslinked samples (A), microDIC analysis for SAMBa7 sample (B), weight change of 24 h crosslinked samples (C).***

4. Conclusion

The conducted research made it possible to evaluate the structural and mechanical properties of the proposed material, changing with the chemical composition. The properties were studied with its possible future application in the form of stents for the urethral stenosis treatment. The analysis suggested strongly a relationship between the preparation process of SAM material and its mechanical and degradation properties. Further steps should be taken to analyze the flow and work of muscles directly affecting the urethra.

Acknowledgments: This research was funded by the National Science Center Poland, grant number DEC-2016/21/B/ST8/01972.

References

[1] DYER R.B., et al., *Complications of Ureteral Stent Placement.* Radio Graphics, 2002, 22:1005-1022.

[2] SALI G.M., JOSHI H.B., *Ureteric stents: Overview of current clinical applications and economic implications.* International Journal of Urology, 2020, 27, 7-15.

[3] CHUTIPONGTANATE S., THONGBOONKERD V., *Systematic comparisons of artificial urine formulas forin vitrocellular study*. Anal. Biochem., 2010, 402, 110-112.

[4] KUROWIAK J., et al., *Analysis of the Degradation Process of Alginate-Based Hydrogels in Artificial Urine for Use as a Bioresorbable Material in the Treatment of Urethral Injuries*. Processes 2020, 8(3), 304.

[5] KLEKIEL T. et al., *Novel design of sodium alginate based absorbable stent for the use in urethral stricture disease*. Journal of Materials Research and Technology, 2020, 9(4).

Is optimal cruising velocity constant during distance running?

R. MAROŃSKI[1]

Key words: *minimum-time running, singular arc*

1. Formulation of the problem

The optimal strategy during the competitive running is reconsidered. The calculus of variations (the optimal control) formalism is applied. The pioneering work is that of Keller [1], [2]. He proves that the distance to be covered may be broken into three sections: initial acceleration; cruise with constant velocity; and final slowing down (finish with decreasing velocity). Keller's model of running bases on two ordinary differential equations: the first one results from Newton's second law, the second one describes the energy conversions in competitors' body. His model relies on the assumption of constant oxygen uptake (constant $V\dot{O}2$). Aftalion, for more realistic energy conversion model, where the oxygen uptake varies with the energy staying at the competitor's disposal, proves that the cruising velocity is not constant, but it decreases with the time [3]. This section of the optimal path refers to so-called singular arc in the optimal control. Aftalion's reasoning is very sophisticated, however. This presentation contains the extension of Aftalion's model given by Bonnans and Aftalion [4], where the oxygen uptake varies for a given range of energy, and it is constant for another one. A non-classical method of calculus of variations is applied – the method of Miele [5]. The optimal run is analysed in the energy-velocity plane. The method gives sufficient and necessary conditions of optimality in relatively simple manner including the singular arcs.

The applied model is as follows:
The first equation relies on Newton's second law

$$dv/dt = f(t) - v(t)/\tau, \tag{1}$$

where t is the time, $v(t)$ is the instantaneous competitor's velocity, $f(t)$ is the variable propulsive force per unit mass, v/τ is the resistive force per unit mass (τ is a constant coefficient).

The second equation represents the power balance per unit mass of the runner

$$de/dt = \sigma(e(t)) - f(t)v(t), \tag{2}$$

where e is the available energy per unit mass, σ is the energetic equivalent of oxygen uptake per unit mass (here depending on the energy e), fv is the power necessary to accelerate and to overcome the resistance of motion. The energetic equivalent of oxygen uptake σ is assumed to be linear function of the accumulated oxygen deficit (cf Bonnans and Aftalion [4])

$$\sigma(e) = \frac{\bar{\sigma}}{1-\phi}\left(1 - e/e_0\right), \tag{3}$$

where $\bar{\sigma}$ is the maximal value of σ, ϕ is the constant coefficient, and e_0 is the energy at the beginning of the exercise. There is a clear interpretation of this equation by a hydraulic analogy (cf Bonnans and Aftalion [4]). These differential equations should be supplemented by boundary conditions:

$$v(0)=v_0, \quad e(0)=e_0, \quad e(T)=0, \tag{4}$$

[1]Warsaw University of Technology, Institute of Aeronautics and Applied Mechanics, Warsaw, Poland,
e-mail: maron@meil.pw.edu.pl

and the inequality constraints:

$$0 \le f(t) \le f_{max} \ , \tag{5}$$

$$e(t) \ge 0 \ . \tag{6}$$

The time T is minimized

$$T = \int_0^T dt \ \Rightarrow \ MIN \tag{7}$$

of covering the given distance D

$$D = \int_0^T v \ dt \ . \tag{8}$$

The considered problem may be regarded as an isoperimetric problem of calculus of variations.

2. Method and results

The classical Pontryagin's maximum principle is applied in Aftalion's approach [3]. The Hamiltonian is linear in the control function – the propulsive force setting *f(t)*. For such the case singular arcs should be considered. An alternative approach is used in the current presentation, a non-classical method of Miele – the method of extremization of linear integrals by Green's theorem [5]. For the considered problem the singular arc referring to the cruise is represented by an algebraic equation

$$\tau\,(1+\lambda v)\, {}^{d\sigma}\!/_{de} + \lambda v + 2 + \lambda\, \sigma(e)\tau / v \ = \ 0\,, \tag{9}$$

where λ is a constant Lagrange's multiplier depending on the distance to be covered. For Keller's model of metabolism $\sigma(e) = \bar{\sigma} = const.$, and $d\sigma / de = 0$. The equation (9) reduces to the simpler form

$$\lambda\, v^2 + 2v + \lambda\, \bar{\sigma}\, \tau = 0 \ . \tag{10}$$

The parameters λ, $\bar{\sigma}$ and τ are constant, therefore the cruising velocity v is constant too (cf Maroński [6]). The singular arc should be considered in its general form (9) for the model of metabolism of Bonnans and Aftalion [4]. The optimal cruising velocity decreases with the distance for energy e above ϕe_0 level. The cruising velocity is constant for e below ϕe_0 level. In such the sense the presented result is generalization of the result of Keller [1], [2], where the cruising velocity is constant, and the result of Aftalion [3], where the cruising velocity decreases.

References

[1] KELLER J.B., *A theory of competitive running.* Physics Today, 1973, 26, 43-47.

[2] KELLER J.B., *Optimal velocity in a race.* Amer. Math. Monthly, 1974, 81, 474-480.

[3] AFTALION A., *How to run 100 meters.* SIAM J. Appl. Math., 2017, 77, 1320-1334.

[4] BONNANS J.F., AFTALION A., *Optimization of running strategies based on anaerobic energy and variations of velocity.* INRIA Research Report n^0 8344 – Août 2013, 24 pages, https://hal.inria.fr/hal-00851182v1.

[5] MIELE A., *Extremization of linear integrals by Green's theorem.* In: *Optimization techniques with application to aerospace system (Litmann G., ed.),* Academic Press, New York, London, 1962, 69-98.

[6] MAROŃSKI R., *Minimum-time running and swimming: an optimal control approach.* J. Biomechanics, 1996, 29, 245-249.

Design process of bioresorbable stent

L.A. MAZURKIEWICZ[1], **J. MAŁACHOWSKI**[2], **J. BUKAŁA**[3]

Key words: *bioresorbable stent, numerical analysis, optimization, FEA*

1. Introduction

Percutaneous coronary intervention (PCI) has revolutionised the treatment of coronary artery disease (CAD) in the last 20 years. A promising alternative approach to the treatment of CAD is the implementation of bioresorbable technologies used for the construction of scaffolds. However developing new polymer-based bioresorbable drug-eluting scaffolds (BVS) requires a new structural geometry, as these polymer materials are characterised by substantially lower stiffness than metallic alloys. Sufficient radial strength of the stent is essential, as insufficient vessel wall support can lead to a significant recoil. The combination of finite element analysis (FEA) with optimisation algorithms has proven to be a valid and efficient method used to investigate and optimise the mechanical behaviour of stents and angioplasty balloons[1].

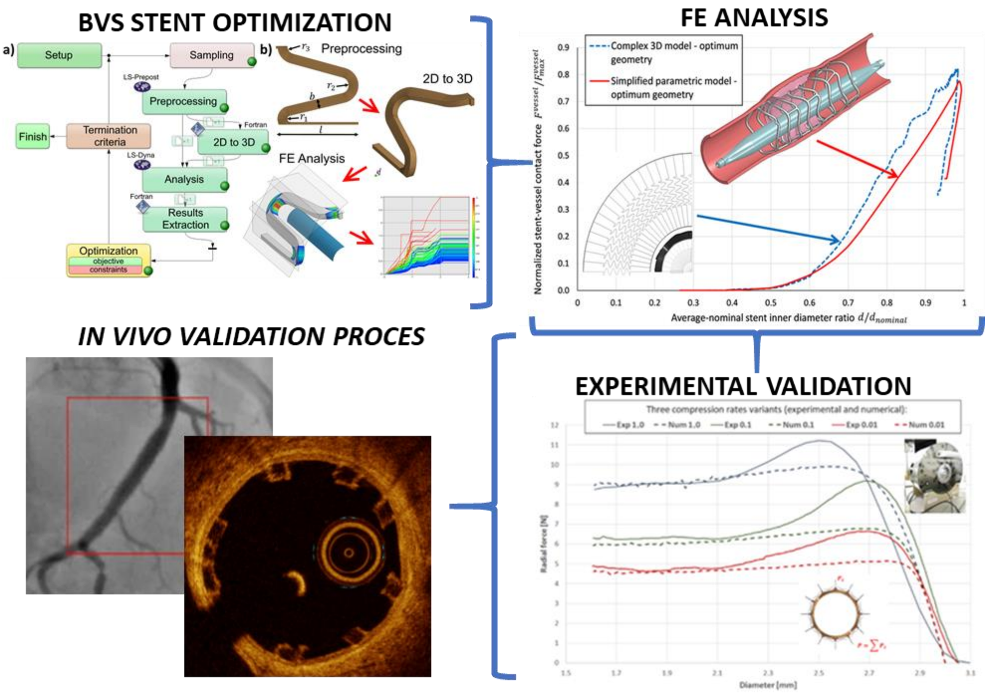

Fig. 1. Stent design flow chart [2]

2. Materials and methods

[1]Military University of Technology, Warsaw, Poland, e-mail: lukasz.mazurkiewicz@wat.edu.pl
[2]Military University of Technology, Warsaw, Poland, e-mail: jerzy.malachowski@wat.edu.pl
[3]Military University of Technology, Warsaw, Poland, e-mail: jakub.bukala@wat.edu.pl

To assess the stress development and deformation of the stent, finite element analysis (FEA) was used. First, a complex FE analysis of both the crimping and inflation processes for the bioresorbable coronary stent (initial design) was performed. The complex analysis included an entire process of coronary stent crimping and inflation of the expandable folded balloon, with minimal simplification. The results of the analysis were used as key parameters in the development of the simplified parametric FE model of the system. Subsequently, an optimization procedure based on the simplified models was performed to obtain the optimum geometrical parameters of the analysed structure. The objective of the optimisation was to maximise the vessel diameter after the BVS implantation. The optimisation procedure was based on the automatic model-generating scripts, numerical analyses and implementation of genetic algorithms. The verification of proposed methodology was performed by comparing the final results obtained from the simplified parametric model with those from the complex model of the optimal stent design. Final, the validation process consist of structural studies, CFD analysis and in vivo testing of developed BVS stent structure (Fig. 1).

3. Results and conclusions

The optimisation procedure generated almost 1000 stent models with varying shape parameters. The FE analyses for each sampling point provided responses as a set of points. From all feasible solutions (satisfying the constraint of maximum plastic strains), an optimal set of parameters was obtained. Subsequently, during the numerical validation, the contact interface forces for the simplified parametric model and the complex 3D model of the optimal stent design were compared). The obtained results confirmed that the simplified model is suitable and efficient for optimisation research in which the computational time plays an important role. In addition, the effective plastic strains are represented correctly in the simplified model.

The validation tests were performed using a specially equipped laboratory crimping machine dedicated to stent compression. The obtained results show a satisfactory correlation [3]. Additionally, the validation performed with the use of the porcine coronary in-stent restenosis procedure indicated a good translation from the mathematical FE model to the in-vivo setting, particularly when regarding the stent delivery, inflation and geometry immediately after the bioresorbable stent implantation, as shown in multiple OCT imaging modalities.

The presented numerical multistage procedure will be used to develop a new series of geometries of bioresorbable coronary stents, while taking into consideration different vessel geometries as well as the blood pressure characteristics. The cooperation between the medical and engineering sciences in order to create new bioresorbable stents will surely improve the comfort and life expectancy of many patients.

Acknowledgments: The study was supported by the NCBiR within project “Apollo” (STRATEGMED), the Interdisciplinary Centre for Mathematical and Computational Modelling (ICM) of the University of Warsaw under grant no GB84-21 and Military University of Technology under research project UGB 877/2021. This support is gratefully acknowledged.

References

[1] Bukala J., Malachowski J., Kwiatkowski P., Numerical analysis of crimping and inflation process of balloon-expandable coronary stent using implicit solution. International Journal for Numerical Methods in Biomedical Engineering 33 (2017) e2890. https://doi.org/10.1002/cnm.2890

[2] Mazurkiewicz, Ł.A., Bukała, J., Małachowski, J., Tomaszewski, M., Buszman, P.P., *BVS stent optimisation based on a parametric model with a multistage validation proces*, Mater. Des. 198 (2021) 109363. BEAR J., *Dynamics of Fluids in Porous Media,* Dover, 1988.

[3] Bukala, J., Buszman, P.P., Malachowski, J., Mazurkiewicz, L., Sybilski, K., Experimental tests, *FEM constitutive modeling and validation of PLGA bioresorbable polymer for stent applications*, Materials, 13(8) (2020) 2003.

Experimental strength analysis of modern dental composites used in layered tooth crown restoration techniques

G. MILEWSKI[1], B. MUSZYŃSKI, A. ŚLEDŹ

Key words: *nano and micro hybrid composites, sandwich restoration technique, strength properties*

1. Introduction

Carious bacteria that invade into the space between filling and tooth wall cavity become the main cause of pulpal irritation in teeth restored with composite materials what results in marginal dental caries, what was proved almost four decades ago [1]. It seems to be the most crucial feature resulting due to the polymerization shrinkage phenomena of resin filling composites applications. High shrinkage and resulting high residual stresses could lead to failure of the adhesive bond between the composite filling and the tooth structures – dentine and enamel [2]. Over the last few years the intense research activity in the studies on the individual contributions of the composite's physical properties and the curing kinetics of the dental resins has been registered. Thanks to them the low shrinkage light curable hybrid and nano filled dental composites have been reported as the resins reducing the most the contraction stresses [3,4]. Despite the fact that much effort has been put into developing dental composites of limited contraction the dentists still have to defy the problem of destructive shrinkage stress in their present practice, mainly due to the application of variant filling techniques. Up-to-day the sandwich filling processing seems to be the most often used in practice method of dental resins polymerization shrinkage reduction, however the number of scientific papers concerning the strength aspects of dental composite materials properties with regards to the thickness of processed layers is relatively low [5].

The paper presents the results of the experimental strength examination of the influence of the different ways of layered polymerization processing on the mechanical properties of modern hybrid micro and nano dental composite materials.

2. Materials and methods

Seven types of the modern dental composite materials were used for the study:

- four nano composite: Charisma Diamond made by Heraeus Kulzer®, Enamel Plus (MicerDent®), OliCoXP and OliREVO made by OliDent®,
- three micro hybrid composites: Boston (Arcona®), Gradia Direct and G-enial Universal Flo (both materials made by GC® in so called flow technology).

The material samples were layered in glass tubes of 7.5 [mm] length and then each of the superimposed layers, in the range 1 to 2.5 mm, were polymerized using a LED polymerization lamp – Fig. 1. For chosen groups of samples alternatively HighPower (1000mW/cm^2) and Soft-Up (from 200mW/cm^2 up to 1000mW/cm^2) power modes were used.

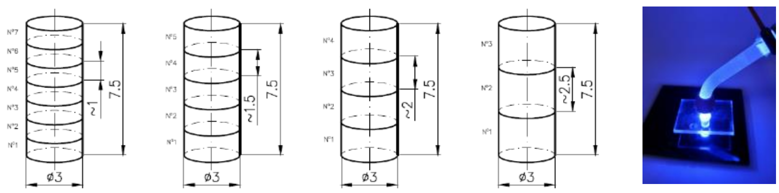

Fig. 1. Four variants of dental composites layered polymerization processing

[1]Cracow University of Technology, Institute of Applied Mechanics, Cracow, Poland,
e-mail: milewskil@mech.pk.edu.pl

Strength tests at compression were done with the use of MTS Insight strength machine for the following properties: compressive strength, modulus of elasticity at compression, strain to fracture, and work to fracture. The applied load head of the strength machine was at the range (0 – 50) kN, while the strain rate was taken 0,5 mm/min. The tests were done at room temperature and standard humidity. Each series of the tests consisted of 6 samples. Standard statistical data analysis was done.

3. Results

As an example, the comparison of the medium values of the compressive strength and work to fracture for nano hybrid Charisma composite material polymerized in the various ways for HighPower mode is shown in Fig. 2.

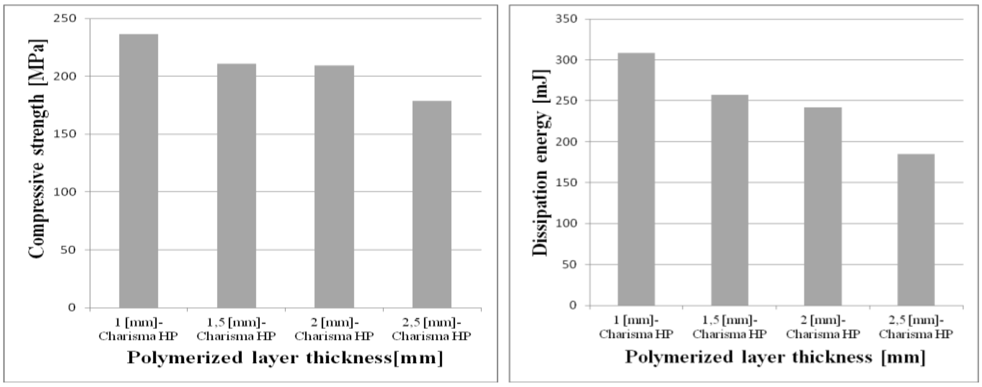

Fig. 2. Influence of the various ways of layered polymerization processing of Charisma Diamond nano composite on its compressive strength and work to fracture

The strength tests proved that 1.0 and 1.5 mm layered polymerization characterize with the highest values for all strength parameters regardless the type of dental composites. For instance, the medium values of compressive strength varied between 220 and 330 MPa for all subsequent group of dental composites, what accomplish the strong requirements for highly effort teeth crown fillings. It is worth mentioning that OliREVO which produces 290 MPa of the medium value of compressive strength was the composite for which the number of layers had the least impact on strength, what makes it the material with the largest spectrum of applications.

4. Conclusions

The layered polymerization processing seems to be the best method to reduce polymerization shrinkage in tooth crown fillings. The registered tendency is: the thinner the layer, the better the strength properties. Two-step light-activation option slows the material reaching the gel point, and thus the material is lower stressed when fully hardened. Increased temperature accelerates the polymerization of the composite and reduces the material viscosity, affects the process of composite material cross-linking what results in the increase of its strength properties.

References

[1] BRÄNNSTRÖM M., VOJINOVIČ O., Response of the dental pulp to invasion of bacteria around three filling materials, J Dent for Children 43 (1976), pp. 15-21.

[2] DAVIDSON C.L., A.J. FEILZER A.J., Polymerization shrinkage and polymerization shrinkage stress in polymer-based restoratives, J Dent., 25(1997), pp. 435-440.

[3] FERRANCE J.L., Resin composite – state of the art, Dental Materials 27 (2011), pp. 29 – 38.

[4] SAKAGUCHI R.L., POWERS J.M., Craig's Restorative Dental Materials, 13th ed., Elsevier Mosby, Philadelphia, USA, 2012.

[5] MILEWSKI G., MAJEWSKI T., Influence of the method of polymerization of composite material for teeth crown fillings on its strength properties, Solid State Phenomena, Vol. 240 (2016), pp. 168-173.

Biomechanics: origin of the concept and the science of movement

J.C. MUÑOZ[1], **F. MONTANÉ**[2], **M.M. VALES FLORES**[3]

Keywords: *Biomechanic, science of movement, first mention, Preyer and Benedikt.*

1. Background

The current historiography in Human Movement and Human Gait assigns the origin of the term "Biomechanics" to Moriz Benedikt, who mentioned it in *Über mathematische Morphologie und Biomechanik*, within the framework of the Congress of Naturalists in Wiesbaden in 1887. However, as G. Toepfer shows (2016) [1], this term was previously used by the physiologist William Preyer.

2. The introduction of a new concept

2.1. William Preyer

William Thierry Preyer (1841–1897) was born in Rusholme, England. He studied in Germany, where he was a Professor of Physiology at the University of Jena. He made a remarkable contribution to the field of Child Psychology and Physiology through several publications. William held the idea of "eternal life", a conception of the existence of the organic life in the Universe as eternal, just like matter. In other words, he considered that life has always existed throughout the universe [2]: "Is not the problem of the origin of life based on a wrong assumption that the living must have come sometime from the non-living? All organisms invariably originate from other living organisms" [3].

Years later, Alexandr Oparin will affirm that "the adherents of the theory of the eternity of life assume that at all times some principle existed eternally, which passed on from organism to organism, and without which the origin of living things would be impossible. Following this path of reasoning, we invariably fall into the pit of vitalistic conceptions" [3]. On the contrary, Mechanism considers that such a vital force does not exist and that the physicochemical reaction that occurs in a living organism follows the same laws that govern inanimate.

2.2. Biomechanik

Concepts such as Biostatik and Biodynamik were already used routinely in the field of Physiology in 1866, as can be seen in Ernst Heinrich Haeckel´s diagram [4], and even earlier, in the first half of the 19th century [5] [6] [7].

However, as far as we have been able to verify, the term Biomechanik appears for the first time in *Über die Erforschung des Lebens* [8], published in 1873. After the preface (Vorwort), towards the end of the fourth page, we find the first and only mention of the term Biomechanics that appears in this book, where it can be read in the German language that: "Die Biomechanik unternimmt es aber keineswegs alle Mysterien des Lebens zu entschleiern. Das kann sie nicht, und sowie sie es versucht, verliert sie an Ansehen." [Biomechanics, however, does not claim to reveal all mysteries of life. It cannot, and as soon as it tries, it loses reputation] (Fig. 1), surely alluding to his ideas about the eternity of life.

Die Biomechanik unternimmt es aber keineswegs alle Mysterien des Lebens zu entschleiern. Das kann sie nicht, und sowie sie es versucht, verliert sie an Ansehen. Ge-

Fig. 1. The first mention of the term Biomechanics (1873) [8]

[1]Instituto de Ciencias de la Rehabilitación y el Movimiento (UNSAM), e-mail: profjcm@hotmail.com
[2]Universidad Nacional Arturo Jauretche, e-mail: montane.favio@maimonides.edu
[3]Universidad Católica de Salta, e-mail: mmvflores@ucasal.edu.ar

Ten years later, Preyer locates the concept of Biomechanics in the introduction (Einleitung) of *Elemente der Allgemeinen Physiologie* (1883), when he refers to the application of physical theorems to the phenomena of life, relating the concepts Biokinetik, Biostatik and Biodynamik: “z. B. [zum Beispiel] Biomechanik, d.i. [das ist] allgemeine Bewegungslehre der Organismen (Biokinetik) , mit denbeiden Unterabteilungen Biostatik oder Lehre vom Gleichgewicht der Organismen, und Biodynamik (Zoodynamik und Phytodynamik] oder Lehre von den Bewegungen der Organismen, im engeren Sinne Phoronomie” [9] [10] [such as, for example, Biomechanics, that is to say, the general science of the movement of organisms (Biokinetics), with two subdivisions, Biostatics or science of the equilibrium of organisms, and Biodynamics (Zoodynamics and Phytodynamics), or science of the movements of organisms, in the proper sense of Phoronomy].

2.3. The birth of a new science

Although the term was used by Preyer to name a science of movement, in the sense of a theory, it will be necessary to wait until Benedikt (1887) begins to assign the value to express a new science. It is due to the significance given by Benedikt that the concept “Biomechanik” spreads, expands and begins to have the importance as a science that we assign to it today [11] [12]. According to him, Biomechanics is the “Lehre von den Bau-Anordnungen, welche das Auftreten von Lebensvorgängen ermöglichen, und von der Art des Betriebes durch die in den Organen aufgehäuften Ladungen” [13] [14], that is to say, science of the building blocks that enable the occurrence of life, and the processes that enable building up, assimilation, elimination and transport of loads through the organs. In this context, “different organs and organisms, their functions, changes, and multiplications, are due only "to the properties of the substances that compose them and to divers combinations of forces" ” [15].

3. Future perspectives

In his 1873 work, Preyer uses the term Biomechanik without any introduction, without giving it the proper status of a new concept. For this reason, it was probably not the first time it was mentioned. The search for the term in other documents is open to interested researchers. It also remains to be elucidated whether, according to Preyer, the concept of Phoronomy was closer to the current Kinematics or to neovitalism [16]. Finally, from a different perspective than the one we propose in this article, Fraefel (1999) will argue that Biomechanics in Benedikt's time cannot be considered a science but rather a protoscience [17]. This is another discussion that we leave open.

References

[1] TOEPFER G., *Historisches Worterbuch der Biologie*, Springer-Verlag, 2016.

[2] WILLS C, BADA J., *The Spark of Life: Darwin and the Primeval Soup*, OUP, 2001.

[3] OPARIN A.I., *The origin of life*, Dover, 1952.

[4] HAECKEL E., *Generelle Morphologie der Organismen*, George Reimer, 1866.

[5] DUNGLISON R, *Medical lexicon: a Dictionary of Medical Science*, Lea and Blanchard, 1848.

[6] KRAUS D., *Grundriß der allgemeinen Biodynamik*, Göttingen, 1820.

[7] WALSER. *Biostatische Studien*, Jahreshefte des Vereins für vaterländische Naturkunde in Württemberg, 1850, 5, 225-252: 229.

[8] PREYER W., *Über die Erforschung des Lebens,* Mauke's Verlag, 1873.

[9] PREYER W., *Element der allgemeinen Physiologie,* Th. Grieben´s Verlag, 1883.

[10] PREYER W., SOURY J (Trad.), *Éléments de Physiologie Générale*, Félix Alcan, 1884.

[11] MUÑOZ J.C., *El pensamiento biomecánico de Moriz Benedikt: aportes al desarrollo de la biomecánica.* Anales de la Sociedad Científica Argentina, 2017, 259(3), 57-70.

[12] MUÑOZ J.C., VALES FLORES, M., MONTANÉ, F. *Following the first mention of Biomechanics*. Ijarset, 2020, 7(11), 15505-15507.

[13] BENEDIKT M. *Das biomechan. [neovitalist.] Denken in d. Medic. u. in d. Biol*. 1903.

[14] BENEDIKT M. *Biomechanik und Biogenesis*. Fischer, 1912.

[15] *A mechanical theory of life.* The literary digest, New York, Funk & Wagnalls, 1903, 27.

[16] HAECKEL E. *The wonders of life: A popular study of biological philosophy,* Harper, 1904.

[17] FRAEFEL U., *Vom suggestiven Wortfeld zur Protodisziplin: Biomechanik 1880–1930,* Historisches Seminar Zurich, 1999.

Analyses of blood flow through trileaflet and bileaflet aortic valve – will a trileaflet valve replace a bileaflet valve in the future?

A. Nieroda[1]**, M. Pawlikowski**[2]

Key words: *aortic valve, mechanical valve, blood flow*

1. Introduction

Abnormal functioning of the aortic valve contributes to improper cardiovascular and a significant load on the heart muscle. Often, artificial aortic valve transplantation is the only and effective solution. A substantial problem associated with transplantation is the need for anticoagulation therapy in operated patients. It has been found that thrombosis formation depends on the non-physiological fluid flow scheme [1]. The simulation of blood flow through an artificial aortic heart valve using the finite element method (FEM) is the main subject of the research. The studies aim to verify the performance of mechanical aortic valves of two types, i.e., bileaflet (BIL) and trileaflet (TRI) valves (Figure 1). The construction of the BIL valve is based on commercially used aortic valves.

The paper presents an easy-to-implement methodology of flow modelling and defines liquid-structure interaction. Haemodynamic analysis of an artificial aortic valve is a crucial element of the study and improvement of its construction.

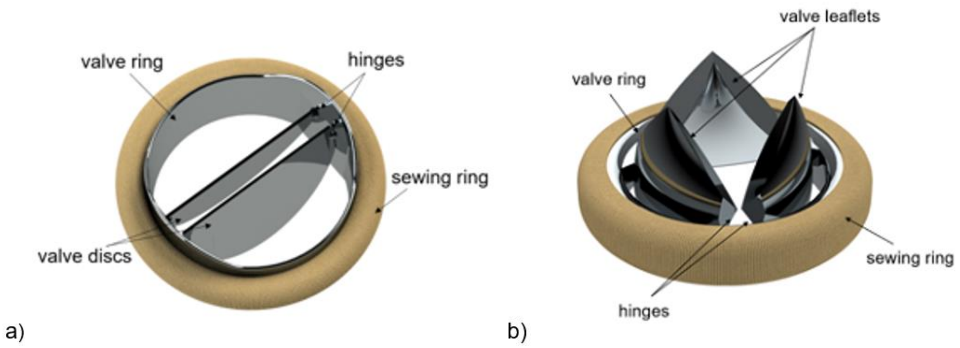

Fig. 1. Model of a) bileaflet and b) trileaflet valves

2. Methods

The numerical model of the system consisted of the left ventricle, valve, and aortic fragment. We analysed the blood flow at four positions of the valves' leaflets defined through an angle to the vertical plane (passing through the symmetry axis of the valve) 60◦ (fully closed valve), 40◦, 20◦, and 0◦ (fully opened valve).

The blood flow was defined in a way reflecting the actual, pulsatile nature of the flow. The correlation of the flow velocity and the time opening of the leaflets was determined utilising the Doppler ultrasound examination in an adult human being [2]. Blood flow through a valve is a complex phenomenon. It includes both the movement of the fluid and the movement of the valve leaflets. The dynamics of blood circulation were determined using ANSYS 2019 R2 software. The use of three modules made it possible to analyse flow characteristics and determine the influence of structural response on cyclic fluid movement.

[1]Warsaw University of Technology, Institute of Mechanics and Printing, Warszawa, Poland,
e-mail: anna.nieroda.dokt@pw.edu.pl
[2]Warsaw University of Technology, Institute of Mechanics and Printing, Warszawa, Poland,
e-mail: marek.pawlikowski@pw.edu.pl

3. Results

The performance of the considered valves was assessed through reduced stress in the valves resulting from the interaction of the flowing blood and the leaflets, shear stress in the aorta wall, and an effective orifice area. Mounting of the leaflets in the valve ring was also analysed. The obtained results give new insights into the strength performance of the design of the leaflet fixation in the annular rings.

Stress distribution in the leaflets of the BIL and TRI valves was calculated as well as the flow through them was characterised. The blood velocity distributions during flow through the valves were also defined. In addition, the flow velocity profile was determined in order to verify symmetry of the flow (Figure 2).

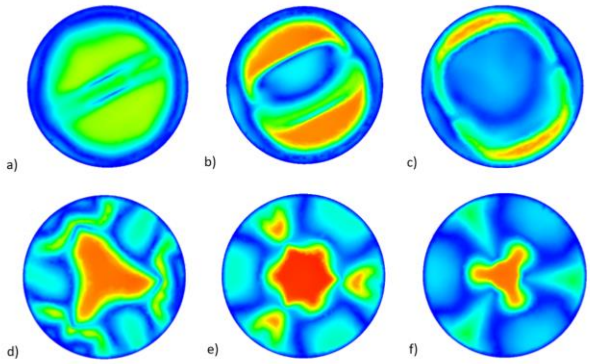

Fig. 2. Flow characteristics for the opening angle of the two-disc valve: a) 0˚, b) 20˚, c) 40˚, for three-leaflet valve: d) 0˚, e) 20˚, f) 40

4. Discussion

The blood flow velocity is higher in the case of the TRI valve, which results from Bernoulli's law. Interestingly, the lower values of blood flow velocity through the partially and fully opened BIL valve correspond to those for the natural trileaflet aortic valve [3]. The maximal stress concentrations were observed in the hinges. Similar results were also obtained by other investigators [4].

The shear stress affects the behaviour of blood cells during flow. Regions of high shear stress can cause a thrombotic response, specifically through haemolysis and shear-induced platelet activation. From the obtained results, we conclude that none of the considered mechanical valves will cause haemolysis.

References

[1] DASI L.P., SIMON H.A., SUCOSKY P., YOGANATHAN A.P., *Fluid mechanics of artificial heart valves,* Clinical and Experimental Pharmacology and Physiology, 2009, 36(2), 225-237.

[2] AMINDARI A., SALTIK L., KIRKKOPRU K., YACOUB M., YALCIN H.C., *Assessment of calcified aortic valve leaflet deformations and blood flow dynamics using fluid-structure interaction modeling,* Informatics in Medicine Unlocked, 2017, 9(C), 191-199.

[3] SUNDSTRÖM E, JONNAGIRI R, GUTMARK-LITTLE I, GUTMARK E, CRITSER P, TAYLOR MD, ET AL. *Hemodynamics and tissue biomechanics of the thoracic aorta with a trileaflet aortic valve at different phases of valve opening,* International Journal for Numerical Methods in Biomedical Engineering, 2020, 36(7), 1-14.

[4] KWON Y.J., *Numerical analysis for the structural strength comparison of St. Jude Medical and Edwards MIRA bileaflet mechanical heart valve prostheses*, Journal of Mechanical Science and Technology, 2010, 24(2), 461-469.

Transtibial amputee ramp gait - preliminary report

J. OTWOROWSKI[1], M. MURAWA[2], A. GRAMALA[3], P. DRAPIKOWSKI[4]

Key words: *Lower limb amputee gait, Prosthetic feet, ramp gait*

1. Introduction

The objective assessment of the effectiveness of the new design solutions for subsequent models of prostheses is becoming a standard of conduct as the three-dimensional movement analysis systems become more and more popular [1], [2]. As the amputee patients should be able to walk efficiently not only on the level ground but also during ascending or descending on uneven ground conditions, more research interest should be focused on this field of development. The purpose of the study was to compare selected biomechanical gait parameters between the amputee patient (equipped with the Otto Bock 1C64 Triton HD prosthesis foot, commonly used by active patients with no mobility limits) and non amputee healthy subjects during walking on the ramp (ascent and descent). The result of this study is also a starting and reference point for the new concept of the foot prosthesis.

2. Materials and methods

2.1. Participants and intervention

34 years old male with TTA amputation (almost 3 years ago) participated in the study. Amputation etiology was trauma. He was equipped with the Otto Bock Harmony prosthesis socket and Otto Bock 1C64 Triton HD prosthesis foot. The control group included 10 healthy adult subjects (5 male and 5 female) at the age of 21,9 ± 1,8 with no medical problem.

2.2. Measurements and calculations

During the study specific designed and constructed ramp with slope angle 11,65 ± 0,41 deg was used. Measurements were carried out using the OptiTrack motion capture system. 25 records for the amputee ascend and descend and 5 records for ascend and descend for each control group participant were registered. 8 markers model based on Helen Hayes lower body model was used to calculate the angles in the ankle joint.

[1]Poznan University of Technology, Faculty of Mechanical Engineering, Poznań, Poland,
e-mail: jakub.i.otworowski@doctorate.put.poznan.pl
[2]Poznan University of Physical Education, Department of Biomechanics, Poznań, Poland,
e-mail: murawa@awf.poznan.pl
[3] Poznan University of Technology, Faculty of Control, Robotics and Electrical Engineering, Poznań, Poland
[4] Poznan University of Technology, Faculty of Control, Robotics and Electrical Engineering, Poznań, Poland

3. Results

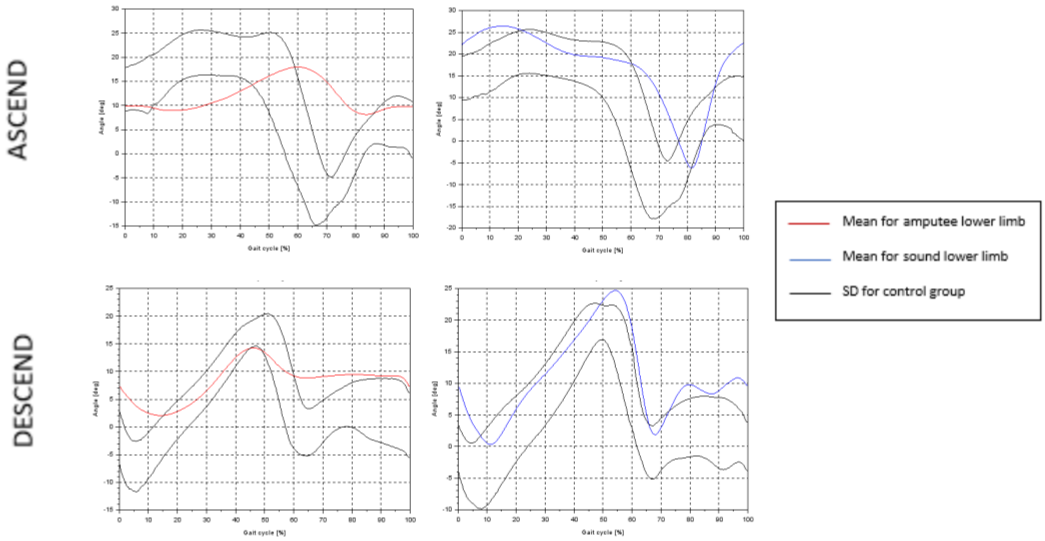

Fig. 1. Ankle dorsi-plantar flexion during ramp gait ascend and descent for amputee lower limb (left) and sound lower limb (right)

4. Discussion

The authors main finding was that the ankle movement pattern for the prosthetic foot characterized with reduced ankle range of motion. The deficits are more significant during ramp descent. The results agree with other studies and proves the need for searching the innovative solutions to restore full range of ankle motion in order to regain a good quality ramp gait [2]. Otto Bock 1C64 Triton HD which works very good during level walking is far away from the optimal solution in terms of ascent and descent types of locomotion.

Acknowledgments: This study was founded by Wielkopolski Regionalny Program Operacyjny na lata 2014-2020, Oś. Priorytetowa 1. Innowacyjna i konkurencyjna gospodarka, Działanie 1.2. „Wzmocnienie potencjału innowacyjnego przedsiębiorstw Wielkopolski" and realized by Enforce Medical Technologies' project named „Wzmocnienie potencjału innowacyjnego przedsiębiorstwa ENforce Medical Technologies Sp. z o.o. poprzez inwestycję w infrastrukturę badawczo-rozwojową oraz przeprowadzenie prac badawczych, celem opracowania prototypu bionicznej protezy stopy".

References

[1] SCHMALZ T., ALTENBURG B., ERNST M., BELLMANN M., ROSENBAUM D., S.C, CARDOS L., *Lower limb amputee gait characteristics on a specifically designed test ramp: Preliminary results of a biomechanical comparison of two prosthetic foot concepts.* Gait & Posture, 2019, 68, 161-167.

[2] FRADET L., ALIMUSAJ M., BRAATZ F., WOLF S.I., *Biomechanical analysis of ramp ambulation of transtibial amputees with an adaptive ankle foot system.* Gait & Posture, 2010, 32(2), 191-198

Long bone locking plate positioning enhancement with finite-element model

M. PALKA[1], R. PERZ[2]

Key words: *long bone, stabilization, locking plate, humerus*

1. Introduction

The long bone fracture is one of the most popular skeletal injury caused by external factors due to its specific structure. Appropriate fracture treatment plays the most important role in its healing. After proper stiffening of the bones, the time factor is essential for the reconstruction of bone tissue.

In the case of long bone fractures, devices that rigidly hold the bone pieces in the correct position with the help of screws inserted in the bone can be helpful. A certain degree of flexibility of the stabilizers is necessary in order for the fracture to heal properly. The stabilizer's stiffness should be as close as possible to that of the bone, if possible.

Locking plate is a device enabling the fusion of two bone fragments, without the need for direct interference with the fracture or inflammatory process [1]. External stabilization is based on the principle of transferring loads through the external system (stabilizing apparatus) bypassing the fracture site or only its partial participation.

The stabilization of the apparatus as well as the type, shape and place of refraction are factors that have a decisive influence on the process of union. The right location and placement of fracture displacements are also important. This is directly related to the change in stress varying in individual bone sections.

The aim of the study was to analyse the configuration of the locking plate screw arrangement in the bone, in which the stress affecting the bone is the LOWEST. Determination of the optimal configuration leads to the least damage to the patient's health. Stresses, displacements and static deformations occurring in the screws and stabilizer embedded in the forearm bone were analysed. This study is to provide insight on the possible FEM usage as an pre-surgery planning enhancement.

2. Methods

For the analysis the human humerus bone was selected and its CT scan was performed. The DICOM medical images of the bone were used to build the model in CAD software. Then ANSYS Workbench software was used to define a finite element model of human femur, which simulate the geometry and bone mechanical properties. It was essential for performing calculations and creating a map of the stresses that appear on stabilizer plate, screws and bone itself in different configurations.

Cortical bone strength material properties: orthotropic material, ρ=1.39 g/cm3, E_1=3880.6, E_2=3880.6, E_3=5712.6, G_{12}=5.71, G_{23}=7.11, G_{31}=6.58, v_{12}=0.4, v_{23}=0.25, v_{31}=0.25 [2].

Locking Plate and screws material properties: isotropic material, taken from ANSYS material base; ρ=4.62 g/cm3, E=96000, G=35294, v=0,36; where E is the elastic modulus for cortical or trabecular bone in MPa, function of bone density ρ in g/cm3, G is the shear modulus in MPa and ν is Poisson ratio [3].

For the study purpose oblique displace type of bone fracture was used (Fig. 1). Depending on case, specific force was applied to the plate model locked with screws, then stress, displacement

[1]Warsaw University of Technology: Institute of Aeronautics and Applied Mechanics, Warsaw, Poland
e-mail: mpalka@meil.pw.edu.pl
[2]Warsaw University of Technology: Institute of Aeronautics and Applied Mechanics, Warsaw, Poland,
e-mail: rafal.perz@pw.edu.pl

and sliding distance in vicinity of the fracture were analysed. Also stresses occurring in screw holes for various configurations of positioning the screws were checked.

In analysis the screws configurations: 2x20° + 2x0°, 4x0°, 4x10° and 4x20° were analysed for bending (both XZ and YZ), compression and tension [4].

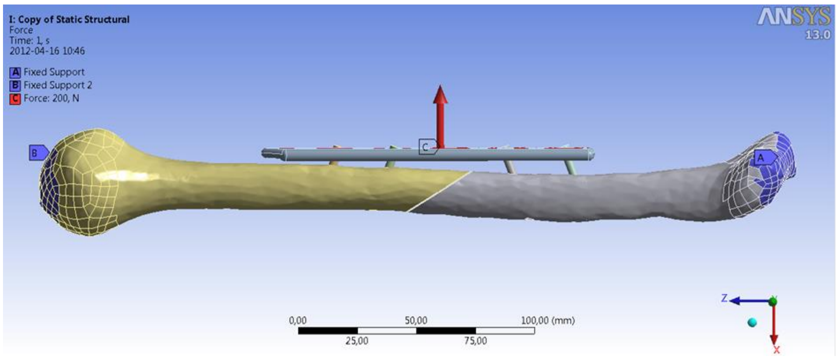

Fig. 1 A humerus model used to simulate pulling a stabilizer plate from the bone

3. Results

The conducted research led to determination of the most optimal configuration of the screw's setup. Out of four analysed setups the best outcome was given by the 2x 20° + 2x 0° configuration, giving values below 30 MPa on average and below 50 MPa at peaks (3 point bending, 1st screw). Stress values in this configuration are the lowest. Other configurations provided satisfactory results but higher than the selected one. All of the stress results were below 70 MPa which gives significant margin from the assumed 100 MPa bone endurance level.

4. Summary

This research proved that pre-surgery planning of the locking plate positioning using FEM modelling might be useful for optimal placement and stress reduction. Such approach can benefit with lowering the risk of locking plate failure and as a result decreasing risk of healing failure. Further plan assumes detailed analysis of the approach and introducing it to medical practice.

References

[1] BĘDZIŃSKI R., *Biomechanika inżynierska, Zagadnienia wybrane*. Oficyna Wydawnicza Politechniki Wrocławskiej, Wrocław 1997

[2] BEER, R. J , EBERHARDSTEINER, J. , KODVANJ, J. , GRIENAUER, W. , GOTTSAUNER-WOLF, F., SKRBENSKY, G., *Mechanical and medical aspects of an implant-bone connection in the femur: A three-dimensional photoelastic study of the load transfer mechanism using gamma radiation for fixing the experimental information. Comparison of two solutions of femur prosthesi,* Acta of Bioengineering and Biomechanics Vol. 2, nr 2, pp. 25-31, 2000

[3] FONSECA E.M.M., LIMA M.J., BARREIRA L.M.S., *Human femur assessment using isotropic and orthotropic materials dependent of bone density*, 3 rd International Conference on Integrity, Reliability and Failure, Porto/Portugal, 20-24 July 2009

[4] WÄHNERT D., WINDOLF M., BRIANZA S., ROTHSTOCK S., RADTKE R., BRIGHENTI V., SCHWIEGER K., *A comparison of parallel and diverging screw angles in the stability of locked plate constructs*, J Bone Joint Surg Br. Sep;93(9), pp. 1259-64, 2011.

Characteristics of nerve roots mechanical properties exposed to uniaxial stretching tests

M. PALMERSKA[1], A. MACKIEWICZ[2], T. KLEKIEL[3], A. NOSZCZYK-NOWAK[4], R. BĘDZIŃSKI[5]

Key words: *nerve roots, radiculopathy, uniaxial stretching tests*

1. Abstract

The article presents the issues of the mechanical response of nerve roots under stretching conditions. There is assumed a relation between deformation, blood flow characteristics, and nerve root impulse transmission. Research proves that vascular hypofusion of peripheral nerves occurs at a deformation of 15%. Impulse conduction disturbances at 6% strains were also observed. From this account it follows that the cause of diseases of the nervous system may be excessive deformation of its structures. One of such diseases is radiculopathy.

Lumbar radiculopathy affects 3 to 5% of the general human population. It is a condition caused by chemical or mechanical factors that destroy the nerve roots, such as herniated discs, inflammation, and iatrogenic causes. Radiculopathy is accompanied by various types of pain and functional deficits that make life difficult for patients. In addition to compression, nerve roots may be exposed to tensile stress, e.g. by adhesions with the surrounding structures as a consequence of inflammation. This phenomenon is often unnoticeable during follow-up MRI examinations, which makes correct diagnosis difficult. It is essential to understand the development of the pathology of nerve roots exposed to mechanical stress to understand the relationship between stresses, strains and the structural and functional reaction of the nerve roots.

Understanding the mechanical response of tissues exposed to certain clinical conditions requires special techniques and complex constitutive models that cannot be solved analytically. Tissue material parameters are therefore tested using numerical approximation methods. In order to do this, it is necessary to experimentally investigate the material characteristics that allow to determine the parameters for the numerical models used.

The aim of investigation was to define the material characteristics of nerve roots. The analysis was performed to obtain data allowing to simulate conditions that can lead to disease states of nerve roots using the finite element method.

The material was obtained from the rabbit's lumbar spine, which was stored in the transplant fluid in a freezer at 5°C by 6 hours. Paraspinal muscles and spinous processes were removed. Samples of the neural structures originating from the spinal cord with the spinal nerve were obtained individually with a scalpel and tweezers, just before the examination. To prevent drying, the samples were soaked in water. Tensile tests were performed with a speed of 0.17 mm / s on testing machine ZWICK. The samples were mounted on specially made holders. The obtained data showed that the rabbit nerve root strength 0.9 ± 0.53MPa, the relative deformation 12.73 ± 4.03%, and Young's modulus 2.53 ± 1.00MPa. The results of the experiment were compared with the results from the literature. The obtained results are partly in line with the results of other researchers, but none of the data is fully consistent with each other. The tensile strain achieved in the studies and data reported in the literature exceed 9%, which in clinical conditions would result in vascular hypofusion, conduction disturbances and tissue changes.

[1] University of Zielona Góra, e-mail: 20000884@stud.uz.zgora.pl

[2] University of Zielona Góra, e-mail: a.mackiewicz@iimb.uz.zgora.pl

[3] University of Zielona Góra, e-mail: t.klekiel@iimb.uz.zgora.pl

[4] Wrocław University of Environmental and Life Sciences, e-mail: agnieszka.noszczyk-nowak@upwr.edu.pl

[5] University of Zielona Góra, e-mail: r.bedzinski@iimb.uz.zgora.pl

References

[1] BERTHELOT J., LAREDO J.D., DARRIEUTORT-LAFFITE C.,MAUGARAS Y., *Stretching of roots contributes to the pathophysiology of radiculopathies*. Joint Bone Spine, 2018, vol.85, 41-45

[2] JU, M.S, LIN C.C.K., FAN J.L., CHEN R.J.,*Transverse elasticity and blood perfusion of sciatic nerves under in situ circular compression.* Journal of biomechanics, 2006, 39.1: 97-102.

[3] SINGH A., LU Y., CHEN C., CAVANAUGH J.M., *Mechanical properties of spinal nerve roots subjected to tension at different strain rates.* Journal of Biomechanics 39, 2006, 1669–167

[4] KHUYAGBAATAR B., KIM K., PARK W.M. KIM Y.H., *Biomechanical investigation of post-operative C5 palsy due to ossification of the posterior longitudinal ligament in different types of cervical spinal alignment.* Journal of biomechanics, 2017, 57: 54-61.

[5] KWAN M.K., RYDEVIK B., MYERS R.R., TRIGGS K., WOO S.L.Y., GARIN S., *Biomechanical and histological assessment of human lumbosacral spinal nerve roots.* Trans Orthop Res Soc., 1989, 14,

The influence of polyurethane double-J stent of various diameters on urological encrustation

K. PASIK[1]

Key words: *urolithiasis, ureteral stent, encrustation, scanning electron microscopy, me-chanical strength, ureterorenoscopic-lithotripsy procedure, surface roughness arthroplasty*

Abstract

Double-J ureteral stents (DJ stents) are commonly used in urology. The most troublesome difficulty in their application is stent encrustation, stent breakage, and recurrent urinary tract infections. This work aimed was to de-termine the causes of a double-J stent complication.

The analysis of DJ stents included microscopic analysis, mechanical strength testing, and surface roughness measurements. The analysis was per-formed on the brand new ureteral stents and ureteral stents implanted after the ureterorenoscopic-lithotripsy (URSL) to treat calcium oxalate stone. Performed analysis of the polyurethane DJ stents concentrated on elaborating the influence of ureteral stent diameter (1.00; 1.33; 1.66 mm) on the affinity to stent encrustation and/or breakage.

The comparison of DJ stents with different diameters confirmed that the risk of encrustation increases with the lower diameter of the ureteral stent. Remaining post-URSL kidney stone fragments deposited on the surface of the DJ stents formed a multilayer structure creating a risk of obstruction or blockage of ureteral stents and block the urine flow. Additionally, a decrease in mechanical strength of the DJ stent related to the implantation time was determined. DJ stent implantation caused an increase in surface roughness.

The performed analysis indicates the need for further exploration of the biomaterials used in DJ stents and modification of their surfaces. This may allow to eliminate the phenomenon of encrustation of urinary stone frag-ments and NaCl crystals on the surface of implanted stents.

[1]Department of Biomedical Engineering, Faculty of Mechanical Engineering, University of Zielona Gora, Zielona Gora, Poland, e-mail: k.pasik@iimb.uz.zgora.pl,

Using Bayesian framework to calibrate Voce model parameters of ductile human parietal bone

M. PEKEDIS[1]

Key words: *Parietal bone, Bayesian model calibration, Voce model, uncertainty quantification*

1. Introduction

Scatter and intrinsic variability in biomechanical properties of hard biological tissues are some of the main sources of uncertainties mostly influenced by several variations such as micro-structure, tissue age and *in-vitro* experimental noises. Hence, mathematical models often needs approaches that captures the randomness due to uncertainties in mechanical response [1]. Here, we address the Voce modelling in a probabilistic framework for the quantification of uncertainties of human parietal bone.

2. Methodological concept

The experimental stress and strain curves used in this study are those reported for the fresh frozen human parietal bone (Figure 1a) [2]. To predict the stress that involves elastic-plastic range of the bone, Voce model is implemented. In this model the flow stress may display non-linearly with increment of plastic strain. The equivalent stress in Voce model:

$$\sigma_{eq} = k_o + Q(1 - \exp(-\beta \varepsilon^{pl})) \tag{1}$$

where k_o, Q and β are calibrated parameters and ε^{pl} is the plastic strain. For uniaxal test $\sigma_{eq} = \sigma_{true}$ where σ_{true} is true stress (Cauchy). We assume isotropic material, and the stress-strain data could be converted to true stress-strain as,

$$\begin{aligned} \sigma_{true} &= \sigma_{eng}(1 + \varepsilon_{eng}) \\ \varepsilon^{pl} &= \ln(1 + \varepsilon_{eng}) - \frac{\sigma_{true}}{E} \end{aligned} \tag{2}$$

where σ_{eng} and ε_{eng} represent engineering stress and strain, respectively.

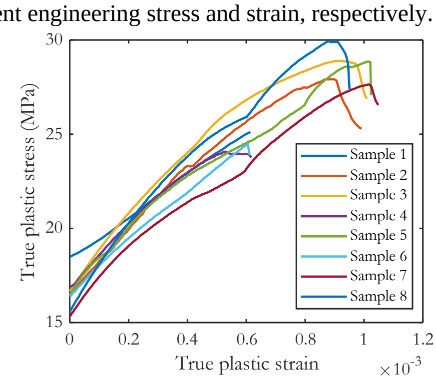

Fig. 1. True plastic stress-strain curves of human parietal bones in plastic (Adapted from Pekedis et al. [2])

The uncertainty bands on the model predicted curves can be computed by sampling the joint probability distribution of the parameters. The framework is based on Bayes's classical theorem of conditional probability that can be described as,

$$P(\theta | D, M) = \frac{P(D | \theta, M) P(\theta | M)}{P(D | M)} \tag{3}$$

[1]Ege University/Department of Mechanical Engineering, Izmir, Turkey, e-mail: mahmut.pekedis@ege.edu.tr

where D represents the data, M is the Voce model, and θ shows the model parameters (k_o, Q and β) to be estimated. After obtaining new data, model parameters are updated by the likelihood function $L(\theta)=P(D|\theta, M)$ and prior joint probability density function (PDF) $P(\theta|M)$. The goal of the Bayesian analysis is to compute the joint posterior PDF $P(\theta|D, M)$. The likelihood function $L(\theta)$ shows the probability of witnessing the data D is based on predictions. In the current study we choose prior for k_o (between 0 and 50), Q (between 0 and 50), and β (between 0 and 1300) to be uniformly distributed. We considered predicting outcomes of σ_{true} having normally-distributed observations.

3. Results

The calibrated results obtained for k_o, Q and β are 16.39±0.08 MPa, 18.71±0.62 MPa and 1053.4± 60.5, respectively. Fig 2a represents stress-strain curves and their uncertainty bands. The model can capture the randomness due to uncertainties for all experimental measurements. The pair wise parameter scatter plots are given in Fig 2b, 2c and 2d which each point represents a sample for the posterior distribution. These plots also indicate whether there is correlation between parameters pairs. In conclusion, the approach we followed here may allow experiments to be accurately reproduced and provide calibrated parameters with randomness for the computational biomechanics simulations.

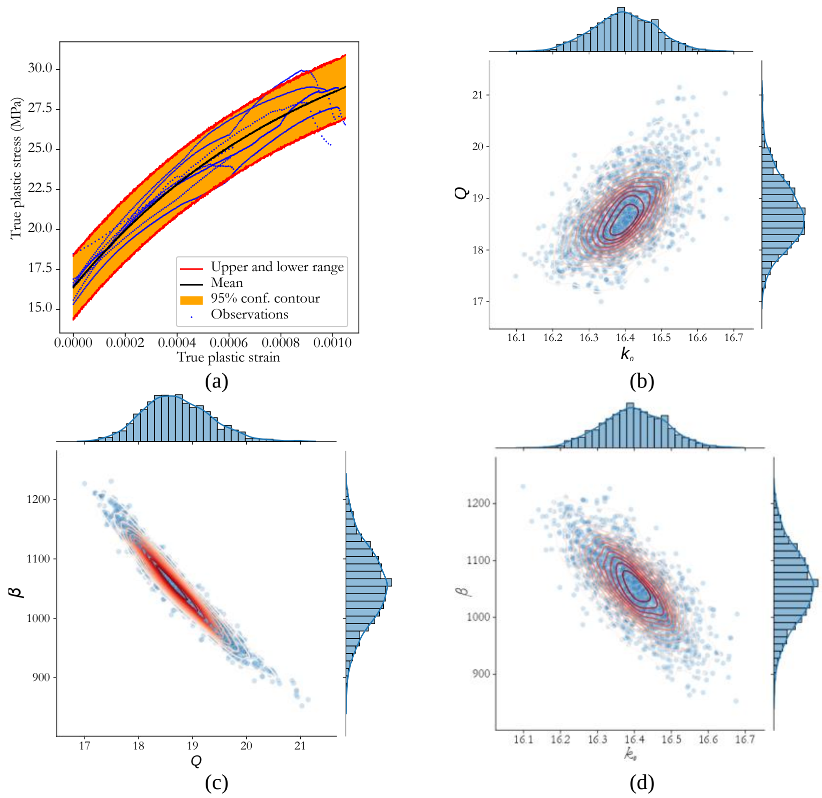

Fig. 2. Model prediction. (a) Predicted true stress-strain curves and their uncertainty bands with 95% confidence contour, (b-d) Joint probability plots of the model pair wise parameters (k_o and Q are in MPa while β is unitless)

References

[1] TEFERRA K., BREWICK P., *A Bayesian model calibration framework to evaluate brain tissue characterization experiments*, 2019, Comput Method Appl Mechanics, 357.

[2] PEKEDIS, M. *et al. Characterization of the mechanical properties of human parietal bones preserved in modified larssen solution, formalin and as fresh frozen*. 2021, Surg Radiol Anat.

The dependence of postural stability on visual stimuli following a flight with different task loads in General Aviation pilots

E. POLAK[1], A. ŚWICZEREWSKI[2], A. GARDZIŃSKA[3]

Key words: *postural stability, flight, Civil Aviation, Romberg ratio*

1. Introduction

People working in the profession of the General Aviation (GA) pilots are required to have high general physical fitness, high efficiency of the circulatory and respiratory systems, as well as high efficiency of the hearing, sight and sense of balance. They should have efficient senses, which include sight and spatial orientation, hearing, feeling (the so-called proprioception) and smell. Usually, the pilot relies on the sense of sight, which, together with the sense of balance and proprioceptors, provide him with information about the position and position of the body in space [1,2]. The accelerations that occur in a plane during the various phases of flight can interfere with the normal perception of the gravity vertical by the otolithic organs. Confusing impressions may cause the pilot a stronger sense of the gravity vertical relative to the aeroplane than to the Earth [1,3].

The results of scientific research confirm the legitimacy of using the monitoring of the psychophysical state of the pilot during the implementation of air operations as one of the methods of improving flight safety and reducing the risk of threats. One example is the conclusions of the Galant research which showed that there is a relationship between the increased GA pilot task load and the level of its physiological parameters [4].

The purpose of this research is the assessment of the dependence of postural stability on visual stimuli following a flight with different task loads in general aviation pilots participated in training for the ATPL (A) license.

2. Material and Methods

The study was carried out at the Aviation Training Centre of the Rzeszów University of Technology in a group of 37 volunteers selected from among students of aviation and astronautics with a specialization in pilotage. The subjects flew, depending on the stage of the training, with aircraft of similar equipment: the single-engine Piper PA-28 “Arrow” or the twin-engine Piper PA-34 “Seneca”. Each pilot carried out flight sessions and performed the tasks specified in the training program, based on the principles of instrument flights. They consisted in practicing the critical phases of flight, i.e., the Standard Terminal Arrival Route (STAR), Standard Instrument Departure (SID) and landing approaches using radio navigation or GNSS systems (RNAV, ILS, VOR) and the improvement of the circles at the airport, using the indications of aircraft instruments.

Before starting the flights, the pilots completed a research card based on the Simulator Sickness Questionnaire (by Kennedy et al.) - a standardized tool used in research related to the verification of the psychophysical state of pilots [2]. The obtained information was used to characterize the subjects, verify the inclusion criteria and divide the studied pilots into two groups. Group 1 included 15 pilots (aged 24,3 ± 0,9 years) who practiced the airport traffic circles and critical phases of flight, and group 2 included 22 pilots (aged 23,0 ± 0,1 years) who practiced navigation skills along the flight route and flight procedures to other airports. The average duration of flight sessions in Group 1 was 1,6 ± 0,3

[1]Rzeszow University of Technology, Academic Sport Centre, Rzeszów, Poland, e-mail: e.polak@prz.edu.pl
[2]Rzeszow University of Technology, graduate of the Faculty of Mechanical Engineering and Aeronautics, Rzeszów, Poland
[3]Rzeszow University of Technology, Academic Sport Centre, Rzeszow, Poland, e-mail: agardz@prz.edu.pl

hour, and in Group 2 2,1 ± 0,4 hours. The pilots in Group 1 performed shorter flights duration but characterized by a greater task load.

To evaluate the postural stability the Romberg test (standing both feet in 30 seconds with eyes open and closed) on the Alfa stabilographic platform (produced by AC International East) was used. The obtained data described the displacements of the Centre of Pressure (CoP) from the geometrically central point of the platform in a two-dimensional coordinate system. Each of the subjects performed the postural stability test twice: before boarding the plane (pre-test) and immediately after leaving it (post-test).

The result analysis included the comparison of the influence of visual stimuli on the control of postural stability of the studied pilots. For this purpose, a comparison of the normalized Romberg ratio for the sway path (Rr SP) and the surface area (Rr SA) with eyes open (EO) and eyes closed (EC) was used. Romberg ratio were calculated according to the formula [5]:

$$Rr = \frac{EC - EO}{EC + EO} * 100 \tag{1}$$

Interpreting the Romberg ratios means that a value close to zero or negative indicates that the amount of body sway is similar or less with eyes closed than with eyes open. This means that the stability of the subject's standing posture is not visually dependent, i.e., information from visual stimuli is less important for the control of postural stability than information provided by proprioceptive stimuli. On this basis, it can also be concluded that a very high positive value of the Romberg index indicates disorders in the interpretation of proprioceptive stimuli [5].

The differences between the results obtained before (pre-test) and after (post-test) the flight session were analysed in both studied groups. To determine the statistical significance of the differences between pre- and post-test (at the level of α = 0.05) the nonparametric U Mann-Whitney test was used.

3. Results

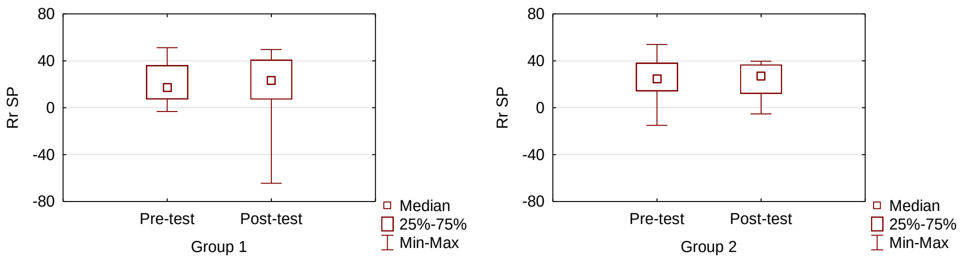

Fig. 1. Normalized Romberg ratios for the sway path of the CoP displacement (Rr SP) in pre- and post-tests.

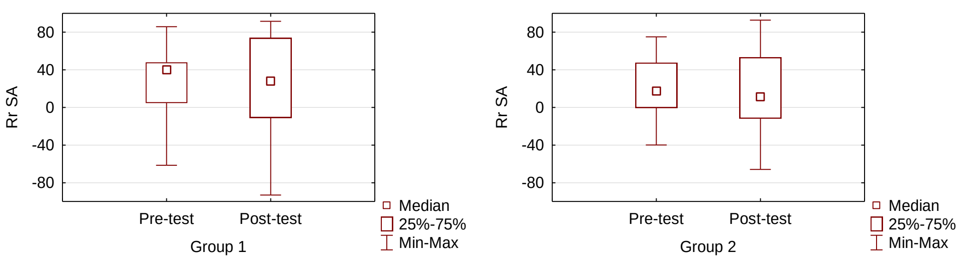

Fig. 2. Normalized Romberg ratios for the surface area of the CoP displacement (Rr SA) in pre- and post-tests.

In order to check whether the dependence of postural stability on visual stimuli changed after the flight session, the differences between ratios in pre- and post-tests were analysed. There were no statistically significant intergroup differences in the pre-tests or post-tests. However, the post-test results indicate a decrease in the mean value of Rr SP and Rr SA in both groups, and thus a lower dependence of postural stability on visual stimuli. Considering the fact that the border between visual dependence and independence in mathematically is determined by the Rr value close to zero, it was observed that the flight session with a higher task load resulted in a greater reduction in both Rr values. Rr SP in Group 1 was reduced from 20,73 ± 16,49 to 19,12 ± 28,59 and in Group 2 from 24,25 ± 17,71 to 23,13 ± 14,80. Rr SA in Group 1 was reduced from 24,73 ± 37,19 to 20,57 ± 54,28 and in Group 2 from 21,89 ± 33,08 to 20,02 ± 44,06. There was also a greater increase in intra-group differentiation in Group 1.

4. Conclusion

The observed changes in the Romberg ratios values for both the path length and the CoP displacement area after the flight sessions showed that in both groups of subjects under the influence of flying sessions, the dependence of postural stability on visual stimuli slightly decreased. A greater difference between the value of Romberg ratios, and thus a stronger reaction to the performance of a flying session, was noted in Group 1, i.e., the group performing flights with a higher task load. The obtained results require confirmation in subsequent studies, which should be performed in a larger group of respondents, taking into account more precise inclusion criteria.

References

[1] GRUSZECKI J., RZUCIDŁO P., *Uproszczony model informatyczny pilota operatora.* Journal of Aeronautica Integra, 2008, 1: 59-67.

[2] STOFFREGEN T.A., HETTINGER L.J., HAAS M.W., ROE M.M., SMART L.J., *Postural instability and motion sickness in a fixed-base flight simulator.* Human Factors, 2000, 42(3): 458–469.

[3] MARYNIAK J., *Zagadnienia symulacji lotu na symulatorach lotniczych - samolot, człowiek, symulator.* Mechanika Teoretyczna i Stosowana, 1990, 3-4(28).

[4] GALANT M., *Ograniczanie ryzyka zagrożeń w lotnictwie ogólnym przez zastosowanie systemu monitorującego stan psychofizyczny pilota.* Rozprawa doktorska. Poznań: Wydział Maszyn Roboczych i Transportu, Politechnika Poznańska, 2017.

[5] TJERNSTRÖM, F., BJÖRKLUND, M., AND MALMSTRÖM, E.M., *Romberg ratio in quiet stance posturography - Test to retest reliability.* Gait & Posture 2015, 42, 27–31.

Experimental evaluation of a novel concept of an implant for direct skeletal attachment of limb prosthesis

P. Prochor[1]

Key words: *stump, strain, bone, ARAMIS*

1. The design of a novel concept of implantation system for bone-anchored prostheses

The proposed implantation system (patent no. 229715) was developed to directly connect prosthesis to bone in order to avoid the disadvantages resulting from the use of prosthetic sockets [1]. The system consists of two parts: the medullary part (made of PEEK GRF30) placed in the reamed medullary cavity of a long bone and a percutaneous part (made of Ti6Al4V), which penetrates soft tissues, allowing to attach an exoprosthesis (Fig. 1). Placing the percutaneous part into medullary part expands its conical, triple-notched section, leading to obtainment of press-fit features. At the same time, helical tooth placed on the outer surface of the conical section, gives the advantages of threaded connection.

Fig. 1. Proposed implantation system, on the left – the percutaneous part, on the right – the medullary part

2. Experimental evaluation of proposed implantation system

The functionality of the proposed system has been estimated through previous analyses [2, 3, 4]. To finally confirm its effectiveness, experimental verification was carried out, which is described below.

2.1. Materials and methods

Simplified and properly scaled versions of a typical press-fit implant and the proposed implant were prepared for the study (Fig. 2a). Six femoral porcine bones (cut in half, leaving the proximal part for testing) were prepared for each implant. The medullary cavity was reamed in a way that allowed to obtain a radial interference of 0.1 mm between the implant and the bone. To obtain adequate support, each bone was stabilised with polyester resin on the level of greater trochanter and femoral head in a rectangular aluminum form (Fig. 2b). Marking with black and white spots were applied on the samples using paints, allowing further tests. ARAMIS 3D 4M vision system (GOM) and 858 Mini Bionix testing machine (MTS Systems Corporation) were used in the research (Fig. 2c). The sampling frequency was set to 50 Hz.

a) b) c)

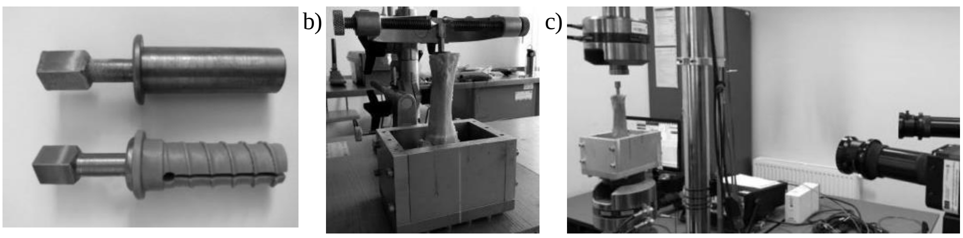

Fig. 2. Steps taken during the experiment: a) simplified and scaled prototypes of typical press-fit (upper) and proposed implant (lower); b) photograph of sample positioning; c) experimental setup for tests with the use of vision system

[1]Institute of Biomedical Engineering, Faculty of Mechanical Engineering, Bialystok University of Technology, Bialystok, Poland, e-mail: p.prochor@pb.edu.pl

The ARAMIS system was used to assess bone deformation during axial loading of the implant head. The axial force simulated the static load bearing exercises (SLBE) performed as rehabilitation activities. The GOM Correlate 2018 (GOM) program was used to process the results. In order to allow an objective comparison of the functionality of the tested implants, a 50 mm x 15 mm bone area, 30 mm below the head of the implants, was selected for each sample, determined each time from the direction of the frontal plane.

2.2. Results

Obtained maps of true strain generated for an applied axial force of 5000 N are presented in Figure 3. A high force value was necessary to observe the deformation occurring on the bone surface.

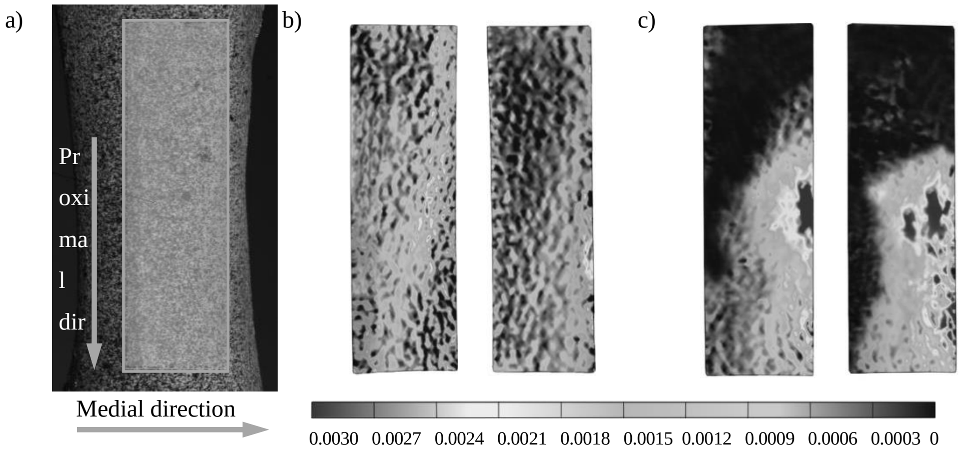

Fig. 3. Obtained results of true strain [ln(mm/mm)] formed in bone during axial loading: a) the analysed area; b) example of results obtained for proposed implant; c) example of results obtained for typical press-fit implant

3. Conclusions

While analysing the obtained strain maps, there can be noticed its strong, local concentrations in the central part of the discussed area, with no noticeable deformation in the distal bone. This suggests that loads are transferred along the entire length of the implant and their concentration in the bone tissue appears along with the end of the structure. In the case of strain maps obtained during axial loading of the proposed implant, deformation occurs in the entire analysed area, with a stronger concentration in the proximal direction. In addition, they are characterised by a strong heterogeneity in relation to the strain obtained when using press-fit implant. This can be caused by the asymmetrical shape of the proposed structure. The data obtained indicate greater functionality, in terms of load transfer method, of the newly designed implant in comparison to typical press-fit solution.

Acknowledgments: Research was funded by Ministry for Science and Higher Education, project number WZ-WM-IIB/3/2020.

References

[1] PITKIN M., *Design features of implants for direct skeletal attachment of limb prostheses,* Journal of Biomedical Materials Research, 2013, 101, 3339-3349.

[2] PROCHOR P, PISZCZATOWSKI S, SAJEWICZ E., *Biomechanical evaluation of a novel Limb Prosthesis Osteointegrated Fixation System designed to combine the advantages of interference-fit and threaded solutions,* Acta of Bioengineering and Biomechanics, 2016, 18(4), 21-31.

[3] PROCHOR P., *Finite element analysis of stresses generated in cortical bone during implantation of a novel Limb Prosthesis Osseointegrated Fixation System*, Biocybernetics and Biomedical Engineering, 2017, 32(2), 255-262.

[4] PROCHOR P, SAJEWICZ E., *A comparative analysis of internal bone remodelling concepts in a novel implant for direct skeletal attachment of limb prosthesis evaluation – a finite element analysis*, Proceedings of the Institution of Mechanical Engineers, Part H: Journal of Engineering in Medicine, 2018, 232:(3):289-298.

Constitutive modelling of abdominal implants as experiment-related problem

D. REZNIKOV[1], A. TOMASZEWSKA[2]

Key words: *ventral hernia, abdominal implant, mechanical test, constitutive modelling, FEM model*

1. Introduction

Surgical meshes are used in ventral hernia treatment when a size of the hernia orifice is too large to sew it. There is a huge variety of meshes, which are different by a substance or biomechanical properties. They can be isotropic or anisotropic, absorbable or nonabsorbable, light- or heavy-weight, micro- or macro-porous, etc [1]. Numerical calculations help to select an implant to a given medical case.

The aim of the present work is to develop a methodology to identify parameters of constitutive model of an anisotropic prosthesis. To study this problem biaxial tests of DynaMesh®-IPOM (FEG Textiltechnik GmbH, Aachen, Germany) have been made with different setups as far as force or displacement control are concerned. The parameters of the Gasser-Ogden-Holzapfel (GOH) material model have been identified based on all tests. All results have been implemented in numerical model of the implant and the diversity of the forces calculated for the mesh fixation points due to (intra-abdominal) pressure load is analyzed in relation to a position of fixation damage observed in experiments [2].

2. Mechanical tests, constitutive and numerical modeling

Nine samples of DynaMesh with a size 65x65mm have been subjected to tests. Previous uni-axial tension tests have showed that '1' direction (along the knitting pattern) is more resilient than '2' direction (perpendicular to '1'). The following setups of the test have been conducted in accordance with the axes 1-2: (i) Force-driven, with the force ratios: 1:1.5; 1.5:1; 1.2:1; 1:1; (ii) Displacement-driven, with the ratios: 1.5:1; 1:1. The tests were conducted using Zwick BIAX machine, equipped with 500N load cell. Displacements were measured by Q-400 DIC Multicamera system (DANTEC DYNAMICS GmbH, Ulm, Germany).

The GOH material model has been used to reflect behaviour of the surgical mesh. The strain energy density function has the following form [3]:

$$\Psi = C_{10}(\bar{I}_1 - 3) + \frac{k_1}{2k_2}\sum_{\alpha=1}^{N}\left(e^{\left[k_2 k(\bar{I}_1-3)+(1-3k)(\bar{I}_{4(\alpha\alpha)}-1)\right]^2} - 1\right) \tag{1}$$

In order to determine five parameters of GOH constitutive equation authors have used "trust-region-reflective" algorithm to solve nonlinear least-squares (nonlinear data-fitting) problems. This algorithm is available in MATLAB with a function "lsqnonlin".

The surgical mesh is a limp structure so it has been modeled using membrane elements M3D4 and M3D3 in the SIMULIA Abaqus 2017 environment, using finite elements (FE) methodology. The model definition follows the idea presented in [4]. Geometry, dimensions, boundary conditions and load have been modeled in accordance with experiment [2]. The abdominal wall is reflected by linear-elastic springs in the model plane (simulation of the point fixation of the prosthesis) and out of the model plane (simulation of the implant and tissue overlap), see Figs. 1a,b. Stiffness of the springs have been obtained in the model validation to the experiment described in [2].

---

[1]Gdańsk University of Technology, Gdańsk, Poland/ Department of Structural Mechanics,
e-mail: danrezni.pg@gmail.com
[2]Gdańsk University of Technology, Gdańsk, Poland/ Department of Structural Mechanics,
e-mail: atomas@pg.edu.pl

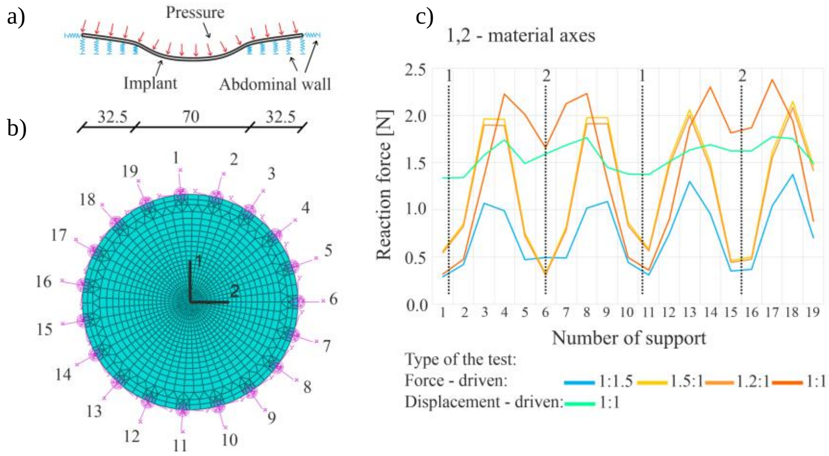

Fig. 1. a) Cross-section of the numerical model; b) Numerical model; c) Reaction forces in supports

4. Results and conclusions

The displacement-driven case 1.5:1 has been rejected from the analysis, because the obtained stress-strain relation reveals multiple stress values for some range of strains (at some point elongation changes into shortening). Reaction forces in joints obtained for other experimental cases are presented in Fig.1c. Displacement-driven test induce isotropic response of the material, which is an opposition to the former results obtained in uniaxial tests. Force-driven tests induce anisotropic response in the FEM model, with the anisotropy axes being oblique to the '1' and '2' axes of the material, which is visible by the reaction forces increase in points 3-4,8-9,13,18. That is in accordance with the experimental observation of the damaged fixation in points 5,7,15,17. However the reaction forces differ between various cases. In the model related to force-driven test 1:1.5 the variability of the reactions values is the smallest. The variability increases when FEM model refers to force-driven tests 1.5:1 and 1.2:1. For the 1:1 test the numerical response is intermediate.

The provided analysis shows the response dependency of the numerical model on the biaxial test setups which results are used to identify parameters of the constitutive model. We can conclude that displacement-driven tests provide inappropriate results while force-driven tests lead to physically confirmed results. However, further studies are needed to quell this issue and recommend force ratio to be applied in test to obtain true relation between forces in different mesh fixation points.

Acknowledgments: This work has been supported by the National Science Centre (Poland) [grant No. UMO-2017/27/B/ST8/02518].

References

[1] DEEKEN C.R., SPENCER P.L., THOMPSON JR. D.M., CASTLE R.M., *Biaxial analysis of synthetic scaffolds for hernia repair demonstrates variability in mechanical anisotropy, non-linearity and hysteresis,* Journal of the mechanical behaviour of biomedical materials, 2014, 38, 6-16.

[2] TOMASZEWSKA A., LUBOWIECKA I., SZYMCZAK C., *Mechanics of mesh implanted into abdominall wall under repetitive load. Experimental and numerical study.* 2018, J Biomed Mater Res Part B 2018:9999:9999:1-10

[3] GASSER T.C., OGDEN R.W., HOLZAPFEL G.A., *Hyperelastic modelling of arterial layers with distributed collagen fibre orientation.,* J.R. Soc., 2006, 15-35.

[4] LUBOWIECKA I., *Mathematical modelling of implant in an operated hernia for estimation of the repair persistence.* Comput Methods Biomech Biomed Engin., 2015, 18:438-445.

Tribological behaviour of tooth enamel in remineralization environments

E. SAJEWICZ[1], M. PIOTRAK

Key words: *remineralization environments, tooth enamel, restorative material, wear*

1. Introduction

It is well-known that remineralization environments lead not only to restore calcium content in the enamel but also to restore its mechanical properties, mainly microhardness, deteriorated during demineralization. However, tribological behavior of tooth enamel in remineralization conditions are studied relatively rare. Hence, the authors decided to carry out a study regarding to analysis of this problem.

2. Materials and methods

Mature, sound molars extracted mainly for orthodontic reasons were used for preparation of the enamel samples. The crown of each tooth was cut in half and cut off from the root. Each tooth fragment was embedded in Duracryl®Plus chemosetting acrylic plastic. The holders in which they were to be flooded were made of PVC pipe with a diameter of 20 and a height of 5 mm. Then each sample was ground flat with 200, 800, and 2000 grit silicon carbide papers consecutively. Finally, the samples were polished with aluminium oxide slurry employing a low-speed metallurgical polisher.

Light-cured restorative dental materials Amelogen®Plus was used for the preparation of the countersamples. These were formed in a shape of truncated cones, using a special form. The tip of the cone (contact plane) has been ground to a diameter of approximately Ø0.5 - Ø0.6 mm. The restorative material was polymerised with Blue Cap 1000 LED Curing Light (Dentazon) for 40 s. After polymerization samples were polished with 1500, 2000 and 2500 grit silicone carbide papers.

As lubrication were used: distilled water, mineral water Cisowianka and yogurt Danone.

The tribological tests were conducted by means of a tribometer UMT2 (Bruker) that simulated oral conditions and the cyclic loading produced during the mastication – the test configuration is described in detail elsewhere [1]. The experimental parameters were as follows: contact pressures were selected in the range of 20 - 60 MPa and changed every 5 MPa; frequency, 1.67 Hz; environment 3 ml of a fluid; the number of cycles was 5500 for every single test.

After the wear tests enamel volumes lost during wear tests were measured using a confocal microscope (Olympus Lext OLS 4000, Japan), and lost volumes of contersamples were calculated on the basis of results of measurement carried out by an optical microscope (Olympus BX51).

3. Results

Wear results of the experimental investigations are presented in Figs. 1,2. Some fluctuations of wear are visible when distilled water or mineral used as the lubricants. Wear is much stable when yogurt use as the environments.

4. Discussion

Results of wear experiments show that the contact pressure does not influence on the volume wear of the investigated material as well as tooth enamel. For distilled and mineral water it has been obtained much higher wear than for yogurt. Moreover, while the reduction in enamel wear in the yogurt environment (clearly increased calcium content) is understandable and is reflected in the

[1]Bialystok University of Technology, Department of Biomedical Engineering, Białystok, Poland,
e-mail: e.sajewicz@pb.edu.pl

literature, the simultaneous decrease in the wear of the dental material is quite surprising and its explanation requires further research.

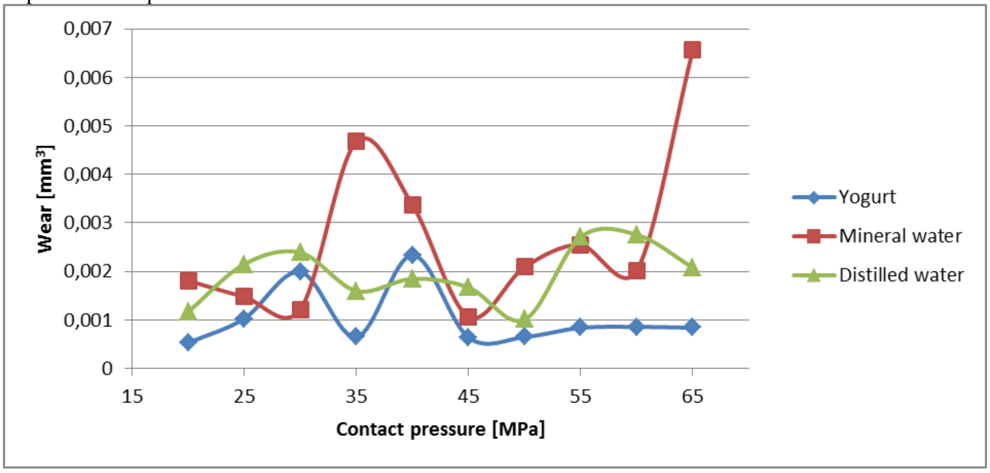

Fig. 1. Wear of tooth enamel at different contact pressures

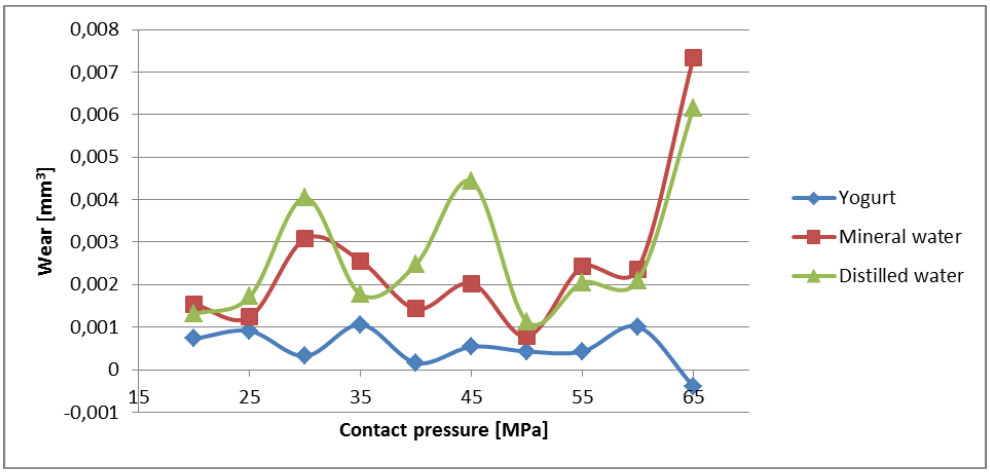

Fig. 2. Wear the composite restorative material at different contact pressures

Acknowledgments

This work was supported by Polish Ministry of Higher Education under the grant No. S/WM/1/2017.

References

[1] SAJEWICZ E., KULESZA Z., *A new tribometer for friction and wear studies of dental materials and hard tooth tissues.* Tribol. Int., 2007, 40, 885-895.

[2] HARA A.T., ZERO D.T., *Analysis of erosive potential of calcium-containing acid beverages.* European Journal of Oral Sciences, 2008, 116, 60-65.

Posture control in relation to the curvature and mobility of the spine in physically active older women

M. Sobera[1], **A. Rutkowska-Kucharska**[2], **A. Sikora**[3], **P. Proskura**[4]

Key words: posture control, physical activity, spine, older women

1. Introduction

Ageing is associated with a progressive decrease in muscle mass, which is described as sarcopenia. This condition leads to disorders in the daily functional capacity, which is manifested in the change in the pattern of locomotion and imbalances. In extreme cases, this condition may lead to falls damaging the movement system [1]. Many authors indicate a relationship between the strength of the muscles which stabilize the spine and the balance of the elderly [2,3]. Also, a decrease in spinal muscle strength leads to spinal instability, which leads to reduced spinal mobility and in consequence leads to low back pain (LBP) [4]. Therefore, it is suggested that the physical activity of the elderly should include both strengthening and stretching exercises stabilizing the spine [5].

This study aimed to define the relationship of the sway of posture and spine curvatures in older women participating in the program of exercise strengthening the muscles stabilizing the spine.

2. Methods

The subjects of the study were 22 women aged above 60 years old. They were physically active from more than 2 years in the regular fitness classes in University School of Physical Education in Wrocław (age 61-75, body mass 45.3 – 86.8 kg, body height 1.49 – 1.75 m). They used to take part in the exercises directed to improve spine musculus force for seniors.

2.1. Measurement

The assessment of the posture control was based on the research with used of two force platform AccuSway (AMTI) set side by side in the 2 mm distance. The subject stood one foot on the left and the second on the right platform involuntary standing position, with parallel feet and hip width. The arms were along to the trunk. The subjects were asked not to move the head or hands during the data registration. The 20-second standing trial was performed just before the fitness classes. The COP time series of the left and right foot (center of pressure) ware recorded. The quantitative posture control indices such as COP amplitude in medio-lateral (COPX) and antero-posterior direction (COPY) were analyzed for the left and right lower limb separately. The indices represent the body sway in the frontal and sagittal plane, respectively.

The Saunders' digital inclinometer was used to the measurements of the lordosis and kyphosis and the spine mobility. The mobility was considered only in the sagittal plane as a bend forward of the trunk in normal standing position as in the EUROFIT test the flexibility trial. It was needed to mark of the spinous processes of the lumbar vertebrae L1 and L5 on the subject's skin on the back before the measurement. Then the inclinometer was zeroed and then a subject performed bend forward. The angles in the points of L1 and L5 were noticed. The difference between the angles was the result of the trunk mobility in the forward bend of the lumbar spine. The measurement was

[1]University School of Physical Education in Wrocław, Department of Gymnastics,
e-mail: malgorzata.sobera@awf.wroc.pl
[2]University School of Physical Education in Wrocław, Department of Biomechanics,
e-mail: alicja.rutkowska-kucharska@awf.wroc.pl
[3] University School of Physical Education in Wrocław, Department of Gymnastics,
e-mail: aleksandra.sikora@awf.wroc.pl
[4] University School of Physical Education in Wrocław, Department of Gymnastics, e-mail: patrysia9214@wp.pl

repeated 3 times to do it correctly and the average of 3 trials was the last data. The bend forward of the spine had been measured just before and just after the classes.

3. Results

The correlation coefficient was computed between the posture control indices and the curvature and forward bend of the spine. It was noticed the significant positive and average correlation of the COP shifts in medio-lateral direction of the right lower limb (Table 1) and the lordosis, forward bend before fitness classes and after that. No significant correlation was found as for the left lower limb.

Table 1. Spearman's correlation of the postural control indices with the curvature and bend of the spine

Variables	COPX left [cm]	COPY left [cm]	COPX right	COPY right
Lordosis [deg]	-0.16	-0.12	0.47*	0.14
Kyphosis [deg]	-0.09	-0.02	0.23	-0.24
Bend forward before [deg]	-0.12	-0.04	0.50*	0.19
Bend forward after [deg]	-0.10	0.02	0.52*	0.19

*significant correlation

That could be the effect of the right lower limb functional domination (we did not verify that) in the subjects and they probably weight bear during bending to the right lower limb more than to the left. That is why the posture control realized by the right lower limb and right foot revealed the dependency on the forward sine bend before fitness as well as after the classes. The spine bend depends on the spine curvatures and the more depends on the lordosis as the results showed (Table 1). Investigators pointed [6] that, the group of women who had experienced at least one fall during the year displayed a significantly larger range, variability and velocity of body sway in the sagittal plane and increased suppression of postural oscillations in the frontal plane. Other authors find that loss of postural control as a result of progressive changes in the ageing process is characterized by the intensity of the body instability in the frontal plane [7]. The results of the study suggests the exercises to increase lumbar lordosis and spine mobility may increase the body sway in the frontal plane but not in the sagittal.

References

[1] CUELLAR W.A., WILSON A., BLIZZARDETAL C.L., *The assessment of abdominal and multifidus muscles and their role in physical function in older adults: a systematic review*. Physiotherapy, 2017, 103(1),21–39.

[2] GOUVEIA É.R., IHLE A., GOUVEIA B.R., KLIEGEL M., MARQUES A., FREITAS D.L., *Muscle Mass and Muscle Strength Relationships to Balance: The Role of Age and Physical Activity.* J Aging Phys Act, 2019, 4,1-7.

[3] GRANACHER U., GOLLHOFER A., HORTOB´AGYI T., KRESSIG R.W., MUEHLBAUER T., *The Importance of trunk muscle strength for balance, functional performance, and fall prevention in seniors: a systematic review.* Sports Medicine, 2013, 43(7), 627–641.

[4] GORDON R., BLOXHAM S., *A Systematic Review of the Effects of Exercise and Physical Activity on Non-Specific Chronic Low Back Pain*. Healthcare, 2016, 4,9-19.

[5] MORENO-SEGURA N., IGUAL-CAMACHO C., BALLESTER-GIL Y., BLASCO-IGUAL M.C., BLASCO J.M., *The Effects of the Pilates Training Method on Balance and Falls of Older Adults: A Systematic Review and Meta-Analysis of Randomized Controlled Trials.* J Aging Phys Act, 2018, 26(2),327-344.

[6] OSTROWSKA B., GIEMZA C., WOJNA D., SKRZEK A., *Postural stability and body posture in older women: comparison between fallers and non-fallers.* Ortop. Traumatol. Rehabil., 2008, 10(5), 486–495.

[7] PUSZCZAŁOWSKA-LIZIS E., BUJAS P., OMORCZYK J., *Postural stability in women in the eighth and ninth decades of life*. Acta of Bioengineering and Biomechanics, 2016, 18(3),115-121.

Development of deformable models of the mandible

K. SYBILSKI[1]**, D. KOLODZIEJCZYK**[2]**, J. MAŁACHOWSKI**[3]

Key words: *FEM, mandible, model, muscle*

1. Introduction

The human stomatognathic system is very complex. It consists of the articular system, the dental-dental system and the tooth-dental system. The stomatognathic system, in addition to processes related to food, is involved in such functions as breathing, making sounds and reflecting emotions. Despite the great development of diagnostic methods and many research works focused on this system, there is still a large group of processes that are difficult to diagnose. This is one of the reasons for the increasing number of interdisciplinary teams being created, combining specialists from various fields of science who, complementing each other, are able to extend the scope of research. This promotes further development of diagnostic methods and more precise diagnosis.

Among the many commonly used diagnostic methods in dentistry are imaging methods using computer tomography (CT) and magnetic resonance imaging (MRI). Their very big advantage is the possibility of very precise imaging of tissues and bones, and thus verification of the presence od adverse changes. The disadvantage is that imaging is performed only for a specific position of the mandible in relation to the skull base (static). On the other hand, diagnostics with the use of systems such as CADIAX, articulators and systems for motion analysis [1] takes into account the kinematics of the stomatognathic system, but only in a simplified manner and without taking into account the deformability of structures. Therefore, it can be complemented by numerical analyses in which it is possible to combine the full kinematics and mandibular movement relative to the skull base, muscle actions and deformability of the structure.

2. Materials and methods

In the present study, a 3D model of the base of the skull and mandible was developed from computer tomography (CT) scans. The main assumption during processing the scans was to divide the entire geometry into four main components: soft bone tissue, stiff bone tissue, periodontium, and teeth. This operation was carried out using Mimics software based on the different greyscale of the aforementioned elements. Despite the numerous literature and data sets on geometry determination based on the Housfield scale (HU) [2], it was not possible to carry out this task automatically. Apart from the material properties, the HU scale depends on the setting of the tomograph and the filters used. Therefore, the HU scale masks were selected individually based on successive iterations. The resulting geometry further processed in Geomagic software to remove artefacts and smooth all surfaces. The model was then filled and transformed into a triangular mesh. In the next step, a FEM mesh was generated. Each component was assigned isotropic material properties..

During the numerical analysis, tooth clenching was analysed. In the first stage, the model was simplified to include only the upper dental arch from the entire skull base, which was fully restrained in its upper part, and the jaw. Additionally, the surface of the temporomandibular joint was modelled against which the condyles were supported. Muscles modelled as 1D elements were used as a load [3]. The maximum force generated by the muscles and the activation level of each muscle are shown in Figure 1. Contacts areas were defined between all collaborating elements.

[1]Military University of Technology, Faculty of Mechanical Engineering, e-mail: kamil.sybilski@wat.edu.pl
[2]Military University of Technology, Faculty of Mechanical Engineering,
e-mail: damian.kolodziejczyk@wat.edu.pl
[3] Military University of Technology, Faculty of Mechanical Engineering, e-mail: jerzy.malachowski@wat.edu.pl

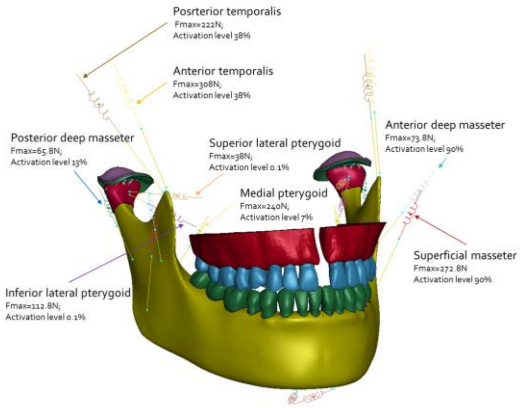

Fig. 1. Preliminary model with maximum force generated by each muscle and activation level

3. Results

The results of the numerical analyses are strain/stress maps as well as the difference in position of the condyles at the beginning (initial contact of the tooth) and at the full clenching stage.

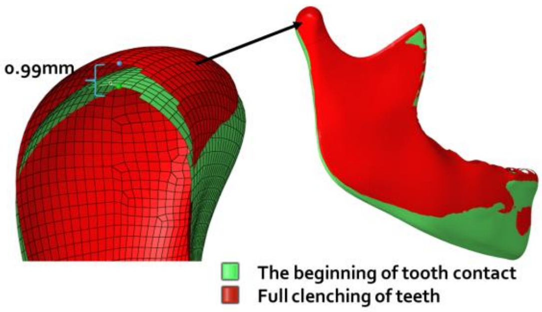

Fig. 2. Condyle displacement difference

Acknowledgments: The study was supported by the NCBiR within project 3D-JAW (The study of 3D temporo-mandibular joint (TMJ) model of bone-cartilage-ligament system mapping for effective commercialization of results in dental prosthetics, orthodontic and orthognathic surgery POIR.04.01.02.-00-0029/17). This support is gratefully acknowledged.

References

[1] PINHEIRO AP, ANDRADE AO, PEREIRA AA, BELLOMO D. A., *Computational method for recording and analysis of mandibular movements*, J APPL ORAL SCI 2008;16:321–7. DOI:10.1590/S1678-77572008000500004

[2] BUJTAR, P., SANDOR, G., BOJTOS, A., SZUCS, A., BARABAS, J., *Finite element analysis of the human mandible at 3 dierent stages of life*, Oral Surg Oral Med Oral Pathol Oral Radiol Endod 110, 301309 (2010)

[3] WOJNICZ W., LUBOWIECKA I., TOMASZEWSKA A., SZEPIETOWSKA K., BIELSKI P., *Jaw biomechanics: estimation of activity of muscles acting at the temporomandibular joint*, AIP Conference Proceedings, 2019, Vol. 2078, iss. 1, s.020105-020113

Objective assessment of the functional status of chronic stroke patients with complex rehabilitation

M. Syczewska[1], K. Nowak[2], I. Sarzyńska-Długosz[3], M. Łukowicz[4], A. Nitera-Kowalik[5,6], R. Owsiński[6], W. Bujalski[6], A. Malec[6], G. Sobota[2]

Key words: *stroke, objective assessment, gait analysis, balance tests*

1. Introduction

The rehabilitation treatment is a key factor for patients' improvement, and requires a coordinated efforts from physiatrists, physiotherapists, occupational therapists, family members and patients themselves [1, 2]. Regardless of the early interventions most stroke survivors require long term rehabilitation treatment, with ongoing functional needs and goals lasting for many years after the stroke incident. According to the Canadian and American guidelines for stroke patients the patients in chronic phase should receive a minimum 45 min per day rehabilitation treatment, 2 to 5 times per week [2, 3], based on the patient's individual needs and goals, provided by multiprofessional team, and should last at least 8 weeks. The reasons for shorter rehabilitation time are: limited number of healthcare centres providing specialist rehabilitation treatment, limited resources and high demand from the patients' side. Use of rehabilitation robots and technologically advanced equipment may help to resolve the problem of the short term rehabilitation treatments and lack of resources [4].

Therefore the aims of this study were as follows:

- First: to check if the relatively short rehabilitation treatment (3 weeks) complemented by complex rehabilitation on advanced equipment improves the functional status of chronic stroke patients,
- Second: which clinical and objective parameters can be used to assess the efficacy of such rehabilitation treatment in chronic stroke patients.

2. Material and methods

28 patients were recruited to the study. The spent 3 weeks of rehabilitation treatment in rehabilitation hospital at Busko Zdrój. At the beginning and at the end of rehabilitation period the pataient underwent a battery of clinical (Time-UP-And-Go, Scandinavian Stroke Scale) and objective tests (balance assessment with eyes open and close condition, 3d gait analysis with GGI [5], GDI [6], GVS and GPS [7] indexes) assessing their functional status.

3. Results

The statistically significant difference (Table 1) was found only for the TUG test. For balance evaluation were found – for 95 % of the ellipsoid area, maximal and minimal axes of the ellipsoid, average sway speed, sway path length and load distribution – significance differences. The GGI and GVS pelvis in sagittal plane indexes showed significant improvement of gait.

[1]Klinika Rehabilitacji, Instytut „Pomnik – Centrum Zdrowia Dziecka", Warszawa, Poland,
[2] Instytut Sportu, Akademia Wychowania Fizycznego im. J. Kukuczki w Katowicach, Katowice, Poland, e-mail: g.sobota@awf.katowice.pl
[3]Klinika Neurologii, Instytut Psychiatrii i Neurologii w Warszawie, Warszawa, Poland,
[4]Klinika Rehabilitacji, CMKP w Otwocku, Poland
[5]Uniwersytet Jana Kochanowskiego w Kielcach, Kielce, Poland
[6]21 Wojskowy Szpitalu Uzdrowiskowo-Rehabilitacyjny w Busku Zdroju, Poland

Table 1. Variables which changed statistically significantly after 3 weeks of therapy in chronic stroke patients. The variables are summarized by medians and ranges (minimum and maximum).

Variable	Before			After		
	Median	Min	Max	Median	Min	Max
TUG	11,6	6,0	13,6	9,7	5,6	13,0
GGI	154,6	21,7	463,9	98,0	17,7	361,9
GVS pelvis sag. plane	7,1	1,2	20,0	6,0	1,7	20,2
Sway path length	293,7	103,1	504,2	429,8	158,5	817,3
Average sway speed	10,3	3,6	17,6	14,9	5,5	28,6
Minor axis of ellipsoid	15,2	5,3	24,9	24,1	16,1	32,4
Major axis of ellipsoid	16,6	4,9	57,3	31,9	15,5	66,4
95 % elipsoid area	244,4	56,6	710,8	536,6	468,5	1176,8
Total ground reaction force left	50,9	39,1	55,0	53,9	41,9	62,6
Total ground reaction force right	36,0	19,9	46,8	42,3	19,0	51,6

4. Summary

The main finding of this study is the improvement of the functional status of chronic stroke patients after relatively short 3 weeks rehabilitation treatment. The addition to the standard rehabilitation treatment provided in the rehabilitation hospital to the patients of the program on the advanced technologically equipment can markedly help these patients to better function in their daily life.

Acknowledgments: This study was supported by the project. „Opracowanie i wdrożenie innowacyjnego programu kompleksowej rehabilitacji pacjentów z dysfunkcjami układu ruchu", realizowany w ramach Działania 1.2 Badania i rozwój w sektorze świętokrzyskiej przedsiębiorczości Regionalnego Programu Operacyjnego Województwa Świętokrzyskiego na lata 2014 - 2020, współfinansowanego ze środków Europejskiego Funduszu Rozwoju Regionalnego".

References

[1] C.M.Stinear, C.E.Lang, S.Zeiler, W.D.Babylow – *Advances and challenges in stroke rehabilitation* – Lancet Neurol 2020; 19: 348 – 360
[2] C.J.Weinstein, J.Stein, R.Arena et al. – *Guidelines for adult stroke rehabilitation and recovery. A guideline for healthcare professionals from the American Heart Association / American Stroke Association* – Stroke 2016; 47: e98 – e169
[3] D.Hebert, M.P.Lindsay, A.McIntyre et al. – *Canadian stroke best practice recommendations: Stroke rehabilitation practice guidelines, update 2015* – Int J Stroke 2016; 11: 459 – 484
[4] V.Klamroth-Marganska – *Stroke rehabilitation: Therapy robots and assistive devices*. – In: P.L.M.Kerkhof, V.M.Miller (eds.) *Sex-specific analysis of cardiovascular function*. Advances in Experimental Medicine and Biology 1065. 2018, Springer, pp. 579 – 587
[5] L.M.Schutte, U.Narayanan, J.L.Stout, P.Selber, J.R.Gage, M.H.Schwartz – *An index for quantifying deviations from normal gait* – Gait & Posture 2000; 11: 25 - 31
[6] M.H.Schwartz, A.Rozumalski – *The gait deviation index: A new comprehensive index of gait pathology* – Gait & Posture 2008; 28: 351 - 357
[7] R.Baker, J.L.McGinley, M.H.Schwartz, S.Beynon S, A.Rozumalski, H.K. Graham, O. Tirosh - *The gait Profile Score and Movement Analysis Profile* - Gait & Posture 2009; 30: 265 – 269

Application supporting rehabilitation with the use of movement patterns registered with MoCap technique

A. SZCZERBA[1], S. PISZCZATOWSKI[2]

Key words: *rehabilitation, Motion Capture, movement, modelling*

1. Introduction

Rehabilitation is an effective method both in restoring efficiency to the human motor system and caring for its proper functioning. One of the key methods in its field are therapeutic exercises recommended by physiotherapists. Outside the rehabilitation room, when the exercise is not supervised, there are often, sometimes harmful, negligence within the accuracy of their performance. According to this problem, as one of the solutions, rehabilitation applications are designed and some of them are widely described in literature, like for example [1,2].

In connection with the current problem in this field, as topic of the presented work, a project for the rehabilitation application was proposed. This application was focused on exercises dedicated to knee joint therapy, which was aimed to strengthening and improving muscles supporting this joint. In order to develop whole rehabilitation application process containing of motion recording, data processing and graphic modelling was executed.

2. Methods

2.1. Collection and processing of the motion data

Data was recorded using the Qualisys Motion Capture system, equipped with cameras - 10 Oqus (Opus 510+) infrared cameras and 1 Oqus Video (Oqus 210C) camera. The exercises selected for registration were performed by one young person with high physical fitness, who did not report any problems with the musculoskeletal system. On the body of exercising person there were placed a total of 56 markers - small (12.5 mm) and large (14 mm), depending on sticking places. As a result of motion registration files containing the movement patterns of all selected exercises in series of 10 repetitions were obtained. A model was developed on the basis of one of them in the Qualisys Track Manager program. All markers used in the study were named in a way that enables their identification and they were connected by segments constituting bone sequences. The model prepared in this way could be used during processing the rest of recorded exercise's movement sequences.

2.2. Graphic modelling and designing of application

Movement patterns, after a multi-stage processing, including the placement of the bones of the animation skeleton between the markers and the addition of appropriate constraints in order to force the skeleton to move, were used to generate animation files in proper format. These files were combined in the next step with the three-dimensional models of the trainers. These activities were crucial for obtaining realistically reproduced movements of the exercising person and required the use of additional templates. After generating connections there were deformations in three-dimensional models of trainers which had to be repaired frame by frame with simultaneously controlling of animation as the whole.

The files, ready in terms of the ability to reproduce the movement, were individually graphically processed, resulting in 10 trainers with different hair colours, hairstyles and clothes. One of them is shown in Fig. 1. Graphic elements, including models of rehabilitation equipment, were inserted into an application, whose functions was individually programmed.

[1]Bialystok University of Technology, Institute of Biomedical Engineering, Białystok, Poland,
e-mail: a.szczerba@doktoranci.pb.edu.pl
[2]Bialystok University of Technology, Institute of Biomedical Engineering, Białystok, Poland

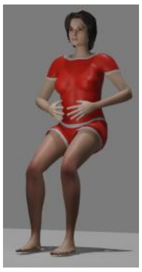

Fig. 1. Model of the trainer

3. Results

Final version of application had menu, list of changeable settings and set of exercises with their descriptions. One of the important functions of application was programmed answer for errors, which can be implied in cooperation with image recognition systems that enable the control of the rehabilitated person at home. The application environment during working was shown in Fig. 2

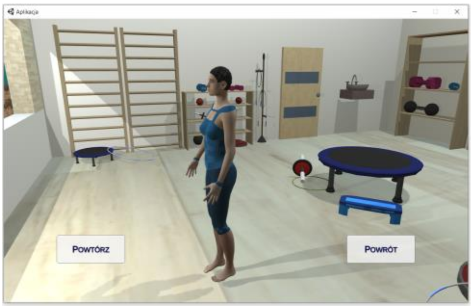

Fig. 2. Scene from working application

4. Conclusions

The final product of the research in the form of a program could be used by the patient at home. Due to the technologies used while working on the program and the programmed feedback, the application has the possibility of further development and cooperation with image recognition systems. The application can improve the therapy of patients by supervising their exercises at home and acting as a virtual rehabilitator. It will be able to facilitate the work of the physiotherapists themselves, because they would be more sure that their patients do not make mistakes, and by exercising in accordance with the recommendations, they ensure the effectiveness of rehabilitation.

Acknowledgments: Research was performed as a part of projects WI/WM-IIB/6/2021, WZ/WM-IIB/3/2020 and financed with use of funds for science from Polish Ministry of Science and Higher Education.

References

[1] ALBIOL-PÉREZ S., FARDOUN H.M., GIL-GÓMEZ H., GIL-GÓMEZ J.A., LOZANO-QUILIS J.A., MASHAT A.S., PALACIOS-NAVARRO G., *Virtual rehabilitation for multiple sclerosis using a KINECT-based system: randomized controlled trial.* JMIR serious games, 2014, 2(2).

[2] CALZÓN S., DÍAZ-PERNAS F., MARTÍNEZ-ZARZUELA M., PEDRAZA M., *Rehabilitation using Kinect-based games and virtual reality.,* Procedia Computer Science, 75: 161-168..

The analysis of the impact of transverse connector of long segments spinal fixation system on mechanical parameters

K. SZKODA-POLISZUK[1], M. ŻAK[2], C. PEZOWICZ[3]

Key words: *thoracolumbar spine, burst fractures, spinal fixation system, finite element methods, mechanical properties*

1. Introduction

The surgical treatment of vertebral fractures in the area of the thoracolumbar spine using spinal fixation system has become a standard in clinical practice in recent years. Therefore the question arises, whether it is beneficial to use transverse connectors in the construction of stabilization, in the case of a compression vertebral fracture, in order to improve the stability of the damaged column of the spine [1-2]. The use of two connectors is a classic stabilization technique, thanks to which the frame system is obtained. However, such systems are increasingly being replaced by a single connector. At the same time, discussions are ongoing on the desirability of using transverse connectors in fixation system.

The main aim of study was the analysis of the impact of using transverse connector of spinal fixation system on selected mechanical parameters of the thoracolumbar spine under conditions of its instability. The analysis was carried out for various transpedicular stabilization configurations (depending on the transverse connector using). The assumed aim of the study was carried out through experimental research (on an animal model of the spine) and numerical simulations using the finite element method.

2. Materials and methods

The experimental study was conducted on preparations of the thoracolumbar spine (Th7-L5) taken from 8 domestic pigs aged 6÷10 months and weighing 90÷110 kg. Conducting experimental analysis required the development of own experimental research protocol. The implementation of the load was possible thanks to the MTS 858 MiniBionix Material Testing System. The preparations were assembled in a specially designed test system, which was equipped with two grips (upper and lower).

On the basis of diagnostic computed tomography (CT), the geometric model of thoracolumbar spine was created in ANSYS Mechanical APDL 18.2 and divided into several structures with different tissues material properties. The vertebrae were modeled of a solid volume (cancellous bone) and a layer of vertebral cortical walls and were described by the isotropic, linear elastic material properties using tetrahedral 10-node elements. In intervertebral disc the difference between the nucleus pulposus and the annulus fibrosus was described by the nonlinear, hyper-elastic Mooney-Rivlin material. Additionally, three cylindrical layers of fibers (outer, middle and inner) of the annulus fibrosus were modeled as a thick shell 4-node elements. The layers were described by the isotropic, nonlinear material properties with alternating fiber inclination (angle of 30º to the horizontal plane). The articulating facet surfaces were modelled using surface to surface contact elements (with a penalty algorithm and a friction coefficient of 0.1). The geometry of the stabilization system (screws, rods and connectors) was described by the isotropic, linear elastic material properties using tetrahedral 10-node solid elements.

[1] Department of Mechanics, Materials and Biomedical Engineering, Wroclaw University of Science and Technology, Wrocław, Poland, e-mail: klaudia.szkoda-poliszuk@pwr.edu.pl

[2] Department of Mechanics, Materials and Biomedical Engineering, Wroclaw University of Science and Technology, Wrocław, Poland, e-mail: malgorzata.a.zak@pwr.edu.pl

[3] Department of Mechanics, Materials and Biomedical Engineering, Wroclaw University of Science and Technology, Wrocław, Poland, e-mail: celina.pezowicz@pwr.edu.pl

In both cases, experimental study and numerical simulations, five configurations of the model were considered: physiological (P), with compression fracture of Th12 vertebra (F), with long segment stabilization (S4), with long segment stabilization and one connectors (S4 C1), with long segment stabilization and two connectors (S4 C2). In each of the considered cases, a pure unconstrained bending moment in flexion (equal to 7 Nm) was applied to the superior endplate of the upper vertebral body (Th7). All configurations of the model were fixed by deducting all the degrees of freedom on the inferior endplate of the lower vertebral body (L3).

3. Results and conclusions

The experimental and numerical study allowed to analyze the stiffness and the dissipation energy, as well as to assess the range of mobility of the spine during the use of various fixation system configurations. The intradiscal pressure in individual intervertebral discs and stresses on the surface of the joint processes were also analyzed. Performing numerical simulations also allowed to assess the distribution of strains and stresses in the construction of the implants subjected to load.

On the basis of the analysis of the impact of transverse connector on the obtained results, it was shown that their use in the constructs of stabilization causes a slight increase in stiffness and limitation of the mobility, in relation to the stabilization without connectors. However, both in the case of a configuration with a one connector as well as with two connectors, the increase in the average value is in the range of 2÷4 Nm/rad (Fig. 1). Additionally, it was shown that statistically significant differences occur between the values obtained for preparations with compression vertebral fracture and long segment stabilization with one transverse connector ($p=0.03$). It should be noted that, the elimination of transverse connectors can contribute to shortening the time of the surgical treatment, additionally avoiding damage to the spinous process and interspinous ligaments.

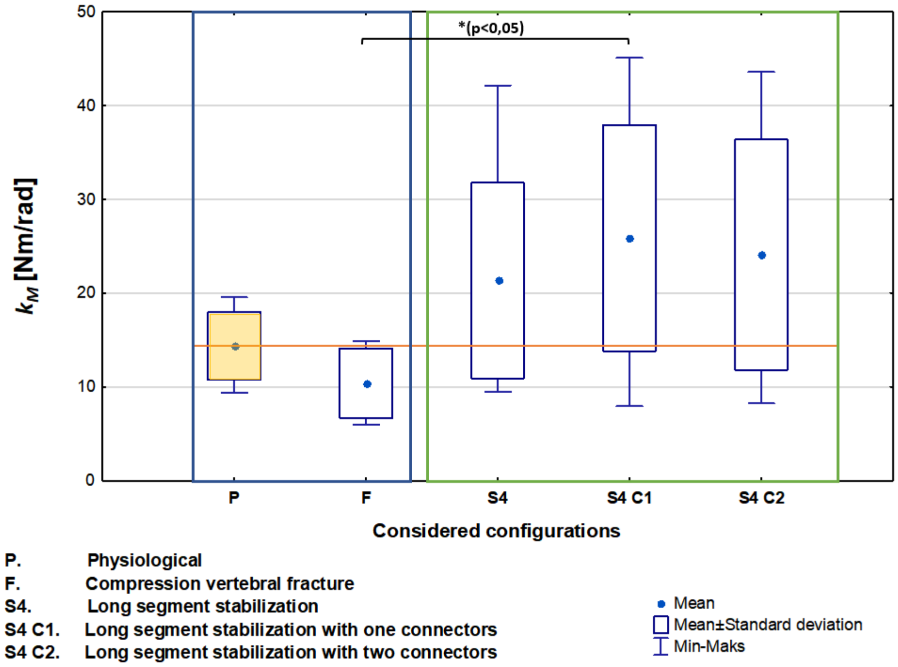

Fig. 1. Average values of the stiffness coefficient obtained for the analyzed configurations in the case of flexion.

Acknowledgments: Calculations have been carried out using resources provided by Wroclaw Centre for Networking and Supercomputing (http://wcss.pl), grant No. 423.

References

[1] ROSENTHAL B.B. ET AL., *Thoracolumbar burst fractures.* Clin spine surg., 2018, 31(4), 143-151.
[2] DAFFNER S.D., T*horacolumbar Fractures.* In Orthopedic Surgery Clerkship. Springer, Cham, 2017, 475-480.

Jumping abilities in patients after liver transplantation and patients qualified for liver transplantation

A. SZULC[1], L. SKLADANÝ[2], K. BUŚKO[3], M. RÁC[4], S. ADAMCOVÁ-SELČOVÁ[5], J. BADINKOVÁ[6]

Key words: *power, height of jump, CMJ, ACMJ, liver transplantation*

1. Introduction

Liver transplantation (LT) surgery saves patients from premature death and provides patients with a chance to return to an active life (quality of life - QOL). With properly selected physical activity, transplant recipients can obtain results comparable to healthy individuals at a similar age [1]. We suspect that lifestyle-driven sarcopenic obesity plays an increasing role in diminishing optimal prognosis and QOL after LT.The aim of the study was to investigate changes of maximal power of the lower extremities and height of jump measured in akimbo counter-movement jump and counter-movement jump in patients after LT surgery and patients qualified for LT.

2. Material and Methods

2.1. Subjects

Ethical approval for this study was provided by the Bioethics Committee of Collegium Medicum of the Nicolaus Copernicus University in Toruń, Poland (No. KB 330/2014). The subjects were informed about the scope and protocol of the study, and of the possibility to withdraw from the study at any moment, and the study was conducted in adherence to the Declaration of Helsinki.

Fifteen patients after liver transplantation (duration after liver transplantation 3.6±2.3 years), 19 people qualified for liver transplantation and 13 healthy participated in the study. Mean (±SD) values of the aged, body height, body mass and BMI are presented in table 1. No significant differences were found between the groups for body height but significant difference was observed between the patients after liver transplantation (PALT) and participant qualified for liver transplantation (PQFLT), control group (CG) for body mass ($F = 5.26$, $P = 0.01$, $\eta^2 = 0.19$), BMI ($F = 4.25$, $P = 0.02$, $\eta^2 = 0.16$) and between PALT and CG for aged ($F = 4.76$, $P = 0.01$, $\eta^2 = 0.18$).

2.2. Measurement methods

The power of lower extremities and the height of rise of the body mass center during vertical jumps were measured on a force plate („JBA" Zb. Staniak, Poland). The MVJ v. 4.0. software package („JBA" Zb. Staniak, Poland) was used for measurement. In the physical model applied the subject's body mass bouncing on the platform was reduced to a particle affected by the vertical components of external forces: the body's gravity force and the vertical component of the platform's reactive force. The maximal power (P_{max} [W]), relative maximal power (P_{max}/mass [W/kg]) and maximal height (h [m]) of rise of the body mass center (COM) were calculated from the registered reactive force of the plate. Each subject performed six vertical jumps with maximal force on the force plate: three akimbo counter-movement jumps (ACMJ) and three counter-movement jumps (CMJ). Akimbo counter-movement jump (ACMJ) – a vertical jump from an upright standing position with hands on the hips and counter-movement of the COM before the take-off. Counter-movement jump (CMJ) – a vertical jump from a standing erect position, preceded by a counter-movement of upper

[1]Adam Szulc, Institute of Physical Education, Kazimierz Wielki University in Bydgoszcz, Sportowa 2, 85-091 Bydgoszcz, Poland, e-mail: aszul@ukw.edu.pl
[2] Lubomir Skladaný, Dept. Internal Medicine, F.D. Roosevelt Teaching Hospital with Policlinic Banská Bystrica, Námestie Ludvíka Svobodu 1, 975 17 Banská Bystrica , Slovakia, e-mail: lubomir.skladany@gmail.com
[3] Krzysztof Buśko, Institute of Physical Education, Kazimierz Wielki University in Bydgoszcz, Sportowa 2, 85-091 Bydgoszcz, Poland, e-mail: kbukw@ukw.edu.pl
[4] Marek Rác, Dept. Hepatology, Faculty Hospital in Nitra, Špitálska 6, 950 01 Nitra, Slovakia, e-mail: racmarek@gmail.com
[5] Svetlana Adamcová-Selčanová, Dept. Div. Hepatology, Gastroenterology and Liver transplantation, F.D. Roosevelt Teaching Hospital with Policlinic Banská Bystrica, Námestie Ludvíka Svobodu 1, 975 17 Banská Bystrica , Slovakia, e-mail: sselcanova@gmail.com
[6] Janka Badinková, F.D. Roosevelt Teaching Hospital with Policlinic Banská Bystrica, F.D. Roosevelt Teaching Hospital with Policlinic Banská Bystrica, Námestie Ludvíka Svobodu 1, 975 17 Banská Bystrica ,Slovakia, e-mail: janka.badinkova@gmail.com

limbs and with lowering of the body mass centre before the take-off. The participants were asked to jump as high as possible in each trial. There were 30 s rest intervals between each ACMJ and CMJ. There was also a 1 min rest interval between each series of jumps. The jump with the highest elevation of the body's COM was chosen for further analysis.

ANOVA procedures with *post-hoc* Scheffé test were employed for comparison of mean values between the groups (Statistica^{TM} v. 13.0). The level of statistical significance was set at p=0.05.

3. Results

Mean (±SD) values of the height of rise of the body mass center, maximal power and relative maximal power during akimbo counter-movement jumps (ACMJ) and counter-movement jumps (CMJ) on a force platform are presented in table 1. The PALT had a significantly smaller absolute maximal power in ACMJ ($F = 5.22$, $P = 0.01$, $\eta^2 = 0.19$) than PQFLT and CG. Significant difference was observe between PALT and PQFLT for absolute maximal power in CMJ ($F = 4.36$, $P = 0.02$, $\eta^2 = 0.17$). The PALT had a significantly smaller relative maximal power in ACMJ ($F = 4.48$, $P = 0.02$, $\eta^2 = 0.19$) and in CMJ ($F = 3.28$, $P = 0.05$, $\eta^2 = 0.13$) than control group. The height of rise of the body mass center in ACMJ and CMJ was similar in the three groups.

Table 1. Mean values (±SD) of the height of rise of the body mass center (*h*), maximal power output (*P*), relative maximal power output (*P/*mass) during akimbo counter-movement jumps (ACMJ) and counter-movement jumps (CMJ) in patients after liver transplantation (PALT), people qualified for liver transplantation (PQFLT) and control group (CG)

Variables	PALT, n = 15	PQFLT, n = 19	CG, n = 13
Aged [years]	57.5±11.9	51.7±6.9	46.7±9.0*
Body height [cm]	165.7±12.8	171.2±7.5	168.3±7.4
Mass [kg]	76.1±16.0	95.8±21.8*	82.5±13.5*
BMI [kg/m^2]	27.60±4.29	32.5±5.8*	29.11±4.51*
$P_{maxACMJ}$ [W]	1739.7±601.0	2385.7±620.4*	2394.8±718.3*
$P_{maxACMJ} \cdot mass^{-1}$ [$W \cdot kg^{-1}$]	22.22±6.75	24.74±4.72	29.12±7.15*
h_{ACMJ} [m]	0.148±0.051	0.163±0.043	0.179±0.063
P_{maxCMJ} [W]	1994.8±701.0	2797.6±877.7*	2730.6±931.4
$P_{maxCMJ} \cdot mass^{-1}$ [$W \cdot kg^{-1}$]	25.58±8.63	28.69±5.73	32.93±8.65*
h_{CMJ} [m]	0.180±0.065	0.197±0.050	0.215±0.075

* - the averages differ significantly from PALT, p <0.05.

4. Discussion and conclusions

In literature has been described that after receiving a donor organ the patients reported improved QOL and were frequently able to successfully return to employment [2]. The main finding of the study is that the maximal power and height of a jump in the ACMJ and CMJ did not differ in the patients after LT and the people qualified to LT with exception of absolute power in ACMJ and CMJ. The results indicate that patients after liver transplantation have lower body mass and BMI than those qualified for LT. The results are proof-of-the-concept that the health potential provided by LT is not sufficiently exploited; our results indicate that we should focus on physical rehabilitation and fitness of physical fitness after LT.

Acknowledgments: The study was supported by Ministry of Science and Higher Education (Grant of Kazimierz Wielki University: BS-2017-N2).

References

[1] STĘPIEŃ-SŁODKOWSKA, M, NIEWIADOMSKA, M, KOTARSKA, K. *Quality of life and physical activity after liver transplantation.* Literature review. Central European Journal of Sport Sciences and Medicine, 2017, 1: 51-60.

[2] TARTER, RE, SWITALA, JA, ARRIA, A, PLAIL, J, VAN THIEL, D. (1991). *Quality of life before and after orthotopic hepatic transplantation*. Arch hit Med., 151, 1521–1526.

Kinematics of the human spine during locomotion in a person with lower limbs discrepancy - preliminary results

P. TABOR[1]**, T. SACEWICZ**[2]**, E. OLSZEWSKA**[3]**, K. GÓRNIAK**[4]**, M. LICHOTA**[5]**, A. MAZURKIEWICZ**[6]**, D. IWAŃSKA**[7]**, A. MASTALERZ**[8]

Key words: *spine kinematic, gait, running body posture*

1. Introduction

Initially, the model of the spine as a passive passenger dominated in gait analysis. Over time, it was undertaken to analyse the kinematics of the spine while walking [1]. Along with the development of measuring possibilities, it was possible to collect data describing mainly the linear movement of the lumbar spine in healthy people and suffering from various types of back pain [2]. Another factor that disturbs the kinematics of gait may be the asymmetrical length of the lower limbs [3]. There is no description of the kinematics of the entire spine during the run, as well as the description of parameters describing body posture. Hence, the aim of this work is to describe the kinematics of the spine during locomotion at different speeds in a person with lower limbs discrepancy.

2. Material and method

The material was a young, healthy male with an absolute length of the right lower limb 1.5 cm shorter and with a normal body weight (179 cm, 68 kg, BMI = 21.2).

The recordings of the spine kinematics were made with the use of a 10-camera Vicon system (200 Hz; 6 cameras positioned at the back of the subject). The Human Plug-in-Gait model was used, supplemented with additional markers located at the apex of thoracic kyphosis (KP), the apex of lumbar lordosis (LL) and the fifth lumbar vertebra (L_5). he marker corresponding to the Th10 position was shifted to the thoracic lumbar (PL) transition. The kinematics of the spine was described using the parameters used in the assessment of body posture [4,5]: thoracic kyphosis angle (KA) - calculated on the basis of sections C_7-KP and KP-PL, lumbar lordosis angle (LA) - calculated on the basis of sections KP-LL and LL-L_5. These angles were the equivalent of the Coba angle. The angle γ of the inclination of the lumbar section (LL-L_5 segment) in relation to the vertical and the torso inclination (C_7 sag) in the sagittal plane (position C_7 in relation to the symmetrical point of the posterior superior iliac spines) is also given. The results are presented as normalized to the 100% left-step cycle with respect to the angular values in the habitual posture. The ranges of variability of the absolute values of the angles KA, GA and γ are also given. The standards of the above-mentioned parameters were determined on the basis of the data indicated by Degenhard [5] (KA-45-55°; LA-32-37°; C_7 sag-± 7mm).

After a standard warm-up, the position of the spine in the habitual position was recorded, followed by a walk for at least 10 walking cycles on a treadmill (10 ° incline) at a speed of 4.6 km/h and a run at a speed of 10, 12, 14 and 16 km/h. There were no rest breaks between individual trials.

[1]AWF Warsaw/Departmen of Biomedical Sciences, Poland, e-mail: piotr.tabor@awf.edu.pl
[2]AWF Biala Podlaska/Departmen of Natural Sciences, Poland, e-mail: tomasz.sacewicz@awf.edu.pl
[3]AWF Warsaw/Departmen of Biomedical Sciences, Poland, e-mail: elzbieta.olszewska @awf.edu.pl
[4]AWF Biala Podlaska/Departmen of Health Promotion, Poland, e-mail: krystyna.gorniak@awf.edu.pl
[5]AWF Biala Podlaska/Departmen of Health Promotion, Poland, e-mail: malgorzata.lichota @awf.edu.pl
[6]AWF Warsaw/Departmen of Biomedical Sciences, Poland, e-mail: anna.mazurkiewicz@awf.edu.pl
[7]AWF Warsaw/Departmen of Biomedical Sciences, Poland, e-mail: dagmara.iwanska@awf.edu.pl
[8]AWF Warsaw/Departmen of Biomedical Sciences, Poland, e-mail: Andrzej.mastalerz@awf.edu.pl

2. Results and discussion

The subject was characterized by excessive tilting of the torso (-21mm; normal -7mm) and reduced thoracic kyphosis and reduced lumbar lordosis (Fig. 1). During locomotion, a clear asymmetry of the spine movement is noticeable for the movement of the right and left lower limbs. In general, an increase in the speed of locomotion is associated with an increase in the variability of the angle and the torso inclination. The exception is walking at a speed of 6 km / h, when the mobility was less than at a speed of 4 km/h, and running at a speed of 16 km/h compared to 14 km/h.

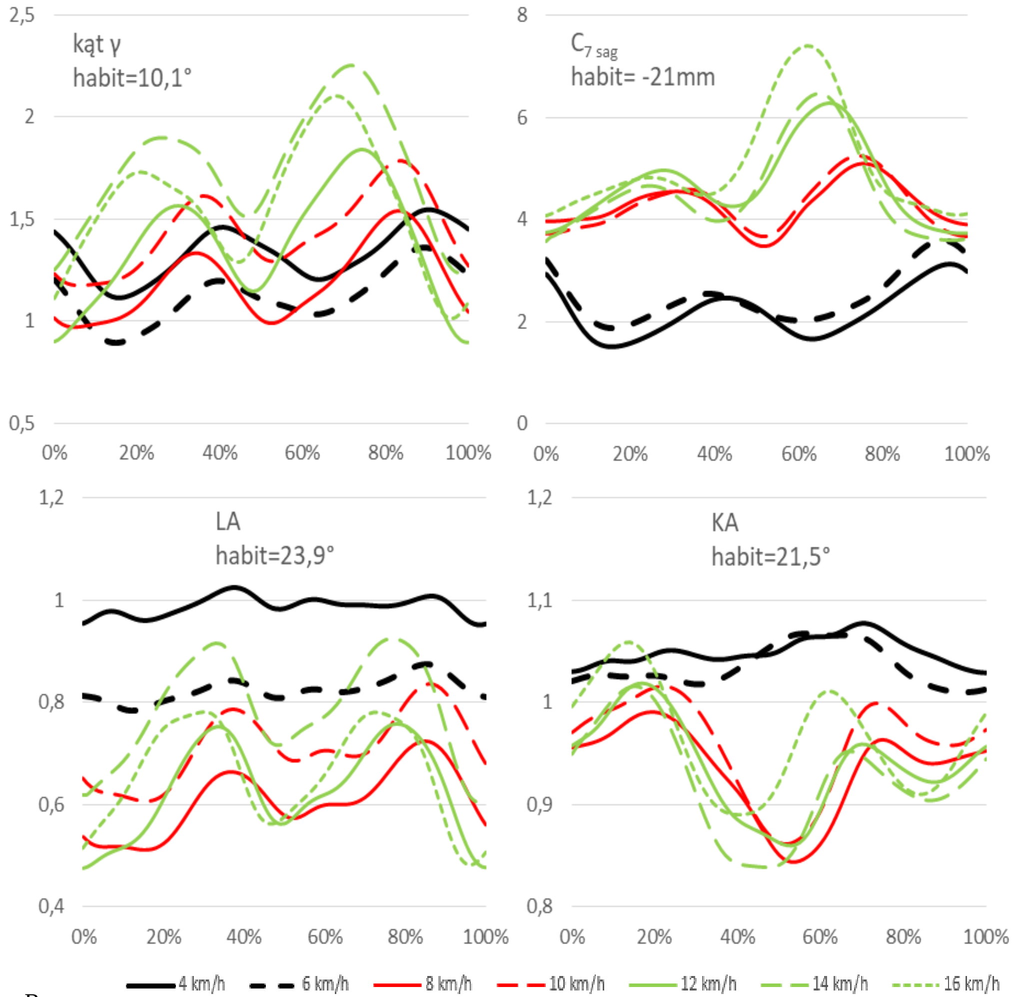

Range							
γ	4.4	4.7	5.8	6.2	9.5	10.3	11
$C_{7\ sag}$	68	142	76	69	119	138	150
LA	1.7	2.2	5.1	5.5	6.7	7.6	7.2

Fig. 1. Relative values of thoracic kyphosis (KA), lumbar lordosis (LA), lumbar inclination angle (γ) and torso inclination (C7 sag) normalized to the gait cycle, as well as the ranges of variability of the absolute values of the above-mentioned parameters.

References

[1] SYCZEWSKA M, ÖBERG T., *Spinal Segmental Movement Changes during Treadmill Gait after Stroke*, J. Hum. Kinet., 2006, 16, 39–56.

[2] GOMBATTO S.P., BROCK T., DELORK A., JONES G., MADDEN E., RINERE C., *Lumbar spine kinematics during walking in people with and people without low back pain*, Gait Posture, 2015. 42539–544.

[3] GURNEY B., *Leg length discrepancy - review*, Gait Posture, 2002, 15, 195–206.

[4] GRABARA M., *A comparison of the posture between young female handball players and non-training peers*, J. Back Musculoskelet. Rehabil, 2014, 27, 85–92.

[5] DEGENHARDT B.F., STARKS Z., BHATIA S., R*eliability of the DIERS Formetric 4D Spine Shape Parameters in Adults without Postural Deformities*, Biomed Res. Int. 2020.

Model development of the cerebral artery using tomography techniques and engineering software

M. TOMASZEWSKI[1], R. RZEPLIŃSKI[2], M. KUCEWICZ[3], M. SŁUGOCKI[4] J. MAŁACHOWSKI[5], B. CISZEK[6]

Key words: *hemodynamic, cerebral circulation, micro-CT, 3D models, CFD flow domain*

1. Introduction

Using hemodynamical analyses to solve medical problems has provided ground-breaking findings [1]. One of the most extensively studied part of cardiovascular system is cerebral circulation. Describing interactions between blood flow and arterial walls is getting us closer to explaining the development of various diseases, such as atherothrombosis, stroke, aneurysms as well as helps us improve treatment [2]. Recent advances in understanding pathogenesis, improving diagnostics and developing new treatment methods for these conditions result from an interdisciplinary approach to the problem. Most common techniques used in such studies include computational fluid dynamics [3-5], which allows for development of 3D models of cerebral vasculature, basing on radiological studies.

The paper presents a method for creating 3D models of small cerebral arteries and perforating branches of major cerebral arteries. By using micro tomography, it was possible not only to visualise the presence of small arteries, but also to precisely reconstruct their course. The anatomical specimens were chosen as a base for the model, due to certain limitations which are related to the examination of living tissues. Possibilities of the used micro CT raises hope to also visualise the level of microcirculation in future investigations. Based on the resulting model, a flow domain will be developed which included branches of diameter less than 0.1mm.

2. Materials and method

2.1. Preparation of the specimen

Firstly, an unfixed brain specimen was obtained from a cadaver. The basal part of the specimen (12cm x 12cm x 5cm block, basal surface of the brain along with the brainstem) was sufficient to visualise the desired vasculature. The contrast medium was prepared by melting together gelatine solution and barium sulphate. The specimen was placed under the microscope and contrast medium was subsequently drawn into a standard 10ml syringe with a PVC cannula.

2.2. Imaging with computed micro tomography

[1] Faculty of Mechanical Engineering, Military University of Technology, Warsaw, Poland, e-mail: michal.tomaszewski@wat.edu.pl

[2] Medical University of Warsaw, Warsaw, Poland, e-mail: radoslaw.rzepliński@wum.edu.pl

[3] Faculty of Mechanical Engineering, Military University of Technology, Warsaw, Poland, e-mail: michal.kucewicz@wat.edu.pl

[4] Medical University of Warsaw, Warsaw, Poland, e-mail: m.slugocki@hotmail.com

[5] Faculty of Mechanical Engineering, Military University of Technology, Warsaw, Poland, e-mail: jerzy.malachowski@wat.edu.pl

[6] Medical University of Warsaw, Warsaw, Poland, e-mail: bogdan.ciszek@wum.edu.pl

Specimens prepared in the aforementioned way were scanned with an industrial grade computed tomography system (Nikon/Metris XT H 225 ST). The specimen rotation was performed using a 5-axis computer-controlled table.

2.3. Creating spatial model of arteries

The images were stored in a DICOM format as a series of x-ray images assigned to a specific axis of the device (tomograph). Image processing was performed with CT Pro 3D software (Metris XT 2.2, Nikon Metrology, Belmont, CA). In this program, the individual shades of grey were separated by plotting their Hounsfield values on a histogram.. The model was then exported as a set of three-node elements forming its surface.. The final geometry was developed by extracting surfaces based on the ".stl" model using the poliNURBS surfaces available in the Altair Inspire system (Fig. 1). The model was then re-imported into Altair HyperMesh where discretisation was performed.

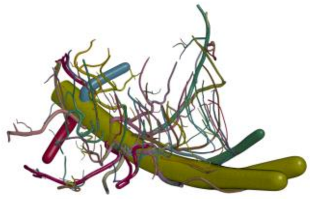

Fig. 1. Geometrical model development in the Altaire Hyper Mesh system.

3. Conclusions

The method presented in this paper is fairly simple, reliable and cost-effective, which makes it applicable for modelling the small vasculature of any other organ of the human body.

The strength of the presented method is the possibility of studying the histopathology of the reconstructed arteries. This opens the unique and valuable possibility of analysing hemodynamics and response of walls of the same artery, allowing drawing inferences about clinical significance of detected patterns of blood flow.

Acknowledgments: The study was founded by the National Science Centre (award number 2020/37/B/ST8/03430, Recipient Jerzy Małachowski, Prof., D.Sc., Ph.D., Eng.).

References

[1] STONE P.H., COSKUN A.U., KINLAY S., *Effect of Endothelial Shear Stress on the Progression of Coronary Artery Disease, Vascular Remodeling, and In-Stent Restenosis in Humans: In Vivo 6-Month Follow-Up Study.* Circulation 108, 2003, 108, 438-44.

[2] MENG H., TUTINO V.M., XIANG J., SIDDIQUI A, *High WSS or Low WSS? Complex Interactions of Hemodynamics with Intracranial Aneurysm Initiation, Growth, and Rupture: Toward a Unifying Hypothesis,* Am J Neuroradiol, 2014, 35, 1254-62.

[3] TOMASZEWSKI M., SYBILSKI K., BARANOWSKI P., MAŁACHOWSKI J., *Experimental and numerical flow analysis through arteries with stent using particle image velocimetry and computational fluid dynamics method.* Biocybernetics and Biomedical Engineering 40, 2020, 740-751.

[4] TOMASZEWSKI M., SYBILSKI K., MAŁACHOWSKI J., WOLAŃSKI W., BUSZMAN P.P., *Numerical and experimental analysis of balloon angioplasty impact on flow hemodynamics improvement*. Acta Bioeng Biomech 22, 2020, 169-183.

[5] MAZURKIEWICZ Ł., BUKAŁA J., MAŁACHOWSKI J., TOMASZEWSKI M., BUSZMAN P.P., *BVS stent optimisation based on a parametric model with a multistage validation process*. Materials and Design, 198, 2021.

Clustering with Self-Organising Maps in the analysis of muscle activity

M. TROKA[1], W. WOJNICZ[2], K. SZEPIETOWSKA[3], I. LUBOWIECKA[4]

Key words: *Electromyography (EMG), muscle activation, temporomandibular joint (TMJ), machine learning, self-organising maps (SOM)*

1. Introduction

The temporomandibular joint (TMJ) is the joint that allows for mastication, swallowing, breathing and speaking. This abstract proposes a classification method of patients based on their Electromyography (EMG) data obtained during specific jaw motions.

For this purpose we used Self-Organising Maps (SOM), an artificial neural network (ANN) model. SOM was applied to interpret post-processed EMG signal and to group patients based on similarities in their data. Overall, this study aimed to demonstrate the use of SOM for visualisation and classification of patients in terms of TMJ behaviour during jaw motion.

2. Material and methods

2.1. EMG

The scope of this study involved acquisition of EMG data of subjects during chosen jaw motions: opening, closing, protrusion and retrusion. Four surface muscles were examined, specifically: masseter right, masseter left, temporalis right and left. Data acquisition and EMG examination is presented in detail in [1].

2.2. SOM – Self-Organising Maps

Self-Organising Map is a system applied to unsupervised problems. This ANN model reduces dimensionality of data without having a bias towards labelled data. Its main task is to project large input datasets onto a 2D representation known as a map [2]. Many varieties of applications of SOM algorithm have been documented over the years including biomedical applications [3]. SOM was applied for simultaneous analysis of all four muscles to find clusters of data.

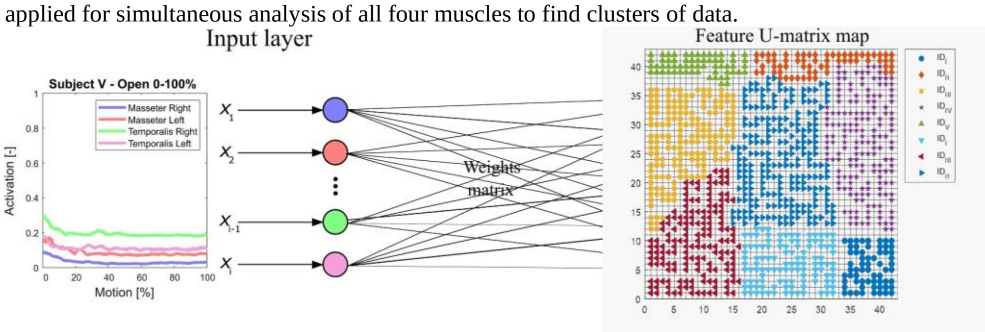

Fig. 1. SOM analysis flow chart.

3. Results

[1] Faculty of Civil and Environmental Engeneering, Gdansk University of Technology, Poland, e-mail: mateusz.troka@pg.edu.pl

[2] Faculty of Mechanical Engeneering, Gdansk University of Technology, Poland,

[3] Faculty of Civil and Environmental Engeneering, Gdansk University of Technology, Poland,

[4] Faculty of Civil and Environmental Engeneering, Gdansk University of Technology, Poland,

Input for SOM analysis are EMG data points as presented in Fig 1. SOM enabled us to analyse multivariate datasets and extract unknown data patterns, features, or tendencies of specific patients from the EMG data. Results of SOM analysis can be depicted with maps, where clusters of data can be identified. Full opening motion output in the form of a U-matrix (unified distance matrix) and labelled map is shown in Fig. 2. Clusters are labelled with the subjects' IDs (I-VII).

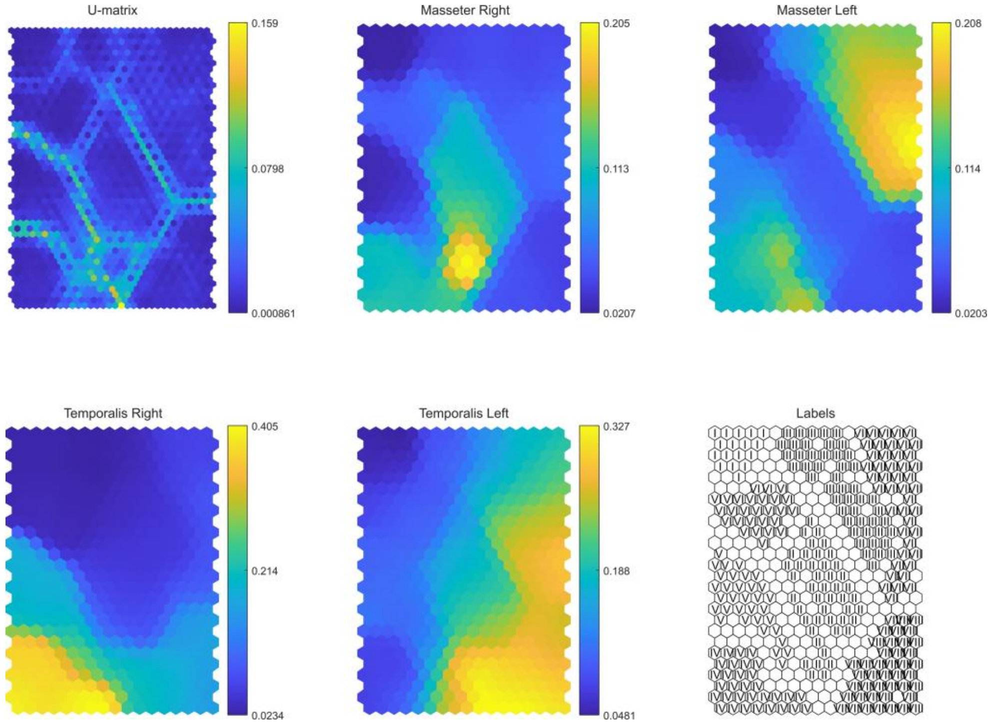

Fig. 2. SOM's output U-matrix maps (0-100% opening motion).

4. Conclusions

The results showed that SOM was able to encode muscular responses and sort them into clusters. This kind of analysis is useful to identify similarities in EMG data between different patients. What is more, the use of SOM algorithm to find clusters in the input data can be broaden to identify unknown input vectors for biomechanical insight regarding the state of TMJ.

Acknowledgments: This study has been performed in the scope of the project "3D-JAW" (The study of 3D temporo-mandibular joint (TMJ) model of bone-cartilage-ligament system mapping for effective commercialization of results in dental prosthetics, orthodontic and orthognathic surgery; POIR.04.01.02-00-0029/17). Calculations were carried out at the Academic Computer Centre in Gdansk (TASK), Poland.

References

[1] W. Wojnicz, I. Lubowiecka, A. Tomaszewska, K. Szepietowska, and P. Bielski, "Jaw biomechanics: Estimation of activity of muscles acting at the temporomandibular joint," *AIP Conf. Proc.*, vol. 2078, no. March, 2019.
[2] M. Cottrell, M. Olteanu, F. Rossi, and N. Villa-Vialaneix, "Self-organizing maps, theory and applications," *Investig. Operacional*, vol. 39, no. 1, pp. 1–22, 2018.

[3] T. Kohonen, “Essentials of the self-organizing map,” *Neural Networks*, vol. 37, pp. 52–65, 2013.

Does the exoskeleton therapy affect gait parameters in patients with cerebral palsy?

A. TRZYNA [1], A. BRACHMAN [2], T. ŁOSIEŃ [3], G. SOBOTA [4]

Key words: *exoskeleton, cerebral palsy, gait, therapy*

1. Introduction

"Cerebral palsy (CP) describes a group of disorders of the development of movement and posture, causing activity limitation, that are attributed to non-progressive disturbances that occurred in the developing fetal or infant brain. The motor disorders of cerebral palsy are often accompanied by disturbances of sensation, cognition, communication, perception, and/or behaviour, and/or by a seizure disorder."[1] The brain injury can affects motor drive, motor patterns, muscle tone, coordination and sensorimotor system. Those neuromuscular deficits have influence on gait in CP.[2] Gait weaknesses are considered to be one of the most important consequences of this disease.[3] Walking is often considered one of the most important activity for daily life and has a great influence on social life. [4] These factors highlight a high urgency for the development and application of new and effective training methods. In recent years exoskeleton therapy has been gaining popularity, hence in this study our aim was to evaluate the influence of exoskeleton therapy on basic spatio-temporal and kinetic parameters in patients with CP.

2. Material

12 young patients with diagnosed CP participated in the study. The mean age was 19.81±3.57 years (range, 15-24), a mean height was 1.67±0.11 m (range, 1.53-1.85) and a mean weight was 63±14.27 kg (range, 43-84). All enrolled participants met the following inclusion criteria: 1) level II of Gross Motor Function Classification System (GMFCS) 2) at least 1,5m height (value required for the technical purposes, because of the exoskeleton size) 3) At least 6 months break since last surgery and/or botulinum toxin injection. Exclusion criteria were as follows: 1) inability to walk on the treadmill even with support on handrails 2) inability to understand the instructions.

3. Methods

Participants trained every day for 8 weeks including 2 week break in the half of the training period. The training session lasted 90 minutes and consisted of exoskeleton training and additional exercises. Exoskeleton part lasted for 60 minutes (including 15 minutes preparation). Subjects walked with crutches/walker and with the help of therapist in exceptional situations (e.g. high spasticity of upper limbs). During the walk, exoskeleton's parameters (step length, step height, stance phase, swing phase) were adjusted to the patient's current abilities. After the exoskeleton part, there was a 30 minutes of resistance exercises and stretching. All objective outcomes were measured before intervention and after completion of the training program. In each trial, subjects walked barefoot on the Zebris FDM–T treadmill with mounted pressure platform. A sampling rate of 100 Hz was used to acquire all data. During each trial participants walked for 30 seconds with preferred speed (Vpref) and then 30 seconds with the maximum tolerated speed (Vmax). Preferred walking speed was constant before and after therapy.

[1]Institute of Sport Sciences, The Jerzy Kukuczka Academy of Physical Education, Katowice, Poland, Department of Biomechanics, SKN "Kinesis" e-mail: 3na-adam@wp.pl
[2]Institute of Sport Sciences, The Jerzy Kukuczka Academy of Physical Education, Katowice, Poland, Department of Biomechanics, e-mail: a.brachman@awf.katowice.pl
[3] Tomasz Łosień, Śląski Uniwersytet Medyczny, Wydział Nauk o Zdrowiu, Katedra Fizjoterapii, Zakład Rehabilitacji Leczniczej, e-mail: tlosien@gmail.com
[4]Grzegorz Sobota, Institute of Sport Sciences, The Jerzy Kukuczka Academy of Physical Education, Katowice, Poland, Department of Biomechanics, e-mail: g.sobota@awf.katowice.pl

4. Results

The results showed that in Vmax participants exhibited a significant improvement for the left step length (p=0.042). The stance phase for left (p=0.036) and right (p=0.033) foot has significantly decreased. Stride time has significantly decreased (p=0.042). Stride Length decreased however it did not reach significance (p=0.059). Cadence (p=0.060) and velocity (p=0.056) has increased nonetheless has not reached significance. The difference between stance phases (left minus right) before and after therapy decreased nearly significantly (p=0.055). Contact time has significantly decreased for: left midfoot (p=0.049), right midfoot (p=0.039) and left heel (p=0.025), and showed a trend towards decrease in left forefoot (p=0.055), right forefoot (p=0.079) and right heel (p=0.052). Maximal force for right forefoot also has increased nearly significantly (p=0.069).

No significant differences between before and after the therapy were found in preferred walking speed condition.

4. Conclusions

This early evaluation shows promising results, however, the small number of participants warrants further and more extensive research, which would include the involvement of the control groups. The interesting finding is that participants improved their walking ability only in maximum walking velocity, no changes in preffered walking speed were found. Durning the third week of the rehabilitation program patients reported fatigue, thus the possible explanation for these results is that maybe the intensity of the trainings was too high or the rehabilitation plan wasn't long enough to evoke adaptive change durning walking with preferred speed.

Acknowledgments:

The study was supported by the National Center for Research and Development Grant under the program TWEC, nr POIR.04.01.04-00-0035/19.

References

[1] Bax, M., Frcp, D. M., Rosenbaum, P., Dan, B., Universitaire, H., Fabiola, R., … Rosenbaum, P. (2005). Review Proposed definition and classification of cerebral palsy. Executive Committee for the Definition of Cerebral Palsy, (April 2005), 571–576.

[2] Zhou, J., Butler, E. E., & Rose, J. (2017). Neurologic correlates of gait abnormalities in cerebral palsy: Implications for treatment. Frontiers in Human Neuroscience, 11(March), 1–20. https://doi.org/10.3389/fnhum.2017.00103

[3] Aycardi, L. F., Cifuentes, C. A., Múnera, M., Bayón, C., Ramírez, O., Lerma, S., … Rocon, E. (2019). Evaluation of biomechanical gait parameters of patients with Cerebral Palsy at three different levels of gait assistance using the CPWalker. Journal of NeuroEngineering and Rehabilitation, 16(1), 1–9. https://doi.org/10.1186/s12984-019-0485-0

[4] Armand, S., Decoulon, G., & Bonnefoy-Mazure, A. (2016). Gait analysis in children with cerebral palsy. EFORT Open Reviews, 1(12), 448–460. https://doi.org/10.1302/2058-5241.1.000052

Design of the device to support the treatment of malocclusion

E. Tymińska[1], M. Kodan[2], S. Wawrzyniak[3], A. Mazurkiewicz[4]

Key words: *malocclusion, orthodontic apparatus, correction of malocclusion*

1. Introduction

The head bone complex is called the skull. In humans, the skull divides on the skull brain, the base of the skull, and the facial skull part connected by sutures. Mandible is connected to the skull through the temporomandibular joint. The muscles of the skull and neck allow the mandible to move. The main muscles that move the mandible are the masseter muscles, which are related to the chewing activity [1].

A malocclusion is defined as an abnormal structure of the teeth, dental arches and their mutual relationship. Occlusion defects can cause slurred speech, difficulty in breathing and eating.

At present, treatment of malocclusions methods are intensively developing in the aim shortening of effective treatment time. Among the modern technologies used in the treatment of malocclusion, we can distinguish [2]:

- Effect of vibrations on teeth. The vibrations set the teeth in motion, which stimulates the bone remodeling and in consequence it changes its shape. In order to achieve this effect in correction the defects, the device should be placed in the mouth daily for a specified period of time, usually about 20 minutes.
- Next technique is placing braces on the internal side of teeth. Such an apparatus has the advantage that it is much less visible than the apparatus placed on external surfaces. The braces are adjusted to the specific structure of the patient's teeth. As a rule, locks and arches are made specifically for each patient. Their shape is selected based on the simulation of the correct setting of the teeth in a new position after the correction is completed.
- Another technique is to use a transparent biocompatible overlay to correct malocclusion. The method is intended for disciplined patients due to the ease of removing the device from the mouth. This solution gives a high degree of aesthetics because of transparent structure of the device.

2. Design the device

The device is designed in the aim to obtain optimal adjustment of the shape of the oral part of the device to the patient's teeth and to obtain the effect of bite correction with the use of vibrations transmitted from the device to the teeth. The device was designed used Inventor software (AutoDesk Inc., USA)

The device consists of four parts:

a) Teether, individually designed to suit the size of the patient's mandible. This part is designed to be removable and has a simple structure. This allows you to take care of hygiene.
b) Body contains the vibrating system and power supply. This part is designed to be as small as possible, which allows for hands-free using device in all conditions.
c) Upper cover of the body. This part provide access to the vibrating mechanism.
d) Battery cover. This part provide access to the battery.

[1]Student Scientific Group “BioMed”, University of Science and Technology, Bydgoszcz Poland,
e-mail: esttym002@utp.edu.pl
[2]Student Scientific Group “BioMed”, University of Science and Technology, Bydgoszcz Poland,
e-mail: monika.kodan7@gmail.com
[3]University of Science and Technology, Mechanical Engineering Department, Bydgoszcz Poland,
e-mail: sylwester.wawrzyniak@utp.edu.pl
[4]University of Science and Technology, Mechanical Engineering Department, Bydgoszcz Poland,
e-mail: adam.mazurkiewicz@utp.edu.pl

2.1. Teether, body and covers

The elements of the device were made with the use of 3D printing in FDM (Fused Deposition Modelling) method. The material was PLA (polylactide) plastic. The printed parts and general view of device are show in Fig. 1.

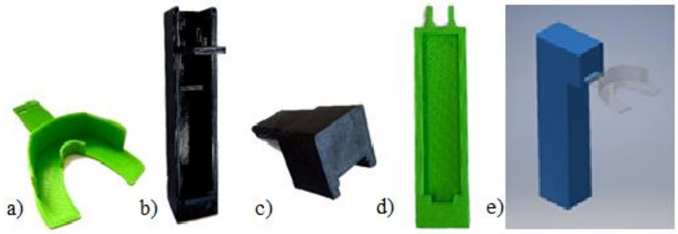

Fig. 1. Printed parts: teether a), body b), upper cover c), battery cover d), general view of device e)

2.2. Vibrating system

The device works based on vibrations transmitted to the teether. The two motors are positioned to transmit vibrations in a multi-directional way (up/down, right/left). Small-size vibration motors have dimensions 10 x 10 x 2.0 mm. The motors are supplied with the voltage from 2.5 ÷ 3.5 V. The source of power supply is a Li-Ion battery with a power of 3.7 V and a capacity of 2600mAh.

2.3. Preparation of teether

The first stage of the project was to make an imprint of the mandible with alginate mass, next then pour the imprint with plaster. In this way a plaster model of the mandible was created. In next step a plaster model of the mandible was scanned using a 3D scanner. The cloud of points obtained as a result of the measurement was transferred to solid. On the base of solid correct shape of the teether was created.

3. Summary

The use of modern technologies made it possible to manufacture a device for the correction of malocclusion. The advantage of the device is simple structure, small number of parts, which makes it available for a low price. The device is easy to use, battery replacement does not generate a problem. The device is designed in such a way that it allows use of the device in hands-free mode. The possibility of detaching the teether makes it easier to take care of hygiene and cleanliness of the device.

References

[1] NETTER F.H., *Human anatomy atl*as, Editor: Elsevier Urban &cPartner, 2011.

[2] GEISSBERGER M., *Stomatologia estetyczna w praktyce klinicznej (Aesthetic dentistry in clinical practice)*, in Polish , Editor: Elsevier Urban & Partner, Wrocław, 2010.

Using stubby prosthesis after bilateral transfemoral amputation: a biomechanical case study

S. WINIARSKI[1], M. KOWAL[2], Ż. FIODORENKO-DUMAS[2], I. DUMAS[2], A. MACHNIKOWSKA[2], E. GIEYSZTOR[2], M. PAPROCKA-BOROWICZ[2]

Keywords: *double amputation; gait analysis; stubby prosthesis; transfemoral amputation*

1. Background

Many unilateral amputations are followed by a contralateral amputation within three years, sometimes presenting bilateral transfemoral amputations [1]. After bilateral transfemoral amputation (BTFA), people may experience limitations in everyday life due to limited mobility and prosthesis problems. Stubby prostheses are an alternative to the standardly used prostheses. Stubbies are short non-articulating prostheses used to improve the gait function, allowing one to load the thigh stumps and improve balance gradually. However, there are concerns that the use of stubbies will worsen the gait with standard prostheses and increase the risk of falling. For this reason, the purpose of this study is to compare the gait function with standard and stubby prostheses used by an individual.

2. Material and method

The case study covered a 54-year-old man after bilateral traumatic amputation of his lower limbs. Transfemoral amputations were performed using Caldwell's method; disproportion in the length of stumps was 5 mm.

According to the Newington model, the motion task was recorded using the SMART-E optoelectronic system (BTS Bioengineering, Milan, Italy). The biomechanical evaluation included measuring angle-time relationships characterizing the range of motion (ROM) in lower limb joints and ground reaction force vertical (vGRF) component. The analyzed tasks were: (A) walking in standard prosthesis with self-selected speed, (B) fast walking and (C) walking in stubby prosthesis with self-selected speed. The following parameters were numerically extracted from the angle-time series: mean value, maximum and minimum values and range of motion and expressed in degrees. The values were calculated to compare in descriptive statistics. Data were also compared to the gait of non-disabled people [2].

3. Results

The temporospatial parameters (Table 1) depended on the gait speed and the prosthetic type used; higher values were recorded at a fast gait while lower ones during the gait with stubby prostheses. Step width was the most similar to the gait of healthy persons walking with stubby prostheses (0.17 ± 0.01 m for healthy people, 29% higher for stubbies, 35%—prosthetic gait with self-selected gait speed and 41% for fast gait speed). However, step width was the smallest when walking with stubbies.

The most significant differences in the range of movement (ROM) occurred in the sagittal plane. The faster the patient moved, the higher the anterior tilt of the shoulder girdle and pelvis. The difference in the shoulder girdle tilt in ROM between a fast gait and a prosthetic gait with stubbies was 57%. Similarly, the pelvic tilt (physiological gait, ROM 1–2°) was constantly in anteflexion during the gait. Regarding the gait with stubbies, the difference was the lowest—49% (self-selected gait speed: 59%, fast gait: 56%). Hip flexion/extension in ROM during the gait with stubbies forced higher flexion and extension values due to the lack of knee joints (20%—gait with stubbies, 8%—

[1]Biomechanics Department, University School of Physical Education in Wroclaw, Wroclaw, Poland,
e-mail: slawomir.winiarski@awf.wroc.pl
[2]Department of Physiotherapy, Wroclaw Medical University, Wroclaw, Poland
e-mail: mateusz.kowal@umed.wroc.pl

self-selected gait speed, 4%—fast gait). Due to the need to provide the required gap from the ground, higher hip flexion/extension values in ROM during the gait with stubbies occurred in the frontal plane. During the gait with stubbies, pelvic obliquity required higher raise to ensure swing (48%—gait with stubbies, 41%—self-selected gait speed, 13%—fast gait). The vGRF waveforms captured during the gait with standard prostheses were similar in shape to the letter "M". During the gait with both the self-selected and fast speed, vF1 and vF3 parameters (overweight at the initial weight acceptance phase and overweight during the terminal stance phase) reached higher values than vF2 parameter (underweight during the middle stance phase). During the gait with stubbies prosthesis, despite the time-shift in the achievement of the parameter, there was no difference in vGRF values obtained by the vF1 parameter. The vF2 parameter reached the lowest value of approx 30% for the stance phase (self-selected gait speed—approx. 50%, fast gait speed—70%). The vF3 parameter obtained maximum values much earlier than in other cases (50%, 70% and 80% for the stance phase in the gait cycle, respectively) and took longer stance phases.

Table 1. Spatiotemporal gait parameters for the main movement tasks.

	Fast walking		**Self-Selected walking**		**Stubby Prostheses**	
	Right	**Left**	**Right**	**Left**	**Right**	**Left**
Spatial parameters [m]						
Stride	1.31 ± 0.1		1.21 ± 0.1		0.71 ± 0.1	
Step width	0.29		0.26		0.24	
Step length	0.66 ± 0.1	0.57 ± 0.1	0.62 ± 0.1	0.54 ± 0.1	0.32 ± 0.1	0.34 ± 0.1
Speeds [m/s]						
Velocity	0.83 ± 0.02		0.69 ± 0.06		0.75 ± 0.06	
Cadence	1.51		1.3		2.14	
Gait phases ratios [%GC]						
Stance ratio	0.63 ± 0.01	0.69 ± 0.03	0.65 ± 0.03	0.7 ± 0.03	0.65 ± 0.02	0.66 ± 0.03
Double Stance ratio	0.18 ± 0.03	0.17 ± 0.02	0.19 ± 0.03	0.18 ± 0.03	0.14 ± 0.03	0.16 ± 0.01
Swing ratio	0.36 ± 0.01	0.31 ± 03	0.34 ± 0.03	0.30 ± 0.03	0.35 ± 0.02	0.34 ± 0.03
Temporal parameters [s]						
Stride time	1.55 ± 0.1	1.33 ± 0.1	1.55 ± 0.2	1.55 ± 0.1	0.94 ± 0.1	0.94 ± 0.1
Stance time	0.84 ± 0.1	0.92 ± 0.1	1.02 ± 0.1	1.01 ± 0.1	0.61 ± 0.1	0.61 ± 0.1
Double Stance time	0.23 ± 0.1	0.22 ± 0.1	0.29 ± 0.1	0.27 ± 0.1	0.13 ± 0.1	0.14 ± 0.1
Swing time	0.48 ± 0.1	0.41 ± 0.1	0.52 ± 0.1	0.46 ± 0.1	0.32 ± 0.1	0.34 ± 0.1

4. Discussion and conclusions

The reduction of body height allows for reducing the risk of fall [1]. The authors of the case study found a limited number of similar scientific studies. Due to the high risk of limited walking capacity in people who have had a double amputation, there is a justified need for further research. The use of stubby prostheses can be an alternative to the daily use of standard ones. The biomechanical analysis results prove that gait with stubbies is comparable to obtained when using standard lower limb prostheses and normal pattern. Moreover, the reduction of body height reduces the risk of falling.

The current limb prosthesis market offers a whole range of products tailored to the patient's needs. Advances in prosthetics are centred around improved materials and designs that increase the performance of a given prosthesis and improve mobility, and a gait analysis makes it possible to create a product that will successfully reproduce a physiological gait.

References

[1] CARROLL M. K., CARROLL K., RHEINSTEIN J., HIGHSMITH M. J., *Functional Differences of Bilateral Transfemoral Amputees Using Full-Length and Stubby-Length Prostheses*, Technol. Innov., vol. 20, no. 1, pp. 75–83, Nov. 2018, doi: 10.21300/20.1-2.2018.75.

[2] PIETRASZEWSKI B., WINIARSKI S., JAROSZCZUK S., *Three-dimensional human gait pattern – reference data for normal men*, Acta Bioeng. Biomech. / Wrocław Univ. Technol., vol. 14, no. 3, pp. 9–16, 2012, doi: 10.5277/abb120302..

COP and head displacements in response to a visual stimuli created in virtual reality

P. WODARSKI[1], **M. CHMURA**[2], **G. GRUSZKA**[3], **A. BIENIEK**[4], **M. PLES**[5], **J. JURKOJĆ**[6]

Key words: *virtual reality, balance, postural stability*

1. Background

Diagnostics of postural stability disorders is performed on the basis of tests performed while standing and walking [1, 2]. In both cases, it is possible to analyse the way in which a person counteracts temporary loss of balance due to stumbling, disorders related to dizziness and other disorders resulting from malfunctioning motor skills. The development of stabilographic measurements may include the use of additional disrupting stimuli, such as simulation of falling down stairs, a moving wall or the entire room [3, 4]. The reaction to such disorders allows for the extension of diagnosis, which increases the possibility of detecting problems with balance, which are impossible to register while standing still. Such assumption require studies that standardize the procedures of such measurements and define the ranges of the values of the analyzed parameters, taking into account the reaction of healthy people and patients to the disorder introduced.

2. Target of research

There were 3 main aims of the research: 1 – to analyse how the simulation of a falling down the stairs, realized by means of virtual reality, affect posture, 2 – to determine if the information about upcoming virtual disturbance, can change the influence of this disturbance, 3 – if there are any differences in analysed parameters obtained for the healthy reference group and a person declaring severe motion sickness and fear of heights.

3. Research methodology

The research group consists of 8 healthy participants (5 women and 3 men, average age – 25, average BMI 23). None of them did not declare any injuries or problems which can cause balance disorders. A person with motion sickness and fear of heights was a woman (age 25, BMI 17,3). VR application was prepared in Unity3D. The avatar was placed on the second floor facing the stairs. After a couple of seconds a simulation of falling down the stairs was simulated. During the research, the COP and head positions were measured using the measuring platform (WinFDM-S, Zebris) and HMD HTC Vive set (used also to present the virtual scenery). The first stage of the research consisted in 60 seconds measurements with eyes open (OO) and closed (OZ). Then, the subjects started the virtual reality test which was divided into two parts – each of them included three measurements. In the first part (BB) a participant was aware of the disturbances, but did not know when it starts. In the second part (BZ) a participant was informed about the beginning of the disturbance 3 seconds before it by red light. Presentation of falling down the stairs lasted 3 seconds, then participants had to stay motionless for 20 seconds. A comparative analysis was performed on the mean values of the COP and head velocities and the value of 95% of the ellipse area plotted by the COP and head movement. For the BB and BZ groups, the occurrence of normal distributions was examined using the Shapiro-Wilk test, and then comparative tests were performed. Due to the lack of normal distributions and the small size of the group, all the above-mentioned values were compared with the use of non-parametric tests. All calculations were made in Statistica version 13.

[1] Department of Biomedical Engineering, SUT, Zabrze, Poland, e-mail:piotr.wodarski@polsl.pl
[2] Department of Biomedical Engineering, SUT, Zabrze, Poland, e-mail:marta.chmura@polsl.pl
[3] Department of Biomedical Engineering, SUT, Zabrze, Poland, e-mail:grzegorz.gruszka@polsl.pl
[4] Department of Biomedical Engineering, SUT, Zabrze, Poland, e-mail:andrzej.bieniek@polsl.pl
[5] Department of Biomedical Engineering, SUT, Zabrze, Poland, e-mail:marek.ples@polsl.pl
[6] Department of Biomedical Engineering, SUT, Zabrze, Poland, e-mail:jacek.jurkojć@polsl.pl

4. Results

As the results of the analyzes showed no significant differences between the values of the studied coefficients for subsequent tests performed for a given person under given conditions, it was decided to combine the values of tests BB1, BB2 and BB3 into one group BB and tests BZ1, BZ2 and BZ3 into the BZ group Initial analysis showed no statistically significant differences both between tests in real and virtual environments, and between measurements with and without the warning stimulus. On the other hand, statistically significant differences were noted between the results of healthy people and a person with motion sickness and fear of heights.

Table 1. Results V– average velocity, EA – ellipse area

	V_{COP} [mm/s]		EA_{COP} [mm2]		$V_{\text{25s from the disturbance moment}}$ [mm/s]				EA [mm2]			
	OO	OZ	OO	OZ	BB		BZ		BB		BZ	
					COP	Head	COP	Head	COP	Head	COP	Head
median	11,5	11,6	107	151	12,5	8,7	14,0	8,3	149	342	148	305
min	7,9	8,1	67	40	9,2	6,4	9,5	6,8	54	174	47	159
max	14,0	19,8	558	696	23,6	12,2	20,7	12,5	487	949	444	891
pp3	16,1	11,1	230	567	18,8	11,7	19,2	12,8	453	971	1450	1687
					13,5	9,2	16,8	11,1	277	530	628	1282
					16,2	10,3	18,5	12,1	386	733	674	848

5. Discussion

The high power of the test (> 0.8), in the absence of statistically significant differences between the results of measurements carried out in individual conditions, allows the conclusion that the introduced destabilizing stimuli did not affect the behavior of the respondents, or indicates the fact that the classical analysis does not provide information allowing for an unambiguous statement if and how the introduced visual stimulus influenced changes in postural stability. A similar conclusion can be drawn by analyzing the results obtained with and without the warning stimulus. No significant differences were noticed here too, which may indicate that among healthy people, the information about a visual stimulus in the form of a fall down the stairs is of no importance for the behavior of the respondents. The analysis of a person with motion sickness and fear of heights showed that among the analyzed values, the area of the ellipse, in particular for the head positions, was the most differentiating it compared to healthy people. This suggests that in this type of research, the measurement of the head may be more important than the measurement of COP.

Acknowledgments: Publication supported as part of program “Inicjatywa Doskonałości – Uczelnia Badawcza” implemented at Silesian University of Technology, year 2020/2021.

References

[1] POLECHOŃSKI J, NAWROCKA A, WODARSKI P, TOMIK R., *Applicability of Smartphone for Dynamic Postural Stability Evaluation*, BioMed Research International, vol. 2019, 2019: 1-6

[2] WODARSKI P, JURKOJĆ J, POLECHOŃSKI J, BIENIEK A, CHRZAN M, MICHNIK R, GZIK M., *Assessment of gait stability and preferred walking speed in virtual reality,* Acta of Bioengineering and Biomechanics, col. 22, No. 1: 127-134

[3] CHANDER, H.; GARNER, J.C.; WADE, C., *Impact on balance while walking in occupational footwear*. Footwear Sci. 2014, 6, 59–66.

[4] JURKOJĆ J, WODARSKI P, MICHNIK R, MARSZAŁEK W, SŁOMKA K. J., GZIK M., *The Use of Frequency Analysis as a Complementary and Explanatory Element for Time Domain Analysis in Measurements of the Ability to Maintain Balance,* Journal of Human Kinetics volume 76/2021, 117-129

Assessment of influence of upper limb light-weight passive exoskeleton on motion performance of DMD patient and healthy young

W. WOJNICZ[1], B. ZAGRODNY[2], M. LUDWICKI[3], A. SOBIERAJSKA-REK[4], J. JABŁOŃSKA-BRUDŁO[5], M. KACZMARCZYK[6], K. FORYSIAK[7], A. JEDNACHOWSKA[8], M. CHODNICKI[9]

Key words: *DMD patient, EMG, kinematic data, upper limb, passive exoskeleton*

1.Introduction

Duchenne muscular dystrophy (DMD) is a genetic neuromuscular disorder causing motor function loss, gait abnormalities, progressive respiratory muscle dysfunction and cardiomyopathy. To maintain normal daily activity each wheelchair DMD patient needs external help and rehabilitation. This can be achieved by designing custom-made exoskeleton (external device) that helps perform chosen motions of upper limb of DMD patient.

We created a light-weight passive exoskeleton (it was a prototype to build an active exoskeleton) and tested its influence on the motion performance of one healthy adolescent (chosen from the control group of healthy teenagers) and one chosen DMD patient.

2. Method of testing

The aim of this study was to compare motion performance of chosen healthy one and DMD patient in two modes: 1) natural motions (unconstrained motions); 2) using light-weight passive exoskeleton (constrained motions).

The study involved recording of kinematic data (Fig. 1) and surface electromyography signals (EMG) of four chosen muscles of dominant upper limb (Fig. 2) by performing chosen motions [1-3]:

1) lifting a 50g/200g/500g weight from the waist height to the shoulder height;
2) moving 100g/200g/500g/1000g weight on the table (on the waist height);
3) raising an arm with a 50g/200g weight from the waist height;
4) tracing a path by the index finger on the waist height;
5) supination of the forearm;
6) bringing food/cup to the mouth;
7) placing fingers on the diagram and pressing a button.

A healthy subject performed each motion five times. A DMD patient performed each motion three times. Kinematic data (normalized differences of coordinate of wrist joint (WJ_x, WJ_y,WJ_z, ΔWJ) and upper limb centre of mass (COM_x,COM_y,COM_z,ΔCOM)) and muscle activations calculated as processed EMG data (RMS normalized data of biceps brachii (EMG_1), lateral head of triceps brachii (EMG_2), anterior part of deltoideus (EMG_3)and trapezius (EMG_4)) were analysed in five arbitrary chosen ranges of performed motions (each motion was normalized to 100% with respect to the time):2% of motion, 10% of motion, 38% of motion, 66% of motion and 96% of motion. Statistical relationships were analysed between muscle activations treated as independent variables (EMG_1,EMG_2,EMG_3,EMG_4) and kinematic data treated as dependent variables (WJ_x, WJ_y ,WJ_z, ΔWJ, COM_x,COM_y,COM_z and ΔCOM) by using linear regression analysis, linear multi-regression analysis and non-linear regression analysis.

[1]Gdansk University of Technology, Gdansk, Poland, email: wiktoria.wojnicz@pg.edu.pl
[2]Lodz University of Technology, Lodz, Poland, e-mail: bartlomiej.zagrodny@p.lodz.pl
[3]Lodz University of Technology, Lodz, Poland, e-mail: michal.ludwicki@p.lodz.pl
[4]Medical University of Gdansk, Gdansk, Poland, email: sobierajska@gumed.edu.pl
[5]Medical University of Gdansk, Gdansk, Poland, e-mail: jjbrudlo@gumed.edu.pl
[6]Gdansk University of Technology, Gdansk, Poland, e-mail:mmkaczmarczyk@go2.pl
[7]Gdansk University of Technology, Gdansk, Poland, e-mail: katarzyna.forysiak@pg.edu.pl
[8]Gdansk University of Technology, Gdansk, Poland, e-mail:a.jednachowska@gmail.com
[9]Gdansk University of Technology, Gdansk, Poland, e-mail: marek.chodnicki@pg.edu.pl

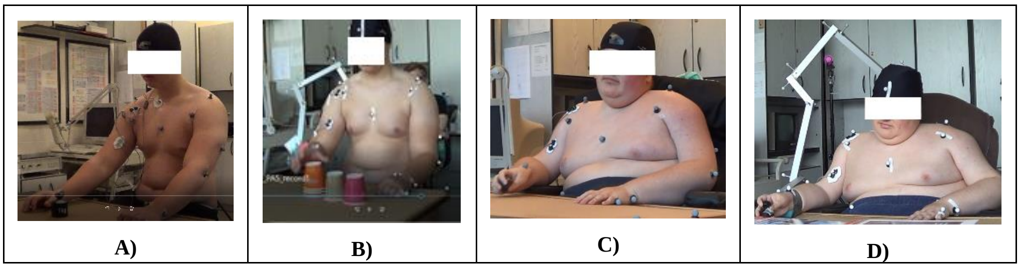

Fig. 1.A) Healthy young, B) Healthy young with a passive light-weight exoskeleton, C) DMD patient, D) DMD patient with a passive light-weight exoskeleton

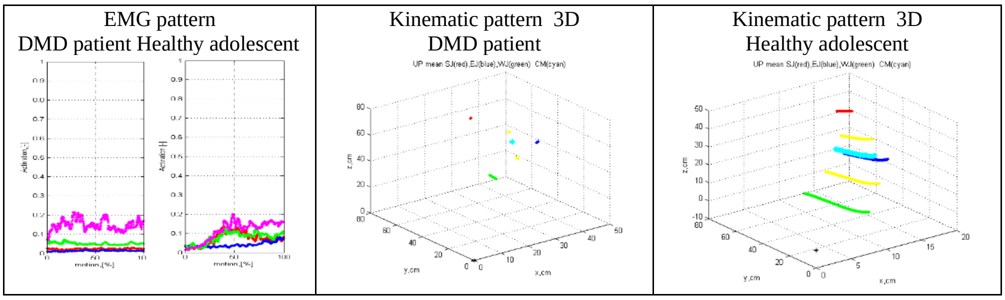

Fig.2. Lifting 50g weight from the waist height to the shoulder height without a passive exoskeleton: EMG data processed (mean value of the RMS normalized data): *biceps brachii* (1, red), *lateral head of triceps brachii* (2, blue), *anterior part of deltoideus* (3, green) and *trapezius* (4, magenta); Kinematic data of Shoulder joint (SJ), Elbow joint (EJ) and Wrist joint (WJ)

Acknowledgments: Project "The 'e-Pionier - using tertiary education institutions' potential to boost ICT solutions in the public sector', No. WG-POPC.03.03.00-00-0008/16-00, subject of the contract: "Custom-made device to assist the motor functions of the upper limb with muscular dystrophy".

References

[1] MAYHEW A., MAZZONE E.S., EAGLE M., DUONG T., ASH M., DECOSTRE V., VANDENHAUWE M., KLINGELS K., FLORENCE J., MAIN M., BIANCO F., HENRIKSON E., SERVAIS L., CAMPION G., VROOM E., RICOTTI V., GOEMANS N., MCDONALD C., MERCURI E., *Performance of the Upper Limb Working Group, Development of the Performance of the Upper Limb module for Duchenne muscular dystrophy*. Dev Med Child Neurol.55(11) 2013, 1038-45

[2] LANDFELDT E., MAYHEW A., EAGLE M., LINDGREN P., BELL C.F., GUGLIERI M., STRAUB V., LOCHMÜLLER H., BUSHBY K., *Development and psychometric analysis of the Duchenne muscular dystrophy Functional Ability Self-Assessment Tool (DMDSAT)*, NeuromusculDisord.25(12) 2015, 937-44

[3] SOBIERAJSKA-REK A., JABŁOŃSKA-BRUDŁO J., DĄBROWSKA A., WOJNICZ W., MEYER-SZARY J., WIERZBA J., *Timed Rolling and Rising Tests in Duchenne Muscular Dystrophy Ambulant Boys: A Feasibility Study*, Minerva Pediatrics, 2021 (accepted for publication)

An investigation of blood circulation biomechanics using computational fluid dynamics (CFD)

W. Wolański[1], M. Sobkowiak-Pilorz[2], M. Ples[3], M. Zimny[4], M. Gzik[5], W. Kaspera[6]

Key words: *Computational fluid dynamics, blood vessels, Middle Cerebral Artery, cardiovascular disease, hybrid imaging*

1. Introduction

Cardiovascular diseases are one of the main causes of mortality in developed and developing countries. One of them is pathological changes resulting in increased lumen of blood vessels (e.g. cerebral arteries) [1]. Existing 3D/4D, CT or MR echo techniques are standard diagnostic procedures but in some cases are insufficient. For this reason, the development of hybrid techniques combining 3D imaging with advanced numerical models (CFD) is desirable [2]. Numerical simulations and analysis of blood flow changes caused by pathological defects can be used to plan treatment and predict postoperative effects.

2. Aims

The study of the blood flow dynamics and the consequences of its influence on the walls of blood vessels requires a profound understanding of the impact of numerous factors, among which are the hemodynamic, mechanical, and morphometric ones. The CFD model will ultimately be a driving tool of the simulation experiments aimed at determination of the fluid-structure interactions significance in blood vessels [3,4]. Numerical simulations and analysis of the changes in blood flow caused by pathological defects can be used for treatment planning and post-operative effects prediction [5].

3. Methods

The following methods were used:

- Development of a 3D geometric and numerical model of the blood vessel,
- Performance of the CFD flow numerical simulations for the analysed blood vessel model,
- Analysis of the results (the hemodynamic parameters) obtained as a result of numerical simulation of CFD flow.

4. Results and discussion

Some of the results of the numerical simulations are shown in Figure 1.

[1]Silesian University of Technology, Faculty of Biomedical Engineering, Department of Biomechatronics, Poland, e-mail: wojciech.wolanski@polsl.pl
[2]Silesian University of Technology, Faculty of Biomedical Engineering, Department of Biomechatronics, Poland, e-mail: marta.sobkowiak-pilorz@polsl.pl
[3]Silesian University of Technology, Faculty of Biomedical Engineering, Department of Biomechatronics, Poland, e-mail: marek.ples@polsl.pl
[4]Medical University of Silesia in Katowice, Department of Neurosurgery, Poland, e-mail: zimny.mikolaj@gmail.com
[5]Silesian University of Technology, Faculty of Biomedical Engineering, Department of Biomechatronics, Poland, e-mail: marek.gzik@polsl.pl
[6]Silesian University of Medicine in Katowice, Department and Clinical Division of Neurosurgery, Poland, e-mail: wkaspera@sum.edu.pl

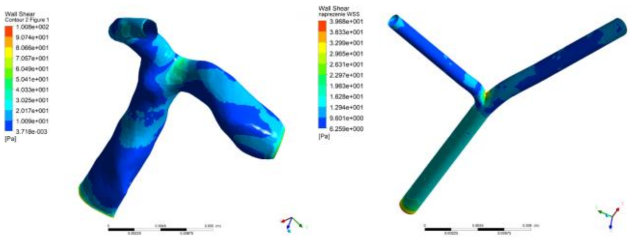

Fig. 1. Results of numerical simulations: on the left – real model (from CT scans), on the right – parametric model

Simulation results for both models (Fig. 1) revealed that the lowest values of pressure and those of the Wall Shear Stress (WSS) were related to the real (anatomical) model. The performed tests demonstrated the usability of the development of parametric models on the basis of anatomical parameters of the Middle Cerebral Artery (MCA) [6]. The models enable the performance of any modifications of the vessel and make it possible to perform the analysis of the artery wall sensitivity.

References

[1] Sforza, D.M., Putman, C.M. and Cebral, J.R., *Hemodynamics of cerebral aneurysms.* Annual Review of Fluid Mechanics. 2009, v41: 91-107.

[2] Levesque, M.J., Liepsch, D., Moravec, S. and Nerem, R.M., *Correlation of endothelial cell shape and wall shear stress in a stenosed dog aorta*. Arteriosclerosis. 1986, v6: 220-229.

[3] Hsu, M.-Ch., Bazilevs, Y., *Blood vessel tissue prestress modeling for vascular fluid-structure interaction simulation.* Finite Elem. Anal. Des. 2011, 47(6)1: 593–599.

[4] Gzik-Zroska B., Joszko K., Wolański W., Gzik M.: *Development of New Testing Method of Mechanical Properties of Porcine Coronary Arteries,* [in] Ed.: Piętka E., Badura P., Kawa J., Więcławek W., Information Technologies In Medicine (ITIB 2016), VOL 2, Springer, 2016, s. 289-297.

[5] Botar, C.C., Vasile, T., Sfrangeu, S., Clichici, S., Agachi, P. S., Badea, R., Cristea, M. V., *Validation of CFD simulation results in case of portal vein blood flow*. Computer Aided Chemical Engineering, 2010, 28(C): 205-210

[6] Sobkowiak, M., Wolański, W., Zimny, M., Gzik, M., Kaspera, W., *Analysis of an Impact of Hemodynamic Parameters in Relation to Variable Morphometric Features of the Middle Cerebral Artery (MCA)*. Innovations in Biomedical Engineering, Proceedings IiBE 2018, Eds. Marek Gzik, Ewaryst Tkacz, Zbigniew Paszenda, Ewa Piętka, Cham: Springer, pp. 200-209, 2019.

Assessment of the impact of ankle athletic taping on spatio-temporal gait parameters in healthy people

S. WÓJTOWICZ[1], **M. BIEDA**[2], **A. DANILUK**[3], **A. BUGALSKA**[4], **K. WIADERNA**[5], **M. GRABOWICZ**[6], **A. HADAMUS**[7]

Key words: *ankle, tape, athletic taping, gait analysis*

1. Introduction

Ankle sprain is one of the most common musculoskeletal injury in athletes affecting lower limb [1]. Due to the complex anatomy of the ankle joint, the most common injury is sprain which leads to stretch of a ligament or, even more often, partial or complete rupture of one or more ligaments. About 20-40% of ankle sprains leads to chronic instability, persistent symptoms and recurrent sprains [2,3]. Athletic taping (AT) is often recommended as a strategy to prevent ankle sprain [4]. Although studies have shown that taping reduces the risk of initial and recurrent ankle sprains [5], the mechanism by which taping works is not completely understood. Furthermore, studies on the effects of taping have mostly been carried out on patients with chronic ankle instability but taping is also used in healthy people as a protection against injury. The aim of this study was to assess the impact of athletic taping of ankle on spatio-temporal gait parameters in healthy people.

2. Materials and methods

2.1. Participants and intervention

The study enrolled 55 healthy individuals aged 23–27 years without ankle sprain in history. The participants were randomly assigned to the experimental group (E-group; N=27) and control group (C-group; N=28). E-group received Mueller athletic tape for ankle joint of the dominant lower limb, while C-group did not. Participants from E-group walked on a treadmill without tape and with tape. Participants from C-group walked two times without tape. Interval between two measurements in both groups was 15 minutes.

2.2. Measurements and calculations

Gait parameters were assessed using H/P Cosmos Mercury Med. instrumented treadmill with Zebris FDM-T software (Zebris Medical GmbH, Germany). The examination was conducted at a constant velocity of 5km/h. Each test attempt took 30 seconds. Following spatio-temporal gait parameters were analysed: step time (s), stride time (s), step length (cm), stride length (cm), step width (cm), stance time (%), swing time (%), loading response time (%), midstance time (%), preswing time (%), cadence (step/min). Statistica 13.1 was used for the statistical analysis. The threshold for significance was set at $p<0.05$.

[1]Department of Rehabilitation, Faculty of Medical Sciences, Medical University of Warsaw, Poland, e-mail: sebastian.wojtowicz@wum.edu.pl
[2]Student Scientific Society for Physiotherapy, Department of Rehabilitation, Faculty of Medical Sciences, Medical University of Warsaw, Warsaw, Poland e-mail: marbied@poczta.onet.pl
[3]Department of Rehabilitation, Faculty of Medical Sciences, Medical University of Warsaw, Poland, e-mail: anna.daniluk@wum.edu.pl
[4]Department of Rehabilitation, Faculty of Medical Sciences, Medical University of Warsaw, Poland, e-mail: aneta.bugalska@wum.edu.pl
[5]Department of Rehabilitation, Faculty of Medical Sciences, Medical University of Warsaw, Poland, e-mail: karolina.wiaderna@wum.edu.pl
[6]Department of Rehabilitation, Faculty of Medical Sciences, Medical University of Warsaw, Poland, e-mail: marta.grabowicz@wum.edu.pl
[7]Department of Rehabilitation, Faculty of Medical Sciences, Medical University of Warsaw, Poland, e-mail: anna.hadamus@wum.edu.pl

3. Results

No differences were observed between the groups before and after the applied intervention. Both in the E-group and in the C-group there were no significant differences in the measured gait parameters. There were also no differences between sides in both groups.

4. Discussion

Some studies have shown that athletic taping and kinesiotaping on ankle applied to patients with chronic ankle instability affect foot motion in the frontal plane and tibial motion in the transverse plane during stance phase of walking [6,7]. Chinn et al. found that, in those with chronic ankle instability, taping resulted in a more neutral ankle position during walking and jogging in shoes on a treadmill [8]. It is also confirmed that ankle-foot orthosis, which is often used for ankle instability disturbs gait [9]. The results obtained above may indicate that ankle taping has no effect on gait parameters in healthy subjects. Therefore, taping can be used as a protection against injury, that do not affect gait parameters, especially symmetry of a gait.

References

[1] WANG D.Y., JIAO C., AO Y.F. ET AL., *Risk Factors for Osteochondral Lesions and Osteophytes in Chronic Lateral Ankle Instability: A Case Series of 1169 Patients.* Orthop J Sports Med, 2020, 8(5): 2325967120922821.

[2] CHEN E.T., BORG-STEIN J., MCINNIS K.C., *Ankle Sprains: Evaluation, Rehabilitation, and Prevention.* Curr Sports Med Rep, 2019, 18, 217-223.

[3] AL-MOHREJ O.A., AL-KENANI N.S., *Chronic ankle instability: Current perspectives.* Avicenna J Med., 2016, 6(4), 103-108.

[4] VERHAGEN E.A.L.M., BAY K., *Optimising ankle sprain prevention: A critical reviewand practical appraisal of the literature.* Br J Sports Med, 2010, 44(15), 1082-8.

[5] VUURBERG G., HOORNTJE A., WINK L. M., ET AL. *Diagnosis, treatment andprevention of ankle sprains: Update of an evidence-based clinical guideline.* Br J Sports Med, 2018, 52(15), 956.

[6] YEN S.C., FOLMAR E., FRIEND K.A., ET AL., *Effects of kinesiotaping and athletic taping on ankle kinematics during walking in individuals with chronic ankle instability: A pilot study.* Gait Posture, 2018, 66, 118-123.

[7] MIGEL K., WIKSTROM E., *Gait biomechanics following taping and bracing in patients with chronic ankle instability: a critically appraised topic.* J Sport Rehabil. 2020, 29(3), 373-376.

[8] CHINN L., DICHARRY J., HART JM., ET AL., *Gait kinematics after taping in participants with chronic ankle instability.* J Athl Train, 2014, 49(3), 322-30.

[9] BŁAŻKIEWICZ, M., LANN VEL LACE K., HADAMUS A., *Gait Symmetry Analysis Based on Dynamic Time Warping.* Symmetry 2021, 13, 836.

Can tattoo influence a thermal image? A case report

B. ZAGRODNY[1]

Key words: *thermal imaging; tattoo; influence of body-tattoo on temperature distribution*

1. Introduction

The aim of this work is to answer the question if a body tattoo can influence thermographic examination and if the results for a new and old tattoo are different. This work is also a continuation of an earlier study devoted to this problem.

2. Materials and methods

The study was conducted on one volunteer with a tattoo made in a professional tattoo parlour, on the upper part of his chest 16 months and 28 months after making a tattoo. To record a skin temperature distribution, an infra-red camera was used.

3. Results

It is shown that a tattoo may have an influence on a local skin temperature distribution. The main applicable conclusion is that during any kind of thermographic examination, the examiner should expect that the tattoo can locally change temperature readings.

4. Discussion

The presented method allows to create repeatable conditions and to minimise the influence of factors that can change the temperature readings. As a result, when using the proposed standardisation, higher repeatability and precision of measurements are obtained.

[1]Lodz University of Technology, Faculty of Mechanical Engineering, Department of Automation, Biomechanics and Mechatronics, Lodz, Poland, e-mail: bartlomiej.zagrodny@p.lodz.pl

Standardisation procedure of infra-red imaging in biomechanics

B. Zagrodny[1]

1. Introduction

The methods of thermal imaging in biomechanics and medicine are still not fully standardised, in contrary to other popular methods of muscle activity examination. This this makes it difficult to compare test results performed in different laboratories or even undermines credibility of some of the results.

2. Materials and methods

The proposed standardisation procedure is based on the International Association of Certified Thermographers, American Academy of Thermology, European Association of Thermology, scientific publications and authors experience. The most restricted recommendations are chosen, described and discussed.

3. Results

The standardisation procedure of infra-red imaging in biomechanics is presented and discussed. Volunteer preparation, laboratory conditions, and tips how to make a thermal image are described. The state of the art. is presented and chosen aspects of thermal imaging pointed out.

4. Discussion

The presented method allows to create repeatable conditions and to minimise the influence of factors that can change the temperature readings. As a result, when using the proposed standardisation, higher repeatability and precision of measurements are obtained.

[1]Lodz University of Technology, Faculty of Mechanical Engineering, Department of Automation, Biomechanics and Mechatronics, Lodz, Poland, e-mail: bartlomiej.zagrodny@p.lodz.pl

Assessment of proprioception in the knee joint in patients after ACL reconstruction – preliminary study

P. Zalewska[1], J. Skubich[2], T. Guszczyn[3], S. Piszczatowski[4]

Key words: *knee joint, proprioception, ACL, reconstruction, Internal Brace*

1. Introduction

Anterior cruciate ligament (ACL) injury is one of the most common injuries of the knee [1]. This ligament is crucial for the stability of the joint. It is presumed that it also plays an important role in the proprioception, and its damage may affect its disturbance [2]. The basic method of ACL reconstruction is to replace the damaged ligament with a graft. Now, however, more and more often the new method named *Internal Bracing* is used, where the damaged ligament is not replaced, but is sutured and reinforced with synthetic tape, which allows for faster recovery [3]. Hence, the aim of this study was to develop the methodology and preliminary assessment of the impact of ligament reconstruction on proprioception in the knee joint.

2. Methods and materials

The preliminary studies involved 16 participants (age 22.0 ± 7.6 years) who underwent ACL reconstruction using one of the two methods - using an autologous graft (11 patients) and the Internal Bracing method (5 patients), as well as the rehabilitation process has been completed. Patients were qualified for the project on the basis of clinical assessment made by an orthopaedist. The research was approved by the bioethics committee. The BIODEX System 4 Pro isokinetic dynamometer was used to test proprioception in the knee joint. First, the whole set of tests was performed for the healthy limb (ACL-I) as a reference, and then for the operated limb (ACL-R).

The study consisted of two stages:

1. Threshold to detect passive motion (TTDPM) in the joint towards extension and flexion, defined as the angular path (in degrees) of the shank passively travelled from its initial position to the position, where limb movement can be detected by participant. In this test, the arm of dynamometer with the participant's shank moved from the starting position (90°) with a speed of 0.25°/s by a maximum of 5° (passive motion mode) in the appropriate direction (depending on movement direction) - the exercise was repeated four times for flexion and extension of the knee joint.
2. Joint position sense (JPS) – defined as ability to reproduce the given angular position (30° and 60°) in the knee joint three times in two ways:
   a. passively (muscles fully relaxed) - joint was moved to an appropriate angle and hold for 10 second (the patient was told to remember the position) and then returned to the starting position (90°). Next, the arm of dynamometer slowly moved participant's shank. When the patient decided that the current position of the limb coincides with the memorized position, he/she stopped the machine with a button and the current angle was recorded,

[1]Bialystok University of Technology, Institute of Biomedical Engineering, Bialystok, Poland,
e-mail: p.zalewska@doktoranci.pb.edu.pl

[2]Bialystok University of Technology, Institute of Biomedical Engineering, Bialystok, Poland,
e-mail: j.skubich.pb.edu.pl

[3]The Medical University of Bialystok Children's Clinical Hospital, Bialystok, Poland,
e-mail: tomasz.guszczyn@umb.edu.pl

[4]Bialystok University of Technology, Institute of Biomedical Engineering, Bialystok, Poland,
e-mail: s.piszczatowski.pb.edu.pl

b. actively (moderately tense muscles) - in this variant, the muscles of the lower limb were maintain in moderate tension during learning and next, the participant reproduced appropriate angular position on his own.

3. Results

Table 1 and Table 2 present the results of the experiment. Results were presented for healthy limb (ACL-I) and operated limb (ACL-R).

Table 1. Threshold to detect passive motion - TTDPM ([°] mean ± SD)

	ACL-I		ACL-R	
	mean	SD	mean	SD
flexion	**1.8**	0.8	**1.7**	0.7
extension	**2.7**	1.1	**2.5**	0.8

Table 2. Joint position sense - JPS ([°] mean ± SD)

	30°				60°			
	ACL-I		ACL-R		ACL-I		ACL-R	
	mean	SD	mean	SD	mean	SD	mean	SD
passive	**8.7**	4.4	**5.4**	3.6	**4.1**	2.3	**3.4**	1.7
active	**4.6**	3.0	**5.4**	2.9	**4.4**	2.9	**6.3**	5.5

4. Summary and conclusions

When analysing the TTDPM (Table 1) it can be noticed that the results for both limbs were very similar, with a slight dominance of the operated limb. Moreover, patients felt the flexion faster than the extension. Analysing the JPS (Table 2), it can be seen that passively angle was reproduced better by operated limb, but actively by healthy limb. The angle 60° was generally better reproduced (except for the operated limb for active angle reproduction).

Summarizing, it can be concluded that there is a visible effect of the damage and reconstruction of the ACL on proprioception in the knee joint. However, further studies is underway in order to gain a deeper understanding of the discussed phenomena. Due to the availability of patients who have undergone ACL reconstruction performed using one of the two methods, it seems reasonable to perform an in-depth analysis the impact of the type of reconstruction for proprioception, which will be done with the selection of an appropriate group of patients. It is also worth including a group of healthy participants in the study as a control group, because general observations and studies show that injury of one knee joint means that the other cannot be considered fully healthy.

Acknowledgments: Research was performed as a part of projects WI/WM-IIB/7/2020, WZ/WM-IIB/3/2020 and financed with use of funds for science from Polish Ministry of Science and Higher Education

References

[1] BENOS L., STANLEY D., SPYROU L., MOUSTAKES K., TSAOPPOULOS D.E., *A Review on Finite Element Modeling and Simulation of the Anterior Cruciate*, Frontiers in Bioengineering and Biotechnology, 2020, 20, 8:967.

[2] JOHANSSON H., SJOLANDER P., SOJKA P., *A sensory role for the cruciate ligaments*, Clinical Orthopaedics and Related Research, 1991, 268, 161-168.

[3] DABIS J., WILSON A., *Repair and Augmentation with Internal Brace in the Multiligament Injured Knee*, Clinics in Sports Medicine, 2019, 38(2), 275-283.

Muscle activity of the knee joint during gait in persons after ACL reconstruction – preliminary study

P. ZALEWSKA[1], J. SKUBICH[2], T. GUSZCZYN[3], S. PISZCZATOWSKI[4],

Key words: *knee joint, ACL, reconstruction, muscle activity, stabilization*

1. Introduction

The stability of the knee joint requires the cooperation of a complex system of anatomical structures working together to prevent excessive bone movement [1]. Apart from the main stabilizers, which are ligaments, this role is also played by all the muscles surrounding the knee, the hip muscles and the gastrocnemius muscle [2]. An ACL injury, the need to undergo reconstruction surgery and then strenuous rehabilitation means that the muscles can adapt to new working conditions and partly take over the function of the ligament. Therefore, the aim of this study is to make a preliminary assessment of muscle activity in patients after ACL reconstruction and the completed rehabilitation process.

2. Methods and materials

The preliminary studies involved 16 participants (age 22.0 ± 7.6 years) who underwent ACL reconstruction using one of the two methods - using an autologous graft (11 patients) and the Internal Bracing method (5 patients), as well as the rehabilitation process has been completed. Patients were qualified for the project on the basis of clinical assessment made by an orthopaedist. The research was approved by the bioethics committee.

The following muscle were selected for the assessment of muscle activity during gait: rectus femoris, vastus medialis, vastus lateralis, biceps femoris, semitendinosus and the two heads of the gastrocnemius muscle (lateral (L) and medial(M)). The electrode was placed according to standardized procedures. Both the healthy limb (ACL-I) and the operated limb (ACL-R) were examined. The test stand consisted of a measuring path, which included two force plates 9260AA (Kistler), which allowed to determine the beginning and end of the gait cycle. The study of muscle activity was carried out on a set from Biometrics Ltd, which included 14 integrated SX230 electrodes. Muscle activity testing during gait was recorded until at least 5 good trials were obtained (each foot cleanly struck on the force platform). In order to normalize the results, the MVC (maximum voluntary contraction) procedure was performed. The obtained results were related to the duration of the gait cycle. Additionally, in order to broaden the analysis, studies of muscle torque during knee extension and flexion was measured using a BIODEX System 4 Pro (isokinetic conditions). Patients performed 4 repetitions of the knee flexion and extension with maximum involvement at an angular velocity of 120°/s. The maximum values for flexion and extension moments were normalised to percentage of subject's body weight [N] multiplied by body height expressed in meters [m] (%BwH).

3. Results

Table 1 and Fig. 1 present the results for healthy (ACL-I) and operated limb (ACL-R).

[1]Bialystok University of Technology, Institute of Biomedical Engineering, Bialystok, Poland
e-mail: p.zalewska@doktoranci.pb.edu.pl

[2]Bialystok University of Technology, Institute of Biomedical Engineering, Bialystok, Poland,
e-mail: j.skubich.pb.edu.pl

[3]The Medical University of Bialystok Children's Clinical Hospital, Bialystok, Poland,
e-mail: tomasz.guszczyn@umb.edu.pl

[4]Bialystok University of Technology, Institute of Biomedical Engineering, Bialystok, Poland, e-mail: s.piszczatowski.pb.edu.pl

Table 1. Maximum values of flexor and extensor moments in isokinetic conditions ([%BwH] mean ± SD)

	ACL-I		ACL-R	
	mean	SD	mean	SD
flexion	**6.2**	1.7	**6.2**	1.5
extension	**9.6**	2.5	**9.5**	1.9

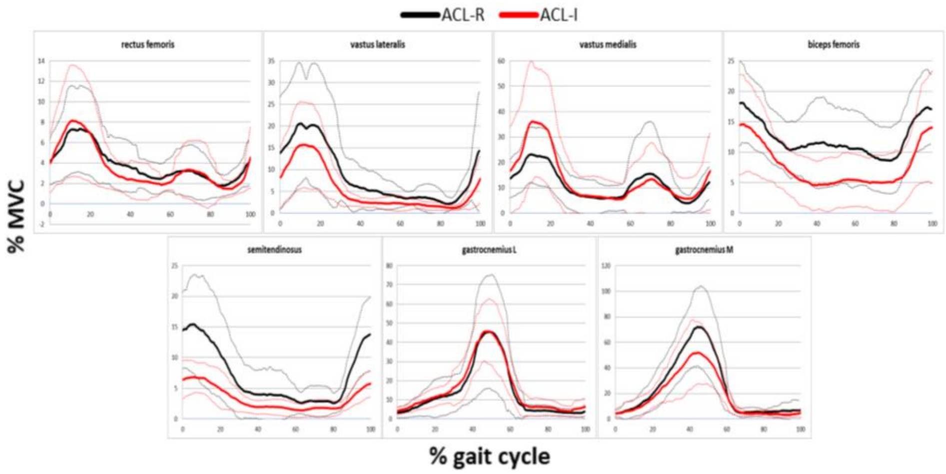

Fig. 1. Muscle activity during gait

4. Summary and conclusions

When analysing Table 1 it can be seen that there were no significant differences between the limbs, which means that there were no differences in the muscle strength of the flexors and extensors. Analysing Fig.1. differences between the operated and the healthy limb can be noticed. It is especially visible in the case of hamstrings, where for biceps femoris higher activity was maintained throughout the gait cycle (GC), and for semitendinosus it was especially noticeable at the beginning and end of the GC, where the differences reached even over a dozen percent. In the case of quadriceps femoris (rectus femoris, vastus lateralis, vastus medialis), a greater difference could be noticed around the first flexion - higher activity for operated limb. In the case of the gastrocnemius, for lateral head it can be seen that the mean value was similar for both limbs, but for operated limb there was a greater SD in the results. In the case of the medial head, higher muscle activity for operated limb was visible at around 40-50% of the GC.

Summarizing, there is a visible effect of muscle activity in persons after reconstruction of the ACL. However, further studies is underway in order to gain a deeper understanding of the discussed phenomena. Due to the availability of patients who have undergone ACL reconstruction performed using one of the two methods, it seems reasonable to perform an in-depth analysis the impact of the type of reconstruction on muscle activity, which will be done with the selection of an appropriate group of patients. It is also planned to include a group of healthy people as a control group.

Acknowledgments: Research was performed as a part of projects WI/WM-IIB/7/2020, WZ/WM-IIB/3/2020 and financed with use of funds for science from Polish Ministry of Science and Higher Education.

References

[1] ZLOTNICKI J.P, NAENDRUP J.H., FERRER G.A., DEBSKI R.E., *Basic biomechanic principles of knee instability*. Current Reviews in Musculoskeletal Medicine, 2016, 9, 114-122.

[2] ABULHASAN J.F., GREY M.J., *Anatomy and Physiology of Knee Stability*. Journal of Functional Morphology and Kinesiology, 2017, 2(4), 34.

Ultrasound based system for objective examination of skeletal muscles stiffness

J. ŻMIGRODZKI[1], S. CYGAN[2], K. WILDNER[3]

Key words: *skeletal muscle, muscle tension, ultrasonography, elastography, muscle biomechanics*

1. Introduction

Developments in ultrasound data processing and analysis has enabled examination of active skeletal muscles under various conditions [1]. Based on the principles of ultrasound elastography, stiffness of muscles can be estimated [2] which can be applied among others in diagnosis of patients with parkinsonian rigidity [3].

2. Materials and Methods

2.1. The proposed system

A new system has been developed for objective measurements of mechanical properties of skeletal muscles (patent pending no 430692). The system consists of an ultrasound scanner, a soft, non-elastic cuff for applying pressure load to the examined tissue, filled with liquid medium allowing for ultrasound imaging through the cuff, a digitally controlled pressure application and monitoring device. The examined model of the system includes a chair for the patient and an arm, where patients arm is immobilized. This arm enables also the measurement of the force developed by the examined muscle. The system enables acquisition of sequences of ultrasonic images registered during application of time varying pressure and/or during voluntary contraction of the muscle. Synchronized acquisition of force and pressure signal is carried out simultaneously.

2.2. Data processing

All data processing methods are implemented in Matlab environment. A previously developed block matching method [4] is used to calculate using acquired ultrasonic 2D radio-frequency image data the following quantities: displacements field u, principal strains ε1, ε2, and their directions, relative area change (area compression) Area compr., mean of absolute values of principal strains εMAP. For each examined case (data sequence) a region of interest is manually defined and for this ROI the mean absolute displacement value ||u||, the mean εMAP and mean Area compr. value are calculated.

For the cases where external pressure load was applied a new measure was proposed – the stiffness coefficient SC, defined by equation:

$$SC = \frac{\max\left(P(t)\right)}{\max\left(\varepsilon_{MAP}(t)\right)}\left[\frac{kPa}{\%}\right],$$

Where max(P(t)) is the maximum pressure value in the deformation cycle. This coefficient gives the value of pressure necessary induce muscle deformation by 1% thus describing its rigidity.

2.3. Experimental verification

The proposed method was verified using a model system incorporating a SonixTouch ultrasound scanner working with a L9-4/38 linear transducer (Ultrasonix, Canada), a Vivitro SuperPump (Vivitro, Canada) for pressure generation, a tip-catheter ANP-529A pressure sensor (Sentron, Netherlands) and a TAS606 – 200kg force sensor (HT Sensor Technology Co. Ltd., China) for measurement of the force generated by the examined muscle.

[1] Warsaw University of Technology, Institute of Metrology and Biomedical Engineering, Warsaw, Poland, e-mail: jakub.zmigrodzki@pw.edu.pl
[2] WUT, Institute of Metrology and Biomedical Engineering, e-mail: szymon.cygan@pw.edu.pl
[3] WUT, Inst. of Metrology and Biomedical Engineering, e-mail: krzysztof.wildner@pw.edu.pl

Experimental data was acquired from the biceps brachii and brachialis muscles of a single healthy volunteer (39 y.o. male, 188 cm, 77 kg) using a section view perpendicular to the muscle fibres.

3. Results

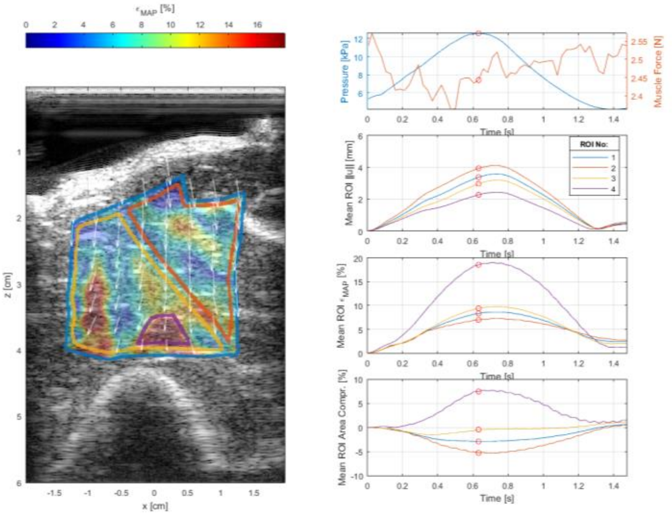

Fig. 1. External pressure applied on a relaxed muscle. Ultrasound image data with ε_{MAP} map in colour on the ROI (left). Time evolutions of registered and calculated quantities (right).

Figure 1. presents the result of an examination of a relaxed muscle under time-varying external pressure applied via the cuff. The left panel shows an ultrasound B-mode image of the examined muscle with the two ROIs covering both examined muscles. Strain maps are coded in colour on those ROIs while the arrows indicate directions of tissue displacements caused by the applied pressure.

4. Discussion and conclusions

This paper presents the basics of a new measurement technique that enables the study (monitoring) of the mechanical properties of muscles based on the use of ultrasound techniques. The first results indicate a significant potential of the proposed method and encourage further work in order to gradually improve it and attempt to analyse the data in order to obtain diagnostically useful information. In particular, the assessment of muscle stiffness and how it varies with the generated force seems to be very interesting from the diagnostic point of view.

References

[1] R. G. P. Lopata *et al.*, “Dynamic imaging of skeletal muscle contraction in three orthogonal directions,” *J. Appl. Physiol.*, vol. 109, no. 3, pp. 906–915, Sep. 2010.

[2] R. Van Der Werff, S. O’Leary, G. Jull, M. Peolsson, J. Trygg, and A. Peolsson, “A speckle tracking application of ultrasound to evaluate activity of multilayered cervical muscles,” *J. Rehabil. Med.*, vol. 46, no. 7, pp. 662–667, 2014.

[3] R. L. Watts, A. W. Wiegner, and R. R. Young, “Elastic properties of muscles measured at the elbow in man: II. Patients with Parkinsonian rigidity,” *J. Neurol. Neurosurg. Psychiatry*, vol. 49, no. 10, pp. 1177–1181, 1986.

[4] J. Żmigrodzki, S. Cygan, B. Leśniak-Plewińska, M. Kowalski, and K. Kałużyński, “Effect of Transmural Extent of the Simulated Infarction in a Left Ventricular Model on Displacement and Strain Distribution Estimated from Synthetic Ultrasonic Data,” *Ultrasound Med. Biol.*, vol. 43, no. 1, pp. 206–217, 2017.

Index of authors

Sponsors

QUALISYS
Motion Capture Systems

Tekscan